

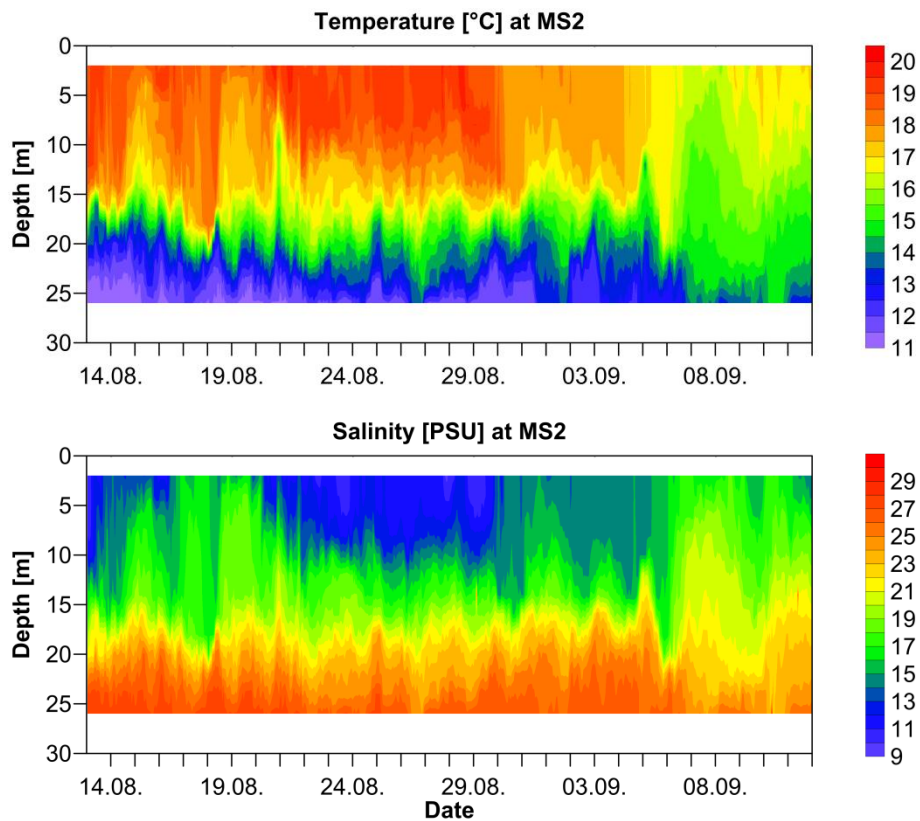
Final Report

**FEHMARNBELT FIXED LINK
HYDROGRAPHIC SERVICES (FEHY)**

Marine Water - Baseline

Hydrography of the Fehmarnbelt Area

E1TR0057 - Volume II



Prepared for: Femern A/S
By: DHI/IOW Consortium
in association with LICEngineering, Bolding & Burchard and Risø DTU

**Responsible editor:**

FEHY consortium / co DHI
Agern Allé 5
DK-2970 Hørsholm
Denmark

FEHY Project Director: Ian Sehested Hansen, DHI
www.dhigroup.com

Please cite as:

FEHY (2013). Fehmarnbelt Fixed Link EIA.
Marine Water - Baseline
Hydrography of the Fehmarnbelt Area.
Report no. E1TR0057 - Volume II

Report: 180 pages

May 2013

ISBN 978-87-92416-28-5

Maps:

Unless otherwise stated:

DDO Orthofoto: DDO®, copyright COWI

Geodatastyrelsen (formerly Kort- og Matrikelstyrelsen), Kort10 and 25 Matrikelkort

GEUS (De Nationale Geologiske Undersøgelser for Danmark og Grønland)

HELCOM (Helsinki Commission – Baltic Marine Environment Protection Commission)

Landesamt für Vermessung und Geoinformation Schleswig-Holstein (formerly Landesvermessungsamt Schleswig-Holstein) GeoBasis-DE/LVermGeo SH

Model software geographic plots: Also data from Farvandsvæsenet and Bundesamt für Seeschifffahrt und Hydrographie

Photos:

Photos taken by consortium members unless otherwise stated

© Femern A/S 2013

All rights reserved.

The sole responsibility of this publication lies with the author. The European Union is not responsible for any use that may be made of the information contained therein.



Co-financed by the European Union
Trans-European Transport Network (TEN-T)



CONTENTS

1	EXTENDED SUMMARY.....	1
1.1	Purpose of the Baseline Investigation	1
1.2	Baseline Monitoring 2009-2011	1
1.3	Bathymetry in the Fehmarnbelt Area	5
1.4	Conditions in the Fehmarnbelt Area.....	5
1.5	Local Conditions in Fehmarnbelt and Adjacent Bights	8
1.6	Selected Flow Features.....	18
1.7	Representativeness of Baseline Period	20
1.8	Present Pressures	22
2	INTRODUCTION.....	25
2.1	Scope of Work.....	25
2.2	Description	25
3	DATA BASIS.....	26
3.1	Baseline Monitoring and Modelling 2009-2011	26
3.1.1	Monitoring stations	26
3.1.2	Monitoring surveys.....	28
3.1.3	Model simulations	30
3.2	Other Data Sources.....	30
3.2.1	Weather stations	30
3.2.2	Water level stations	32
3.2.3	River inflow.....	33
3.2.4	Sea Ice.....	34
3.2.5	German and Danish light-vessels.....	34
3.2.6	Belt Project.....	35
3.2.7	HELCOM COMBINE Programme.....	35
3.2.8	Fehmarn Belt Feasibility Study	35
4	SETTING AND DRIVING FORCES.....	37
4.1	Bathymetry.....	37
4.2	Oceanographic conditions in the North Sea	39
4.3	Hydrology of the adjacent watershed	39
4.4	Meteorological conditions.....	41
4.5	Water Masses.....	41
4.6	Local Driving Forces	43
4.6.1	Bathymetrical features: sills, turnings and buffers.....	45
4.6.2	Tides.....	45
4.6.3	River inflow.....	46
4.6.4	Wind	47
4.7	Effects to water level.....	50
4.8	Distributions in the Fehmarnbelt.....	50
4.9	Sea Ice.....	51
5	METEOROLOGICAL CONDITIONS	52
5.1	Long-term Meteorological Conditions.....	52
5.2	Meteorological Conditions in Baseline Period.....	58
5.3	Summary	66



6	HYDROGRAPHIC BASELINE OBSERVATIONS	68
6.1	Water Level	68
6.2	Waves.....	72
6.3	Current	77
6.4	Salinity and Temperature	93
6.5	Sea Ice	114
7	SELECTED FLOW FEATURES IN BASELINE OBSERVATIONS	116
7.1	Outflow and Inflow Conditions in the Belt Sea	116
7.2	Horizontal Distribution of Water Masses in Fehmarnbelt.....	118
7.3	Velocity Distribution in the Link Corridor.....	119
7.4	Mesoscale Eddies.....	120
7.5	Upwelling	120
7.6	Comparisons of Flow Distributions across Fehmarnbelt	126
7.7	Water level difference and velocity	129
7.8	Volume and Salt Transports	131
8	HISTORICAL OBSERVATIONS OF HYDROGRAPHY.....	133
8.1	Water Level	133
8.2	Waves.....	136
8.3	Current	137
8.4	Salinity and Temperature	144
8.5	Sea Ice	149
9	REPRESENTATIVENESS OF BASELINE PERIOD	159
9.1	Meteorology	159
9.2	Water Level	160
9.3	Current	161
9.4	Salinity and Temperature	163
9.5	Sea Ice	169
9.6	Partial Conclusion	170
10	PRESENT PRESSURES	171
10.1	Major Constructions	171
10.2	Ship Traffic and Its Effects	171
10.3	Expected Climate Change	173
11	ASSESSMENT OF IMPORTANCE	175
12	REFERENCES	177

Lists of figures and tables are included as the final pages

APPENDICES

- A: ADCP transects across Fehmarnbelt during baseline years
- B: Summary of wave model setup



GLOSSARY

BSH: Bundesamt für Seeschifffahrt und Hydrographie, German Federal Shipping and Hydrography Authority

DWD: Deutscher Wetterdienst, German Weather Service

FEHY: Fehmarnbelt Fixed Link Hydrographical Services

HELCOM: Helsinki Commission, the governing body of the "Convention on the Protection of the Marine Environment of the Baltic Sea Area"

ICES: International Council for the Exploration of the Sea

IOW: Leibniz-Institut für Ostseeforschung Warnemünde, Leibniz Institute for Baltic Sea Research Warnemünde

KMS: Kort & Matrikelstyrelsen, Danish National Survey and Cadastre.

SII: Statens isbrydnings- og ismeldetjeneste. Danish ice breaking and ice warning service, transferred to Danish Naval Forces Operational Command in 1996.

SMHI: Sveriges meteorologiska och hydrologiska institut, Swedish Meteorological and Hydrological Institute

SOK: Søværnets Operative Kommando, Danish Naval Forces Operational Commando

Note to the reader:

In this report the time for start of construction is artificially set to 1 October 2014 for the tunnel and 1 January 2015 for the bridge alternative. In the Danish EIA (VVM) and the German EIA (UVS/LBP) absolute year references are not used. Instead the time references are relative to start of construction works. In the VVM the same time reference is used for tunnel and bridge, i.e. year 0 corresponds to 2014/start of tunnel construction; year 1 corresponds to 2015/start of bridge construction etc. In the UVS/LBP individual time references are used for tunnel and bridge, i.e. for tunnel construction year 1 is equivalent to 2014 (construction starts 1 October in year 1) and for bridge construction year 1 is equivalent to 2015 (construction starts 1st January).



1 EXTENDED SUMMARY

1.1 Purpose of the Baseline Investigation

The present report provides the technical documentation of the baseline investigation on hydrography (flow and stratification) in the Fehmarnbelt area. In addition meteorology (at sea surface) has been included in the baseline description. The baseline investigation for the larger Baltic Sea can be found in FEHY (2013a). The core of the baseline investigation is a two year long baseline monitoring with three fixed monitoring stations and monthly surveys in the Fehmarnbelt area.

The purpose of the hydrographic baseline study is to document the baseline conditions in Fehmarnbelt and adjacent areas based on the data collected during the two-year monitoring campaign and 3D oceanographic simulations of flow and stratification in the transition area.

The measurements collected in the monitoring campaign are related to available historical information such as:

- Information extracted from journal papers and engineering reports;
- German and Danish light-vessel measurements; and
- Historical monitoring campaigns.

1.2 Baseline Monitoring 2009-2011

In 2009 an intensive monitoring of hydrographical and chemical parameters in Fehmarnbelt and nearby area was initiated. Most of the baseline monitoring terminated in early 2011.

This measurement campaign includes two permanent moorings in Fehmarnbelt and one mooring in the Mecklenburg Bight.

Another integral part of the monitoring is monthly ship surveys that measures along predefined survey lines in and near Fehmarnbelt.

The three permanent main stations are named MS01, MS02 and MS03 and their locations can be seen Fig. 1.1. The main station measurements comprised in this baseline include two annual cycles from March 2009 to February 2011 with data coverage mainly above 90%.

Fig. 1.2 shows the instrumentation on one of the main stations. Every main station is equipped with three WQMs (Water Quality Monitor), some Microcats for salinity and temperature and one ADCP placed on the sea bottom. The WQMs and Microcats are mounted with a spacing of 2 m.

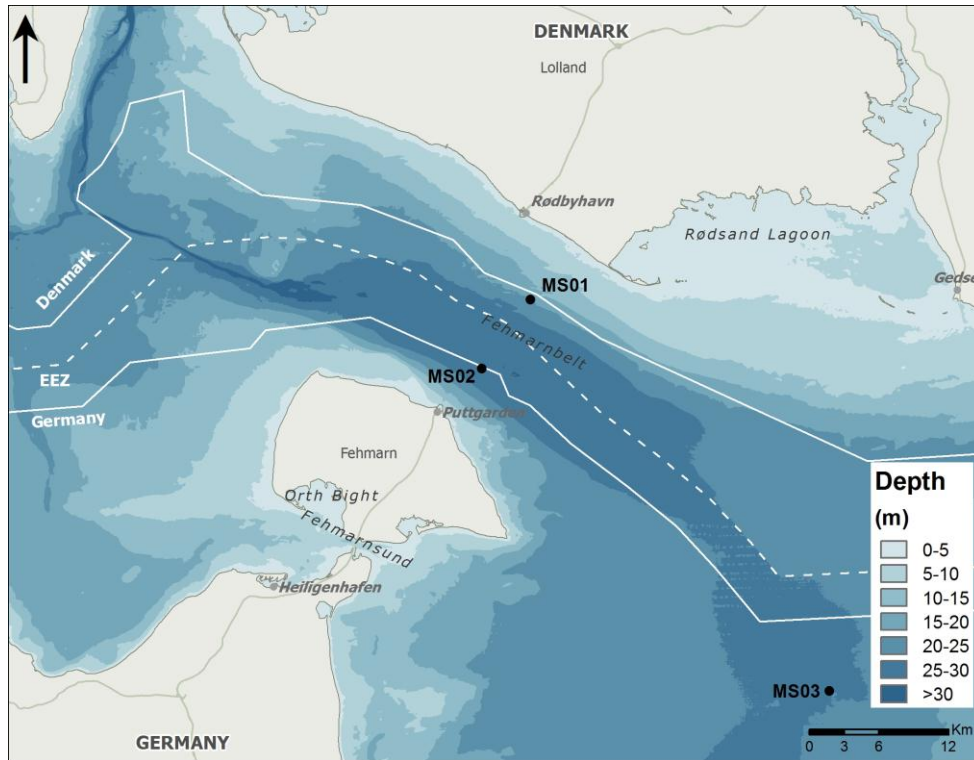


Fig. 1.1 Map with the monitoring stations MS01, MS02 and MS03.

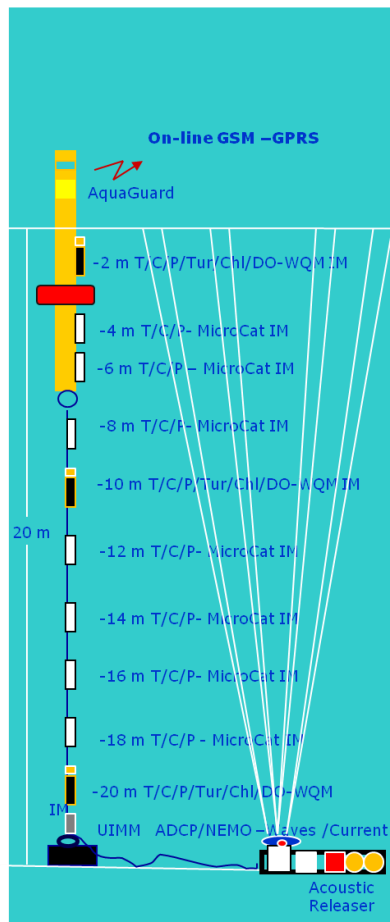


Fig. 1.2 Instrumentation at one of the three main stations (all three station have in principle the same instrumentation, but the precise instrumentation depends on the local water depth).

From these three stations time-series are collected of:

- Current
- Waves;
- Salinity;
- Temperature;
- Turbidity;
- Fluorescence of chl-a; and
- Oxygen.

Monitoring surveys are carried out on a monthly basis. The vessel applied is either RV JHC Miljø or RV Prof. A. Penck. A map with survey lines can be found in Fig. 1.3.

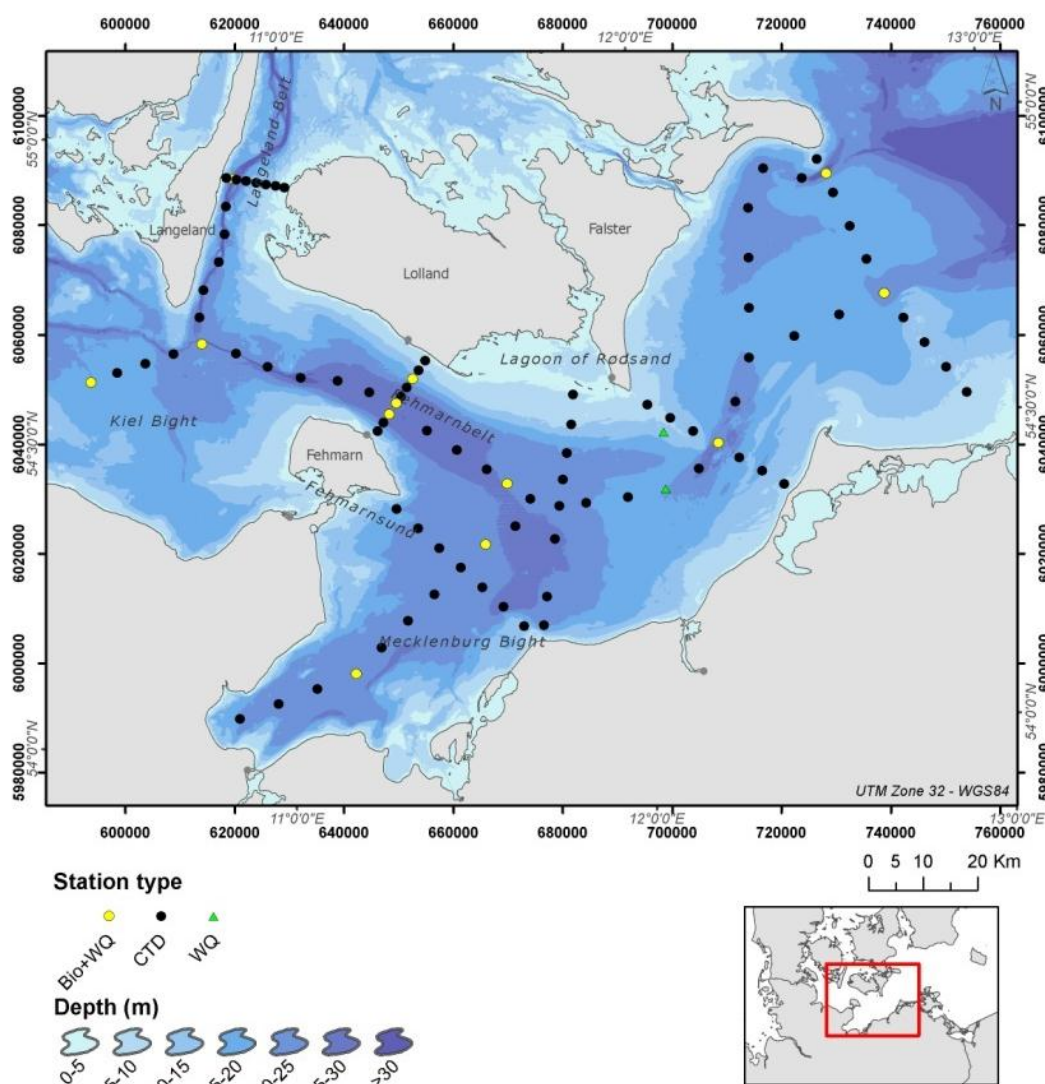
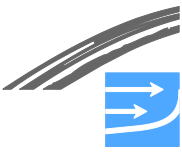


Fig. 1.3 Map with survey lines applied in monthly surveys. The hydrochemical/water quality stations are marked with green and yellow symbols.



The surveys focus on the survey line across Fehmarnbelt, but do also resolve the hydrographic conditions in the adjacent bights and upstream and downstream cross-sections from Langelands Belt to Darss Sill.

Meteorological information such as for example time-series of wind and air temperature has been taken from five stations, see Fig. 1.4:

- Westermarkelsdorf on island Fehmarn;
- MARNET station at Darss Sill;
- MARNET station in the Arkona Basin; and
- Nysted.

The data from Westermarkelsdorf are provided by the German Weather Service (DWD).

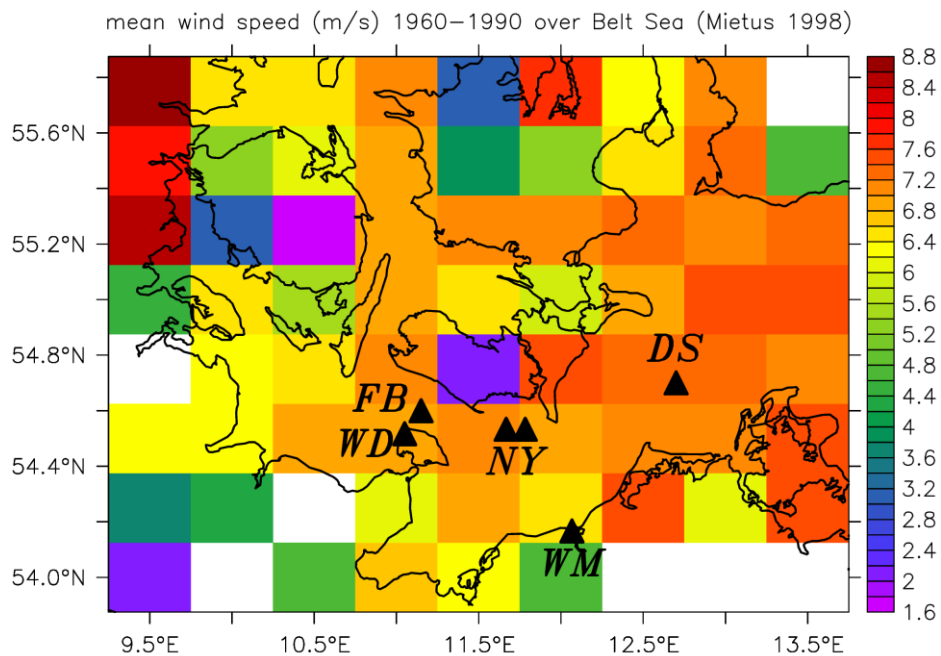


Fig. 1.4 Location of meteorological stations used for analysis: Fehmarnbelt buoy (FB), Westermarkelsdorf (WD), Nysted (NY), Warnemünde (WM), and Darss Sill (DS). The background shows mean wind speed derived from ship observations in 1961-1990 compiled by Mietus (1998).

These stations were selected for the following reasons:

- Station located at open sea or near the coast at sea level;
- Focus on the Fehmarnbelt region; and
- Availability of multi-year time-series.

1.3 Bathymetry in the Fehmarnbelt Area

Fehmarnbelt is bordered by the Danish island Lolland to the northeast and the German island Fehmarn to the southwest, see Fig. 1.5. The adjacent marine areas are Mecklenburg Bight and Kiel Bight, both with depths similar to the depth of Fehmarnbelt.

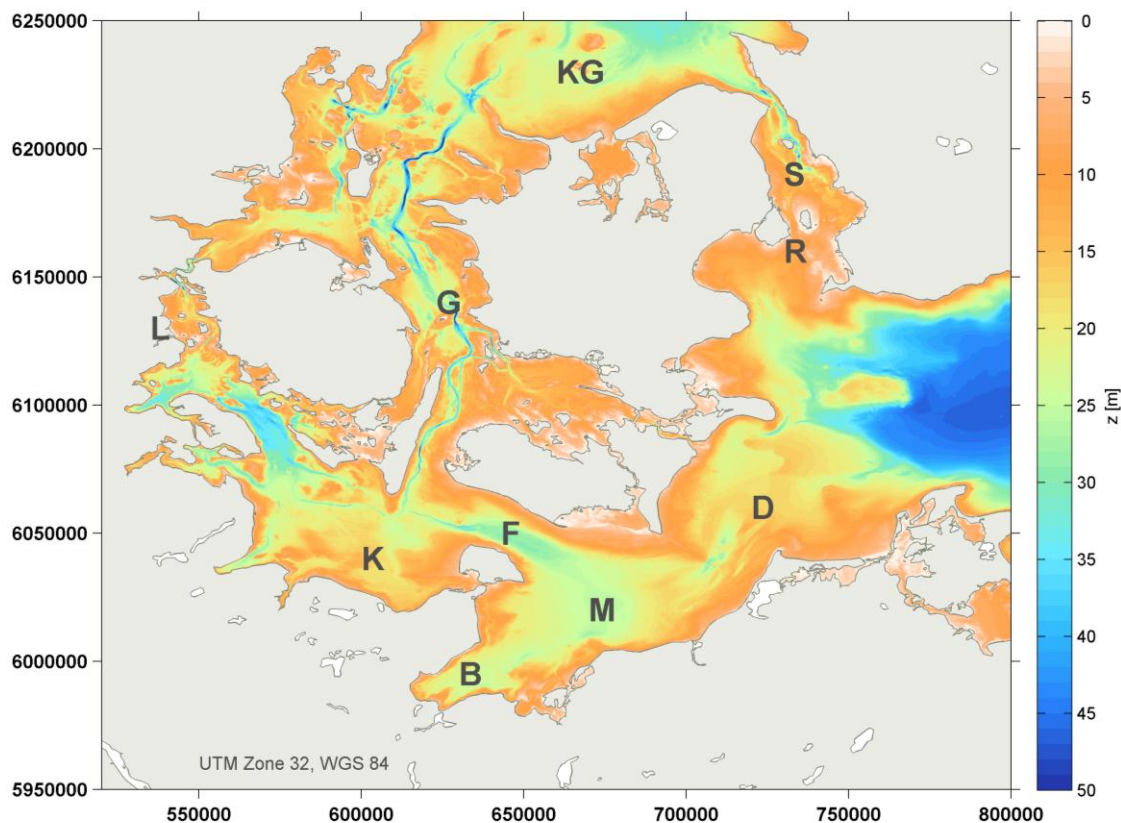


Fig. 1.5 Bathymetry of the Belt Sea: southern Kattegat (KG), Little Belt (L), Great Belt (G), Sound (S), Fehmarnbelt (F), Kiel Bight (K), Mecklenburg Bight (M), Lübeck Bight (B), Darss Sill (D) and Drogden Sill (R).

Fehmarnbelt has a maximum depth of about 30 m and a width varying between 18 km and 25 km. The narrowest section lies between Rødbyhavn and Puttgarden, the proposed site of the link. On the German side the depth increases quite fast to more than 20 m, while the seabed slopes more gently on the Danish side.

North of Kiel Bight is Langelands Belt that is turned 90° compared to Fehmarnbelt. East of Mecklenburg Bight is the Darss Sill with a maximum depth of 18 m bordering the Central Baltic Sea.

1.4 Conditions in the Fehmarnbelt Area

Fehmarnbelt is part of the transition area between the Central Baltic Sea and the North Sea. The flow and stratification in the Fehmarnbelt cannot be understood without relating it to the water exchange between the North Sea and the Central Baltic Sea.



The water masses in the Fehmarnbelt consist of low saline water from the Central Baltic Sea, which, close to the surface, flows through the Belt Sea and the Kattegat, and high saline water from the North Sea, which forms a lower layer. In June, the wind conditions are typically weak, and the two-layer exchange flow between the North Sea and the Central Baltic Sea is clearly identified to provide a strongly stratified water column in the Fehmarnbelt.

The dominating driving force for the flow in the transition area is the meteorological conditions over the North Sea and the Baltic Sea, i.e. not the local wind field over the transition area, not the runoff to the Baltic Sea, not the tidal flow or the density driven flow. The density driven flow is a relatively slow outwards directed flow.

High and low air pressure fields pass Scandinavia on a weekly time-scale and set-up or set-down the water levels in the North Sea and Baltic Sea.

In a situation where a low pressure field over Scandinavia with a cyclonic wind field, the related wind field causes set-ups and -downs in the North Sea and Baltic Sea, respectively, with:

- High water levels along the west coast of Jutland and in the Skagerrak and Kattegat;
- Low water levels in the south-western Central Baltic Sea; and
- High water levels in the north-eastern Central Baltic Sea.

High water levels in Kattegat and low water level in the south-western Central Baltic Sea force an inflow to the Central Baltic Sea, see example in Fig. 1.6:

- Initially the inflowing water masses propagate from Langelands Belt into the Kiel Bight. It continues until the water level inside the Kiel Bight is high enough to turn the water masses directly from Langelands Belt into Fehmarnbelt;
- The longer the inflow lasts the higher the salinities are of the inflowing water masses, and it goes for both the upper and the lower layers; and
- The inflow has to last some days before high saline water masses are lifted over the Darss Sill and continue into the Central Baltic Sea.

If it instead is a high air pressure field over Scandinavia with an anti-cyclonic wind field the situation is reversed with:

- Low water levels along the west coast of Jutland and in the Skagerrak and Kattegat;
- High water levels in the southwestern Central Baltic Sea; and
- Low water levels in the northeastern Central Baltic Sea.

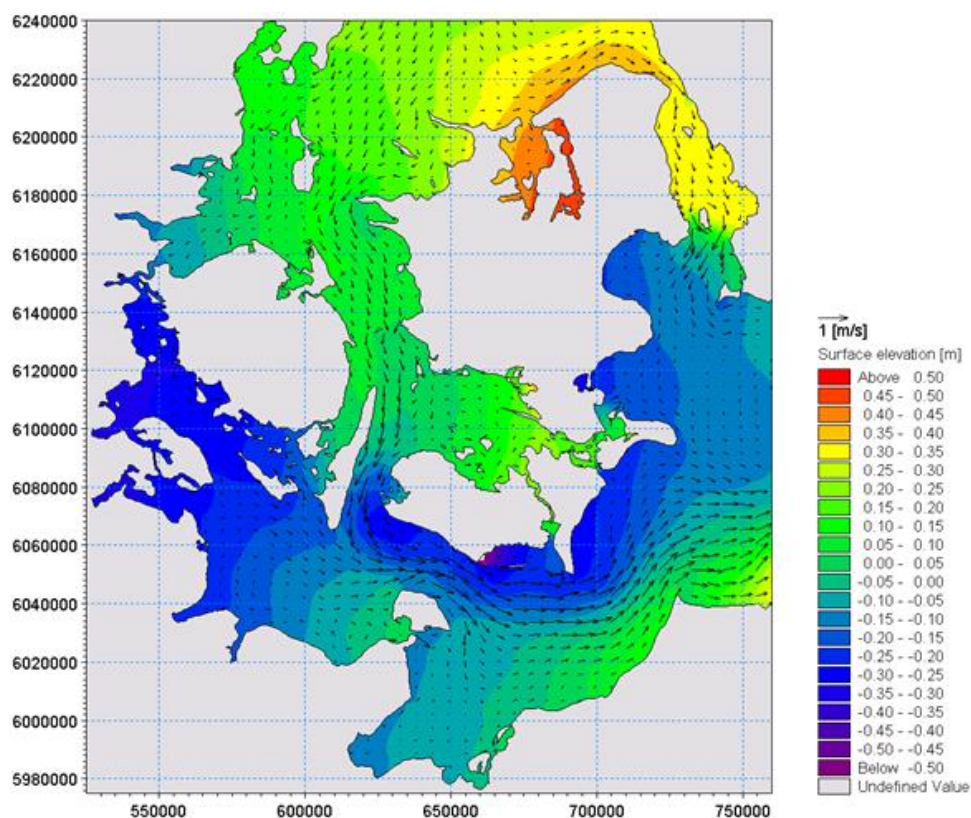


Fig. 1.6 Simulated water levels and current velocities in Belt Sea during strong inflow event.

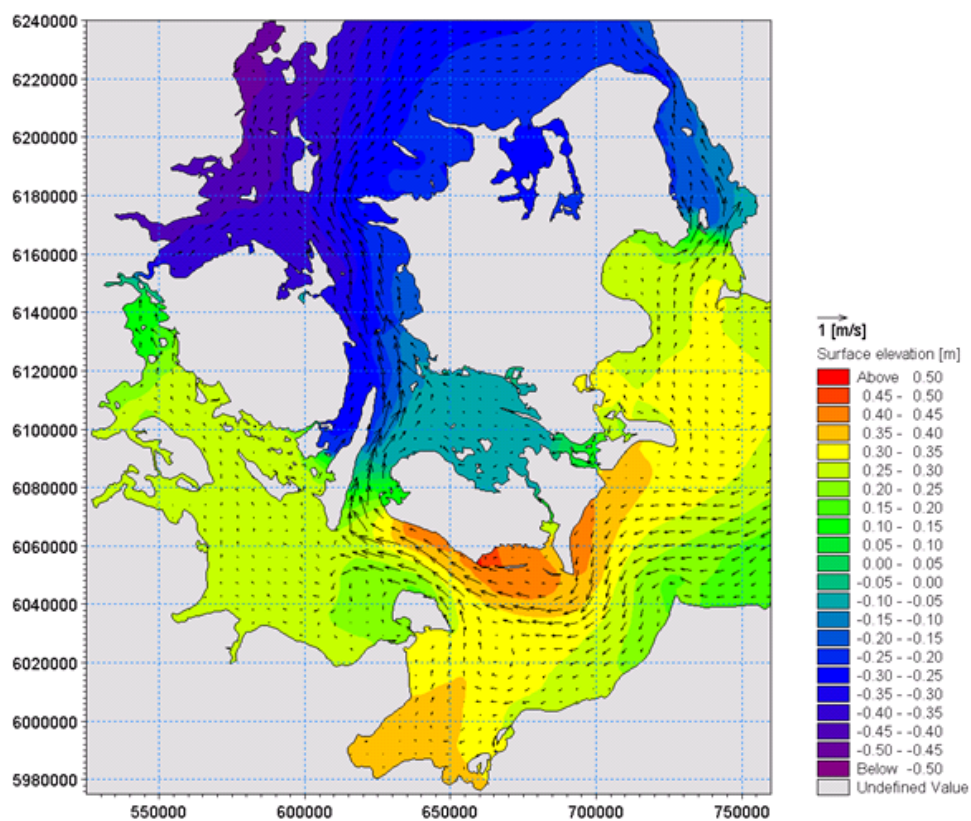


Fig. 1.7 Simulated water levels and current velocities in Belt Sea during strong outflow event.



Low water levels in Kattegat and high water levels in the south-western Central Baltic Sea force an outflow from the Central Baltic Sea through the Belt Sea (and the Sound), see example in Fig. 1.7:

- Initially the outflowing low saline water masses from the Central Baltic Sea propagate along the northern coastline in Fehmarnbelt and turns directly from Fehmarnbelt into Langelands Belt; and
- The longer the outflow lasts the wider the outflow will be. After some time it will occupy the upper layer in the Fehmarnbelt in its full width.

1.5 Local Conditions in Fehmarnbelt and Adjacent Bights

Stormy wind will cause a strong mixing of water masses in the Fehmarnbelt area and thus time scales between days and inter-annual variations have to be considered to characterize the meteorological forcing and the response of the sea. On the other hand the local weather is also influenced by the nearby coasts as can be shown for wind speed and direction and the daily cycle of air temperature in the Fehmarnbelt.

Waves in the Fehmarnbelt area are governed primarily by the local wind conditions and the fetch limitations due to land such as Fehmarn to the South, Lolland to the North, Falster and Mecklenburg-Vorpommern to the E-SE and Langeland and Schleswig-Holstein to the W.

However, occasionally waves from the south eastern Baltic Sea (Arkona Basin) can contribute to the wave climate in the Fehmarnbelt area.

The wave conditions in Fehmarnbelt are generally mild:

- The mean significant wave heights are 0.57 m and 0.52 m at MS01 and MS02, respectively;
- The maximum significant wave heights in 2009-2011 are 2.37 m and 2.49 m; and
- The waves are short with over 90% of the mean wave periods below 4.0 s and peak wave periods generally less than 6.5 s.

Wave roses at MS01 and MS02 are presented in Fig. 1.8.

They show that the dominant wave direction at MS01 is W-WNW, i.e. more or less perpendicular to the link corridor.

However, a significant fraction of waves occurs also from the SE directions.

The conditions at MS02 are very similar to those at MS01, except that the dominant directions are shifted to respectively WNW and ESE.

Waves from N-NE and SSE are low in amplitude and occur infrequently.

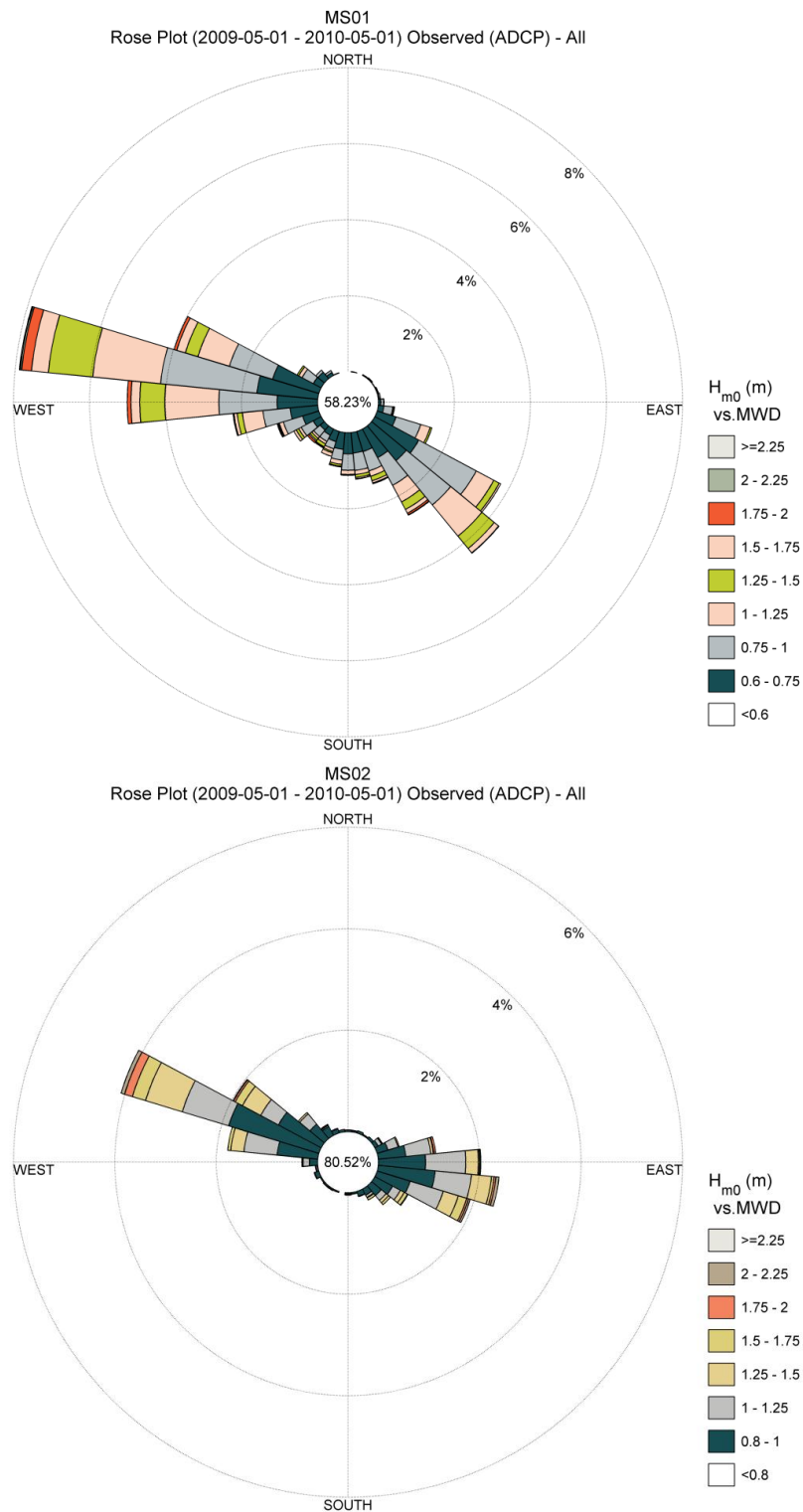
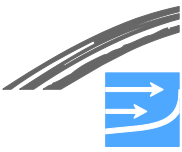


Fig. 1.8 Wave roses at MS01 (top, $H_{m0} > 0.60$) and MS02 (bottom, $H_{m0} > 0.80$).

The current in the Fehmarnbelt is affected by the vertical stratification that can decouple the upper and lower layers. During outflow conditions the outflow is restricted to the upper part of the water column, whereas the dense saline lower part may show insignificant currents or even reversed flow.



The mean measured current profile at MS02 shows (see Fig. 1.9) that the maximum current speeds are reached at the surface while bottom friction and baroclinic pressure reduces current speeds near the bottom.

The mean current is outwards towards the North Sea in the upper 15 m and inwards towards the Baltic Sea below 15 m depth. This vertical current distribution has opposite current directions in the upper surface layer and in the lower bottom layer.

The stratification also acts to reduce the flow resistance as it reduces the turbulence at the interface between the upper and lower layer, thus reducing the flow friction. Furthermore, it creates the separation of the upper and lower layer that can contribute to the development of oxygen depletion in the bottom waters.

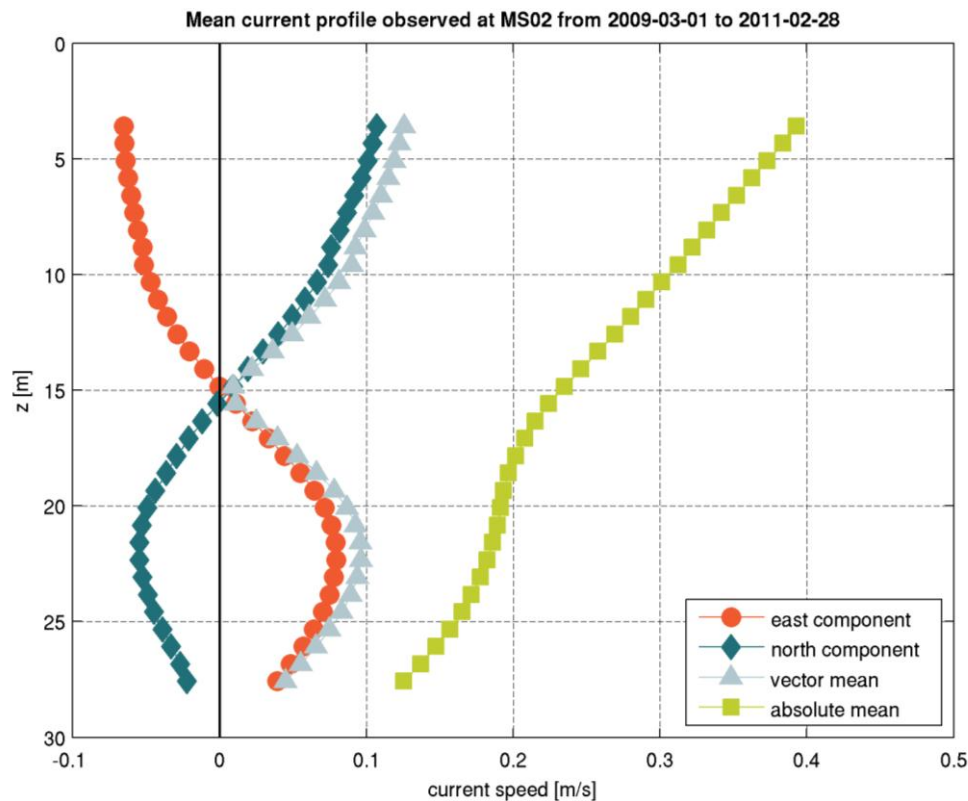
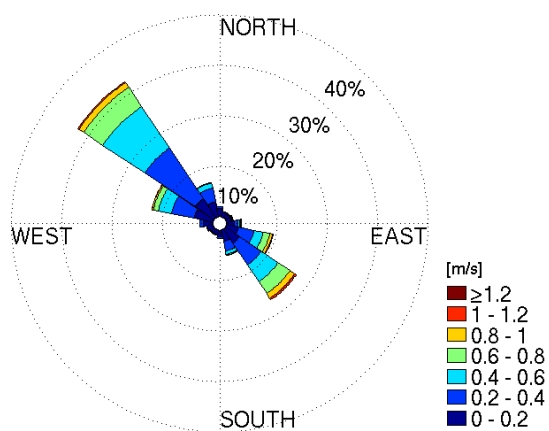


Fig. 1.9 Measured mean current profile at MS02 during the baseline period. Inflow with a south-westerly current dominates below 15 m depth. Maximum current speeds are reached at the surface while bottom friction reduces current speed near the bottom.

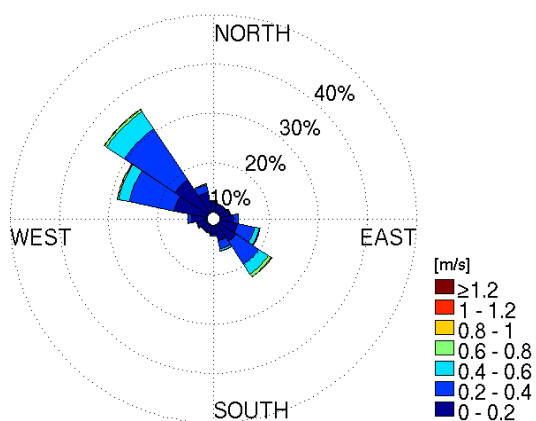
Current roses for the three main stations in Fehmarnbelt are shown in Fig. 1.10, Fig. 1.11 and Fig. 1.12. The current speeds are highest in the uppermost level and lowest in the lowermost level. The current rose shown in Fig. 1.11 based on measurements collected in the biggest water depth clearly shows a reversed current closer to the sea bed.

The current roses for MS01 and MS02 in the Fehmarnbelt also show that the currents follow the direction of the Fehmarnbelt channel. I.e. the currents are influenced by the bathymetry and geometry of coastlines. The mean surface speed is 0.34 m/s at MS01 and the maximum hourly speed monitored is 1.36 m/s. The current rose for MS03 in the more open Mecklenburg Bight area shows less pronounced main directions. I.e. the currents are less influenced by the bathymetry and geometry of coastlines and the current speeds are lower than in the Fehmarnbelt.

Frequency classes of 2009-2011 Fehmarnbelt observed velocity at MS01 in 5.08 m depth. $\Delta t=10$ min



Frequency classes of 2009-2011 Fehmarnbelt observed velocity at MS01 in 12.58 m depth. $\Delta t=10$ min



Frequency classes of 2009-2011 Fehmarnbelt observed velocity at MS01 in 18.58 m depth. $\Delta t=10$ min

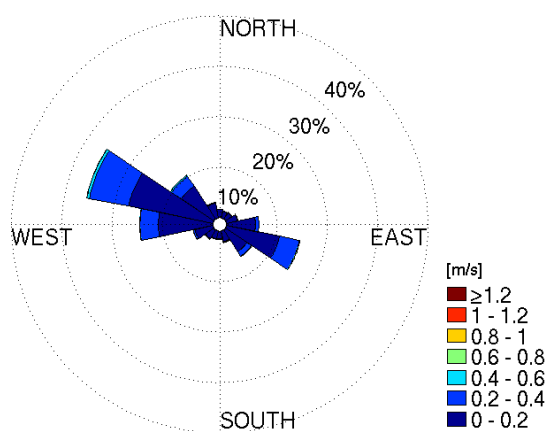
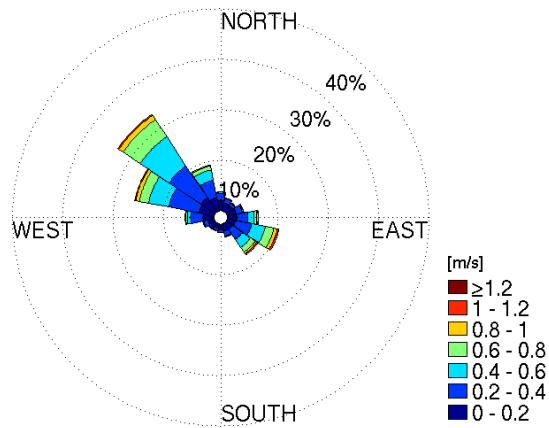


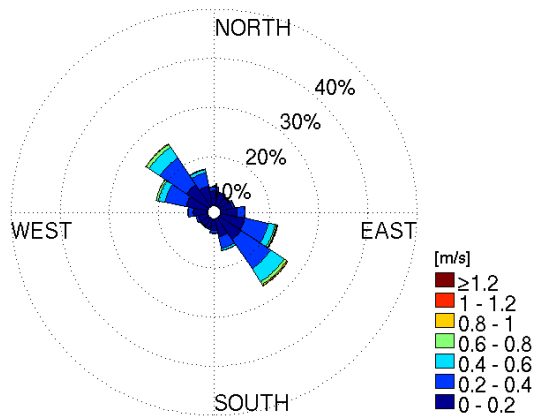
Fig. 1.10 Current roses based on measured current at MS01. The roses are shown in the three levels 5.08 m, 12.58 m and 18.58 m.



Frequency classes of 2009-2011 Fehmarnbelt observed velocity at MS02 in 5.08 m depth. $\Delta t=10$ min



Frequency classes of 2009-2011 Fehmarnbelt observed velocity at MS02 in 15.58 m depth. $\Delta t=10$ min



Frequency classes of 2009-2011 Fehmarnbelt observed velocity at MS02 in 27.58 m depth. $\Delta t=10$ min

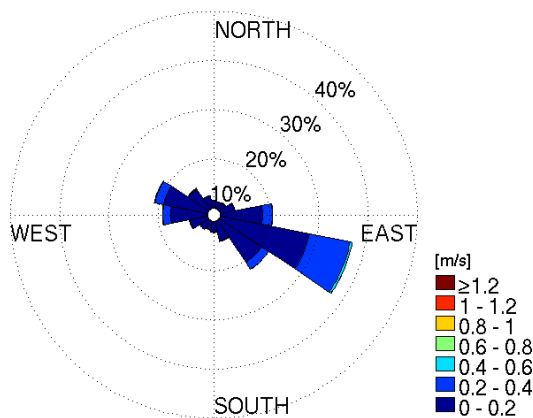
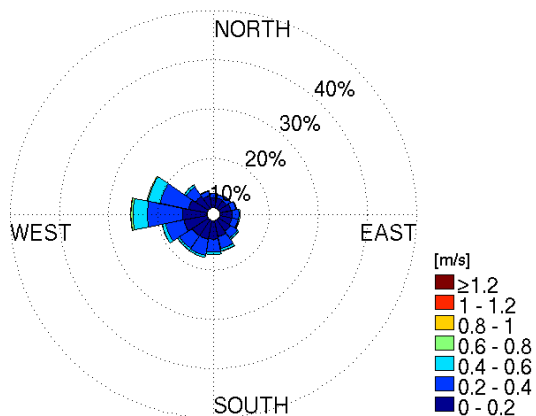
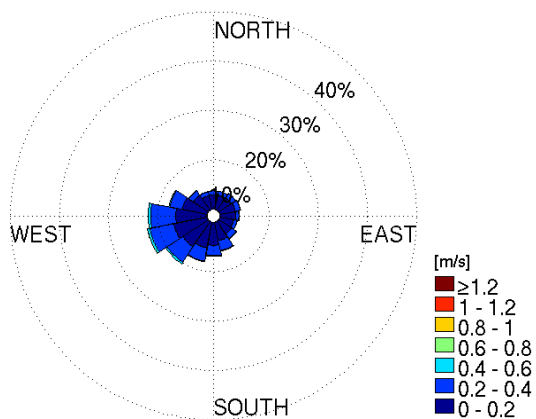


Fig. 1.11 Current roses based on measured current at MS02. The roses are shown in the three levels 5.08 m, 15.58 m and 27.58 m.

Frequency classes of 2009-2011 Fehmarnbelt observed velocity at MS03 in 5.03 m depth. $\Delta t=10$ min



Frequency classes of 2009-2011 Fehmarnbelt observed velocity at MS03 in 12.53 m depth. $\Delta t=10$ min



Frequency classes of 2009-2011 Fehmarnbelt observed velocity at MS03 in 23.03 m depth. $\Delta t=10$ min

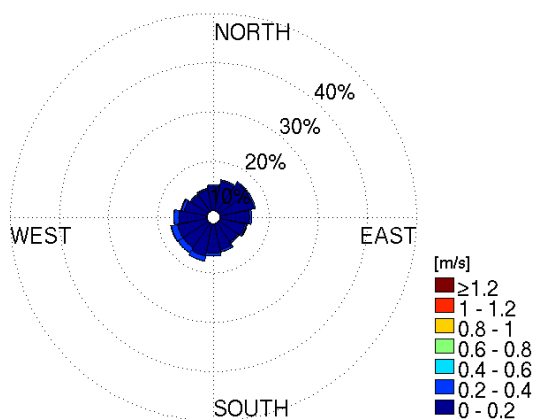


Fig. 1.12 Current rose based on measured current at MS03. The roses are shown in the three levels 5.03 m, 12.53 m and 23.53 m.



Detailed variation of currents at MS01 in the Fehmarnbelt is shown in Fig. 1.13.

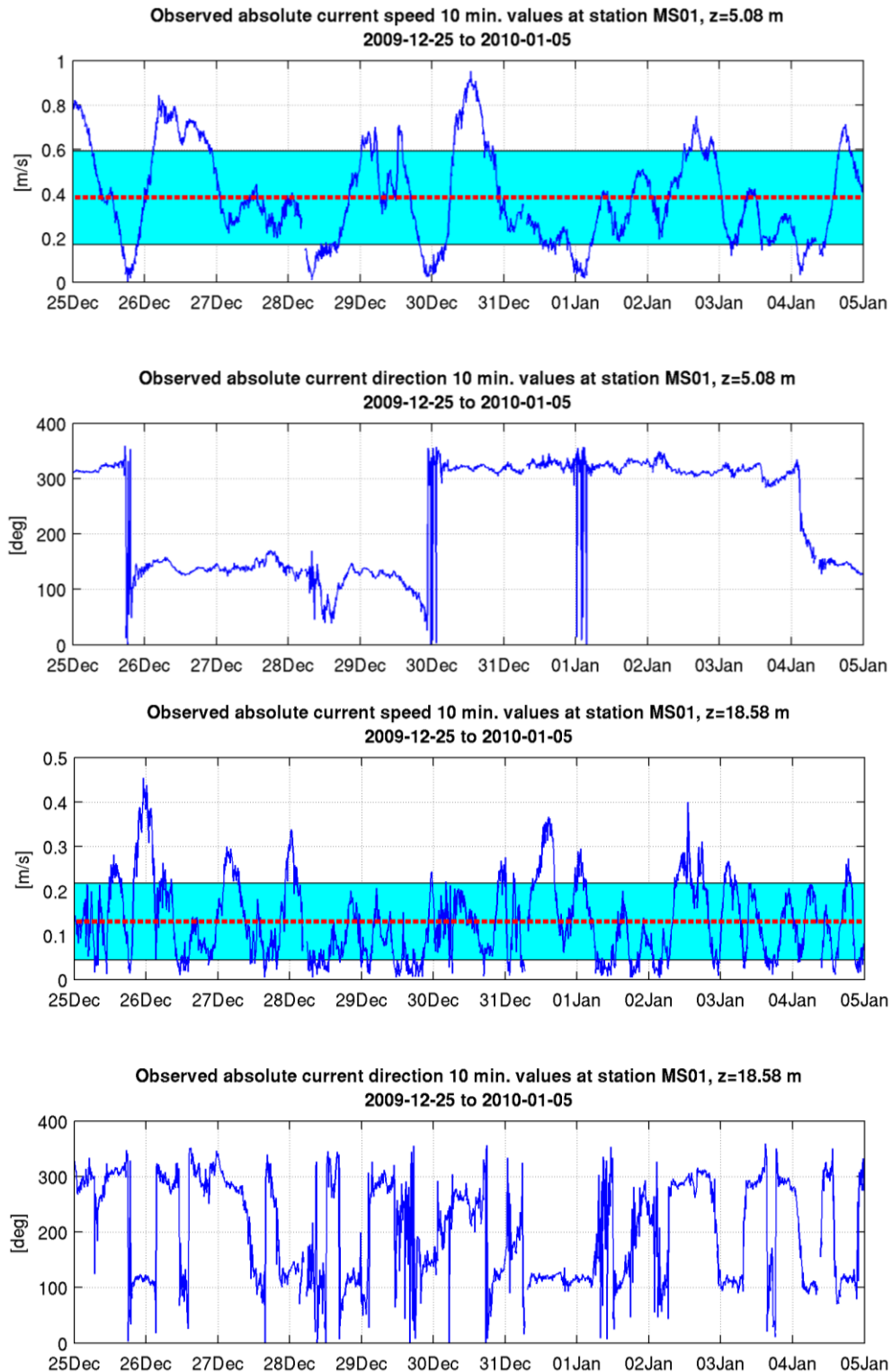


Fig. 1.13 Observed current speed and direction at MS01 from 2009-12-25 to 2010-01-05 at z=5.08 m (upper panel) and z=18.58 m (lower panel) with mean speed (red lines) and standard deviation of current speed.

In the upper layer first the last one day of an outflow is identified. It is followed by 4 days inflow event and a five days outflow event. At the end a situation with reversal towards inflow is found.

The currents are driven partly by a water level difference between the Arkona Basin and the Kattegat and partly by tides from Kattegat. The tides are especially pronounced in the lower layer. In the upper layer the tides are superimposed on top of a stronger water level driven current.

The tidal signal is delayed in the lower layer compared to the upper layer.

Long-term salinity and temperature variations at Fehmarn Belt light-vessel (its location is shown in Fig. 3.8) are shown in Fig. 1.14. A seasonal variation in both salinity and temperature is observed.

No important long-term trends in the salinities and temperatures are identified in the Fehmarnbelt light-vessel data.

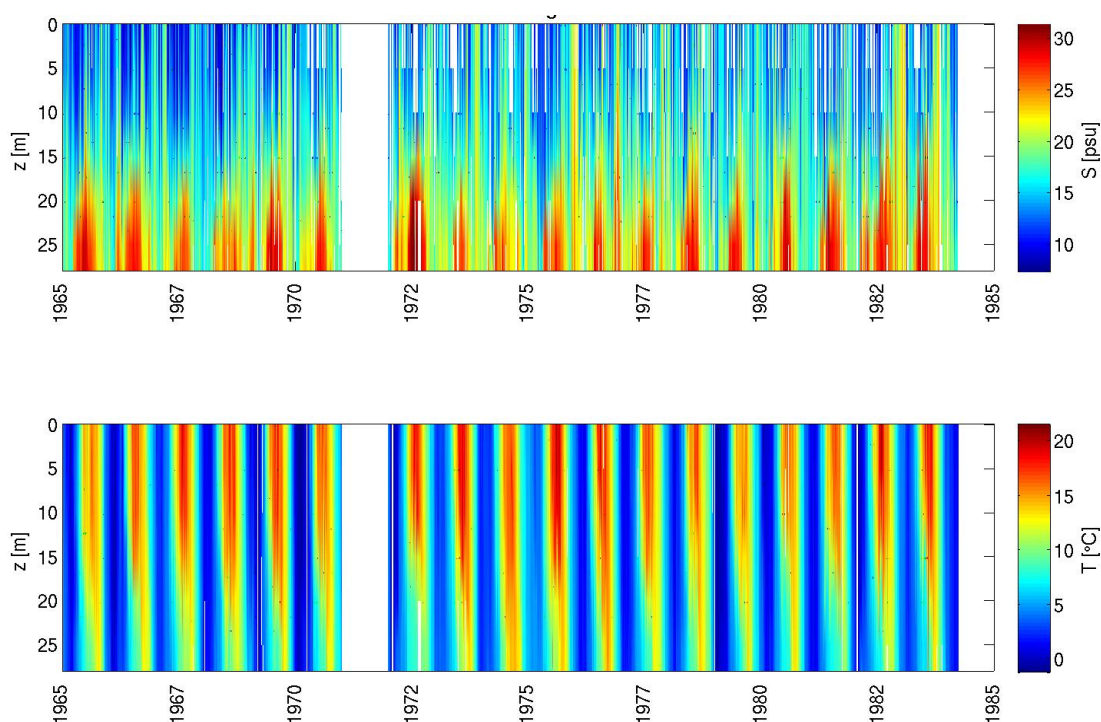


Fig. 1.14 Measured salinity and temperature variation at the Fehmarnbelt light-vessel from 1965 to 1984. Note the cyclic nature of bottom salinity with infrequent inflows of saline North Sea water.

Distribution of salinity and temperature at MS01 and MS02 are shown in Fig. 1.15 and Fig. 1.16 below.

A medium saline inflow to the Central Baltic Sea is detected in October 2009 with salinities around 22 psu over the entire water column at the Darss Sill. The saline inflow in October 2009 was recorded at MS02 as a more or less continuous highly saline layer of $S > 22$ psu at depths below 15 m. The flows of saline North Sea water into the Baltic Sea follows the southern slope of the Fehmarnbelt channel. Hence the lower layer is more dominating at MS02 than at MS01.

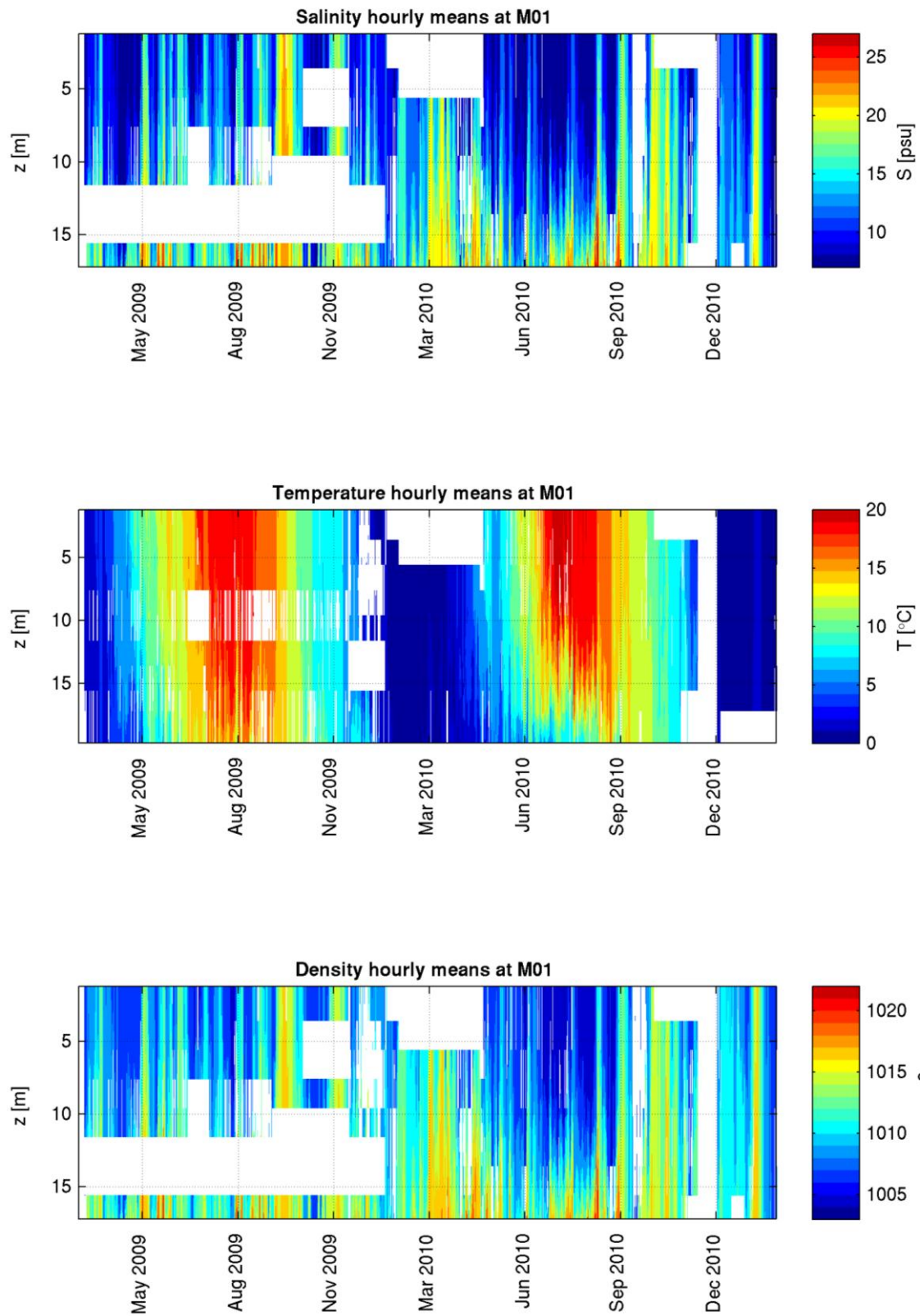


Fig. 1.15 Measured salinity, temperature and density (kg/m^3) at MS01 in Fehmarnbelt (southeast of Rødbyhavn) during the baseline monitoring.

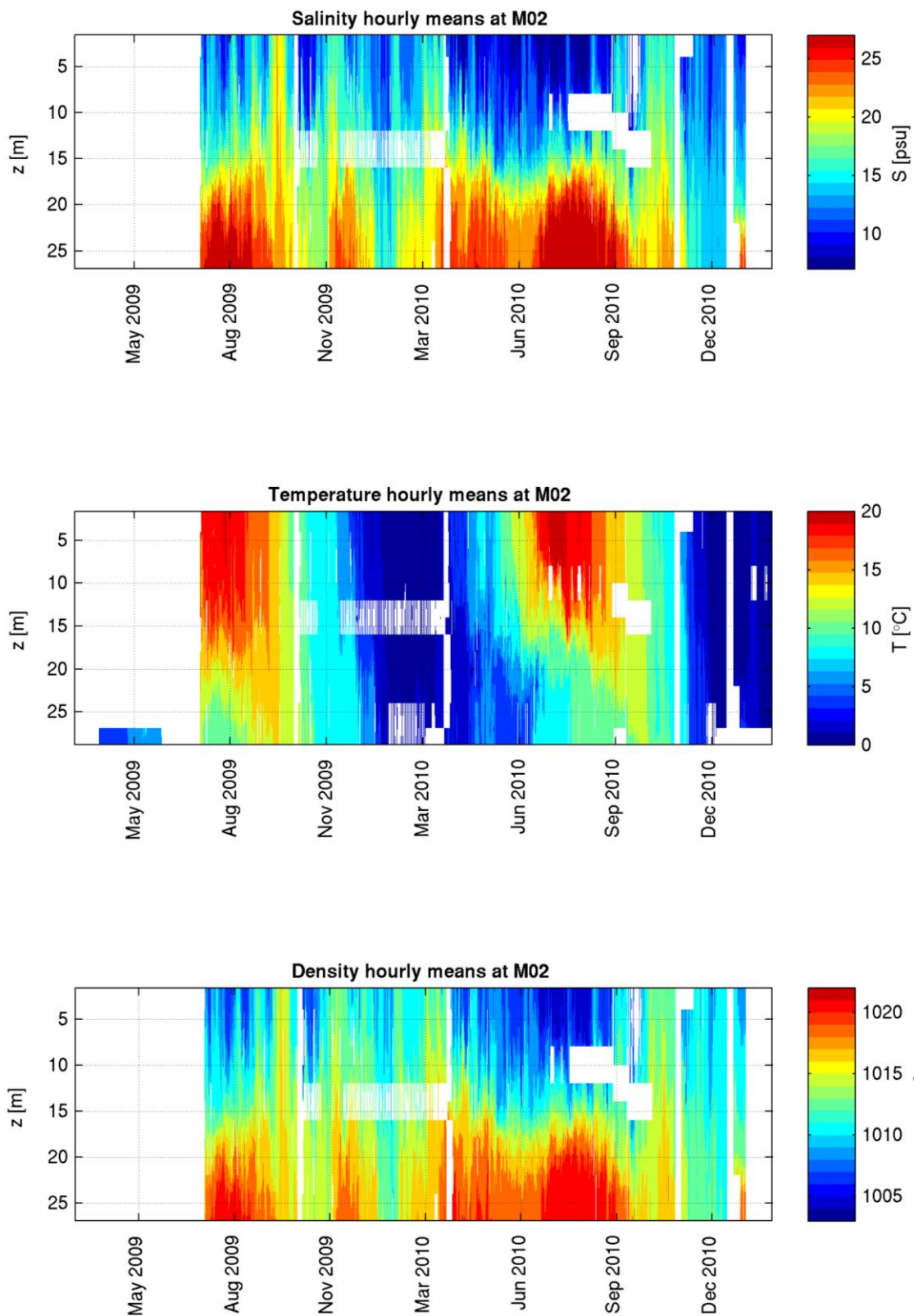


Fig. 1.16 Measured salinity, temperature and density (kg/m^3) at MS02 (north of Puttgarden) during the baseline monitoring.

Salinity profiles at MS01 are analysed in Fig. 1.17. The salinity profiles are divided into inflow and outflow conditions. It shows higher salinity during inflow than during outflow.

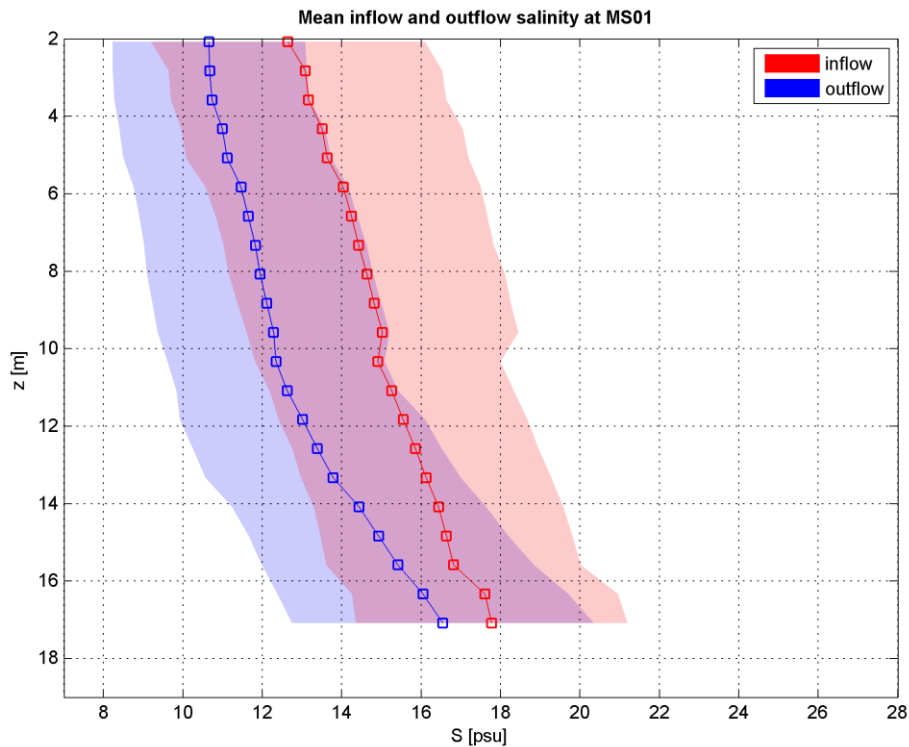


Fig. 1.17 Measured salinity profile at MS01 during the baseline period divided into inflow or outflow conditions. Mean profile with standard deviation indicated.

1.6 Selected Flow Features

Measured velocity distributions in the Fehmarnbelt cross-section are shown in Fig. 1.18. The red and yellow colours refer to inflow and the blue colours refer to outflow. The current is not homogeneous, but varies over the cross-section.

The current conditions and distributions are affected by:

- Barotropic and baroclinic pressure gradients;
- Shear stresses, including the local wind stress on the sea surface;
- The momentum of the flow when entering via Darss Sill or the Great Belt area;
- The necessary change in flow direction due to bathymetry; and
- The Coriolis force resulting from the rotation of the Earth.

The result becomes a complex flow pattern with large scale eddies, fronts, up and down-welling and coastal jets. And when the exchange flow reverses either from inflow to outflow or vice versa then complicated transient flow situations and distributions develop.

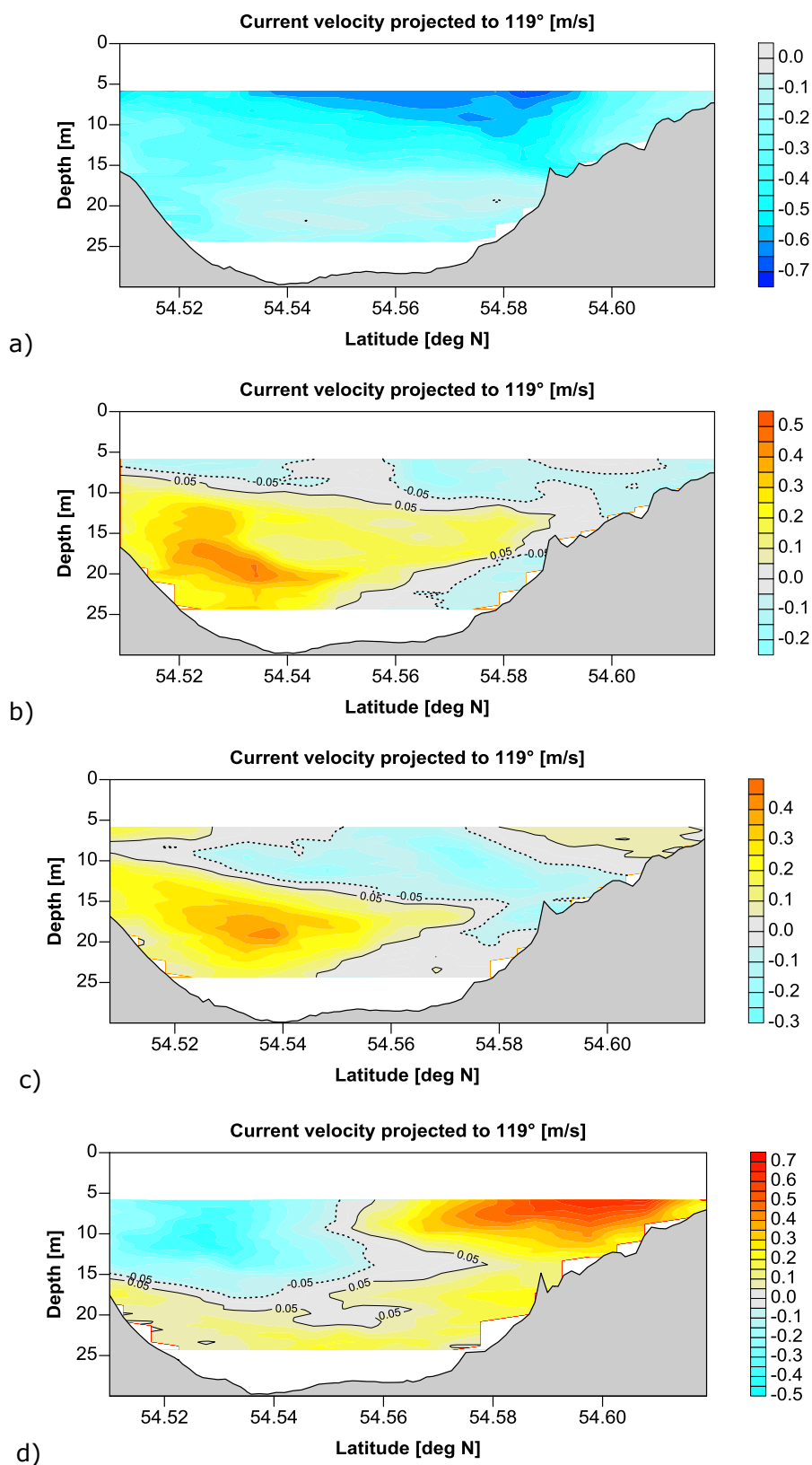


Fig. 1.18 Along-channel current velocity in the link corridor during the survey in August 2009. Positive values indicate flow in the direction of the Central Baltic Sea. The current pattern changed rapidly. The data were collected within a week: a) 24 August 2009; b) 27 August 2009; c) 28 August 2009; and d) 31 August 2009.



The selected patterns above depict uniform flow, two and three layer flow, dipole and quadrupole structures, respectively. The actual flow pattern depends on a complex superposition of the actual wind forcing, remote driven barotropic and baroclinic pressure gradients and on local stratification. Additionally, it will be modified by tides. The isohalines (not shown) indicate geostrophic balance of currents and cross-channel pressure field. The current has a spatial cross channel structure and varies in both the vertical and horizontal direction. The speed ranges from -80 to +80 cm/s.

Upwelling at the northern or southern rim of the Fehmarnbelt is often found. It is induced by along channel winds and the geostrophical adjustment of the flow.

In Fig. 1.19 an example of measured upwelling is shown. It was measured during south-easterly winds. The south-easterly wind caused a cross channel Ekman transport towards north-east in the surface layer of about 10 m thickness. Below the surface layer a compensating flow is found. The saline bottom layer depicts no cross channel current component. The along channel current shows a strong inflow signal at the southern rim of the Fehmarnbelt with a slight increase of current velocity towards the bottom. This current pattern coincides with an upward lifted belt of inflowing saline bottom water.

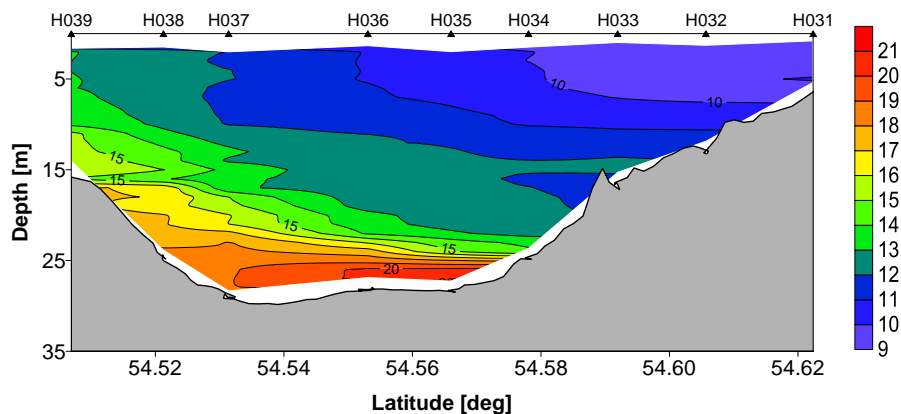


Fig. 1.19 Measured salinity (PSU) distribution in the Fehmarnbelt. Upwelling is observed at the southern coastline.

1.7 Representativeness of Baseline Period

The variation of the monthly mean salinity and temperature at MS01 and MS02 during the baseline period are compared to a selected 6-years means at Fehmarnbelt light-vessel, see Fig. 1.20. This comparison enables one to evaluate whether the baseline period yields representative hydrographic conditions.

It is found that in the Fehmarnbelt:

- Surface salinity is in general lower during the baseline period than in the 6-years average. The winter months shows a difference of up to 4 psu between the baseline and the 6-years average; and
- Bottom salinity at MS01 is lower in the baseline period than in the 6-years average with the biggest difference of 5 psu occurring during summer. At MS02 the bottom salinity only deviates slightly from the 6-years average.

It is noted that the different locations of the main stations and the light-vessel will also influence the comparison and therefore some difference in salinities should be expected. Another factor for increased average salinity in the long-term records is the frequent occurrence of Major Baltic Inflows (MBI), i.e. strong inflows of highly saline North Sea water into the Baltic Sea. The frequency of these inflows has considerably decreased since the 1980s and only three such events have been recorded since 1984 when the light-vessel was retired (Matthäus 2008). In autumn 2009 during the baseline period a medium inflow event was recorded which did however not suffice to raise the average baseline salinity to historical levels.

Water temperatures in the Fehmarnbelt during the baseline period are characterized by extremes. The main stations records show an unusually cold winter 2009-2010 from January to March with negative water temperatures in February near the surface at station MS02. At MS01 the February surface data is missing due to impact of drift ice. Also MS02 was affected by ice close to the sea surface in February.

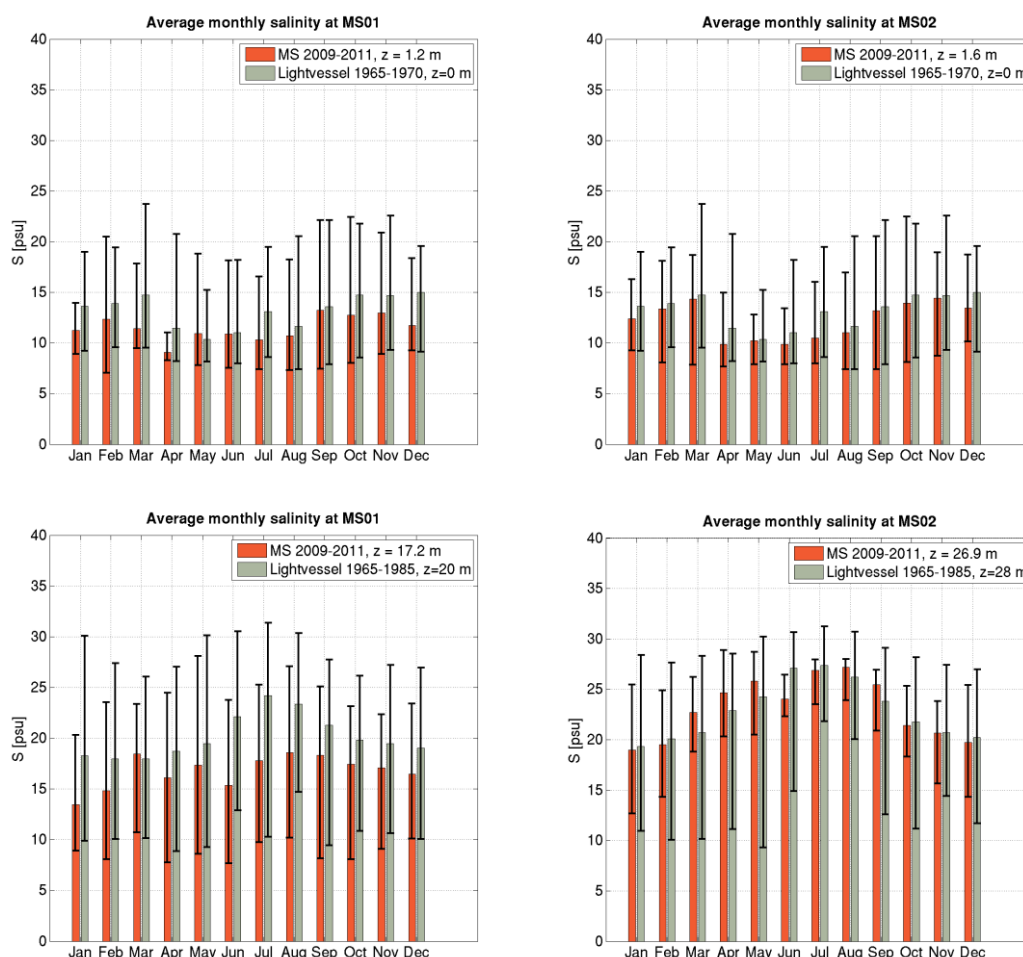


Fig. 1.20 Monthly means of salinity at MS01 (left hand row) and MS02 (right hand row) at surface (upper panels) and bottom (lower panels) layers compared to corresponding 6-years means at surface and long-term at bottom at Fehmarnbelt light-vessel. Black range bars indicate monthly all-time minima and maxima.

While the winter season was colder than average, the rest of the year appears warmer than the 20-year record and both close to the surface and the bottom. While still within the all-time maximum range, bottom temperature in the summer months was up to 5°C higher at MS01 than the 20-years average. Also the bottom



temperature at the southern channel slope, which is normally influenced by cold inflowing North Sea water, was 3°C higher in summer than the 20-years average.

The salinity variation is more important for the density than the temperature. Based on the comparison of salinities it is concluded that the baseline period can be applied to assess the hydrographic impacts of the different considered link solutions.

Meteorological conditions did not differ significantly from average during the baseline period. Only the cold and snowy winters in 2009/10 and 2010/11 were considerably off the average (Fig. 1.21). July 2009 was the warmest month in the baseline exceeding the long-term average by 3°C. Strong winds occurred more often in May, November and December 2010 than in the long-term average (Fig. 1.22). In May, August and November 2009 high precipitation was observed.

1.8 Present Pressures

The present pressures include:

- Major constructions;
- Ship and ferry traffic; and
- Expected climate change.

The bridges across the Danish Straits are hydrographically implemented as zero solutions, designed to not affect the Baltic Sea after their implementation. Hence they should not impact the Fehmarnbelt.

The breakwaters of the Rødbyhavn and Puttgarden harbours extend up to 600 m offshore, which has a blocking effect on the flow. The size of this effect has not been documented.

Existing offshore wind parks at Nysted (Rødsand) together with planned new offshore installations also have an impact on the hydrography. They tend to block the exchange flow through the Belt Sea and create mixing of the stratified water masses unless compensating dredging is carried out as for the fixed links. The mixing efficiency of the turbulence production by a Wind Turbine Generator (WTG) foundation is close to the mixing efficiency of the turbulence production by a bridge pier. But often the offshore wind farms are located in shallower water with homogenous water column.

On the Great Belt – Fehmarnbelt route the ship intensity is increasing and especially the traffic of oil tankers is ever more increasing.

An investigation on the mixing of water masses caused by ferries on the Rødby-Puttgarden route showed that the mixing in the ferries wakes is limited. Hence their environmental impact is only of minor importance. Never the less if the number of ferries and other vessels increases or their size increases then their impact will increase.

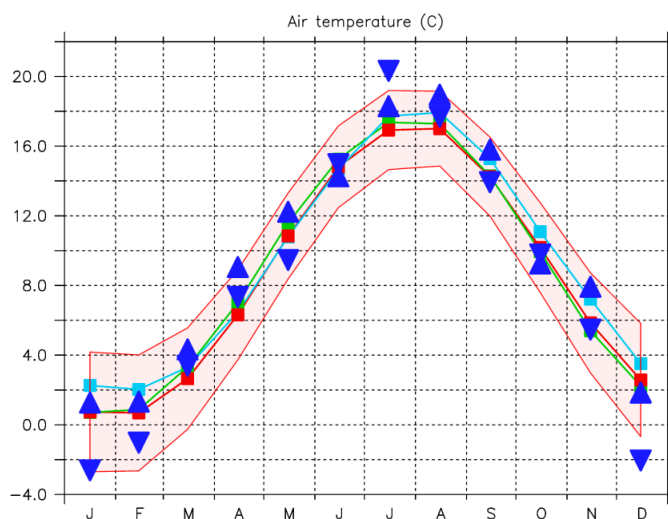


Fig. 1.21 Annual cycle of air temperature (°C). Coloured lines with small symbols indicate climatological monthly means at Warnemünde (green), Westermarkelsdorf (red), and Darss Sill. The shaded region corresponds to ± 1 standard deviation. Triangles denote conditions in baseline years 2009 (upward) and 2010 (downward).

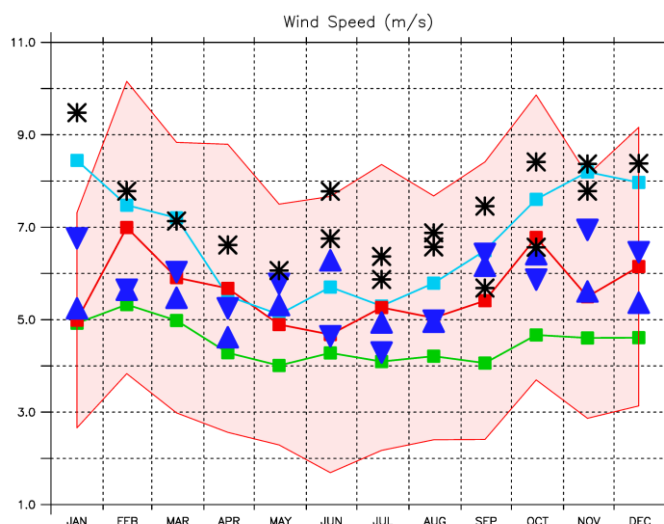


Fig. 1.22 Annual cycle of magnitude of wind speed (m/s). Coloured lines with small symbols indicate climatological monthly means at Warnemünde (green), Westermarkelsdorf (red) and Darss Sill (cyan). Shaded regions correspond to ± 1 standard deviation. Triangles denote conditions in baseline years 2009 (upward) and 2010 (downward) and star the monthly means at Nysted from June 2004 to November 2005.

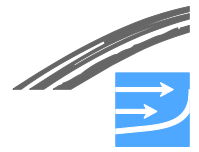
It is anticipated that climate change will raise water levels and increase extreme storm wind speeds in the future. For example +1 m and + 3 m/s by year 2100 (Fehmarnbelt Fixed Link 2009). Both effects will lead to higher water levels in the Belt Sea:

- If the water levels in the world oceans are raised by 1 m then it will cause the water levels in the Belt Sea to be permanently raised by 1 m; and
- If extreme storm wind speeds are increased, then storm surge levels will go up. If storm wind speed for example is increased from 27 m/s to 30 m/s, then the storm surge set-up is increased by roughly 23%.



The higher water level will reduce the resistance of the Belt Sea and hence increase the salinity.

The mesoscale local dynamics of the Fehmarnbelt are mainly driven by local wind forcing and remote pressure gradients. These forcing factors are highly sensitive to interannual and climate changes. It is not obvious how a change in mesoscale dynamics will impact the ecosystem as a whole.



2 INTRODUCTION

2.1 Scope of Work

The Fehmarnbelt Baseline Report shall present a state-of-the-art compilation of hydrographical knowledge about the Fehmarnbelt and nearby areas.

Focus shall be on the baseline monitoring during the years 2009 to 2011. This monitoring includes a number of fixed stations and monthly ship surveys.

But the analyses shall also consider:

- Previously published scientific and engineering studies;
- Data from German and Danish national monitoring campaigns; and
- Numerical simulations of the present conditions carried out as part of the on-going investigations.

The key hydrographic parameters to analyse are flow and stratification, i.e. current, waves, salinity and temperature.

The hydrographic conditions during the baseline shall be compared to long-term hydrographic conditions, for example established from light-vessel observations. This shall be done to ensure that the baseline conditions are representative and satisfactory to apply in the environmental studies.

2.2 Description

The collected data are plotted as time-series and cross-sectional distributions.

Furthermore simple statistical values as mean, standard deviation and minimum and maximum are determined.

Finally the data are interpreted and conceptual descriptions provided.

At the end an evaluation of if the baseline period is representative or not is given.



3 DATA BASIS

The baseline conditions in the Fehmarnbelt area are established on the basis of measurements from:

- National weather stations (wind and more);
- German and Danish light-vessels;
- Belt Project;
- HELCOM COMBINE Program;
- Monitoring during Fehmarn Belt Feasibility Study; and
- Monitoring and modelling as part of Fehmarnbelt Fixed Link Hydrographic Services (present work).

Details on the measurements are presented in the following. References are also provided where more details on the data can be found.

3.1 Baseline Monitoring and Modelling 2009-2011

In 2009 an intensive monitoring of hydrographical and chemical parameters in Fehmarnbelt and nearby area was initiated. This measurement campaign includes two permanent moorings in Fehmarnbelt and one mooring in the Mecklenburg Bight. Another integral part of the monitoring is monthly ship surveys that measure along predefined survey lines in the Fehmarnbelt and nearby areas.

3.1.1 Monitoring stations

Three permanent main stations, named MS01, MS02 and MS03, are placed in Fehmarnbelt and nearby area, see Table 3.1 and Fig. 3.1. The main station measurements comprised in this baseline include two annual cycles from March 2009 to February 2011 with data coverage mainly above 90%.

Table 3.1 Positions of the Main Stations

Station	Latitude	Longitude	Period
MS01	54.586°	11.356°	2009-03-31 to 2011-02-28
MS02	54.534°	11.288°	2009-07-14 to 2011-02-28
MS03	54.275°	11.733°	2009-03-31 to 2011-02-28

Fig. 3.2 shows the instrumentation of one of the main stations. Every main station is equipped with three WQMs (Water Quality Monitor), with some Microcat salinity/temperature sensors and one ADCP on the bottom. The WQMs and Microcats are mounted with a spacing of 2 m.

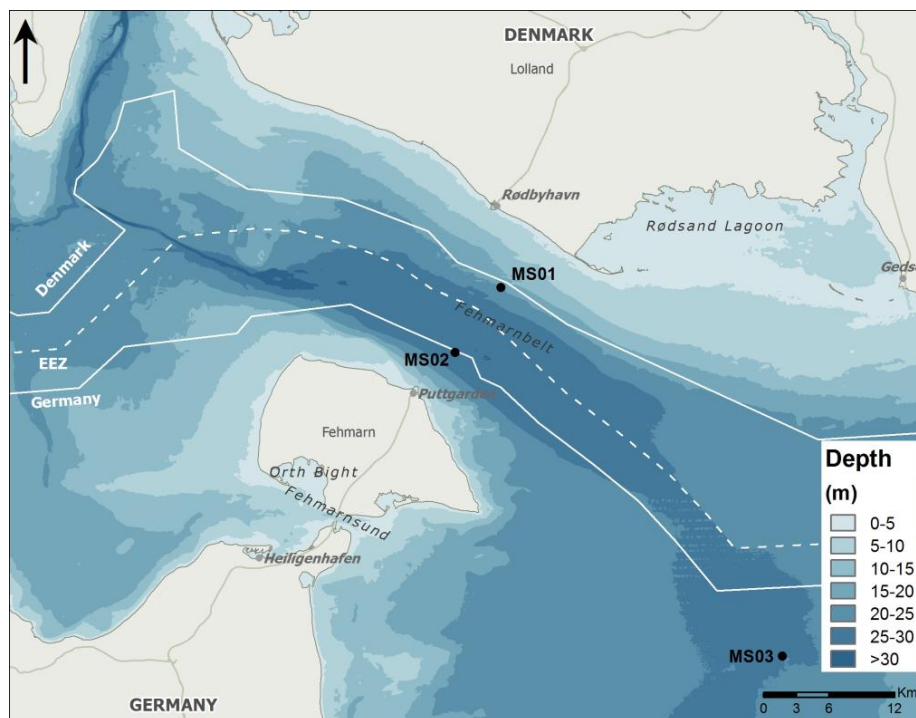


Fig. 3.1 Map with the monitoring stations MS01, MS02 and MS03.

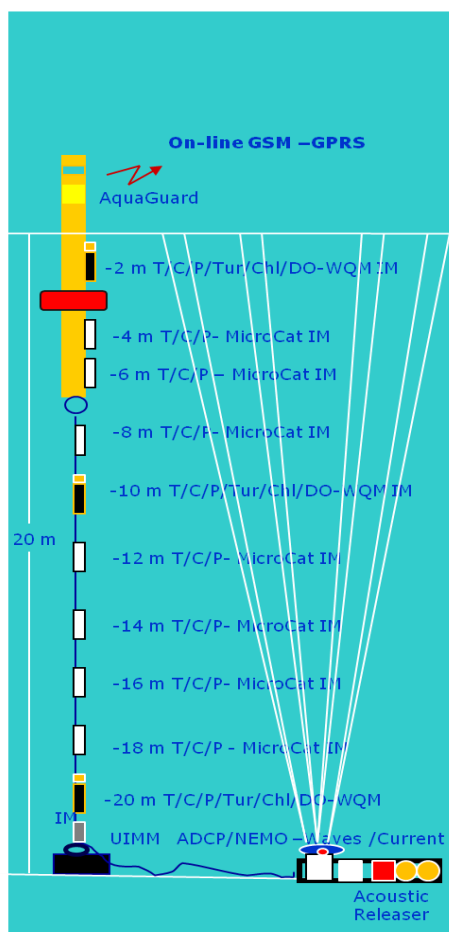
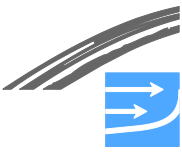


Fig. 3.2 Instrumentation of one of the three main stations. The instrumentation at the three main stations are very similar, but depends on the actual water depth



From these stations time-series are measured of:

- Current
- Waves;
- Salinity;
- Temperature;
- Turbidity;
- Fluorescence of chl-a; and
- Oxygen.

A list of monitoring equipment is shown in Table 3.2.

3.1.2 Monitoring surveys

Monitoring surveys are carried out on a monthly basis in the period March 2009 to December 2010 with profiling at preselected stations and ADCP current measurements in transects. The vessel applied is either RV JHC Miljø or RV Prof. A. Penck (see Table 3.2). A map with survey lines can be found in Fig. 3.3.

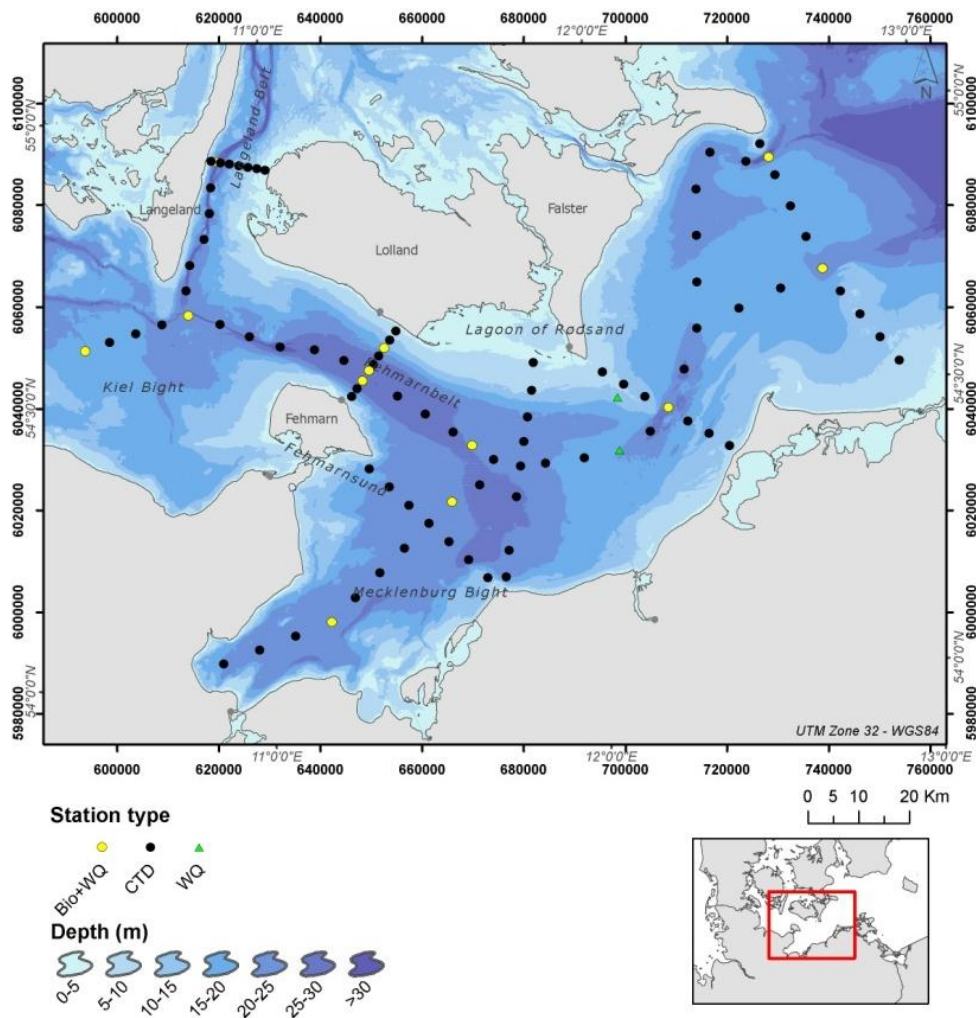


Fig. 3.3 Map with survey lines applied in monthly surveys. The hydrochemical/water quality stations are marked with green and yellow symbols.



The survey lines focus on the link transect across Fehmarnbelt but also resolve the hydrographic conditions in the adjacent bights and upstream and downstream cross-sections from Langelands Belt to Darss Sill.

Table 3.2 List of instruments used in the FEHY baseline monitoring

Instrument	Quantity (range) [uncertainty]
SD-CTD	Temperature Salinity Oxygen Pressure
Vessel mounted ADCP	Velocity [0.04 m/s]
Water Sampler	Volume: 5l
Towed ADCP	Velocity [0.04 m/s]
Towed thermistor chain	Temperature [0.01 K] Pressure [0.2 dbar]
Microstructure Profiler (MSP)	Temperature [0.005 K] Salinity [0.01 mS/cm] Dissipation [0.2 order of Magnitude] Turbidity Pressure [0.2 dbar]
Seabird-CTD	Temperature [0.005 K] Salinity [0.005 mS/cm] Oxygen [0.2 ml/l] Fluorescence Turbidity Pressure [0.2 dbar]
Towed undulating CTD (Scanfish-CTD)	Temperature [0.005 K] Salinity [0.005 mS/cm] Oxygen [0.2 ml/l] Fluorescence Turbidity Pressure [0.2 dbar]
Vessel mounted weather station	Wind speed and direction
Moored ADCP	Velocity [0.005 m/s] Pressure [0.2 dbar]
SBE MicroCats	Temperature [0.008 K] Salinity [0.01 mS/cm] Pressure
ADCP & NEMO	Velocity Temperature Wave height Wave period Pressure
SBE 37-IM ShallowCAT	Temperature (-5 - 35 °C) [0.002 °C] Conductivity (0 - 7 S/m) [0.0008 S/m] Pressure (0 - 250 m/dbar) [0.1%]
Water Quality Monitors (WQM)	Temperature (-5 - 35 °C) [0.002 °C] Conductivity (0 - 9 S/m) [0.003 S/m] Oxygen (0 - 100 %) [2%] Fluorescence (0 - 50 µg/l) [0.2%] Turbidity (0.01 - 25 NTU) [0.01 NTU] Pressure (0 - 200 m/dbar) [0.1%]



In addition to the monthly cruises one special cruise was undertaken in June 2009 to obtain high resolution hydrographic data of short term variability (e.g. tides) of flow and mass field. By applying the latest available advanced technologies the cruises have provided substantially more detailed and comprehensive data-sets than previous investigations.

3.1.3 Model simulations

Numerical model simulations are used as a supplement to resolve and describe spatial patterns and large-scale phenomena in the transition area with focus on physical phenomena taking place in the Fehmarnbelt area.

Most of the simulation results are extracted from a model applied to simulate the hydrographic conditions in the Fehmarnbelt area during the period from 1 January 2009 to 30 September 2009.

The model setup, calibration and validation are described in the impact assessment reporting (FEHY 2013c) for all of the hydrographic modelling tools applied, including MIKE, MOM or GETM.

The applied wave model tool is described in this report (Appendix B).

3.2 Other Data Sources

3.2.1 Weather stations

The present baseline focuses on the hydrographic conditions in the Fehmarnbelt area. For that reason the meteorological measurements by themselves are treated in a separate chapter. The meteorological information is also applied in the analysis of the hydrographic features in the Fehmarnbelt area.

Meteorological information such as for example time-series of wind and air temperature has been taken from five stations, see Fig. 3.4 and Table 3.3:

- Westermarkelsdorf on island Fehmarn;
- MARNET station at Darss Sill;
- MARNET station in the Arkona Basin; and
- Nysted.

The data from Westermarkelsdorf are provided by the German Weather Service (DWD).

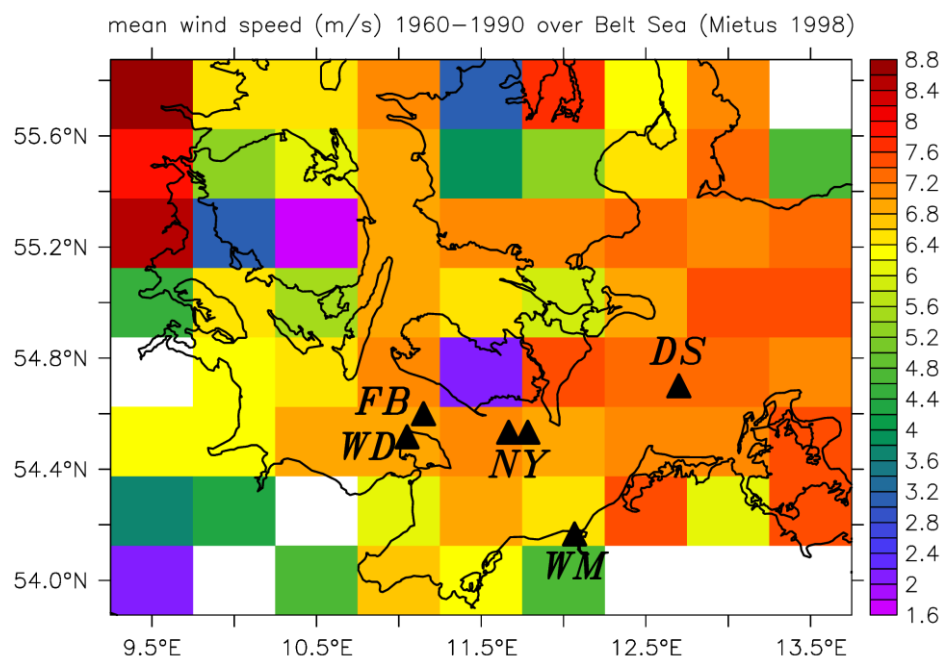


Fig. 3.4 Location of meteorological stations used for analysis: Fehmarnbelt buoy (FB), Westermarckelsdorf (WD), Nysted (NY), Warnemünde (WM), and Darss Sill (DS). The background shows mean wind speed derived from ship observations in 1961-1990 compiled by (Mietus 1998).

Table 3.3 List of meteorological stations for which data of air pressure (P), air temperature (T), wind (W), cloudiness (C), relative humidity (R) and precipitation (N) were available. Frequency denotes basic time resolution.

Station	Longitude	Latitude	Period	Frequency	Data coverage
Fehmarnbelt buoy (BSH)	11°09'E	54°36'N	1985-2007	hourly	10-22% (P,T,W)
Westermarckelsdorf Fehmarn (DWD)	11°03'E	54°31'N	1947-2010	daily	67% (P) 86% (T,W,C,R,N)
Nysted (Danmark)	11°40'E 11°47'E	54°32'N	06/2004- 11/2005	hourly	100% (P,W) wind speed only
Warnemünde (DWD)	12°04'E	54°01'N	1947-2010	daily	56% (W) 94-100% (T,W,C,R,N)
Darss Sill (IOW)	12°42'E	54°42'N	2000-2010	hourly	87-91% (T,W,R)

These stations were selected for the following reasons:

- Station located at open sea or near the coast at sea level,
- Focus on the Fehmarnbelt region, and
- Availability of multi-year time-series.

The first criterion is relevant since meteorological measurements at land are biased by so-called orographic effects, i. e. the influence of changing land height and varying surface roughness. This bias plays a role in Belt Sea, and especially in the Fehmarnbelt region, because of the nearby coasts, but it is assumed to be small at



Darss Sill, see Fig. 3.4. The spatial scale of land influence is set by the nearest distance to the coasts, which is around 10 km in Fehmarnbelt and 20 km at Darss Sill.

The open sea station Darss Sill belongs to the German monitoring network MARNET operated by IOW on behalf of Federal Maritime and Hydrographic Agency (BSH). These are two open sea records with a data coverage around 90% running from February 2000 and October 2002 until now. The data time resolution is one hour derived from averaged samples taken every 10 minutes. Measurements from the buoy in Fehmarnbelt, provided by BSH, are not used because only 10-22% of the period is covered by data. Air pressure and wind speed could be compared for the Fehmarnbelt region by means of the measurements taken at two adjacent mast stations located at a wind park at Rødsand near Nysted, south off Lolland. However, these data cover the rather short period June 2004 to November 2005 where only air pressure and wind speed (no direction) is provided. The daily time-series provided by Deutscher Wetterdienst (DWD) are long-term records at coastal stations covering the period from 1947 until now. Darss Sill was included in order to take into account one more open sea station. These data cover roughly a decade of time which also allow for the consideration of long-term averages like climatological monthly and seasonal means and the discussion of inter-annual variations.

Mietus (1998) compiled a meteorological data set for the Baltic Sea within the climate period 1961-1990 from voluntary ship observations. This data set is provided by web site (ICOADS 2010). Because spatial and temporal resolution by ships of opportunity is arbitrary, these data can be used to calculate long-term averages on Baltic scale (100 km). For a grid resolution of (0.5x0.25) degrees, corresponding to a spacing of approximately 30 km, the time averaged ship data appear somewhat noisy. However, they well reflect, in accordance with station measurements (see below), the tendency to higher mean wind speed over open sea basins as is shown in Fig. 3.4. Hence, (Mietus 1998) data are considered as background information about mean meteorological conditions and variability within the reference period 1961-1990.

A comparison of the hourly station data at Nysted and Darss Sill revealed that only state-of-the-art weather forecast models, which apply a high ground resolution around 10 km, are able to reproduce the local wind speed and wind direction in the Belt Sea.

3.2.2 Water level stations

Changes in water levels may cause both local and regional currents. Therefore water level records from three gauge stations in the Fehmarnbelt area have been evaluated in this report. The resolved period is from year 2004 to 2010. For locations of the gauges see Fig. 3.5 and Table 3.4.

Table 3.4 Positions of the gauge stations

Station	Latitude	Longitude	Period
Kiel-Holtenau	54.367°	10.150°	2004-2010
Warnemünde	54.018°	12.083°	2004-2010
Gedser	54.900°	11.933°	2004-2010

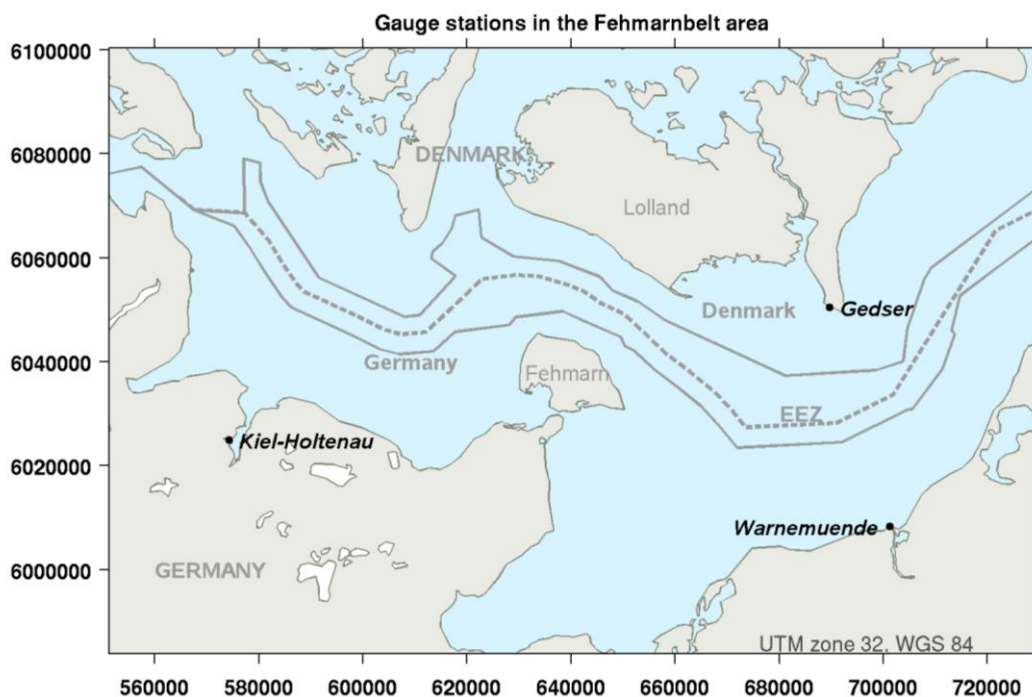


Fig. 3.5 Water level gauges in the Fehmarnbelt area that have been evaluated in this report.

3.2.3 River inflow

River inflow to the Belt Sea and Sound during the years 1999 to 2009 has been collected and analyzed. The rivers considered are shown in Fig. 3.6. The data are calculated by the Swedish runoff model HBV (Bergström 1976; Graham 2000).

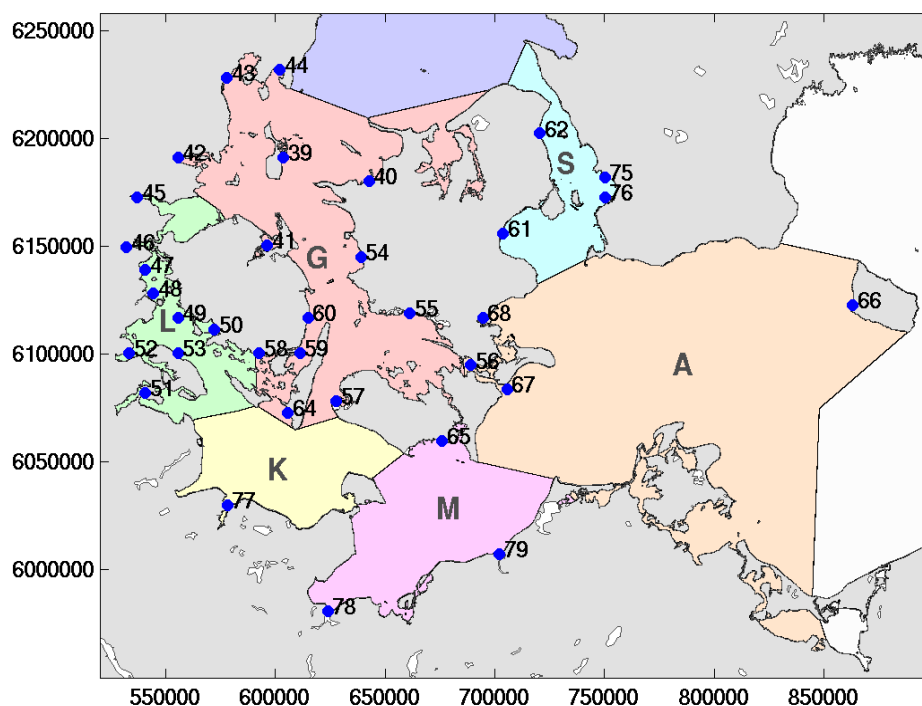


Fig. 3.6 Rivers considered are indicated by blue dots and the river identification number. Coloured polygons show sub-basins of Belt Sea according to HELCOM (polygons taken from Feistel et al. 2008a). Acronyms denote: southern Kattegat (K), Little Belt (L), Great Belt (G), Sound (S), Kiel Bight (K), Mecklenburg Bight (M), Arkona Basin (A).



There are no detailed Belt Sea data available for comparison with the FEHY river data set. The annual river runoff reported by HELCOM does not provide estimates for Belt Sea discharge, see (HELCOM 2009).

3.2.4 Sea Ice

Sea ice conditions in the Danish Waters are published every year. Earlier in annuals as for example the one shown below:

- The State of the Ice and the Navigational Conditions in the Danish Waters during the Winter from 1941-42, published by Statens Isbrydnings- og Ismeldingstjeneste, Copenhagen, A/S J. H. Schultz Bogtrykkeri, 1942.

And later in annuals as for example this one:

- Ice and Navigational Conditions in Danish Waters during the Winter from 2008-2009. Søværnets Operative Kommando, Istjenesten.

The annual reports present information on both frost indexes, ice thickness a.m. Both data and figures are extracted from the annuals and applied (a detailed analysis for data collected at Anholt was recently carried out, see (DONG 2010).

Local sea ice conditions in the Fehmarnbelt area are provided from four German stations by Bundesamt für Seeschifffahrt und Hydrographie: Ice Data Bank; see Fig. 3.7. The data covers the 40 winters from 1960/61 – 1999/2000.

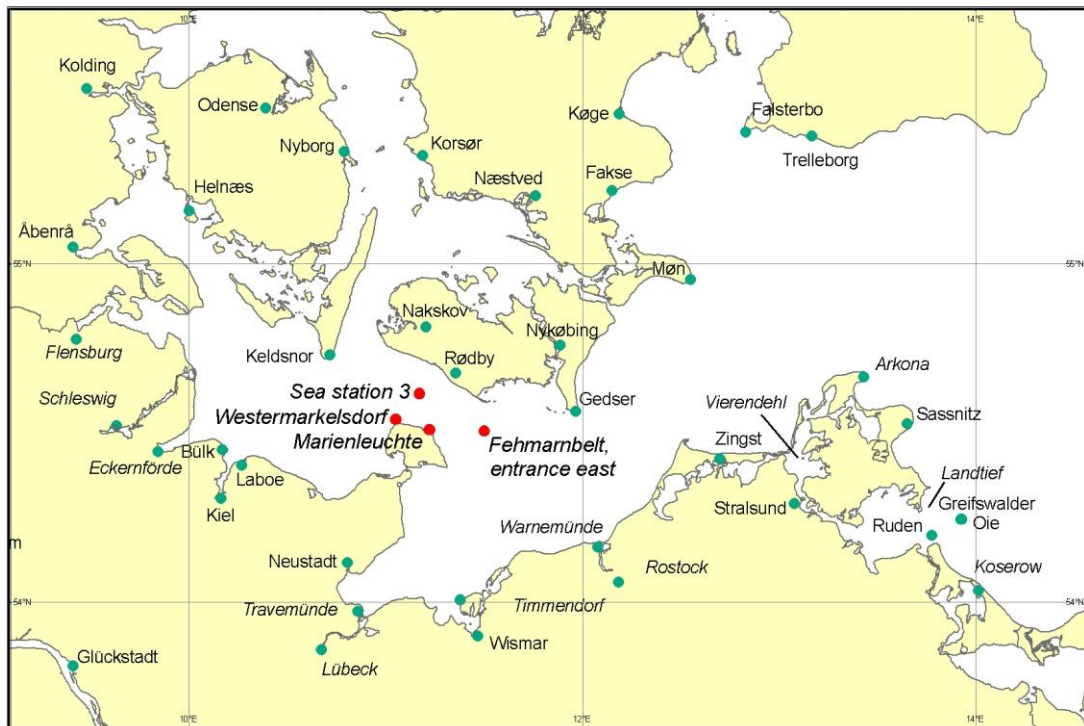


Fig. 3.7 Map of area with the four monitoring stations (red points). Data are provided by Bundesamt für Seeschifffahrt und Hydrographie: Ice Data Bank.

3.2.5 German and Danish light-vessels

The Fehmarn Belt light-vessel was from 1965 to 1984 operated by German shipping authorities, see Fig. 3.8. Only one major temporal gap in the operation is found in 1971. Daily hydrographical observations were collected from the vessel: Water salinity and temperature in 0, 5, 10, 15, 20, 25 and 28 m depth. In 1985 the manned

light-vessel was replaced by an automated buoy that continues the hydrographical and meteorological monitoring. The quality of the buoy data is low and there are long periods without data. The buoy data-set is for that reason disregarded in the further data analysis.

Information and statistical analysis of the light-vessel data can be found in (Lange et al. 1991) and (Middelstaedt et al. 2008).

Information on Danish light-vessels in the transition area can be found in (Sparre (1982, 1984a and 1984b).

3.2.6 Belt Project

The Belt Project was carried out from 1974 to 1977. Belt Project stations in the Fehmarnbelt are also shown in Fig. 3.8. Information and detailed analysis of the Belt Project data can be found in (Kruse et al. 1980; Jacobsen 1980; Ærtebjerg Nielsen et al. 1981) and (Fehmarn Belt Feasibility Study 1996 and 1997).

3.2.7 HELCOM COMBINE Programme

HELCOM monitoring stations provide infrequent temperature, salinity, oxygen and nutrient records in the years from 1960 to 2010. The measurements are collected from vessels. Measurements from a number of these stations have been obtained from ICES (ICES 2010). These stations are also shown in Fig. 3.8.

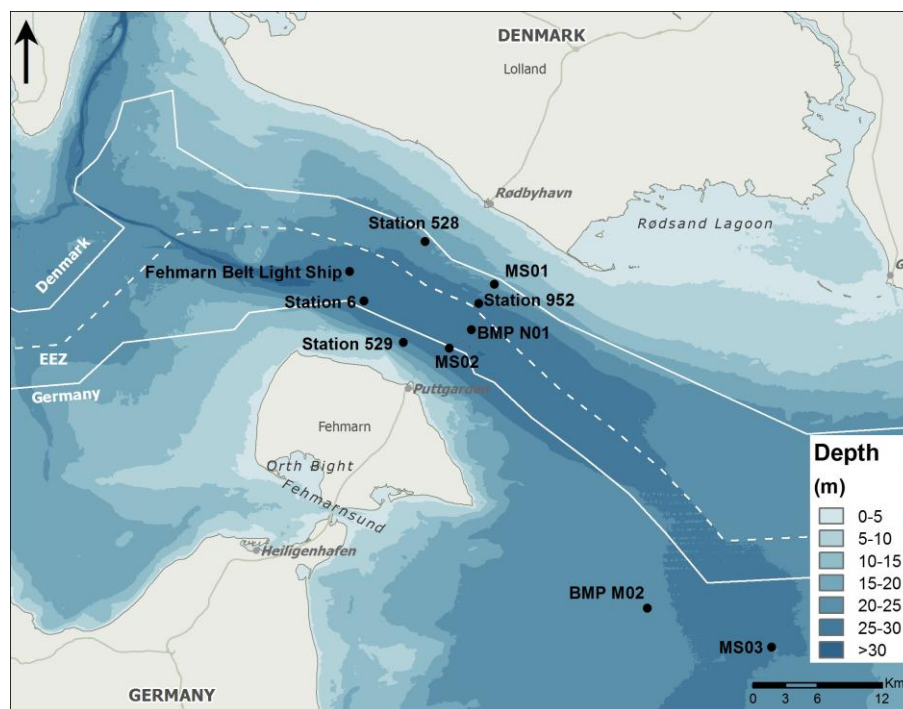


Fig. 3.8 Map with stations in the Fehmarnbelt: Fehmarn Belt light-vessel, Belt Project stations (station 6, 528, 529 and 952) and HELCOM COMBINE monitoring stations (BMP N01 and M02).

3.2.8 Fehmarn Belt Feasibility Study

The Fehmarn Belt Feasibility Study monitoring took place from 15 October 1996 to 15 October 1997 and included two intensive hydrographic surveys. The fixed stations and survey lines in the monitoring are shown in Fig. 3.9. Details on and analyses based on these measurements can be found in Fehmarn Belt Feasibility Study (1998).

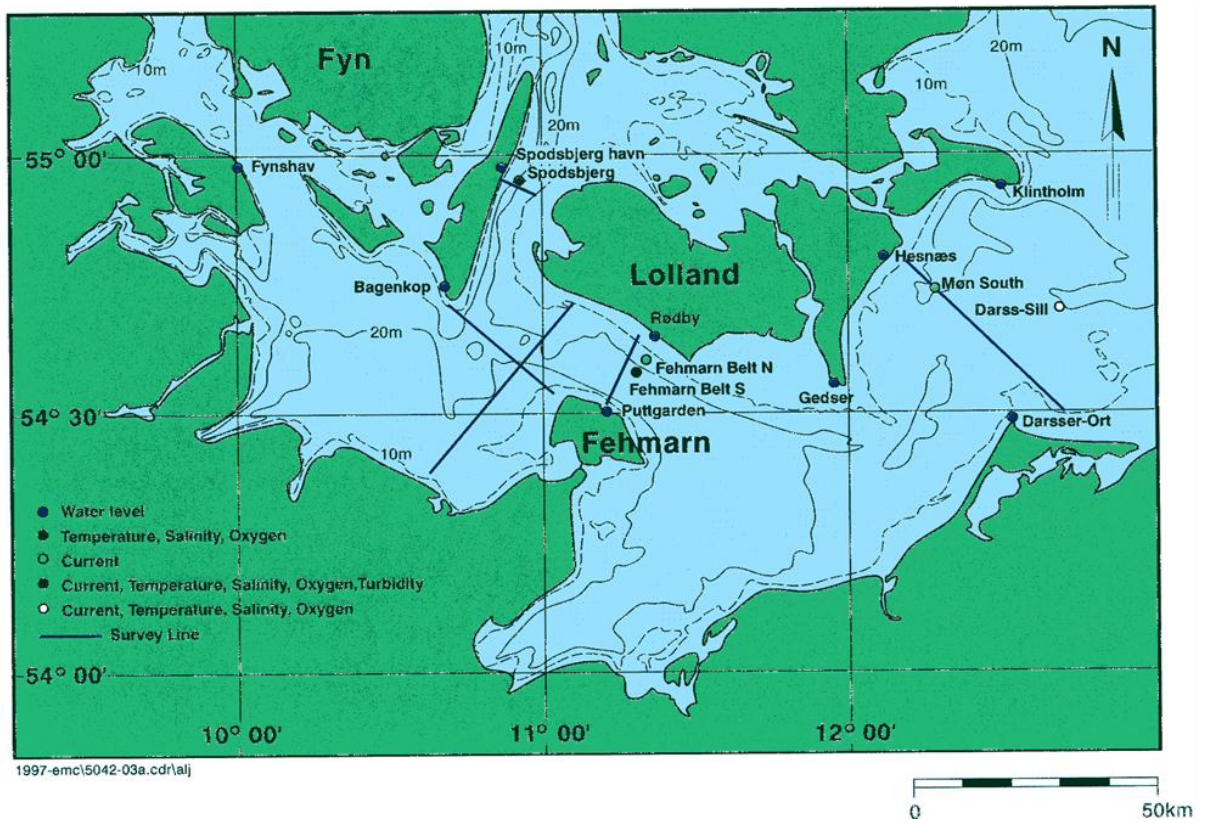


Fig. 3.9 Map with Fehmarn Belt Feasibility Study monitoring stations.

4 SETTING AND DRIVING FORCES

In the following the frame for the later descriptions of hydrography in the Fehmarn-belt area are presented.

4.1 Bathymetry

The total surface area of the Baltic Sea is 411,700 km² and the volume 21,100 km³. The bathymetry of the Baltic Sea is characterised by contractions and sills that influences the currents and mixing between the water masses, see Fig. 4.1.

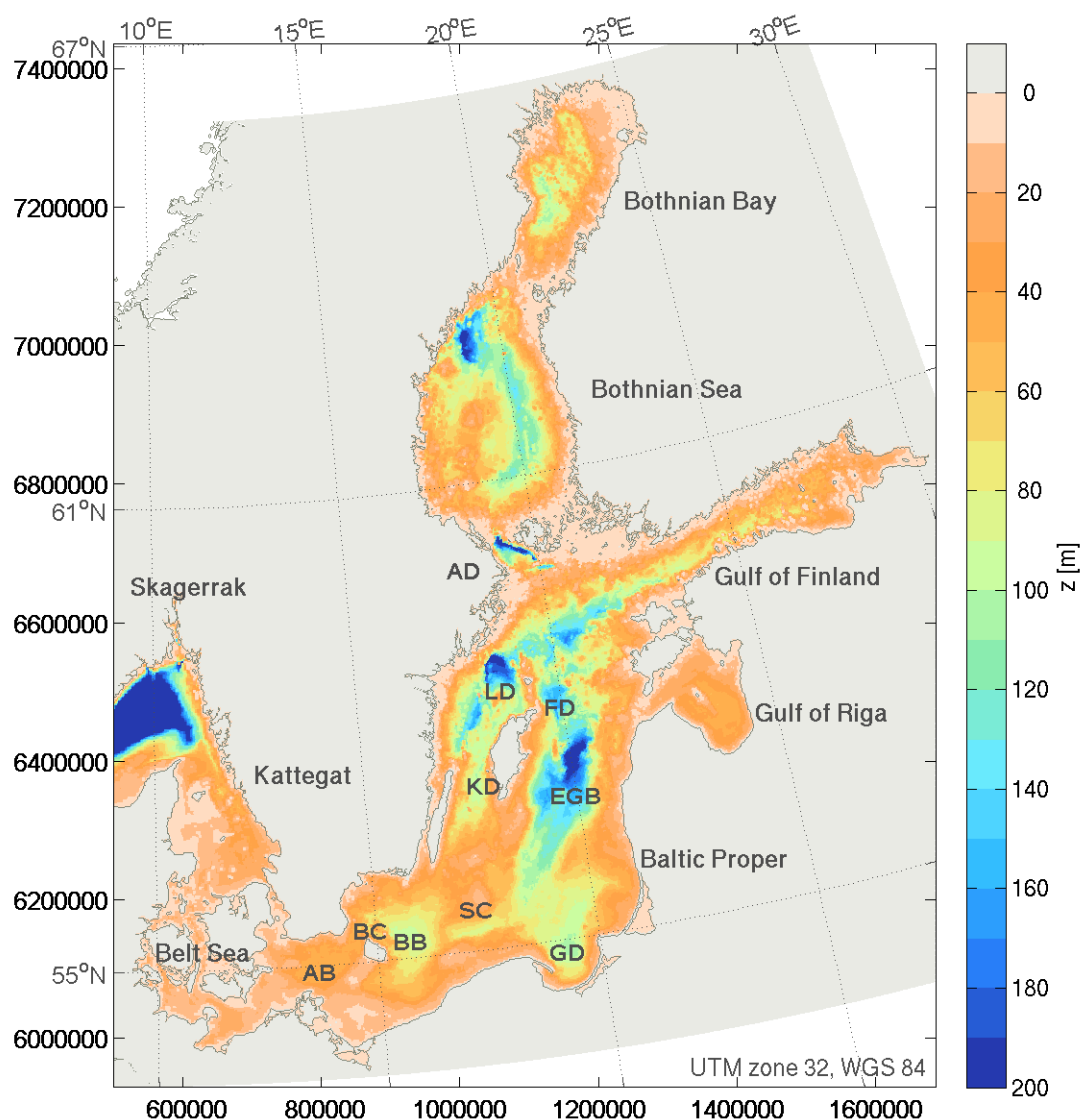
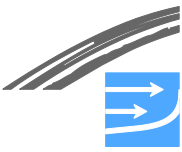


Fig. 4.1 Bathymetry and geographical structures of the Baltic Sea. Water depths refer to (Seifert et al. 2001). Water depth is cut off at 200m. Acronyms indicate some basins and connecting channels: Arkona Basin (AB), Bornholm Channel (BC), Bornholm Basin (BB), Stolpe Channel (SC, also called Slupsk Furrow), Gdansk Depression (GD), Eastern Gotland Basin (EGB), Landsort Deep (LD), Fårö Deep (FD), Karlsö Deep (KD) and Aland Deep (AD).

The first bathymetrical feature to note is the Baltic transition area, which is the relatively shallow, contracted connection between the North Sea and the Central Baltic Sea. It contains the sea areas Kattegat, northern part of Sound, Great Belt, Little



Belt and Fehmarnbelt. The border between the Baltic transition area and the Central Baltic Sea are the Darss and Drogden sills. The maximum depth at the two sills is only about 18 m and 7 m, respectively. The transition area limits the inflow of highly saline water from the North Sea into the Central Baltic Sea and in this manner it has a significant impact on the hydrographical conditions inside the Central Baltic Sea. If and when highly saline water masses originating from the North Sea pass the two sills, they are trapped inside the Central Baltic Sea by the sills and propagate further into the Central Baltic along the bottom. The highly saline water masses can only leave the Central Baltic Sea again by being entrained into the upper less saline water mass at the surface and together with it they flow out of the Baltic Sea again.

The second bathymetrical feature to notice is the three basins in the southwestern Central Baltic Sea, named the Arkona, Bornholm and Gotland Basins. The deepest connection between the Arkona and Bornholm Basin is the Bornholm Channel located north of Bornholm, and the deepest connection between the Bornholm and Gotland Basins is the Stolpe Channel (or Slupsk Furrow). When highly saline water flows across the sills into the Central Baltic Sea it propagates along the deepest connections, i.e. from the Arkona Basin through the Bornholm Channel into the Bornholm Basin and there from though the Stolpe Channel into the Gotland Basin.

Fehmarnbelt is part of the transition area between the North Sea and Central Baltic Sea, see Fig. 4.2.

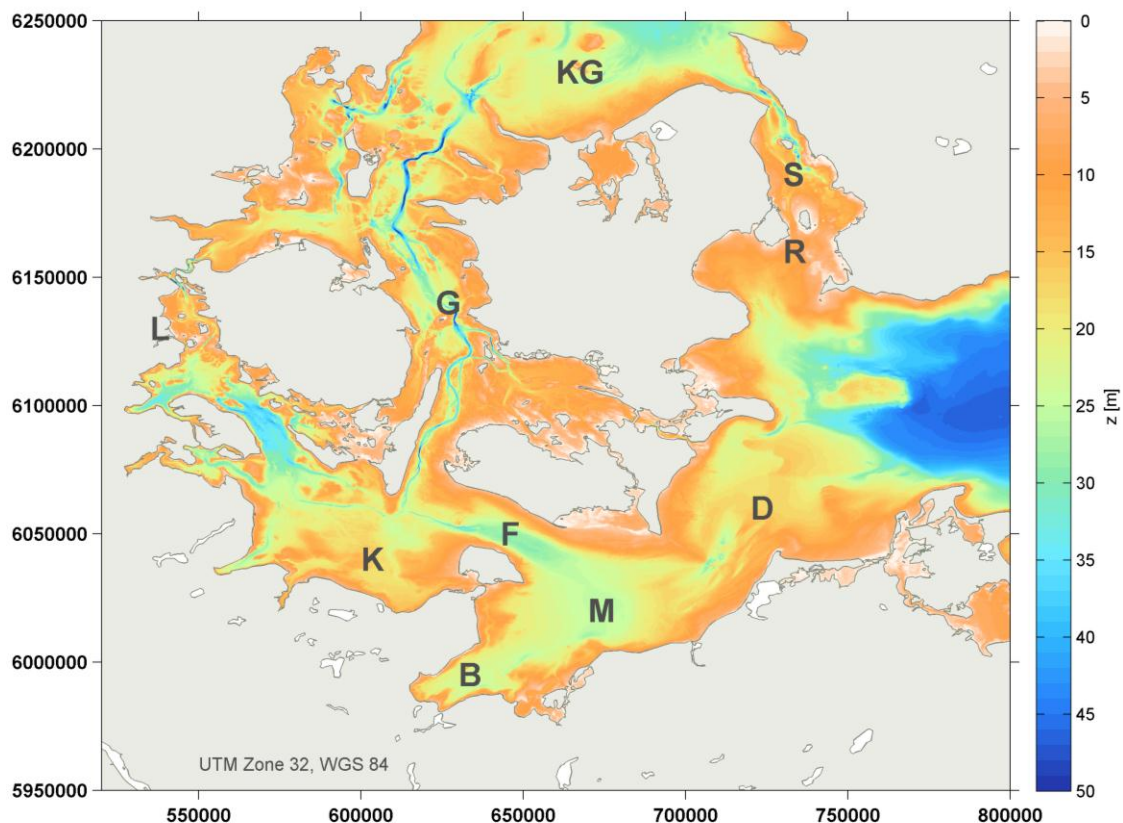


Fig. 4.2 Bathymetry and geographical structures in the Belt Sea. Acronyms indicate some basins, connecting channels, and sills: southern Kattegat (KG), Little Belt (L), Great Belt (G), Sound (S), Fehmarnbelt (F), Kiel Bight (K), Mecklenburg Bight (M), Lübeck Bight (B), Darss Sill (D), and Drogden Sill (R).

Fehmarnbelt is bordered by the Danish island Lolland to the northeast and the German island Fehmarn to the southwest, see Fig. 4.2. The adjacent marine areas



are Mecklenburg Bight and Kiel Bight, both with depths similar to the depth of Fehmarnbelt.

Fehmarnbelt has a maximum depth of about 30 m and a width varying between 18 km and 25 km. The narrowest section lies between Rødbyhavn and Puttgarden, the proposed site of the link. On the German side the depth increases quite fast to more than 20 m, while the seabed slopes more gently on the Danish side.

North of Kiel Bight is Langelands Belt that is turned 90° compared to Fehmarnbelt. East of Mecklenburg Bight is the Darss Sill with a maximum depth of 18 m bordering the Central Baltic Sea.

4.2 Oceanographic conditions in the North Sea

The average salinity in the North Sea is 35 psu and close to the salinity in the oceans, because of the North Sea's wide opening towards the Atlantic Ocean. Therefore water masses in the North Sea are denser than water masses in the Baltic Sea being brackish. In the northern Kattegat or southeastern Skagerrak the North Sea water masses subside (at the Northern Kattegat front, see e.g. Jakobsen 1997) and flow under the lighter water masses in the Baltic transition area, towards the bathymetrical restriction at the two sills at Drogden and Darss. In connection with wind-driven exchange flow between the North Sea and the Central Baltic Sea, the dense water mass is then lifted across the two sills and continues into the Central Baltic Sea. In recent years, inflow events have also been observed under calm forcing conditions during summer. These relatively warm, saline plumes could be tracked into the Central Baltic Sea (Feistel et al. 2003c).

Tidal waves propagate from the Atlantic Ocean into the North Sea and continue along an anti-clockwise path through the North Sea. They separate at the Skagerrak and only partly propagate into the Baltic Sea. On their way, the tidal amplitudes decrease dramatically and they are only of limited importance for the flow and stratification in the Central Baltic Sea. But they do contribute to the instantaneous flow through the transition area and the vertical mixing of the water masses.

4.3 Hydrology of the adjacent watershed

Fig. 4.3 shows the main rivers of the Baltic Sea. The mean runoff is 14,136 m³/s (standard deviation of annual values \pm 1,545 m³/s) according to HELCOM (2009). The difference of direct precipitation and evaporation P - E to and from the surface of the Baltic Sea is estimated to range from around 700 m³/s (Lindau 2002) to 1,300 m³/s (HELCOM 1986), which corresponds to roughly 5%-10% of the river runoff.

The runoff specifications for the ten largest rivers are summarized in Table 4.1.

The fresh water surplus to the Baltic Sea creates a low saline water mass close to the sea surface that flows towards the North Sea, wherefore the water masses in the Baltic Sea are stratified.

If there was no river inflow to the Baltic Sea the water masses in the Baltic would be oceanic, see also (Bo Pedersen and Møller 1981) and its ecosystem would be completely different. Hence the river inflow is of crucial importance for the conditions in the Baltic Sea.

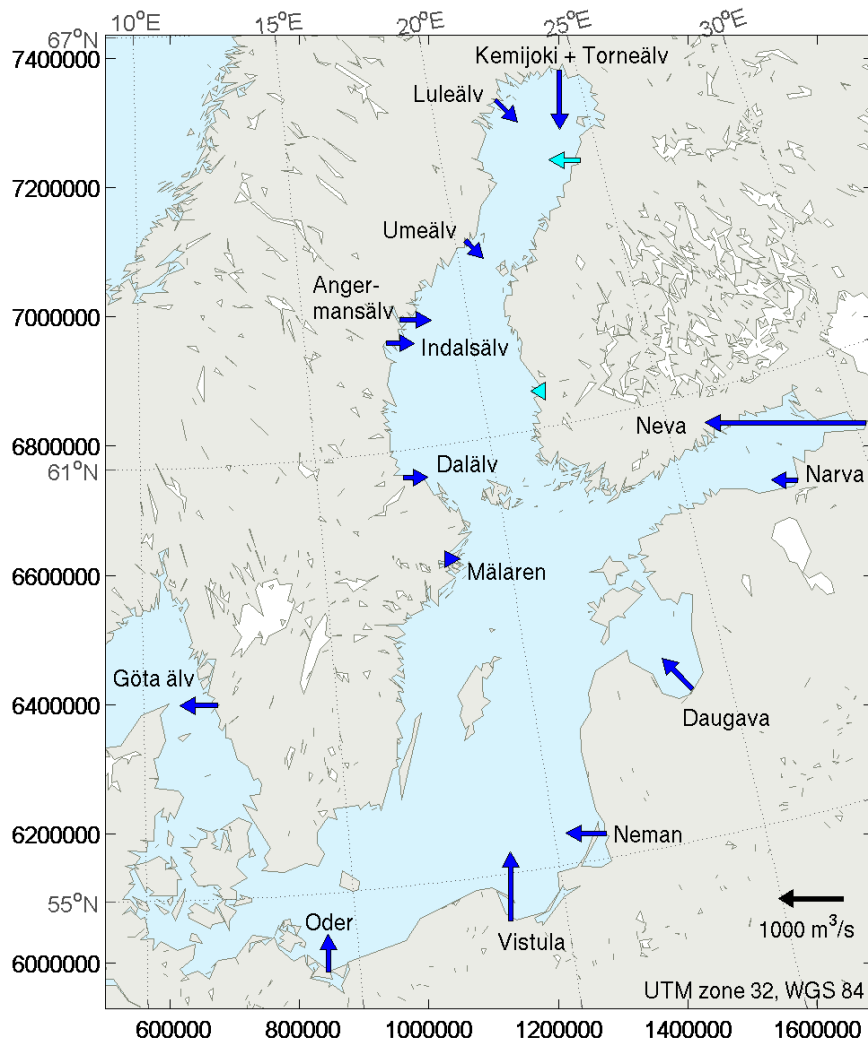


Fig. 4.3 Major rivers contributing to the Baltic Sea water budget. Dark blue arrows indicate specific river runoff, light blue arrows show accumulated diffuse sources. The Göta Älv is shown for although it empties into the Kattegat. Torneälv and Kemijoki have been summed up as their mouths are located only 15 km apart. Values from (Mikulski 1970) and (Bergström & Carlsson 1994).

Table 4.1 The ten largest rivers of the Baltic Sea system, including the Belt Sea, Sound and Kattegat, their approximate drainage area and mean annual runoff 1950-1999 (Bergström & Carlsson 1994)

River	Drainage area (km²)	Mean annual runoff (m³/s)
Neva	281,000	2,460
Vistula	194,400	1,065
Daugava	87,900	659
Neman	98,200	632
Göta Älv	50,100	574
Oder	188,900	573
Kemijoki	51,400	562
Ångermanälven	31,900	489
Luleälven	25,200	486
Indalsälven	26,700	443



4.4 Meteorological conditions

High and low air pressures fields pass Scandinavia on a weekly time-scale and raise or depress the water levels in the North Sea and Baltic Sea, respectively. The water level difference it causes between the North Sea and the Central Baltic Sea drives an exchange flow between the two seas that either transports low saline waters from the Central Baltic Sea out to the North Sea or higher saline water masses from the North Sea into the Central Baltic Sea. Hence the wind driven exchange flow enhances the estuarine circulation. Actually the wind driven exchange in the Danish Straits is an order of magnitude bigger than the net outflow generated by the freshwater runoff and therefore it is difficult to identify and quantify the density driven circulation in flow measurements collected in the straits. Furthermore the wind shear stress on the sea surface produces turbulence that mixes the water masses.

As just described, the wind can set-up and set-down water levels in the North Sea and Baltic Sea, respectively. When the wind changes or ceases, two-dimensional seiches are generated, i.e. the wind set-up oscillates (and partly turns in a counter clockwise direction) in the North Sea and inside the semi-enclosed Central Baltic Sea. The seiching can cause an extra exchange flow in the transition area.

Inside the Central Baltic Sea, and also, but with less importance, in the transition area, the wind also creates:

- Ekman current in the more open sea areas;
- Coastal jets closer to the coast line;
- Kelvin waves on sea surface, thermocline or halocline; and
- Upwelling of water masses from below either the thermocline or the halocline.

All these resulting currents have an impact on the redistribution and mixing of the waters in the area and the water chemistry.

Furthermore, during summer the water masses are heated and during winter they are cooled by the heat exchange with atmosphere. The heating creates a warm low-density layer at the surface with a thermocline located in the upper 20-30 m of the water column, both in the North Sea and in the central Baltic Sea.

4.5 Water Masses

The estuarine circulation is a relatively slow continuous exchange flow driven by the freshwater surplus in the Baltic Sea, partly diminished by the bathymetry constraints, mainly the Darss and Drogden Sills, and enhanced by the wind driven exchange flow.

In the estuarine circulation only two original water masses are involved:

1. Water from the Baltic rivers with a salinity of 0 psu; and
2. Water from the Atlantic Ocean with a salinity of 35 psu that has flown into the North Sea



All water masses found in the Baltic Sea are a mixture of these two original water masses (only a limited amount of water from the German Bight can be found in the Kattegat, see e.g. Jakobsen (2000)). On the basis of a water mass salinity in the Baltic Sea one can determine the ratio of the two original water masses. E.g. a water mass with the salinity 17.5 psu consists of half river water and half Atlantic water. In the summer, the original water masses are both warm and in winter they are both cold. This triviality is mentioned, because it is important for the temperature of the lower layers inside the Baltic Sea, see later.

The river water flows in the upper layer at the surface towards the North Sea (Fig. 4.4). Along the path lower laying higher saline water are entrained and mixed with the river water, whereby both its salinity and its volume increases. In the Arkona Basin the salinity has increased to be 8 psu (23% Atlantic water). Through the transition area the salinity increases further to be about 25 psu (71% Atlantic water). Finally it leaves the Kattegat and continues as the Norwegian Coastal Current towards the Atlantic Ocean.

Atlantic water in the North Sea subsides in the southeastern Skagerrak or in the northern Kattegat and flows below the upper layer along the sea bed and through the transition area, and regularly, but not continuously, into the Central Baltic Sea. Note that its last contact with atmosphere is at the entrance to the Baltic transition area. Along the path in the transition area, upper laying lower saline waters are entrained and mixed with the Atlantic water, whereby its salinity decreases. In the Fehmarnbelt the salinity has decreased to be about 21 psu. When the bottom water is lifted across the sills, it plunges into the Arkona Basin and continues into the Central Baltic Sea initially as a dense bottom current (cf. Fig. 4.4). This dense bottom current follows the deepest connections, while being diluted, until it meets a water mass with identical density. At this point it leaves the sea bed and intrudes the water column and continues as an intermediate layer. Hence inside the Central Baltic Sea the structure of the water column below the upper layer is complicated with many intrusions and both the salinity and temperature can vary. Only major inflows can replace the lowest water masses at the bottom in the Central Baltic Sea. And the longer the water mass stays at the bottom the lower its density will be because of mixing and the bigger the chance of replacement by another inflow.

Beside the Fehmarnbelt (Darss Sill) pathway the Sound (Drogden Sill) exchanges water with the Central Baltic Sea. The Sound exchange was studied in details as part of the Øresund fixed link study (ØL 1997). The Sound can for most purposes be considered a stratified channel, where the water discharge through the channel is driven by the water level difference between Kattegat and Arkona Basin. The water discharge is only to a minor extent driven by the local wind over the Sound and the density difference between the boundaries due to the shallow Darss Sill. During southwards flow high saline water from Kattegat can be lifted locally across the Drogden sill. And in general larger parts of the Drogden sill area are stratified during a south flowing current than during a north flowing current. During northwards flow the narrow contraction at Helsingør-Helsingborg can act as an internal hydraulic control on the flow and hence impact the extent of the salt water wedge in the Sound. Even the density differences in the Sound are not important in driving the flow through the Sound, the stratification lubricates the flow, i.e. decreases the retarding friction on the flow. Hence the stratification in the Drogden Sill area decreases the contribution to the specific resistance of the Sound from the sill area.

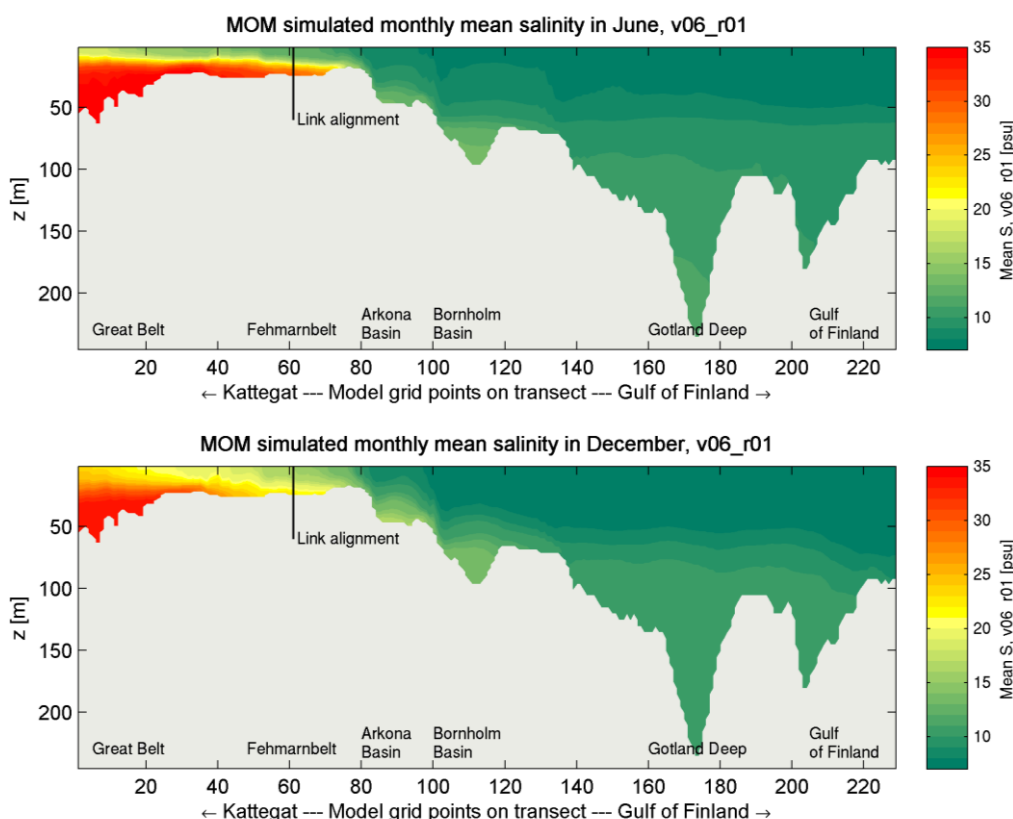


Fig. 4.4 Cross-section showing simulated longitudinal salinity distribution as monthly means from Great Belt through Fehmarnbelt and into the Baltic Proper, where the vertical line shows the position of the planned link (FEHY MOM model, version v06_r01).

The heat (and oxygen) exchange with the atmosphere only takes place in the water mass at the sea surface. Hence if the Atlantic water in the North Sea water is cold when it subsides and flows into the Baltic Sea, then it stays cold and the temperature is only increased through mixing with warm water masses and vice versa. In this manner the temperature of the intrusions in the Central Baltic Sea signals when they subsided on their way into the Baltic Sea. The travel time can range from months to years (it is noted that the 'older' the water mass, the lower the oxygen content; which is important for marine biology).

The residence time for the upper layer in the Central Baltic Sea is about 30 years. The waters below the upper layer consist of numerous layers and intrusions with different salinity, temperature and age (taken from when it flew into the Central Baltic Sea). Hence it is more difficult, or at least makes less sense, to define one residence time for the lower laying water masses in the Central Baltic Sea. Even so values between 1 to 10 years can be found in literature. It has been noted that in general the higher the salinity of a water mass flowing into the Central Baltic Sea is, the longer its residence time in the Central Baltic Sea will be.

4.6 Local Driving Forces

The flow and stratification in the Fehmarnbelt cannot be understood without relating it to the water exchange between the North Sea and the Central Baltic Sea. In the following the exchange of water and salt between the two seas are explained with focus on its importance for the conditions in the Fehmarnbelt.

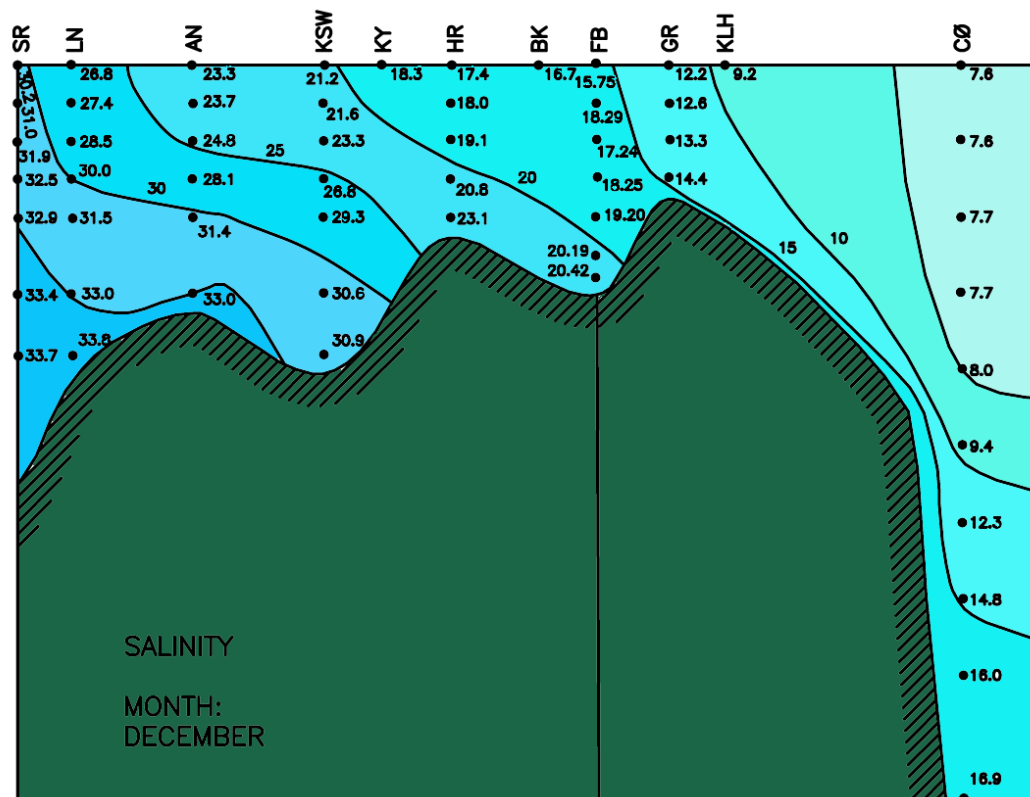
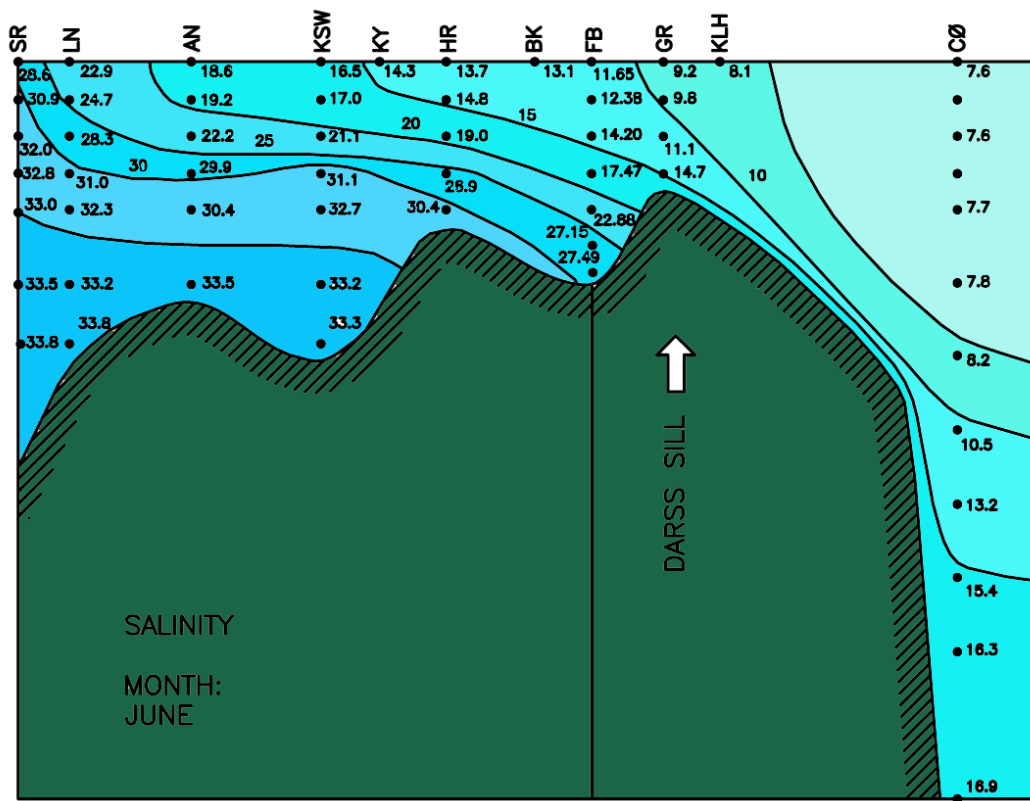
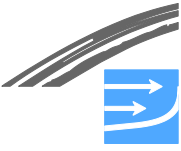


Fig. 4.5 Cross-section showing the longitudinal salinity distribution as monthly means from Skagerrak through Fehmarnbelt and into the Central Baltic Sea (the vertical link shows the position of the planned link). Drawn by data given in (Sparre 1984a), (Lange et al. 1991) and (Jakobsen 1991).



The water masses in the Belt Sea and the Kattegat consist of low saline water from the Central Baltic Sea, which, close to the surface, flows through the Belt Sea and the Kattegat, and high saline water from the North Sea, which forms a lower layer. In June, the wind conditions are weak, and the two-layer exchange flow between the North Sea and the Central Baltic Sea is clearly identified to provide a strongly stratified water column in the Belt Sea, see Fig. 4.5.

The driving forces that determine the flow and stratification in the transition area including Fehmarnbelt can be divided into:

1. Local bathymetrical features: sills, turnings and buffers;
2. Conditions in the Kattegat (high salinity, wind set-up and tide);
3. Hydrology of the adjacent watershed (river discharge and low salinity); and
4. Meteorological conditions (wind, air pressure and heat exchange).

The flows these driving forces cause are described based on the above division with focus on the impacts on the local conditions in the Fehmarnbelt.

4.6.1 Bathymetrical features: sills, turnings and buffers

The important bathymetrical features to note in the Fehmarnbelt and nearby areas are:

- The shallow Darss Sill at the entrance to the Central Baltic Sea;
- The about 90° turning between the Fehmarnbelt and the Langelands Belt; and
- The Kiel Bight and Mecklenburg Bight on either side of the Fehmarnbelt that act as reservoirs that buffers water.

These features are for example important because:

- High saline water has to flow over the Darss Sill to enter the Central Baltic Sea and after passing the sill it is trapped inside the Central Baltic Sea. Hence the sill limits the inflow of dense water through the Fehmarnbelt.
- During inflow the water level inside the Kiel Bight has to rise to turn the flow from Langelands Belt into Fehmarnbelt. Until the water level has increased the inflowing water propagates from Langelands Belt into the Kiel Bight.

4.6.2 Tides

The tides decrease through the Danish straits. The tidal constituents at Hornbæk and Gedser are shown in Fig. 4.6 and Fig. 4.7. The constituents are determined on the basis of approximately 5 years data.

In Kattegat at Hornbæk the tidal amplitude, or intensity coefficient, is 15 cm (sum of four tidal constituents: M2 + S2 + K1 + O1). In the Great Belt it is 20 cm (Schmager et al. 2008). The amplitude decreases through the Danish Straits and is 7.5 cm in the Sound and also in the southwestern Central Baltic Sea at Gedser. The tidal signal is reduced about 50% from Hornbæk to Gedser.



The tides cause an oscillation of water level in and water flow through the Fehmarnbelt. The tidal flow is not able to transport high saline water masses across the Darss Sill and into the Central Baltic Sea.

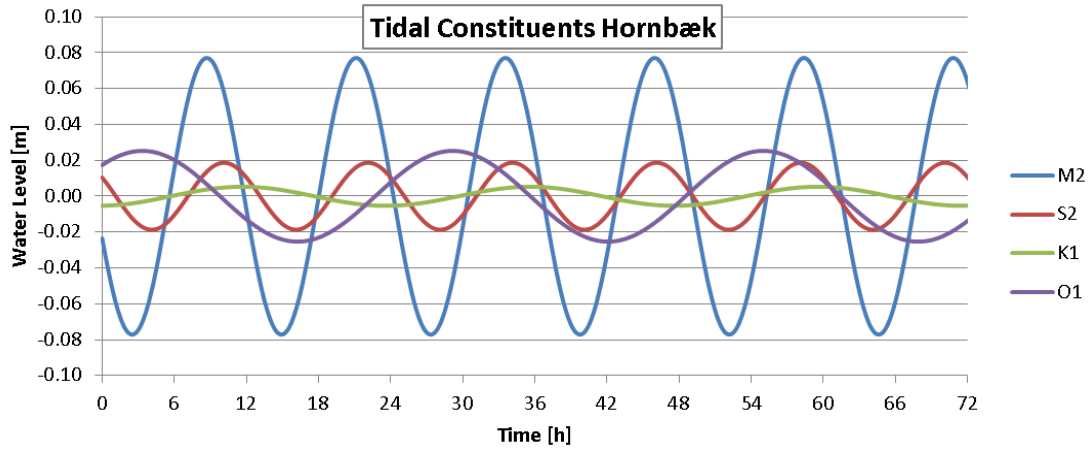


Fig. 4.6 Main tidal constituents for Hornbæk gauge.

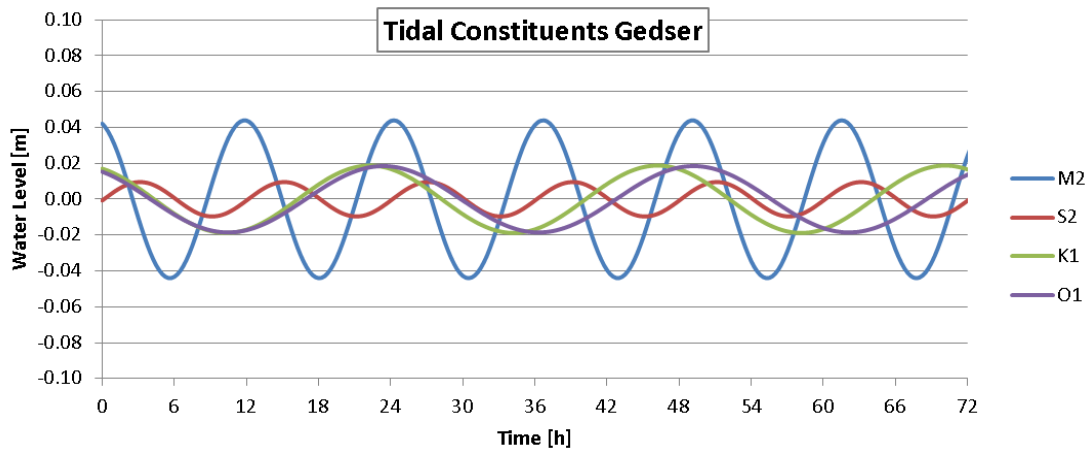


Fig. 4.7 Main tidal constituents for Gedser gauge.

4.6.3 River inflow

Within the Belt Sea including the Fehmarnbelt there are no major local river inflows affecting water levels and stratification. But as it is part of the transition zone between Baltic and North Sea, river inflow to the Central Baltic Sea has an impact on water levels in the Danish Straits including the Fehmarnbelt.

The annual river discharge of into the sub-basins of the Belt Sea is displayed in Fig. 4.8 and Table 4.2. The inter-annual variation is between ± 0.2 to ± 0.8 km³/year leading to 6.7 ± 2.0 km³/year for the whole area.

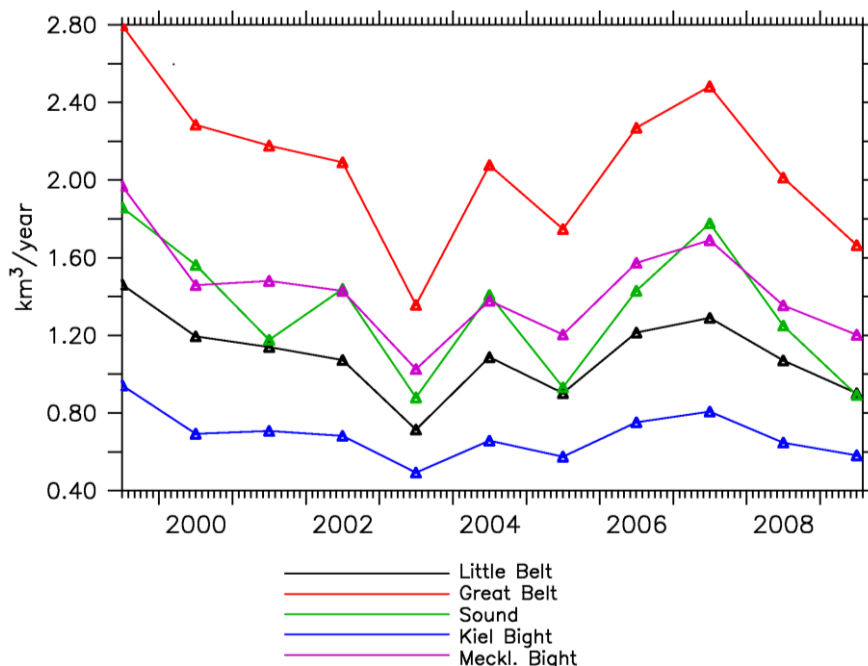


Fig. 4.8 Annual river discharge (km³/year) into the sub-basins of Belt Sea.

Table 4.2 Mean annual river discharges into Belt Sea and its sub-basins in 1999-2009 according to FEHY river data set. The local importance of river inputs is characterized by relation to the sea surface, yielding a hypothetical rise of the sea level (cm/year).

Sub-basin	Sea surface (km ²)	River discharge (km ³ /yr)	Sea surface rise (cm/yr)
Little Belt	2,491	1.1	44
Great Belt	8,891	2.1	24
Kiel Bight	3,349	0.7	21
Mecklenburg Bight	4,673	1.4	30
Sound	2,284	1.3	57
Belt Sea and Sound	21,688	6.6	30

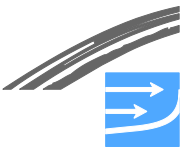
4.6.4 Wind

The dominating driving force for the flow in the transition area is the meteorological conditions over the North Sea and the Baltic Sea, i.e. not the local wind field over the transition area.

High and low air pressure fields pass Scandinavia on a weekly time-scale and set-up or set-down the water levels in the North Sea and Baltic Sea.

In a situation where a low pressure field over Scandinavia, the related cyclonic wind field causes set-ups and -downs in the North Sea and Baltic Sea, respectively, with:

- High water levels along the west coast of Jutland and in the Skagerrak and Kattegat;
- Low water levels in the south-western Central Baltic Sea; and
- High water levels in the north-eastern Central Baltic Sea.



High water levels in Kattegat and low water level in the south-western Central Baltic Sea force an inflow to the Central Baltic Sea. An example of water level distribution for an inflow situation in the Belt Sea is given in Fig. 4.9.

The actual value of high and low water levels depends on the air pressure and wind fields (the wind shear stress on the sea surface increases with the wind speed to power 2-3).

If it instead is a high air pressure field over Scandinavia with its anticyclonic wind field the situation is reversed with:

- Low water levels along the west coast of Jutland and in the Skagerrak and Kattegat;
- High water levels in the southwestern Central Baltic Sea; and
- Low water levels in the northeastern Central Baltic Sea.

Low water levels in Kattegat and high water levels in the south-western Central Baltic Sea force an outflow from the Central Baltic Sea through the Belt Sea. An example of water level distribution for such an outflow situation is given in Fig. 4.10.

Major Baltic inflows of some 100 km³ of saline water are induced if a high air pressure over Scandinavia is followed by a stable low-low air pressure field over Scandinavia. This occurs mainly during autumn and winter.

It is repeated that it is the wind field over the North Sea and Baltic Sea that mainly impacts the flow in the Fehmarnbelt. The local wind is of less importance.

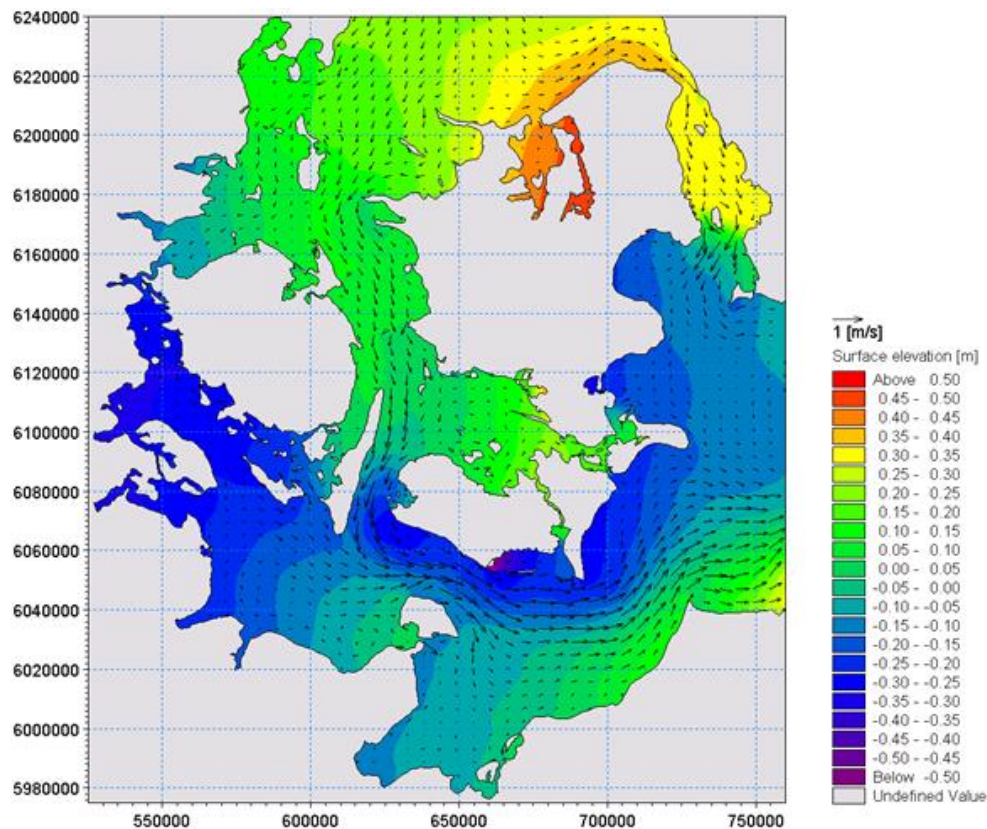


Fig. 4.9 Simulated water levels and current velocities in Belt Sea during strong inflow event.

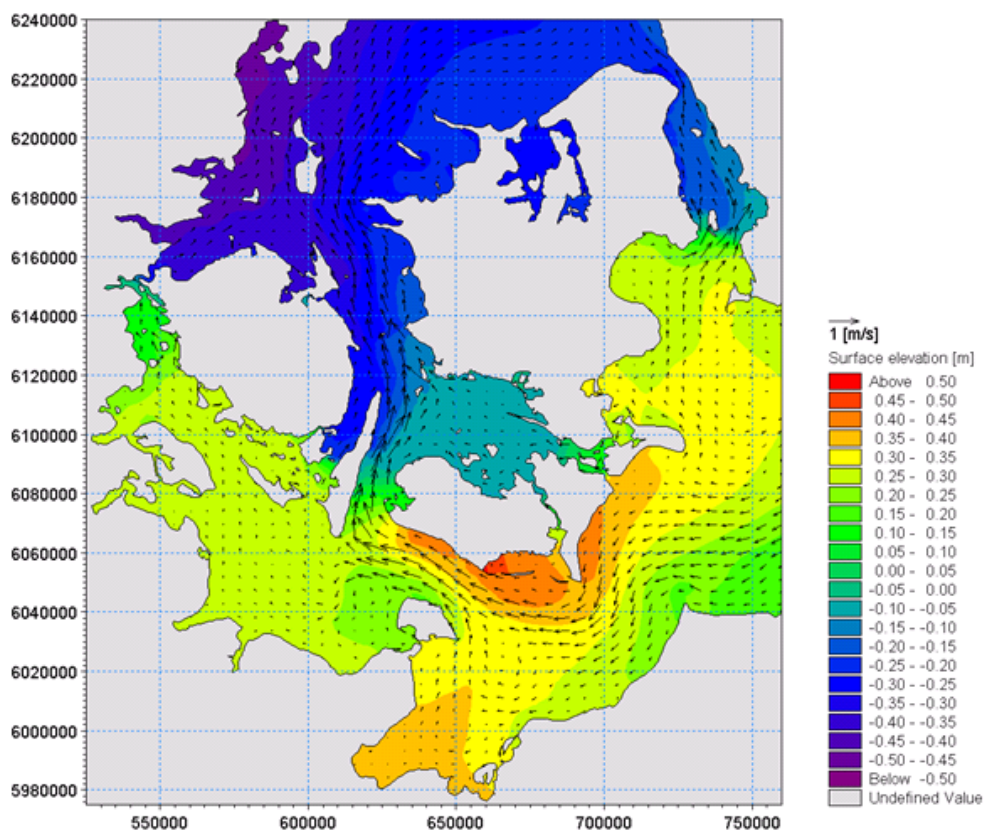


Fig. 4.10 Simulated water levels and current velocities in Belt Sea during strong outflow event.

Wind rose based on measurements collected at Westermarkelsdorf is shown in Fig. 4.11.

Frequency classes of daily wind speed and direction from 1947 to 2010 at Westermarkelsdorf/Fehmarn

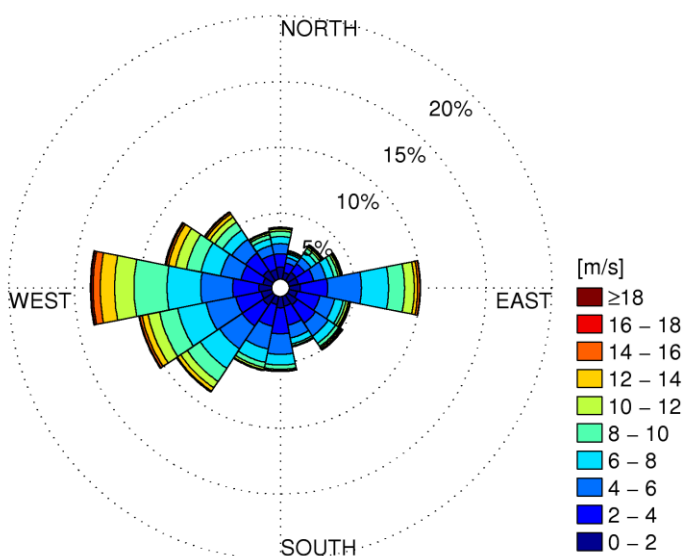


Fig. 4.11 Wind rose at Westermarkelsdorf.

Still, in the Fehmarnbelt, Kiel Bight and Mecklenburg Bight the local wind creates:



- Ekman current in the more open sea areas;
- Coastal jets closer to the coast line;
- Kelvin waves on sea surface, thermocline or halocline; and
- Upwelling of water masses below either the thermocline or the halocline.

All these currents have an impact on the redistribution and mixing of the waters and the biology.

4.7 Effects to water level

Due to the large rivers flowing into the Central Baltic Sea the water level is higher inside the Central Baltic Sea than in the Kattegat and the North Sea and there is a salinity gradient through the Baltic Sea. The water level lift is nearly constant inside the Central Baltic Sea but varies over the Danish Straits.

Because of the river inflow the water level is lifted to be located about 4 cm higher in the southwestern Central Baltic Sea than in the Kattegat.

Water levels in the Danish Straits and around Fehmarnbelt are also affected by density differences between fresher water in the Baltic Sea and salty water in the North Sea.

Salinity at sea surface increases from 8 psu in the southwestern Central Baltic Sea to a mean value of 25 psu in the northern Kattegat, see also Fig. 4.5. The higher the salinity, the higher the density (ignoring the variation in temperature) and hence also the density of the water increases from the Central Baltic Sea towards the North Sea. The biggest salinity and density gradients are found in the Danish Straits.

The density variation causes a water level lift. The highest lift is found in the Central Baltic Sea wherefrom it decreases gradually towards the North Sea. The water level is located about 4 cm higher in the south-western Central Baltic Sea than in the Kattegat, because of these density differences.

Hence the water level difference caused by the river inflow and related salinity gradient through the Belt Sea sums up to be in total about 8 cm (see Fig. 6.4).

As mentioned in Chapter 4.6.3, the local river inflow plays only a minor role for the hydrography in the transition zone, because it is very small compared to the outflow from the Baltic Sea.

4.8 Distributions in the Fehmarnbelt

The first mode baroclinic Rossby radius is about 2.5 to 4 km in spring and summer, but only 1.5 km during winter. Hence it is smaller than the width of the Fehmarnbelt of 18 to 20 km. For that reason the baroclinic flow is less influenced by the bathymetry than the barotropic flow.

The current patterns observed in Fehmarnbelt can be divided into a barotropic inflow or outflow, which is driven by large scale sea level differences between the Baltic Sea and Kattegat, and a baroclinic current on the local scale, which depend on the local bathymetry, stratification and wind.

Subinertial ageostrophic flows in the Fehmarnbelt are the Ekman flows generated by the local wind in the mixed surface layer and by the bottom friction of the geostrophic channel flow. In case of cross channel Ekman flows, mass conservation is established by corresponding compensation flows in the layers below the surface mixed layer and above the bottom mixed layer. In case of uni-directional flow of wind and geostrophic channel flow one cross circulation cell will develop in the upper layer of Fehmarnbelt, while in case of opposite directed wind and channel flow, oppositely directed cross circulation cells may develop (Fig. 4.12).

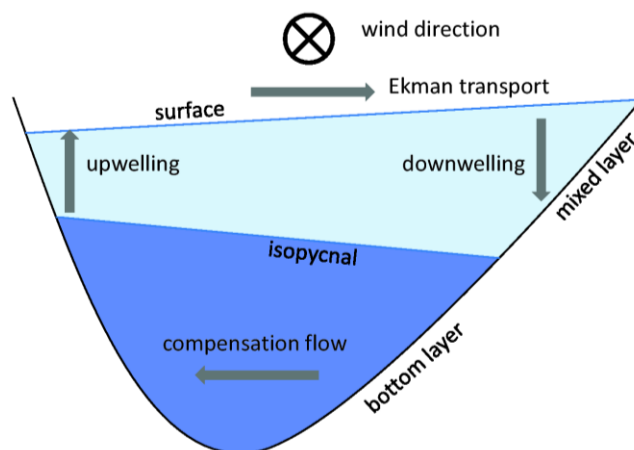


Fig. 4.12 Sketch of wind-driven cross circulation in Fehmarnbelt in case of along channel wind, coastal upwelling and downwelling, surface Ekman transport and deep cross-channel compensation flow.

As a result of this flow conditions, coastal upwelling at the northern or southern rim of the Fehmarnbelt is often induced.

4.9 Sea Ice

Sea ice formation depends on local cooling and the salinity of surface water. During winter season it typically builds up close to the coastline and in shallow semi-enclosed areas. The colder the winter is the thicker and further from land the ice will grow.

Especially cold winter periods enhancing the ice growth are often related to stable high air pressure fields that cover the Scandinavian region. It causes a cold wind from east that furthermore drives cold low-saline water from the Central Baltic Sea into the transition zone. In the transition zone the cold waters form a thin upper layer of low-saline water that rapidly lose its heat to the atmosphere, whereby its temperature quickly drops to the freezing point. The most rapid cooling occurs in the shallow coastal waters and enclosed bays of limited water exchange with adjacent waters. In these areas ice formation forms first and gradually spreads out to the more open areas with continued freezing. Drift ice forms in the shipping routes. When the high air pressure fields is replaced by a low air pressure fields rising air temperatures and inflow of warm water from the North Sea lead to a rapid deterioration of the sea ice.

Sea ice observations from the Fehmarnbelt area show that during the years 1956 to 2005 sea ice occurs in 20%-30% of the winter (Schmelzer et al. 2008). In severe winters, these areas are completely ice covered.



5 METEOROLOGICAL CONDITIONS

Meteorological conditions are not part of hydrographic conditions, but the most important forcing for the hydrographic conditions. Hence the meteorological conditions in the Fehmarnbelt area are outlined in the following. Still it is noted that it is the meteorological conditions over the North Sea-Baltic Sea system that is the main driver of the flow through the Belt Sea.

Despite the small spatial scales of 20 km across channels and 40-80 km across basins, the Belt Sea region is sensitive to local meteorological forcing. The shallow channels and basins are subject to strong mixing by stormy winds. Because of the stratification of the brackish sea water, the spatial scale of dynamic response patterns, like eddies and coastal currents, is only some 1-4 km (see Fennel et al. 1991). Hence, even the narrow channels and small basins, like Fehmarnbelt, Kiel and Mecklenburg Bight, develop peculiar current patterns which vary quickly with changing weather on the time scale of days. Consequently, time scales between days and inter-annual variations have to be considered to characterize the meteorological forcing and the response of the sea. On the other hand the local weather is also influenced by the nearby coasts as can be shown for wind speed and direction and the daily cycle of air temperature.

The meteorological conditions in the Belt Sea region are characterized on the basis of available data which are shortly described in the previous Chapter 3.2.1. The long-term time-series recorded at Westermarkelsdorf on island Fehmarn, see Fig. 3.4, are considered as the main reference for the region of interest. The observations at Darss Sill provide open sea measurements. The average meteorological forcing is described in Chapter 5.1 by long-term means and selected data limits specifying the probability of occurrence of typical and extreme weather. Inter-annual variation is shown by means of yearly mean values, which indicate a positive trend of air temperature after 1990. The seasonal cycle is resolved on monthly time scale to describe the baseline conditions during 2009-2010 in Chapter 5.2. Daily time resolution is applied to identify strong wind events. Focus is set on wind speed and air temperature as the main forcing factors. The general weather conditions have been described in the Baltic Sea Baseline Report (FEHY 2013a).

5.1 Long-term Meteorological Conditions

The basic statistical characteristics of selected meteorological parameters, calculated over the full observation periods, are specified in Table 5.1 to Table 5.8. Usually average long-term conditions and variability are described by the mean value and by the standard deviation of data. The typical range of observations is assumed within a range of ± 2 to ± 3 standard deviations around the mean value. Extreme events are characterized by the absolute minimum and maximum values which were measured. These characteristics are given in the second column of the tables. However, all weather conditions show deviations from Gaussian normal distribution, see for example the daily mean air temperature observed at Westermarkelsdorf in Fig. 5.3, which has a bimodal distribution. The typical meteorological conditions are more completely characterized by so-called percentiles, which specify the data limits according to a certain degree of probability. The percentiles listed in the tables have the following meaning: The median is another kind of mean value, which corresponds to 50% probability, i. e. one half of the observations lie below and the other half above the median. Discrepancies between median and arithmetic mean



indicate deviations from a symmetric Gaussian distribution. The percentiles of 5% and 95% give two pieces of information:

1. These values describe the 90% probability range of observations; and
2. The lower and upper data limits for rather rare events.

There is only a probability of 5% that an observation lies below the 5% percentile or above the 95% percentile. The data range in between describes the typical conditions, which occur in 90% of all cases. In the same sense the 1% and 99% percentiles define an extended data range (of 98% probability) and the bounds for rare events, which occur with only 1% probability.

Table 5.1 Basic statistics of mean daily/hourly wind speed observed at meteorological stations, see Table 3.3 and Fig. 3.4. The second column specifies the overall mean value, the standard deviation and the absolute minimum and maximum values. The percentiles in the third column characterize rare events (below 1% or 99% probability, the 90% data range (between 5-95%), and the median of data (50%).

Station	wind speed (m/s) at 10m height			
	min/ mean±std /max	1/5/ 50 /95/99%	samples	frequency
Westermarkelsdorf	0.0/ 5.7±3.5 /25.5	0.4/1.1/ 5.1 /12.3/15.5	19673	daily
Fehmarnbelt buoy	0.0/ 6.3±3.3 /26.1	0.5/1.6/ 6.0 /12.4/15.2	42664	hourly
	0.4/ 6.3±2.8 /16.4	1.6/2.4/ 6.0 /11.5/13.9	1664	daily
Nysted	0.2/ 7.2±3.3 /24.2	1.2/2.3/ 6.9 /12.9/15.6	11886	hourly
	2.0/ 7.2±2.8 /22.3	2.5/3.2/ 6.9 /12.2/14.3	504	daily
Warnemünde	0.0/ 4.6±2.9 /20.2	0.5/1.1/ 4.0 /10.4/14.2	13047	daily
Darss Sill	0.0/ 7.5±3.6 /27.0	1.1/2.3/ 7.1 /14.0/17.1	88038	hourly
	0.1/ 6.7±3.3 /18.5	0.7/1.8/ 6.4 /12.7/14.9	3694	daily

The average strength of wind forcing is described by the statistical parameters in Table 5.1. The mean wind speed amounts to 4-7 m/s, with clear indication that wind blows stronger on open sea (6-7 m/s) than over land (4-6 m/s). This effect is obvious even for the coastal stations at Westermarkelsdorf on island Fehmarn and at Warnemünde. Fehmarn is exposed to stronger winds because westerly directions are predominant, see Fig. 5.2. The median of wind speed is always somewhat smaller than the mean indicating that lower winds are more frequent.

The ship observations compiled by Mietus (1998) confirm the regional trend in mean wind speed by yielding total averages of 7.0, 4.7 and 7.3 m/s for the large grid cells corresponding to Westermarkelsdorf, Warnemünde and Darss Sill. Standard deviation of ship winds is around 3 m/s, which compares well with the station measurements. A direct comparison of the overlapping 4634 hourly samples at FB buoy and at Nysted via linear regression analysis (not shown) reveals that the mean wind speed over Fehmarnbelt is on average 80% of the wind speed at Nysted, the mean difference (bias) is -1.5 m/s. However, there is large scatter between data expressed by a squared correlation of 0.55 and root mean square (rms) deviations around ±2 m/s. The comparison of 1161 overlapping daily samples with Westermarkelsdorf yield a mean 10% enhancement of wind speed over Fehmarnbelt with a bias of +0.7 m/s, again with large scatter of 0.65 squared correlation and ±1.5 m/s rms deviations. The role of natural small scale fluctuations of the wind might be estimated from the two adjacent wind records at Nysted (approximately 7 km apart). Here the bias is zero, the slope of the regression line is around unity, but the squared correlation is 0.91 and 0.97 and the rms deviations are 0.5



and 1.0 m/s at hourly and daily time scale, respectively. Hence, the wind speed over Fehmarnbelt is generally somewhat stronger than at Westermarkelsdorf, but compared to more open basins limited by the nearby coast.

The 5% and 95% percentiles indicate that daily winds vary typically between 2-13 m/s. The 1% and 99% percentiles show that calm days with mean wind speed below 1 m/s and stormy days with mean winds above 15 m/s are rare events. Larger standard variations and probability ranges for hourly data imply that the variability of wind speed is higher on shorter time scales. This becomes evident if gustiness is expressed by the maximum recorded wind speed. The statistics in Table 5.2 shows that the maximum daily wind gusts are on average 11-14 m/s, i. e. two times stronger than the mean wind speed. A similar relationship also applies to the peak events expressed by a maximum daily mean wind speed around 20-25 m/s (see Table 5.1) accompanied by gusts of 30-40 m/s. On hourly time scale the relation between mean and maximum wind speed yields an average factor of 1.3 on open sea till 1.9 over rough land surface according to the U.K. Meteorological Office as cited by (Brasseur 2001). The percentiles show that on calm days the maximum wind speed reaches 4-7 m/s, whereas 20 m/s are exceeded on stormy days in more than 5% of observations. Note that a 1% percentile corresponds to 3-4 days per year and 5% to 18 days.

Table 5.2 Basic statistics of maximum daily wind speed observed at meteorological stations, see Table 3.3 and Fig. 3.4

Station	Maximum daily wind speed (m/s)		
	min/mean±std/max	1/5/ 50 /95/99%	samples
Westermarkelsdorf	1.2/ 12.5±4.8 /40.0	4.1/5.8/ 12.0 /21.1/26.8	11438
Warnemünde	0.0/ 11.7±5.6 /41.0	0.0/0.0/ 11.4 /21.0/26.8	16128
Darss Sill	2.6/ 14.0±5.0 /30.0	5.0/6.8/ 13.4 /23.0/28.7	2566

The frequency of wind direction is discussed by means of wind rose plots for Darss Sill in Fig. 5.1 and for Westermarkelsdorf in Fig. 5.2. The directional segments correspond to the 16 main wind directions, i. e. north (N), northnortheast (NNE), northeast (NE), eastnortheast (ENE), east (E) etc. Colours denote the observed wind speed. These directional diagrams clearly show the predominance of westerly and easterly winds. At Darss Sill 50% of winds come from WNW to SSW, most frequently from W and WSW. Around 25% of winds blow from easterly directions between ENE and SE. Northerly and southerly winds are rare events but can also reach daily mean wind speed above 10 m/s. Albeit rare, northeasterly wind is potentially dangerous because it can pile up extreme water levels in the Belt Sea region. This was, for example, the case during the big flood in November 1872.

The wind measurements at Westermarkelsdorf indicate a channelizing effect of the nearby coasts. The distribution of westerly winds, to which the station at the northwestern edge of island Fehmarn is exposed, is similar to Darss Sill, but winds coming from the Baltic Sea are concentrated around the eastern direction, compare Fig. 5.1 and Fig. 5.2. A similar effect is observed by the shift of the most frequent wind direction at Darss Sill from W to WSW corresponding to the southeast-northwest inclination of the adjacent Danish and German coasts. The wind guiding effect of the coasts is also discussed by Tiesel (2008) for the "Warnemünder Wind" blowing especially strong from northwesterly directions. Another consequence of the surrounding land is the decrease of mean wind speed at Westermarkelsdorf and Warnemünde in comparison to Fehmarnbelt buoy, Darss Sill and Nysted, see Table 5.1 and Fig. 5.7. Because of the limited wind fetch peak wave heights in the Belt Sea are lower than in the open Baltic Sea as discussed in Chapter 8.2.

Frequency classes of daily wind speed and direction from 2000 to 2010 at Darss Sill

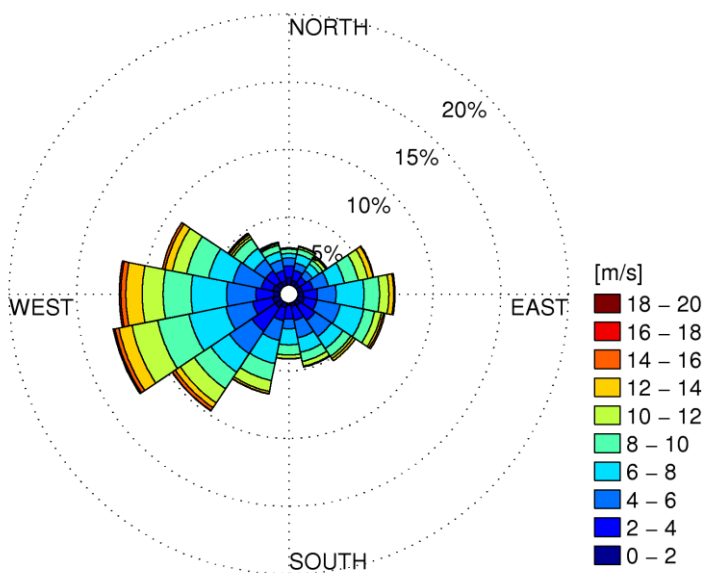


Fig. 5.1 Rose plot of daily mean wind observed in 2000-2010 at open sea station Darss Sill (see Fig. 3.4). Slices show the frequency of wind directions and colours correspond to wind speed.

Frequency classes of daily wind speed and direction from 1947 to 2010 at Westermarkelsdorf/Fehmarn

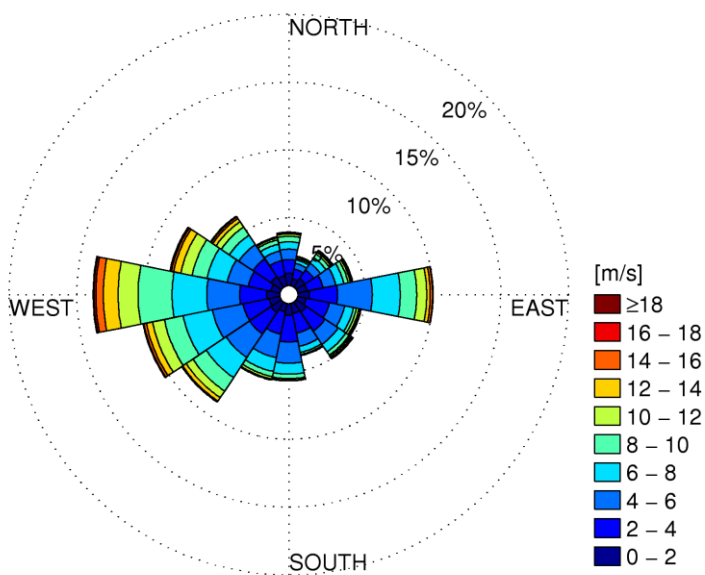


Fig. 5.2 Rose plot of daily mean wind observed in 1947-2010 at coastal station Westermarkelsdorf on island Fehmarn (see Table 3.3). Slices show the frequency of wind directions and colours correspond to wind speed.

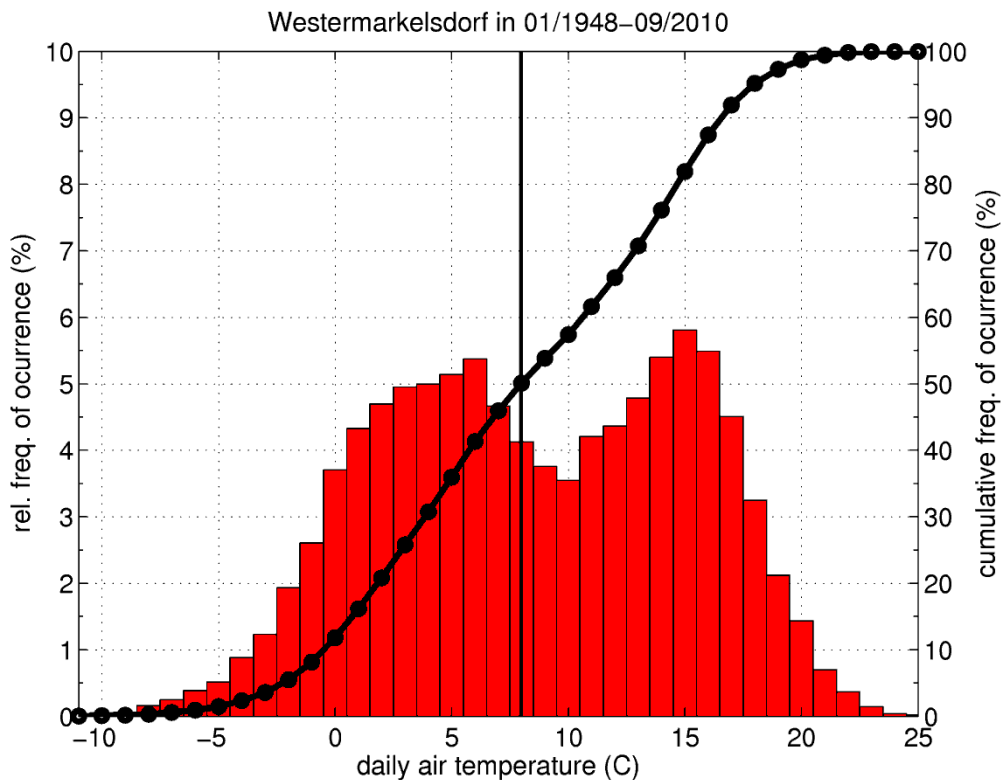


Fig. 5.3 Frequency of occurrence of daily mean air temperature in bins of 1°C, observed at Westermarkelsdorf on island Fehmarn by Deutscher Wetterdienst (DWD). The bold vertical line indicates the median mean value.

The bimodal structure of the frequency distribution of air temperature, shown in Fig. 5.3, is not reflected by the statistic parameters given in Table 5.3. Mean and median values are nearly equal around 8.5°C at Westermarkelsdorf. The lower frequency peak at 6°C corresponds to the mean monthly air temperature in April and November, see Fig. 5.4, whereas daily temperatures around 15°C are typical during June and September. Coastal and open sea stations show comparable data ranges, however, mean air temperature is higher at Fehmarnbelt and Darss Sill, mainly because of heat release during the cold seasons. Frost days with mean temperature below zero occur only in 5% of time, as well as warm days with daily air temperatures above 19°C. Hourly samples meet extended minimum and maximum temperatures but yield the same general statistics because of the strong yearly signal, see also Fig. 5.4.

Table 5.3 Basic statistics of mean daily/hourly air temperature observed at meteorological stations, see Table 3.3 and Fig. 3.4. The second column specifies the overall mean value, the standard deviation and the absolute minimum and maximum values. The percentiles in the third column characterize rare events (below 1% or 99% probability, the 90% data range (between 5-95%), and the median of data (50%).

Station	Air temperature (°C) at 2m height			
	min/mean±std/max	1/5/50/95/99%	samples	frequency
Westermarkelsdorf	-11.9/ 8.6 ± 6.6 /25.1	-5.3/-1.8/ 8.5 /18.5/20.7	19841	daily
Fehmarnbelt buoy	-7.6/ 10.0 ± 6.0 /24.5	-1.9/0.9/ 9.7 /19.1/21.1	45699	hourly
	-6.6/ 10.0 ± 5.9 /21.8	-1.8/1.1/ 9.6 /18.8/20.5	1729	daily
Warnemünde	-14.8/ 8.8 ± 6.9 /27.8	-6.9/-2.3/ 8.8 /19.2/22.1	23433	daily
Darss Sill	-10.1/ 9.6 ± 6.3 /27.5	-2.8/-0.3/ 9.3 /19.2/21.5	87557	hourly
	-8.0/ 9.6 ± 6.3 /23.6	-2.7/-0.3/ 9.3 /19.1/21.2	3689	daily



The compensating influence of the storage and release of heat by the sea is more distinctly seen in the daily variation of air temperature. The heating by solar irradiation during daytime and nocturnal cooling by emission of long-wave radiation leads to typical temperature differences of 2-12 degrees over land and in extreme cases to 14-21 degrees, see coastal stations Westermarkelsdorf and Warnemünde in Table 5.4. In contrast to that, daily temperature variations at sea are damped to around 3 degrees. 90% of observations at Fehmarnbelt buoy and Darss Sill range within 1-5 degrees and extreme events are confined to 6-10 degrees.

Table 5.4 Daily range of air temperature, i. e. difference between daily minimum and maximum values, observed at meteorological stations, see Table 3.3 and Fig. 3.4

Station	Daily range of air temperature (°C)		
	min/mean±std/max	1/5/50/95/99%	samples
Westermarkelsdorf	0.3/ 5.3±2.8 /19.0	1.1/1.8/ 4.8 /10.9/13.6	19841
Fehmarnbelt buoy	0.2/ 2.8±1.3 /10.5	0.8/1.1/ 2.5 /5.0/6.9	1729
Warnemünde	0.5/ 5.8±3.0 /21.1	1.3/2.0/ 5.2 /11.7/14.4	23433
Darss Sill	0.0/ 2.4±1.2 /10.3	0.6/0.9/ 2.2 /4.6/6.2	3686

Basic statistics is summarized for air pressure, cloudiness, relative humidity and precipitation in Table 5.5 to Table 5.8. There are no distinct regional tendencies observed for these parameters. In the range of latitudes covered by the meteorological stations the long-term mean air pressure is around normal pressure at 1013-1014 hPa. The differences of ±1 hPa is attributed to uncertainty of measurement, because such pressure differences may not occur permanently over the short distances between the stations. Regression analysis (not shown) of air pressure at Westermarkelsdorf, Fehmarnbelt buoy and Nysted yields biases between 0.6-0.9 hPa and rms deviations of ±0.7-1.6 hPa with slopes and correlation around unity. The analysis of air pressure for the entire Baltic Sea in the Baltic Sea Baseline Report (FEHY, 2013b) has shown that the mean seasonal air pressure varies by 3-4 hPa over the latitudinal range 54-66°N. The ship data of (Mietus 1998) show the same latitudinal decrease. The typical range of inter-annual variations of yearly mean air pressure lies within ±3 hPa. The standard deviation of 10 hPa reflects the high variability of air pressure on daily time scale. The extreme values and probability distribution imply that strong cyclones are accompanied by air pressure below 990 hPa, whereas 1030 hPa are exceeded during intense high pressure conditions.

Table 5.5 Basic statistics of mean daily air pressure observed at meteorological stations, see Table 3.3 and Fig. 3.4. The average percentiles for probability levels 1, 5, 50, 95, 99% are 987, 996, 1014, 1029, 1036 hPa.

Station	Air pressure (hPa) at sea level		
	min/mean±std/max	1/5/50/95/99%	samples
Westermarkelsdorf	967/ 1013±10 /1049	987/996/ 1014 /1019/1036	15520
Fehmarnbelt buoy	976/ 1014±10 /1044	987/996/ 1014 /1031/1038	1181
Nysted	971/ 1014±9 /1037	988/999/ 1014 /1029/1032	504
Warnemünde	964/ 1013±10 /1046	987/996/ 1014 /1029/1035	23433
Darss Sill	972/ 1014±10 /1046	988/997/ 1014 /1020/1038	3627

The measurements of relative humidity show a slight tendency to higher moisture levels above sea, see Table 5.6. However, average conditions may be characterized by the median and mean values around 85% and a typical range of variation between 60-100%.



Table 5.6 Basic statistics of mean daily relative humidity observed at meteorological stations, see Table 3.3 and Fig. 3.4. The average percentiles for probability levels 1, 5, 50, 95, 99% are 60, 68, 85, 97, 99 % of relative humidity.

Station	Relative humidity (%) at 2 m height		
	min/mean±std/max	1/5/50/95/99%	samples
Westermarkelsdorf	44/84.4±8.6/100	62/69/85/97/99	19841
Warnemünde	31/81.7±9.6/100	54/64/83/95/98	21972
Darss Sill	48/85.9±9.3/100	61/68/87/98/99	3672

Data records of cloud cover and precipitation are available only for the stations operated by Deutscher Wetterdienst (DWD) at Westermarkelsdorf and Warnemünde. Both parameters show one-sided frequency distributions leading to asymmetric estimates of the typical data range. Cloudiness is registered by octal numbers between 0 for clear conditions and 8 for total overcast. Hence, a mean cloudiness of 5.2-5.5 corresponds to 65-70% coverage. On monthly scale cloudiness shows an annual cycle with mean cover around 75% in winter and 60% in summer, see Fig. 5.11 below.

Table 5.7 Basic statistics of mean daily cloudiness observed at meteorological stations, see Table 3.3 and Fig. 3.4. The average percentiles at 1, 5, 50, 95, 99% are 0, 1, 5.5, 8, 8 indicating 5% of probability for very bright and 5% for overcast cloud cover.

Station	Total cloudiness (octals)		
	min/mean±std/max	1/5/50/95/99%	samples
Westermarkelsdorf	0/5.2±2.3/8	0/0.7/5.6/8/8	19841
Warnemünde	0/5.5±2.2/8	0/1.0/5.9/8/8	21972

Percentiles of frequency distribution are explicitly specified for precipitation in Table 5.8 to show the median is around zero, meaning that on average the probability of precipitation is 50% or less. The mean values are around 1.5-2 mm/day indicating a total precipitation of 45-60 mm per month and 550-730 mm per year, which is typical for the Baltic region, see (Lindau 2004), (Leppäranta and Myrberg 2009). The annual variation ranges from monthly means of 30-40 mm in February to April to 60-70 mm in July and August. Strong precipitation events reach to 20-70 mm per day.

Table 5.8 Basic statistics of mean daily precipitation observed at meteorological stations, see Table 3.3 and Fig. 3.4. The second column specifies the overall mean value, the standard deviation and the absolute minimum and maximum values. The percentiles in the third column characterize rare events (below 1% or 99% probability, the 90% data range (between 5-95%), and the median of data (50%).

Station	Daily precipitation (mm/day)		
	min/mean±std/max	1/5/50/95/99%	samples
Westermarkelsdorf	0/1.5±3.5/68.7	0.0/0.0/0.0/7.9/16.6	19840
Warnemünde	0/1.7±3.8/61.6	0.0/0.0/0.0/8.5/17.7	21972

5.2 Meteorological Conditions in Baseline Period

The meteorological forcing conditions in the Fehmarnbelt region during the baseline years 2009 and 2010 are evaluated against the background of the long-term observations analyzed in the previous Chapter 5.1. Monthly time resolution is applied to differentiate the baseline conditions from the typical annual cycle. Short-term weather events are identified on daily time scale.

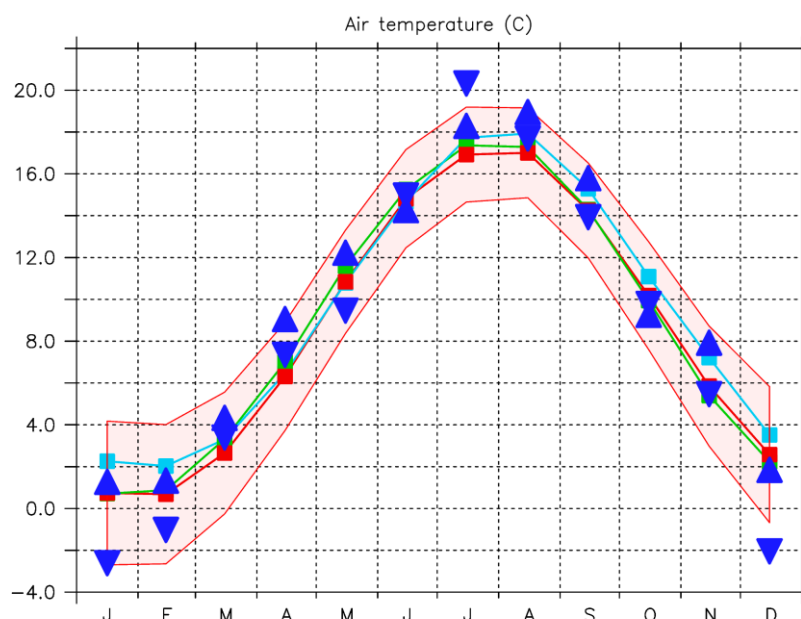


Fig. 5.4 Annual cycle of air temperature (°C). Coloured lines with small symbols indicate climatological monthly means at Warnemünde (green), Westermarkelsdorf (red), and Darss Sill, see Table 3.3 and Fig. 3.4 The shaded region corresponds to ± 1 standard deviation. Triangles denote conditions in baseline years 2009 (upward) and 2010 (downward).

The annual variation of air temperature is displayed in Fig. 5.4 by climatological monthly means, i. e. the mean monthly temperature averaged over all available observations. The shade region indicates the standard deviation of the monthly means at Westermarkelsdorf, which is around $\pm 2^\circ\text{C}$ during winter (December to March), and $\pm 1^\circ\text{C}$ to $\pm 1.4^\circ\text{C}$ otherwise. In comparison to the coastal stations the climatological curves indicate a delayed rise of air temperature during spring due to heat storage by the sea. The effect of heat release during autumn and winter is more pronounced, raising monthly mean air temperature by 1-2°C over sea. The baseline conditions at Westermarkelsdorf are indicated in Fig. 5.4 by upward triangles for 2009 and downward triangles for 2010. This shows that April, November 2009 and July 2010 were warmer than the long-term mean, whereas January and December 2010 were exceptionally colder with respect to one standard deviation. Although the cold February 2010 was within this range it is also listed in the overview in Table 5.9 below.

The annual cycle of air temperature between 0-18°C is reflected by the typical range of daily observations between 5% and 95% of probability, see Table 5.3. The daily variation is of comparable magnitude as seen in Fig. 5.5 derived from the observations at Westermarkelsdorf. On average air temperature varies about 4-5°C during one day from October till March and about 6-7°C from April till September. However, daily temperature differences above 10°C are observed during the whole year. On the other hand also days with nearly no temperature variation occur in every month. The range of daily temperature variations is smaller by a factor of two over sea, see Table 5.4, and has no distinct annual cycle (not shown).

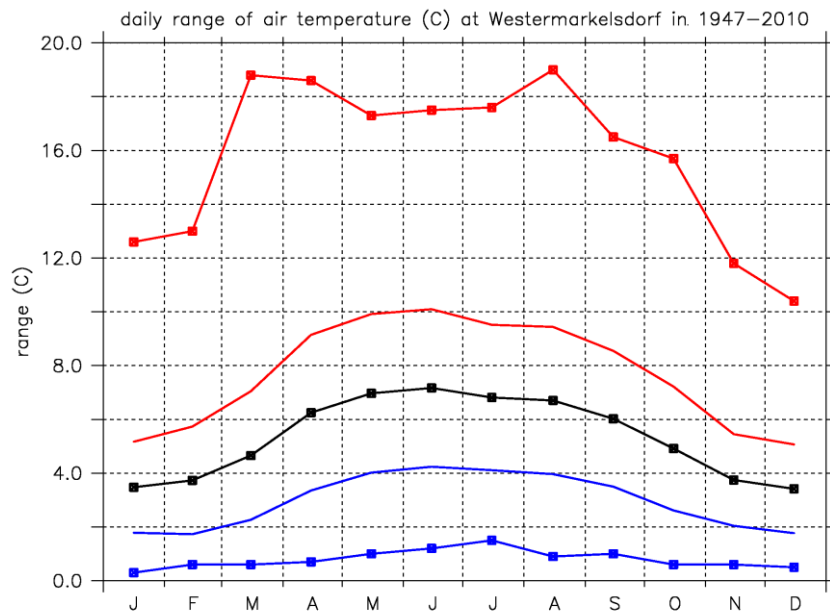


Fig. 5.5 Annual cycle of the daily variation of air temperature (°C) at Westermarkelsdorf. Lines with symbols show monthly minimum (blue), mean (black), and maximum values. Simple lines indicate one standard deviation from the monthly means.

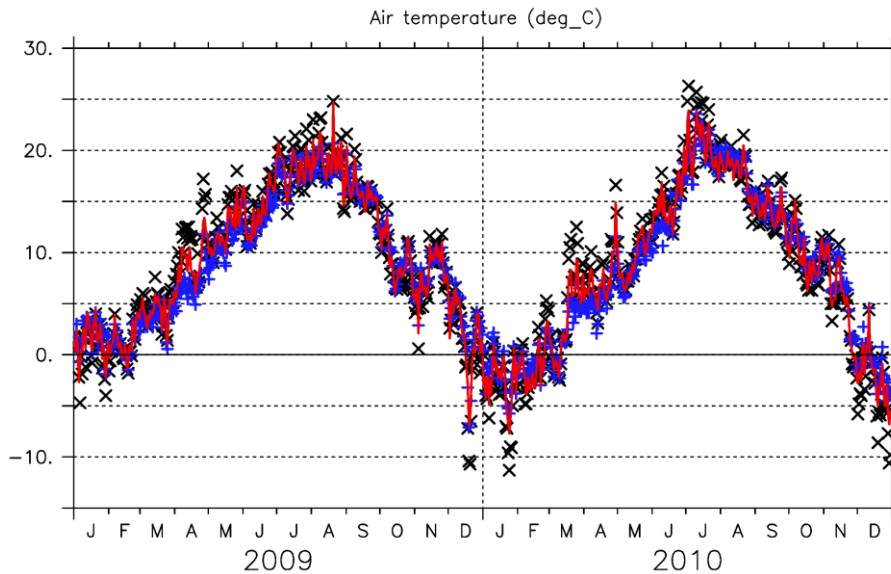


Fig. 5.6 Daily mean air temperature observed at Westermarkelsdorf during the baseline period 2009-2010. Symbols indicate the measurements taken at Warnemünde (black) and Darss Sill (blue).

The daily records of air temperature at Westermarkelsdorf are shown in Fig. 5.6. This time resolution reveals that warming in spring and cooling in autumn proceed with temperature fluctuations around $\pm 5^{\circ}\text{C}$. In comparison to the other available data sets daily temperature variations are more pronounced at Warnemünde (black symbols) but smaller at sea as mentioned above. The warm phase in November 2009, the hot July 2010, and the prevailing frost in January/February and December 2010 are clearly seen as special events during the baseline period. However, the warm April 2009 becomes more evident by monthly mean air temperature, see Fig. 5.4.

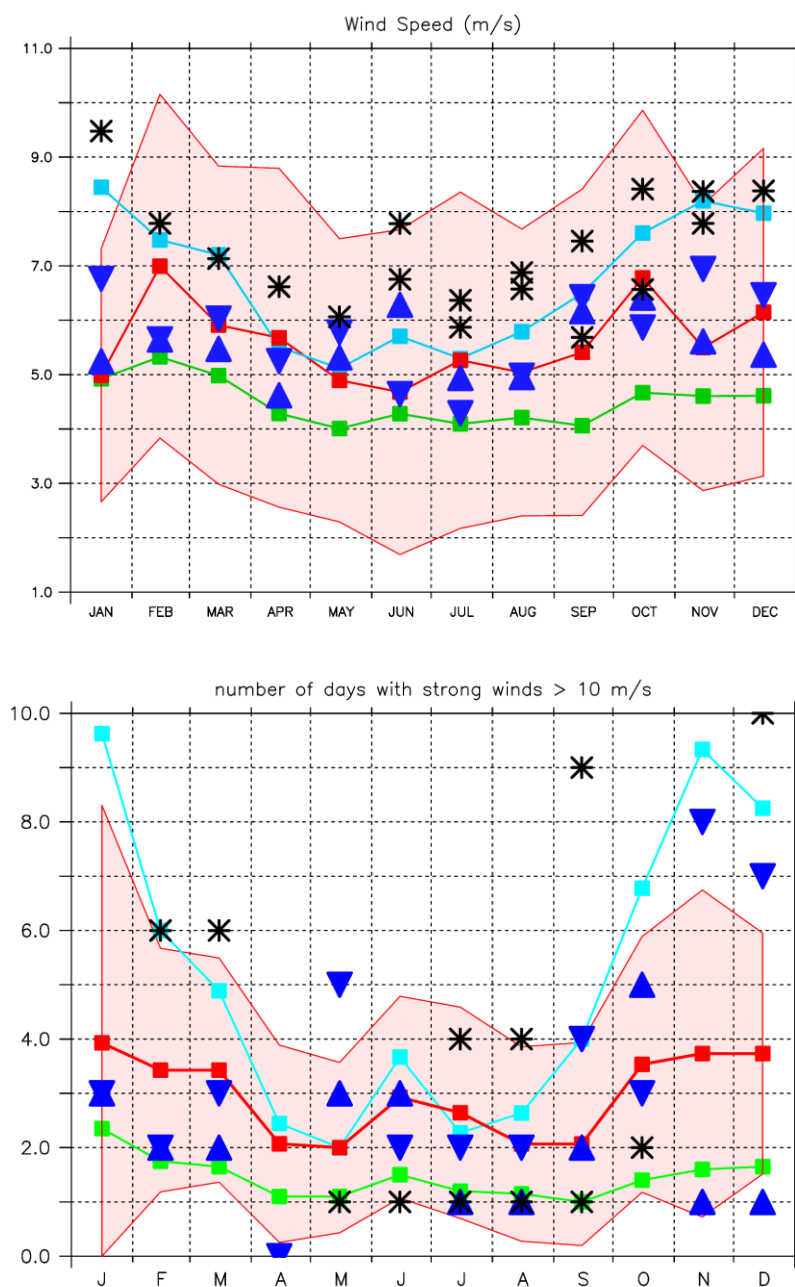


Fig. 5.7 Annual cycle of magnitude of wind speed (m/s) in upper panel, and number of days with strong wind (daily mean > 10 m/s) in lower panel. Coloured lines with small symbols indicate climatological monthly means at Warnemünde (green), Westermarkelsdorf (red) and Darss Sill (cyan), see Table 3.3 and Fig. 3.4. Shaded regions correspond to ± 1 standard deviation. Triangles denote conditions in baseline years 2009 (upward) and 2010 (downward) and star the monthly means at Nysted from June 2004 to November 2005.

The baseline period 2009-2010 was rather normal with respect to mean daily wind speed. With exception of enhanced mean winds in June 2009 the monthly averages are scattered around the long-term means within the range of one standard deviation as is displayed for Westermarkelsdorf in Fig. 5.7. The magnitude of wind speed, which is shown, refers to monthly averages over the absolute values of daily mean wind, i. e. magnitude expresses a mean daily wind speed. This is considered as a more appropriate measure for estimating wind impact on long time scales, since the mean wind vector tends to become small for long-term averages, because of the changing wind directions. Comparison with the other stations shows that



both, mean wind speed and seasonal variation, are generally stronger at open sea, i.e. at Nysted and Darss Sill.

Strong winds are of special importance because the wind stress exerted on the sea surface and on structures increases with the second power of wind speed. That means the wind action doubles if the wind accelerates from 7 to 10 m/s. The wind stress then amounts to approximately 0.2 N/m^2 which generates waves of 1.5 m height in the Fehmarnbelt region, see (Schmager 1979). The limit of 10 m/s was chosen to identify wind events during the baseline period from the daily observations at Westermarkelsdorf as shown in Fig. 5.8.

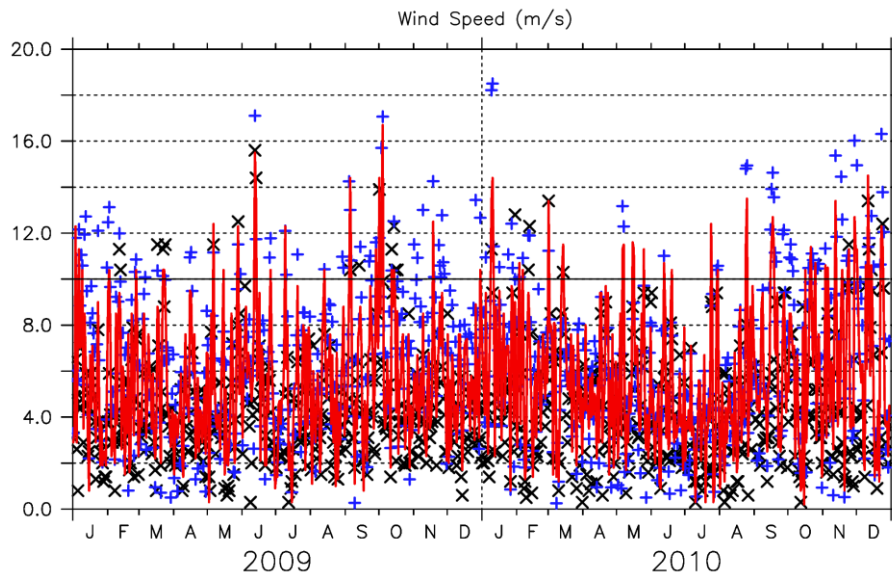


Fig. 5.8 Daily mean wind speed observed at Westermarkelsdorf (red curve). Symbols indicate the measurements taken at Warnemünde (black) and Darss Sill (blue). The limit of 10 m/s, used for identifying strong wind events, is indicated.

Besides the daily mean wind speed also the maximum gusts and the wind direction on the selected days are listed in the monthly overview in Table 5.9 below. Wind gusts above 20 m/s indicate stormy weather. Strong winds came predominantly from westerly and easterly directions. There were only two days in mid-October 2009 with strong wind from the north, a 3-days period with storm from northeast on 9-11 January 2010, and strong to stormy winds from northerly directions from mid-November to December 2010. In total 24 days with strong wind were identified in 2009 and 39 days in 2010, which are comparable with the long-term mean of 36 days per year observed at DWD station Westermarkelsdorf between 1997-2010. Obviously, an enhanced number of days with strong winds were observed in May, November and December 2010, while April, November and December 2009 were rather calm, as seen from the monthly plot in Fig. 5.7.

The distributions of wind directions show also some deviations from the long-term means in 2009-2010, compare for example Fig. 5.2 with Fig. 5.9. The winds at Fehmarn were more focused to westerly directions, especially in case of strong wind events, see Table 5.9. Frequent easterly winds again indicate the channelizing effect of Mecklenburg Bight, however, the storm in January 2010 came from north-east.

Frequency classes of daily wind speed and direction in 2009/2010 at Westermarkelsdorf/Fehmarn

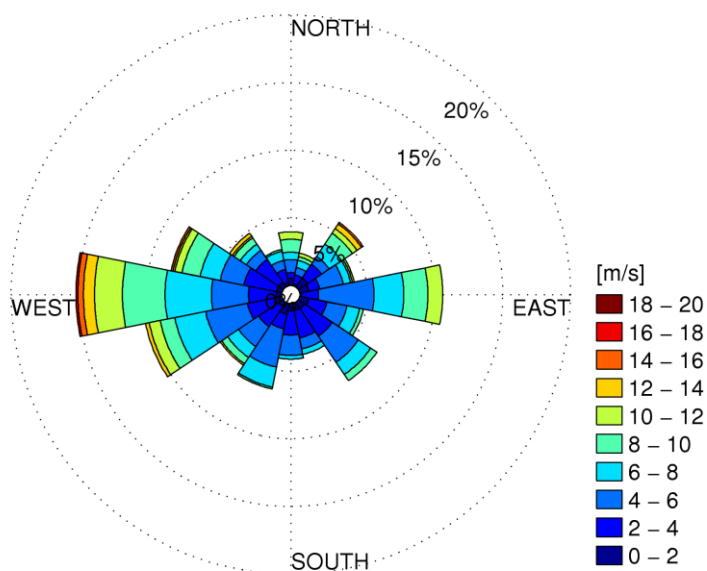


Fig. 5.9 Rose plot of daily mean wind observed in 2009/2010 at coastal station Westermarkelsdorf on Fehmarn island (see Fig. 3.4). Slices show the frequency of wind directions and colours correspond to wind speed.

Frequency classes of daily wind speed and direction in 2009/2010 at Darss Sill

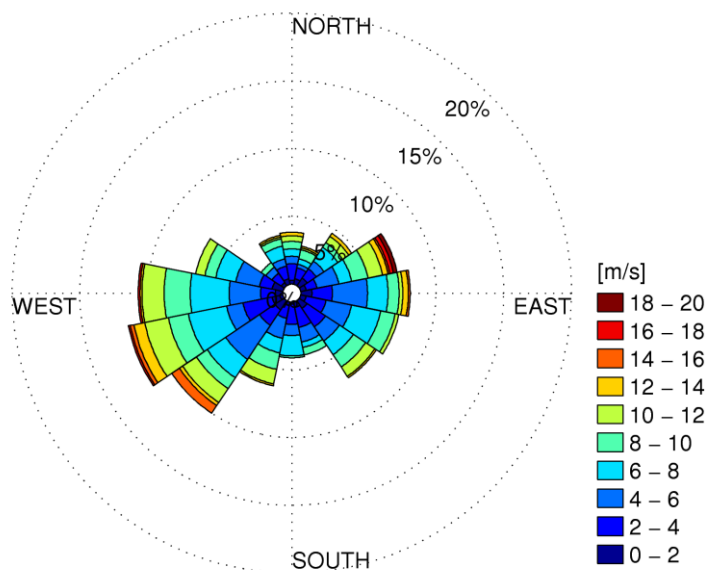


Fig. 5.10 Rose plot of daily wind observed in 2009/2010 at open sea station Darss Sill (see Fig. 3.4). Slices show the frequency of wind directions and colours correspond to wind speed.

From the open sea observations at Darss Sill the directional distribution can be derived from daily averaged measurements, which are displayed in Fig. 5.10. This confirms the high frequency of strong winds from westerly directions and the occurrence of stormy winds from NE during the baseline period. But comparison to daily



means (not shown) reveals that the irregular enhancement of some wind directions, as seen in Fig. 5.9, is an artefact of the averaging.

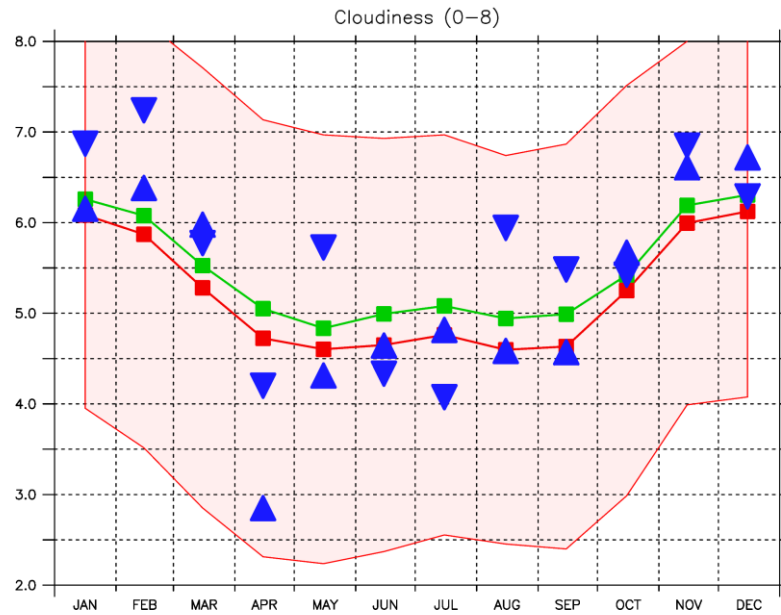


Fig. 5.11 Annual cycle of cloudiness (0-8). Coloured lines indicate climatological monthly means at Warnemünde (green) and Westermarkelsdorf (red), see Table 3.3 and Fig. 3.4. Triangles denote conditions at Westermarkelsdorf in baseline years 2009 (upward) and 2010 (downward).

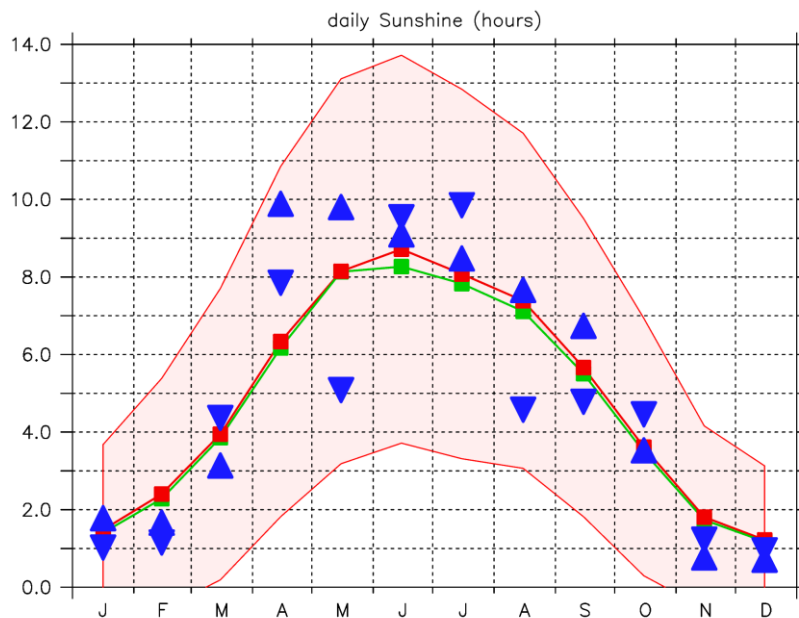


Fig. 5.12 Monthly mean of daily sunshine duration (hours). Coloured lines indicate climatological monthly means at Warnemünde (green) and Westermarkelsdorf (red), see Table 3.3 and Fig. 3.4. Triangles denote conditions at Westermarkelsdorf in baseline years 2009 (upward) and 2010 (downward).

Cloudiness has a clear annual cycle between 6/8 during winter (November till February) and 5/8 in summer (April till September), which is shown in Fig. 5.11. Extraordinary clear conditions were observed during April 2009. The extended cloud cover in May and August 2010 was accompanied by high precipitation, see Fig. 5.13 below.

The duration of daily sunshine shows a regular annual variation corresponding to changing day length reaching its maximum in June, cf. Fig. 5.12, which is modified by the amount of cloud cover. Near overcast conditions reduce the monthly means to approximately 2 hours during November till February, while sunshine can last for more than 12 hours on bright summer days. The monthly means are around 8-9 hours since cloudy days also occur in summer.

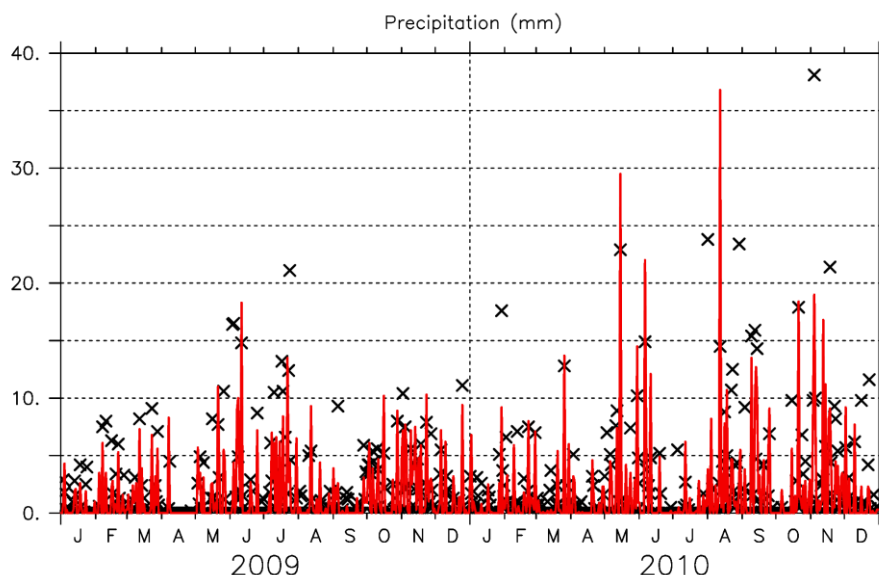


Fig. 5.13 Daily precipitation (mm) observed at Westermarkelsdorf (red curve) and Warnemünde (black symbols) during the baseline period 2009/2010.

Precipitation within the baseline period is presented on daily time scale in Fig. 5.13, showing that typical events yield around 5 mm/day and that 10 mm/day are rarely exceeded, see basic statistics in Table 5.8. On average precipitation occurs half of the time but the sequence is rather irregular. Comparison to nearby Warnemünde, indicated by symbols, shows that precipitation also varies considerably on the spatial scale. Because of that the mean annual cycle is weak and superposed by large fluctuations. Therefore, the monthly picture is not shown, but monthly precipitation is noticed qualitatively in Table 3.3.

Finally, the monthly distribution of relative humidity is shown in Fig. 5.14, which indicates a difference of the annual cycle over land and sea. The coastal stations at Westermarkelsdorf and Warnemünde show a decrease in spring, a seasonal minimum in early summer (May/June), and an increase in autumn, whereas humidity is high in spring and low in autumn at open sea. With respect to the long-term means humidity was low in autumn 2009 and during the warm July 2010.

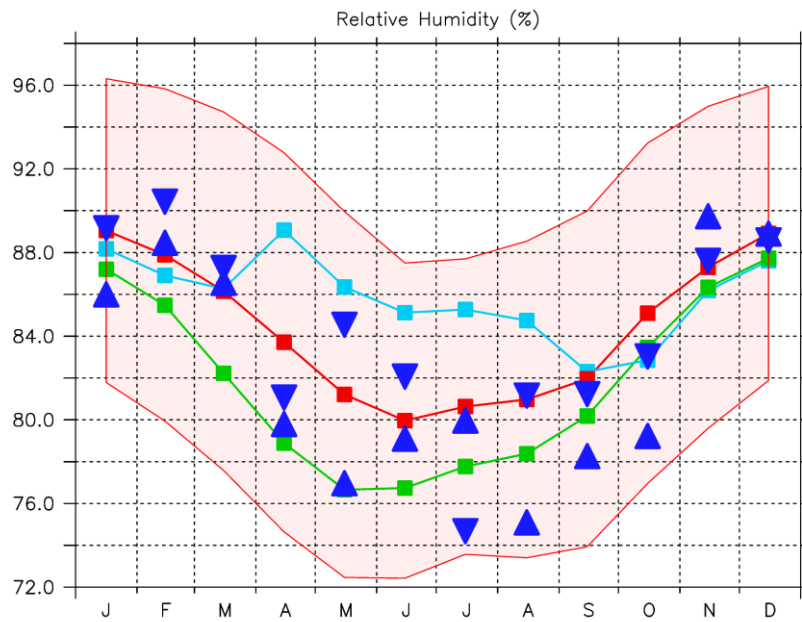


Fig. 5.14 Annual cycle of relative humidity (%). Coloured lines with small symbols indicate climatological monthly means observed at Warnemünde (green), Westermarkelsdorf (red) and Darss Sill (cyan), see Table 3.3 and Fig. 3.4. Triangles denote conditions at Westermarkelsdorf in baseline years 2009 (upward) and 2010 (downward).

5.3 Summary

In summary the overview of deviations from the long-term means, as collected in Table 5.9, show that most weather conditions were on average during the baseline period in 2009-2010.

January 2009 was dry with a monthly sum of precipitation of 15 mm. April 2009 was warm and very dry due to intensive irradiation through low cloud cover (monthly mean around 35% instead of 60%). June 2009 showed an enhanced wind speed on monthly time scale but only two days with strong wind above 13-15 m/s, which are comparable with stormy periods in beginning of October 2009 and in January 2010. November 2009 brought exceptionally low air pressure accompanied by relatively warm air and prevailing precipitation summing up to 87 mm. January and February were cold with a period of strong winds on 9-11 January 2010 and low air pressure during February, but medium precipitation around 30 mm. However, precipitation came down as snow accumulating from December 2009 to February 2010 leading to heavy snow conditions which were not observed since the 1980ies. May and August in 2010 showed enhanced cloudiness of 70-75% with heavy precipitation events of 29 and 37 mm/daily. November 2010 was comparable to 2009 with similar low mean air pressure around 1004 hPa, mean cloudiness of 7/8 and the highest monthly precipitation in the baseline period of 110 mm. Despite the average air temperature of 5.5 C precipitation was mostly snow in the end of November. In December 2010 began the early onset of the next strong winter season. The monthly mean air temperature of -2 C, which corresponds to January 2009, is distinctly below the long-term standard deviation range as seen in Fig. 5.4. Snow conditions became critical already in December.

The frosty and snowy winters were the most exceptional weather phenomenon observed during the baseline periods. The main difference between both winter seasons is the high number of days with strong winds in November and December 2010 in contrast to 2009.



Table 5.9 Monthly weather conditions observed at Westermarkelsdorf by Deutscher Wetterdienst (DWD) during baseline period 2009-2010. Besides wind events above 10 m/s only deviations from long-term averages are noted.

year	month	daily wind events				monthly tendency				
		days	mean (m/s)	max. (m/s)	direction	air press.	air temp.	cloud cover	rel. hum.	precipitation
2009	Jan	3/6/9	10-12	16-20	W					dry
	Feb	2	10	17	E					
		26	10	17	W					
	Mar	22/23	10	17-18	W					
	Apr						warm	low		dry
	May	6	12	21	WNW	high			low	
		15	10	17	E					
	Jun	28	12	19	NW					
		12/13	13-15	22-24	W					
	Jul	26	10	17	E					
		9	12	18	W					
	Aug	13	10	18	W				low	dry
5		14	20	W	high				dry	
Sep	28	11	18	W						
	1/3/4	12-17	23-25	W/SW				low		
Oct	12/14	10	16-18	N						
	18	13	29	WSW	low	warm			wet	
Dec	30	10	18	E						
2010	Jan	9-11	10-14	17-24	NE		cold	high		
	Feb	3	11	22	WSW	low	(cold)	high		snow
		6	10	16	E					
	Mar	1	13	20	W					
		13/14	10-11	17-20	W/WNW					
	Apr					high				
	May	6/7	11	18	E/ENE	high		high	high	wet
		15/16	11-12	19	WNW/W					
	Jun	25	11	18	W					
		12	11	18	W					
	Jul	19	10	21	WSW					
		24	12	17	NW		warm		low	dry
	Aug	30	10	17	W					
		24/25	11-13	22-23	WSW/W			high		wet
Sep	15/18	10-13	19-22	WSW/W					wet	
Oct	16	10	17	NE						
	21	11	23	W						
	25	10	22	WNW						
Nov	3/5	10		W	low				wet	
	12	13		WSW						
	18	10	16	E						
	23/24	10-11	16-17	N-NW						
Dec	29/30/1	11-13	19-24	NE-E						
	9/11/12/14	10-14	15-22	NW-N		cold			snow	
	23-24	11-12	18	NE						



6 HYDROGRAPHIC BASELINE OBSERVATIONS

The presented data and analyses are based on the monitoring and modelling undertaken in the baseline period 2009-2010. It is divided into:

- Water level;
- Waves;
- Current;
- Salinity and temperature; and finally
- Sea ice.

In the following each measured parameter is basically treated by itself. Relationships between the parameters are provided in Chapter 7 (it includes and presents survey measurements).

6.1 Water Level

Measured water level time-series at stations close to Fehmarnbelt are shown in Fig. 6.1 to Fig. 6.3. The observations cover the baseline period.

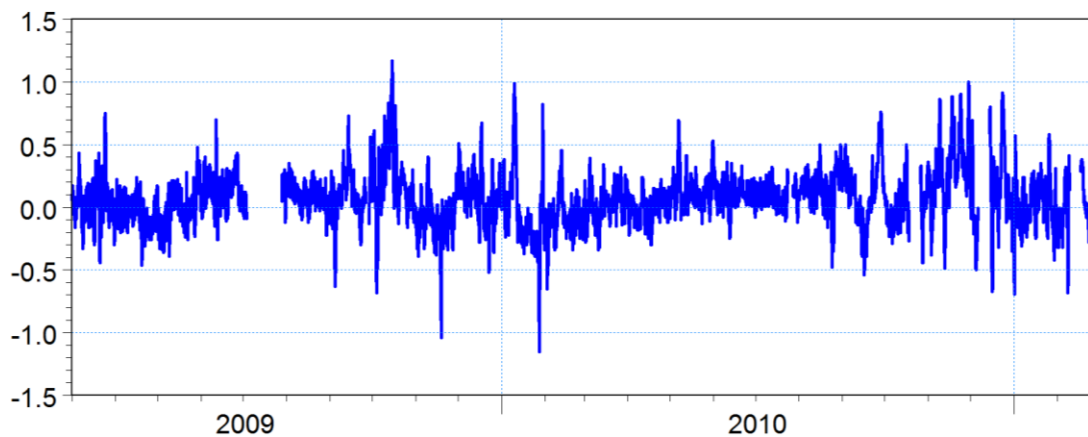


Fig. 6.1 Measured water level (m) at Warnemünde station.

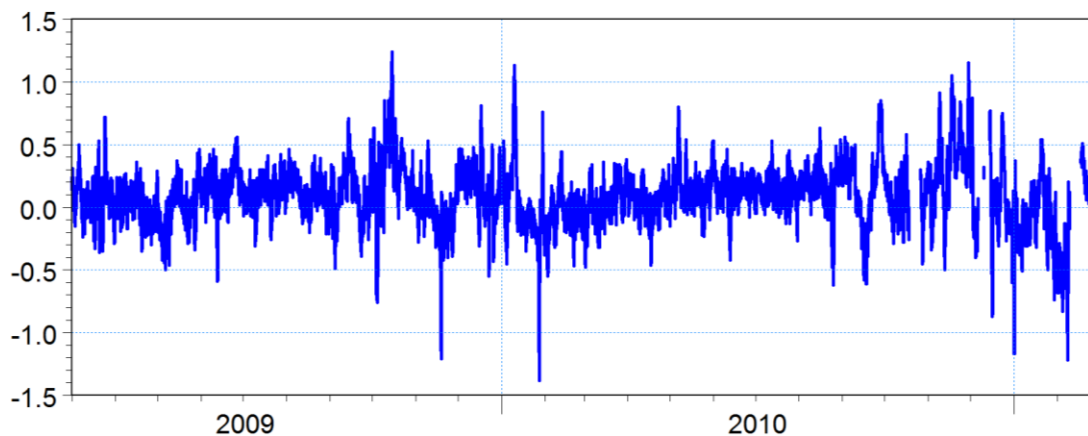


Fig. 6.2 Measured water level (m) at Gedser station.

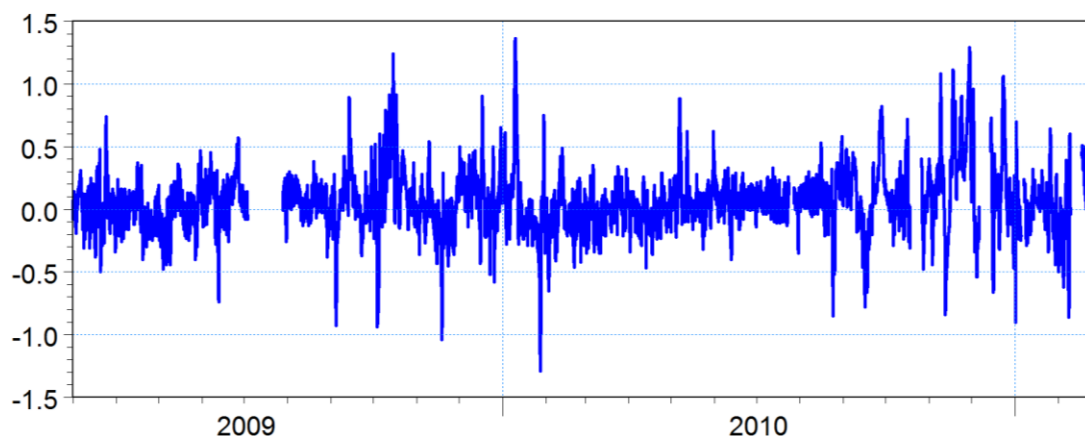


Fig. 6.3 Measured water level (m) at Kiel-Holtenau station.

Rapid variations caused by changing wind fields, seiching and tides are observed in the data. The water level varies on the same tide-scale as the air pressure fields and tides (from 6 hours to some days).

The measured water levels typically stay within the range from -0.5 m to +0.5 m.

Some high and low water levels are observed in the time-series. These high and lows are caused by storms passing Scandinavia. Most of them are found in the period from September to February.

Simulated water level distributions and derived statistical parameters are shown for the period 1 January 2009 to 30 September 2009. The simulation results are extracted from a MIKE Local model simulation.

Fig. 6.4 and Fig. 6.5 show mean and maximal water levels in Belt Sea and around Fehmarnbelt in the simulated period.

At two locations close to Puttgarden and Rødbyhavn water level time-series are extracted, see Fig. 6.6.

Statistics for these two locations can be found in Table 6.1. Slightly higher mean water level (+2 cm) and standard deviation (+1 cm) are found at Rødbyhavn, whereas maximal and minimal values are higher at Puttgarden (+3 cm and -6 cm).

Table 6.1 Statistical parameters for simulated water levels at Puttgarden and Rødbyhavn in the period 1 January 2009 to 30 September 2009.

Water level	Puttgarden (m)	Rødby (m)
Mean	0.04	0.06
STD	0.16	0.17
Min	-0.80	-0.74
Max	0.68	0.65

These data are reflected in the histogram of water levels (Fig. 6.7) where a slightly flatter and broader distribution at Rødbyhavn can be seen.

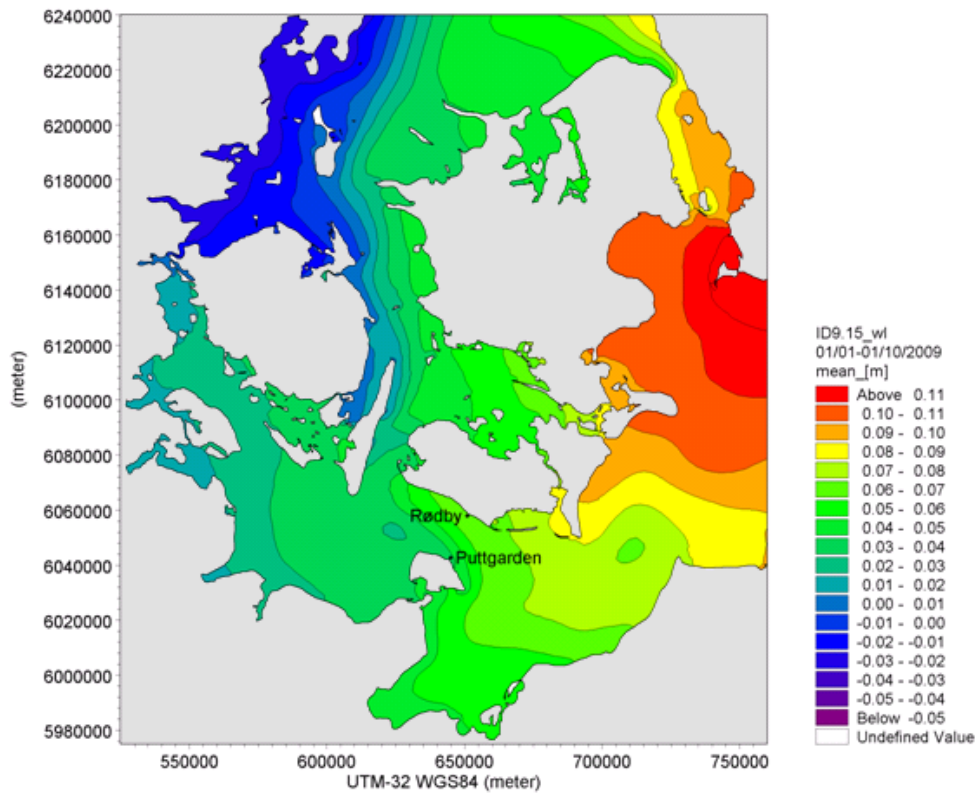


Fig. 6.4 Mean simulated water levels in the Belt Sea in the period 1 January 2009 to 30 September 2009.

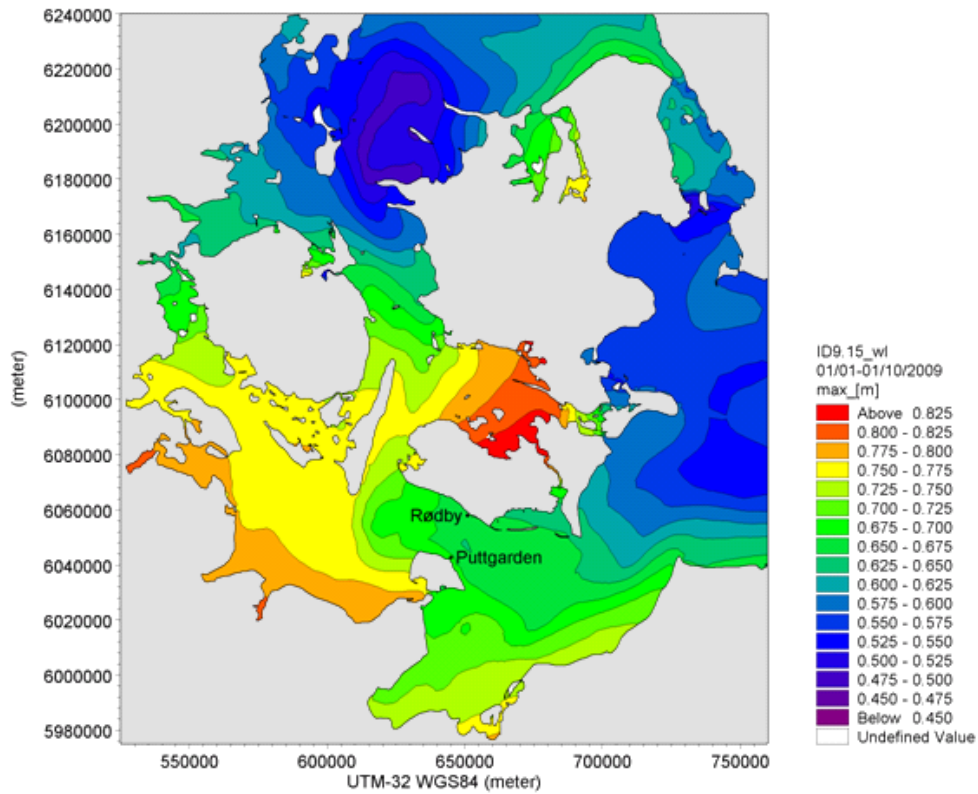


Fig. 6.5 Maximal simulated water levels in the Belt Sea in the period 1 January 2009 to 30 September 2009.

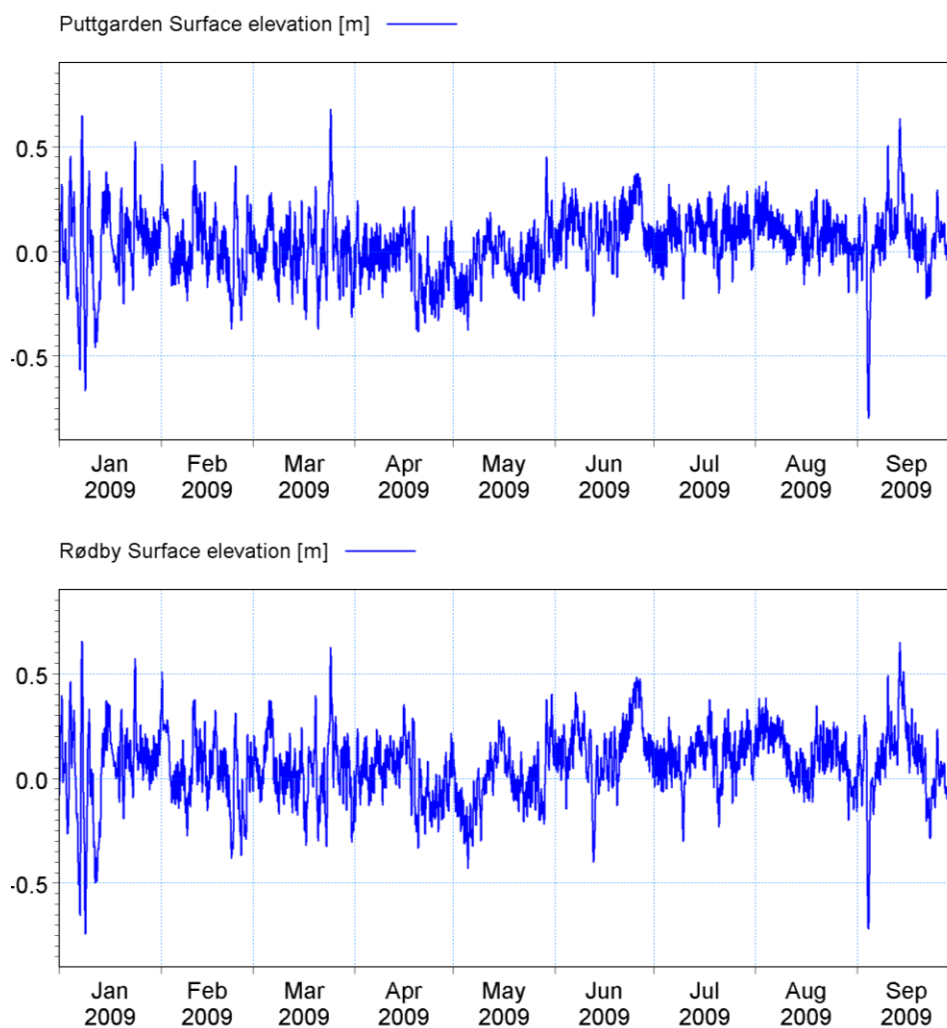


Fig. 6.6 Simulated water level time-series close to Puttgarden and Rødbyhavn.

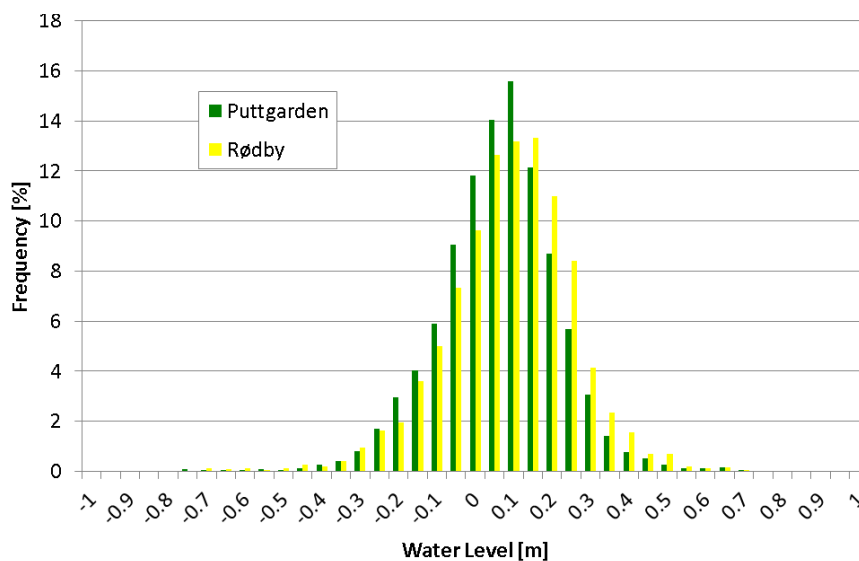


Fig. 6.7 Histogram based on simulated water levels at Puttgarden and Rødbyhavn in the period 1 January 2009 to 30 September 2009.



6.2 Waves

Waves in the Fehmarnbelt area are governed primarily by the local wind conditions and the fetch limitations due to land such as Fehmarn to the South, Lolland to the North, Falster and Mecklenburg-Vorpommern to the ESE and Langeland and Schleswig-Holstein to the west. However, occasionally waves from the south eastern Baltic Sea (Arkona Basin) may contribute to the wave climate in the Fehmarnbelt area.

The following assessment of wave conditions in the Fehmarnbelt area is based on a combination of local wave measurements and results of numerical wave modelling:

- The wave measurements are adopted from the bottom mounted ADCP's at the Fehmarnbelt main stations MS01 and MS02, and applied for detailed assessment of the local wave conditions at the locations of deployment; and
- Wave model data is adopted from the FEHY coastal morphology baseline study (FEHY 2013b) and applied to assess the geographical variability. A short description of the wave model is included as Appendix B in this report.

The wave conditions at MS01 and MS02 are representative of the local offshore waves in the Fehmarnbelt. The ADCP's have been deployed since March 2009 (and remain deployed at time of writing, June 2011), and provides 1-hourly values of integral wave parameters:

- Significant wave height (H_{m0});
- Peak wave period (T_p);
- Mean wave period (T_{01}); and
- Mean wave direction (MWD)) based on 20 minutes measurements.

Time-series covering 1 year (2009-05-01 – 2010-05-01) of the integral parameters at MS01 and MS02 are presented in Fig. 6.8.

It is seen that the wave conditions in Fehmarnbelt are generally mild. The mean significant wave heights during the presented 1 year period are 0.57 m and 0.52 m at MS01 and MS02, respectively, and the maximum significant wave heights are 2.37 m and 2.49 m. The waves are short with over 90% of the mean wave periods below 4.0 s and peak wave periods generally less than 6.5 s.

Wave roses at MS01 and MS02 are presented in Fig. 6.9, showing that the dominant wave direction at MS01 is W-WNW, i.e. more or less perpendicular to the link corridor. However, a significant fraction of waves occurs also from the SE directions. The conditions at MS02 are very similar to those at MS01, except that the dominant directions are shifted to respectively WNW and ESE. Waves from NNE and SSE are low in amplitude and occur infrequently.

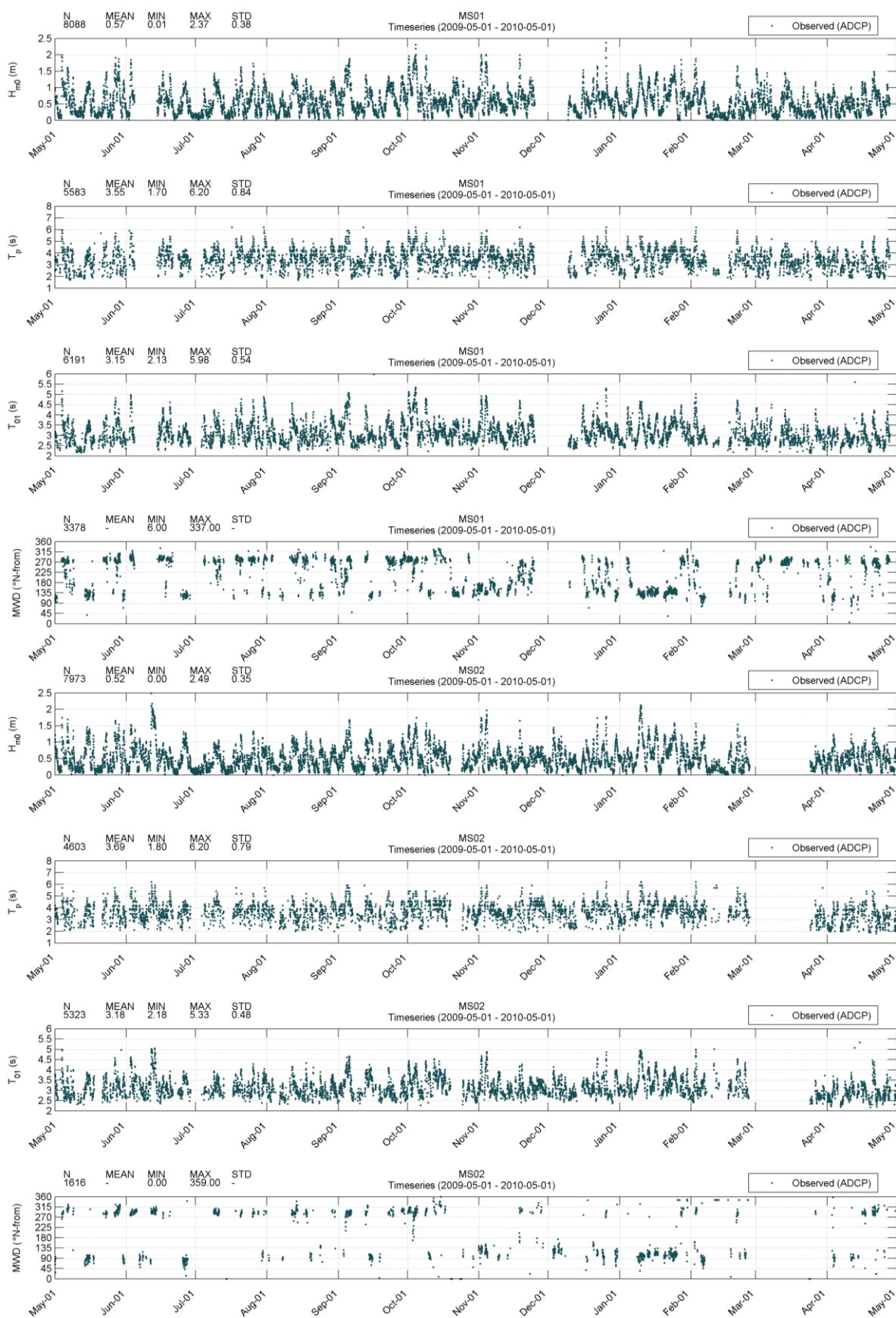


Fig. 6.8 Time-series of H_{m0} , T_p , T_{01} and MWD at MS01 (top) and MS02 (bottom).

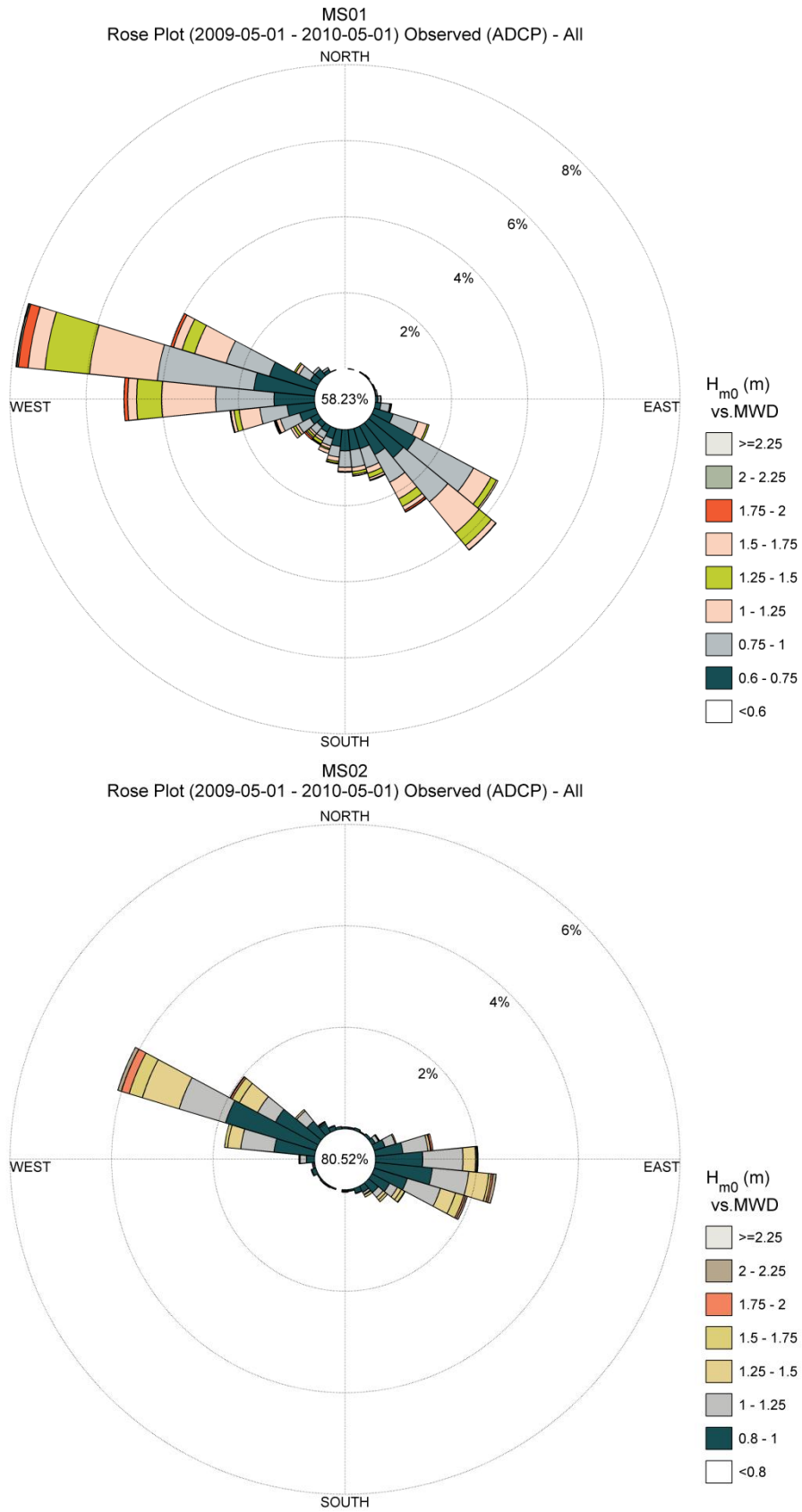


Fig. 6.9 Wave roses at MS01 (top, $H_{m0} > 0.60$) and MS02 (bottom, $H_{m0} > 0.80$).

Fig. 6.10 shows scatter diagrams of H_{m0} vs. T_p , T_{01} and wind speed (U_{10}) at both stations. Wind was not measured at the main stations, MS01 and MS02, and wind speed data is therefore adopted from the WATCH-EN5 meteorological model data set (FEHY 2013b). Due to the dominance of locally generated wind-waves in Fehmarnbelt there is a strong correlation between wind speed and wave height and between wave period and wave height as seen from the scatter diagrams. The conditions are generally similar at MS01 and MS02 with respect to wave heights and periods.

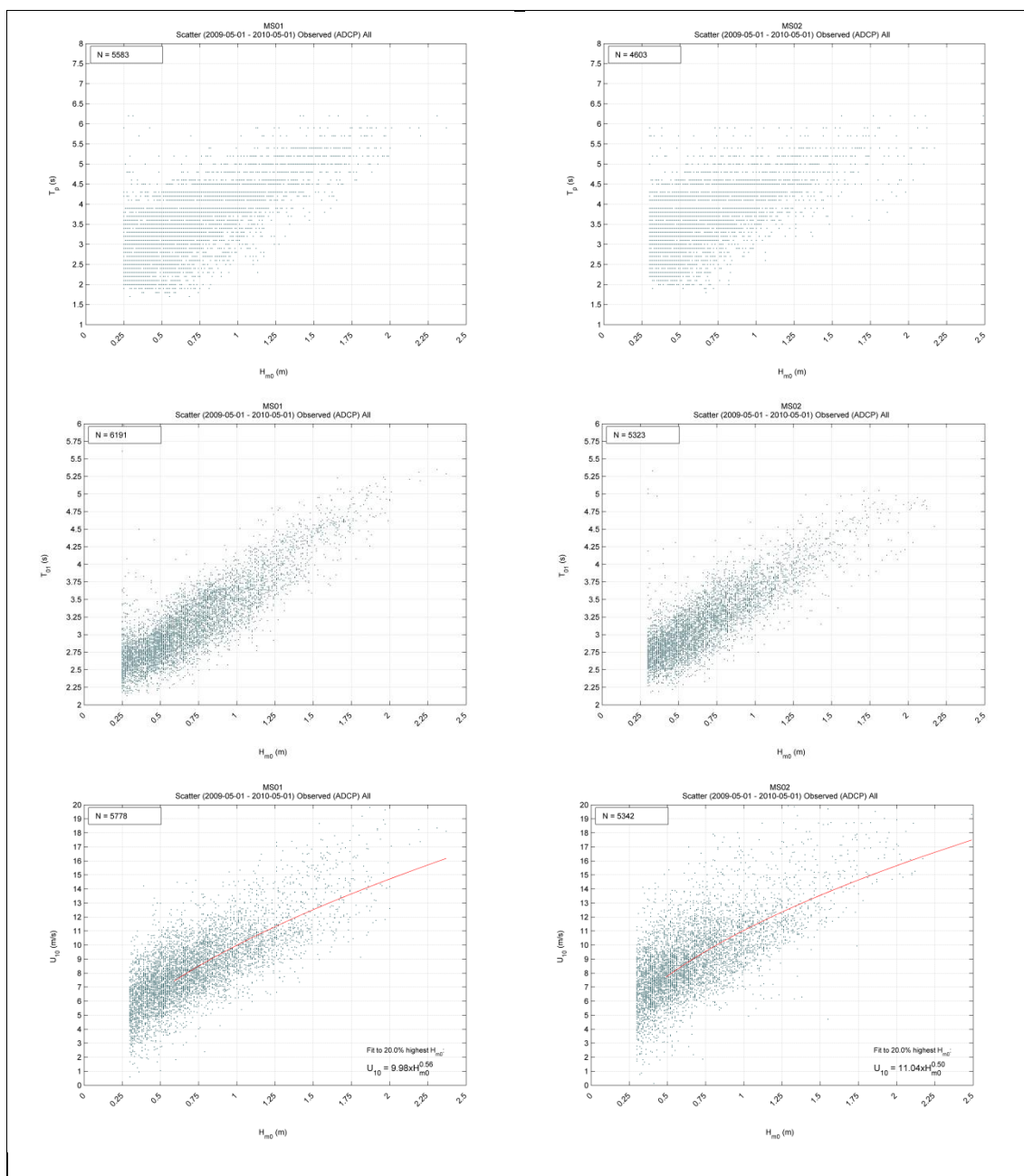


Fig. 6.10 Scatter diagrams of H_{m0} vs. T_p , T_{01} and U_{10} at MS01 (left, $H_{m0} > 0.25$) and MS02 (right, $H_{m0} > 0.30$).

Exceedance diagrams of H_{m0} , T_p and T_{01} are shown in Fig. 6.11 showing e.g. that a significant wave height of 1 m is exceeded about 15% of the year. As seen from the time-series, this occurs primarily during autumn and winter, i.e. during periods of



stronger wind speeds. The mean and peak wave periods associated with a 1 m significant wave height are typically $T_{01} \sim 3.0 - 4.0$ s and $T_p \sim 4.5 - 5.0$ s, cf. Fig. 6.10.

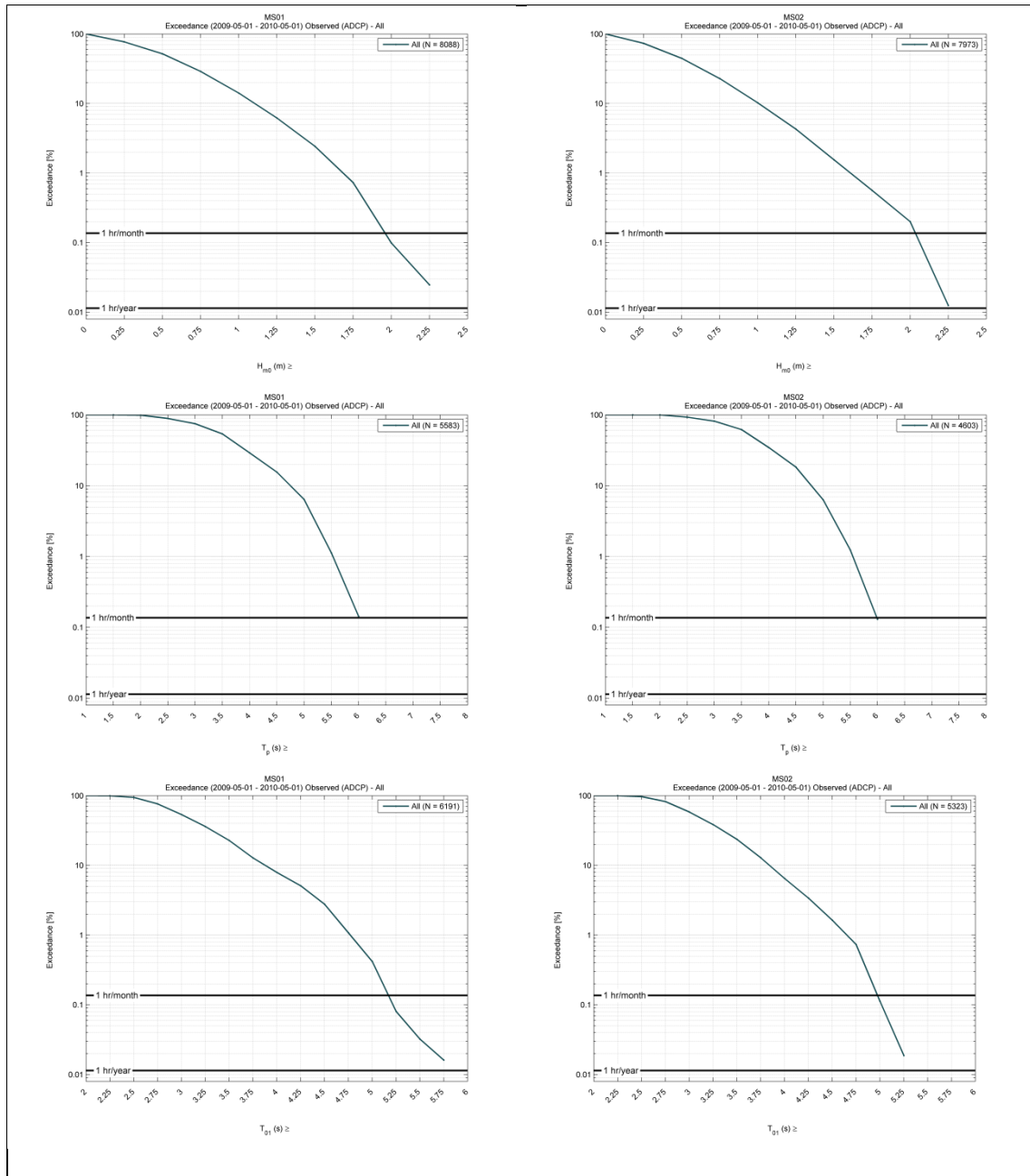


Fig. 6.11 Exceedance diagrams of H_{m0} , T_p and T_{01} at MS01 (left, $H_{m0} > 0.25$) and MS02 (right, $H_{m0} > 0.30$).

Wave model data covering the entire Fehmarnbelt was obtained by simulation of time and space varying wave fields applying the numerical spectral wave model, MIKE 21 SW. MIKE 21 SW is a third generation spectral wind-wave model that simulates the growth, decay and transformation of wind generated waves and swells in offshore and coastal areas. The wave model data presented below is adopted from the FEHY coastal morphology baseline study (FEHY 2013b).

Examples of wave patterns in Fehmarnbelt for the two dominant directions (westerly and easterly) are shown in Fig. 6.12 and Fig. 6.13. Going from deep water to shallow water the waves are transformed due to bottom friction effects (such as shoaling and refraction) and due to different fetch and wind conditions.

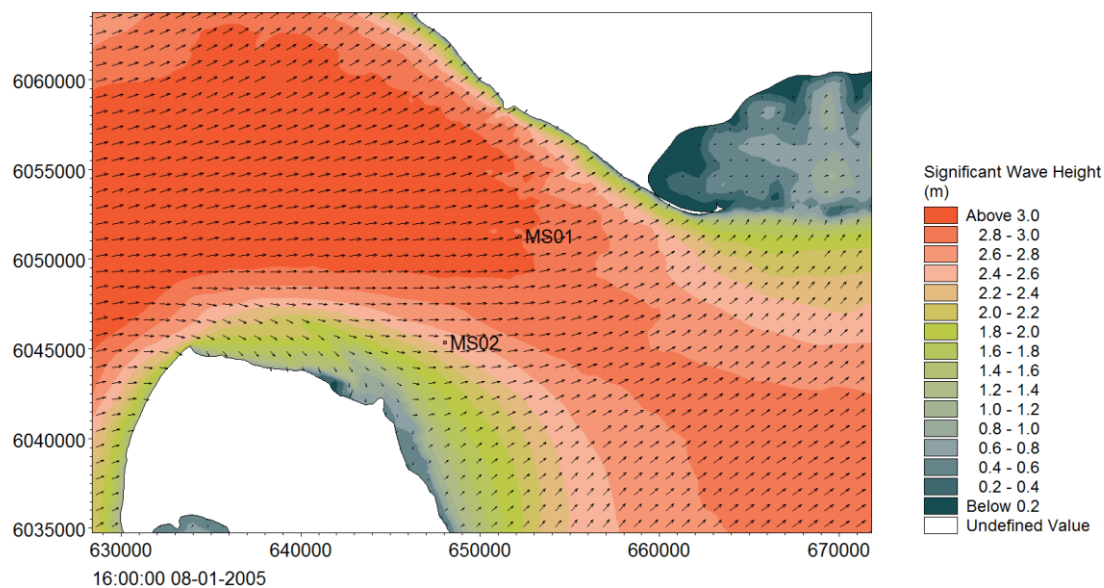


Fig. 6.12 Example of westerly wave pattern in Fehmarnbelt. Date: 08.01.2005.

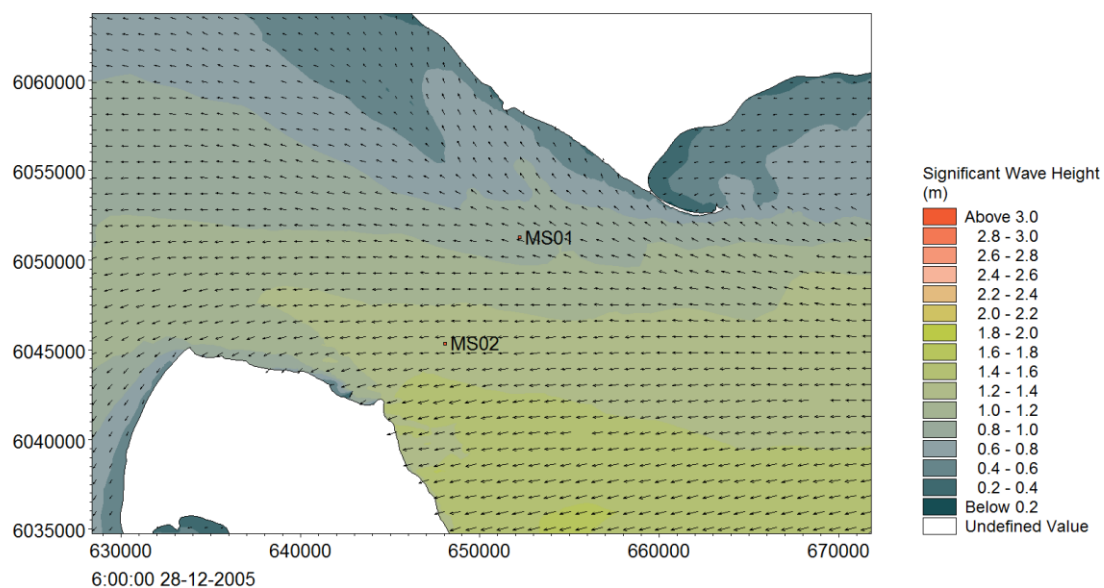


Fig. 6.13 Example of easterly wave pattern in Fehmarnbelt. Date: 28.12.2005.

6.3 Current

The mean measured current profile at MS02 shows that the maximum current speeds are reached at the surface while bottom friction and baroclinic pressure reduces current speeds near the bottom (Fig. 6.14).

The mean current is outwards towards the North Sea in the upper 15 m and inwards towards the Baltic Sea below 15 m depth. This vertical current distribution has opposite current directions in the upper surface layer and in the lower bottom layer.



The current in the Fehmarnbelt is affected by the vertical stratification that can decouple the upper and lower layers. During outflow conditions the outflow is restricted to the upper part of the water column, whereas the dense saline lower part may show insignificant currents or even reversed flow.

The stratification also acts to reduce the flow resistance as it reduces the turbulence at the interface between the upper and lower layer, thus reducing the flow friction. Furthermore, it creates the separation of the upper and lower layer that can contribute to the development of oxygen depletion in the bottom waters.

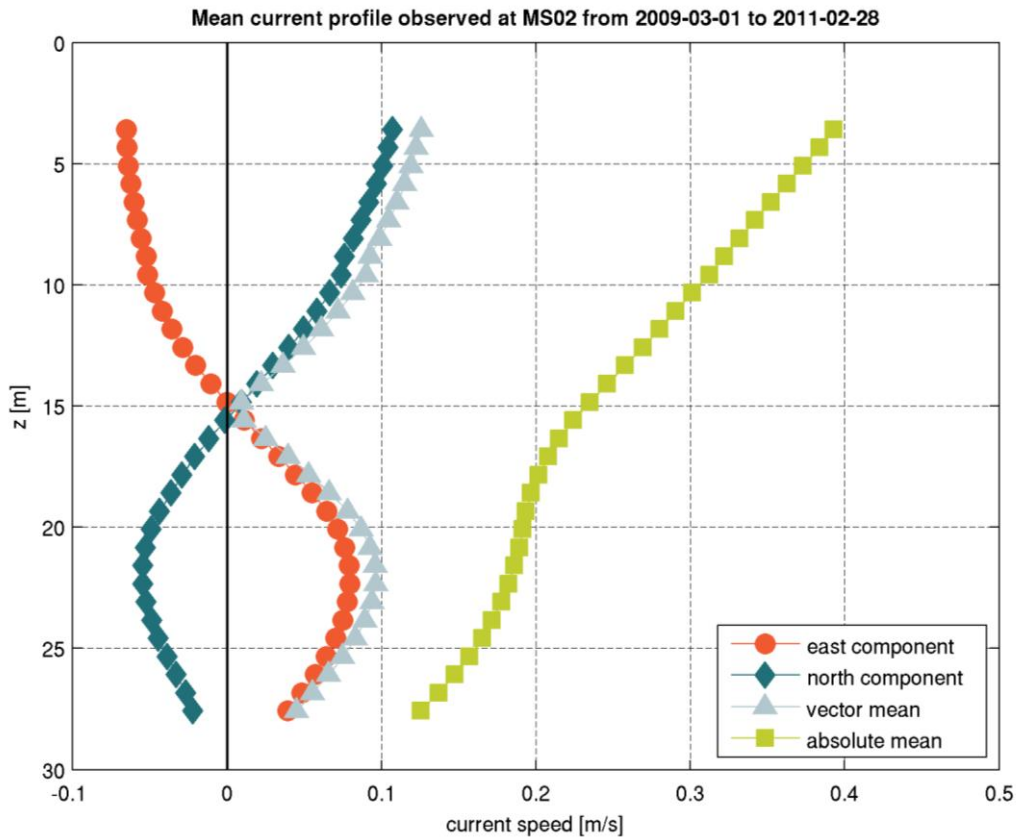


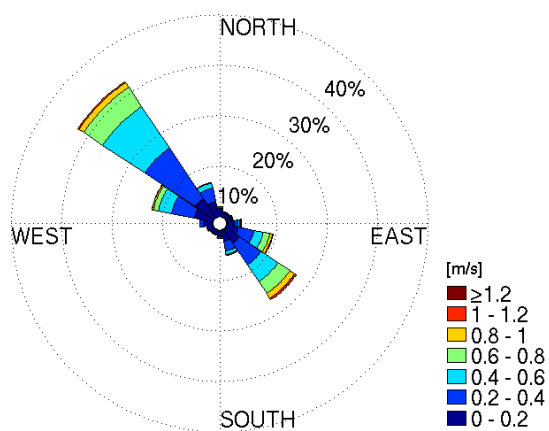
Fig. 6.14 Measured mean current profile at MS02 during the baseline period. Inflow with a south-westerly current dominates below 15 m depth. Maximum current speeds are reached at the surface while bottom friction reduces current speed near the bottom.

Current roses for the three main stations in Fehmarnbelt are shown in Fig. 6.15, Fig. 6.16 and Fig. 6.17.

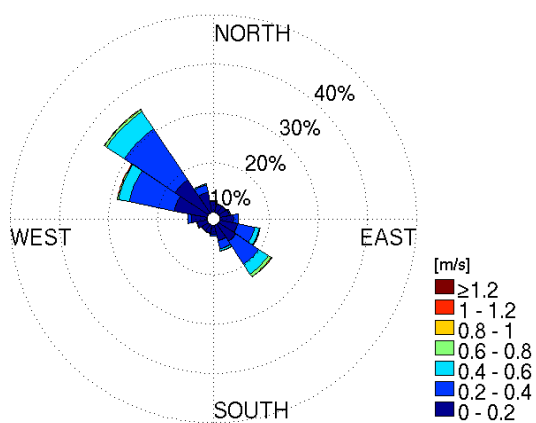
The current speeds are highest in the uppermost level and lowest in the lowermost level. The current rose shown in Fig. 6.16 is based on measurements collected in the biggest water depth and clearly shows a reversed current closer to the sea bed.

The current roses for MS01 and MS02 in the Fehmarnbelt show that the currents follow the direction of the Fehmarnbelt channel. I.e. the currents are influenced by the bathymetry and geometry of coastlines. The mean surface speed is 0.34 m/s at MS01 and the maximum hourly speed monitored is 1.36 m/s. The current rose for MS03 in the more open Mecklenburg Bight area shows less pronounced main directions. I.e. the currents are less influenced by the bathymetry and geometry of coastlines and the current speeds are lower than in the Fehmarnbelt.

Frequency classes of 2009-2011 Fehmarnbelt observed velocity at MS01 in 5.08 m depth. $\Delta t=10$ min



Frequency classes of 2009-2011 Fehmarnbelt observed velocity at MS01 in 12.58 m depth. $\Delta t=10$ min



Frequency classes of 2009-2011 Fehmarnbelt observed velocity at MS01 in 18.58 m depth. $\Delta t=10$ min

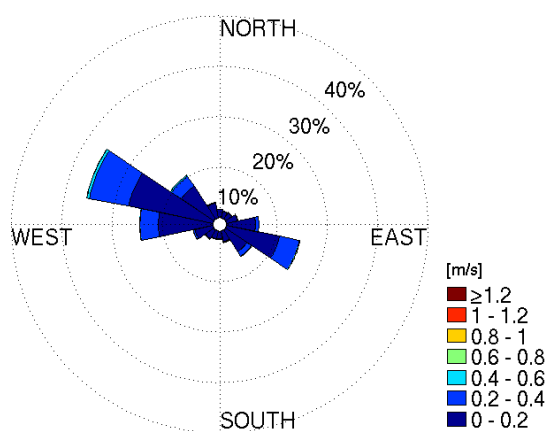
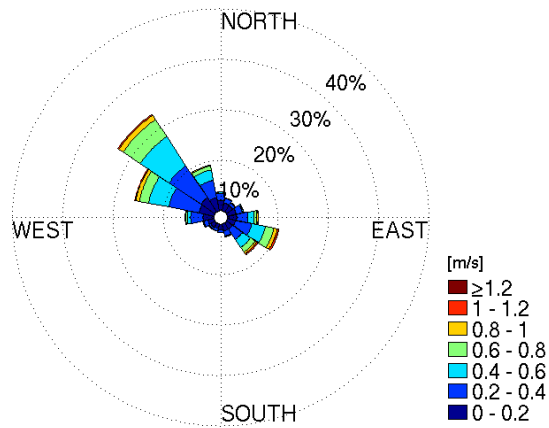


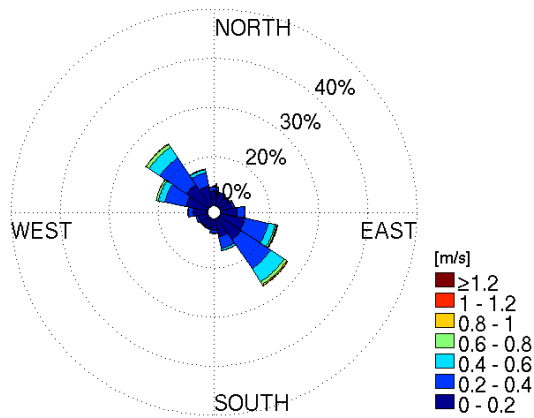
Fig. 6.15 Current roses based on measured current at MS01. The roses are shown in the three levels 5.08 m, 12.58 m and 18.58 m.



Frequency classes of 2009-2011 Fehmarnbelt observed velocity at MS02 in 5.08 m depth. $\Delta t=10$ min



Frequency classes of 2009-2011 Fehmarnbelt observed velocity at MS02 in 15.58 m depth. $\Delta t=10$ min



Frequency classes of 2009-2011 Fehmarnbelt observed velocity at MS02 in 27.58 m depth. $\Delta t=10$ min

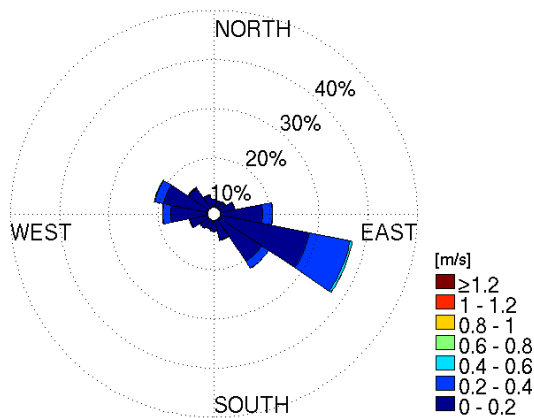
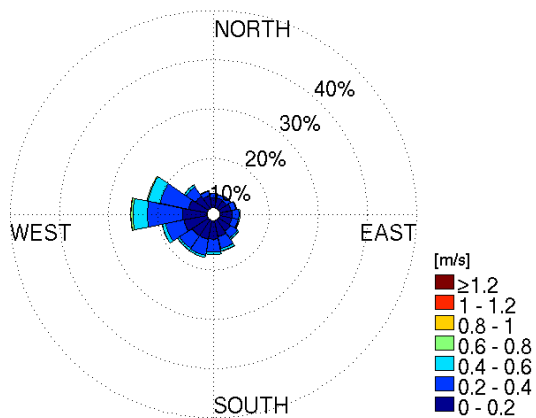
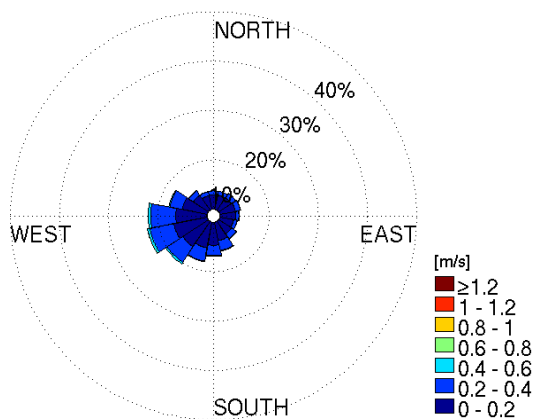


Fig. 6.16 Current roses based on measured current at MS02. The roses are shown in the three levels 5.08 m, 15.58 m and 27.58 m.

Frequency classes of 2009-2011 Fehmarnbelt observed velocity at MS03 in 5.03 m depth. $\Delta t=10$ min



Frequency classes of 2009-2011 Fehmarnbelt observed velocity at MS03 in 12.53 m depth. $\Delta t=10$ min



Frequency classes of 2009-2011 Fehmarnbelt observed velocity at MS03 in 23.03 m depth. $\Delta t=10$ min

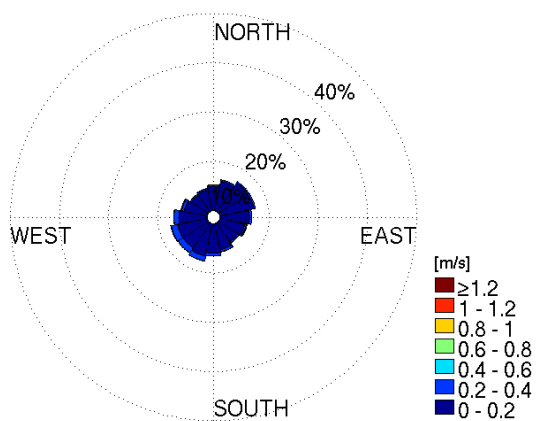


Fig. 6.17 Current rose based on measured current at MS03. The roses are shown in the three levels 5.03 m, 12.53 m and 23.53 m.



The 1-hour average current speed and direction at the three main stations in three levels are shown in Fig. 6.18 to Fig. 6.26. The three levels are the same as for the current roses. An idea about the data coverage, the ranges and the rapid variation of the currents can be seen, but not detailed short-term variation. Such details are presented in later figures.

The data coverage is high at all three stations and in all three cases more than 90% of time.

In the Fehmarnbelt the directional variation shows longer periods of either inflow or outflow at uppermost levels than in the lower levels. In the lowest levels it is difficult to separate in- and outflow events.

Frequent short-periods with high current speeds are observed and these events are found during all four seasons of the year. The maximum 1-hour averaged current speed is typically about 1 m/s in the Fehmarnbelt.

Current direction at MS01 in the northern Fehmarnbelt has two major directions near the surface of about 320° and 135° , and directional shifts within hours to days are very common (Fig. 6.18). These directional preferences are still found at an intermediate depth of 12.58 m (Fig. 6.19), but they are not as prominent near the bottom (Fig. 6.20) where the shifts between inflowing and outflowing water masses are the most frequent.

Station MS02 in the southern Fehmarnbelt also shows two main directions near the surface (Fig. 6.21) but already at the intermediate depth of 15.58 m the shifts in current direction begin to blur the bands of the two main directions (Fig. 6.22). Near the bottom the current direction is again too unstable to observe any preferred directions in the hourly time-series (Fig. 6.23).

In the Mecklenburg Bight at station MS03 the currents are generally circulating at all depth levels without any directional preference (Fig. 6.24 to Fig. 6.26). The only feature is a dominant outflow into various westward directions from near the surface to intermediate depths.

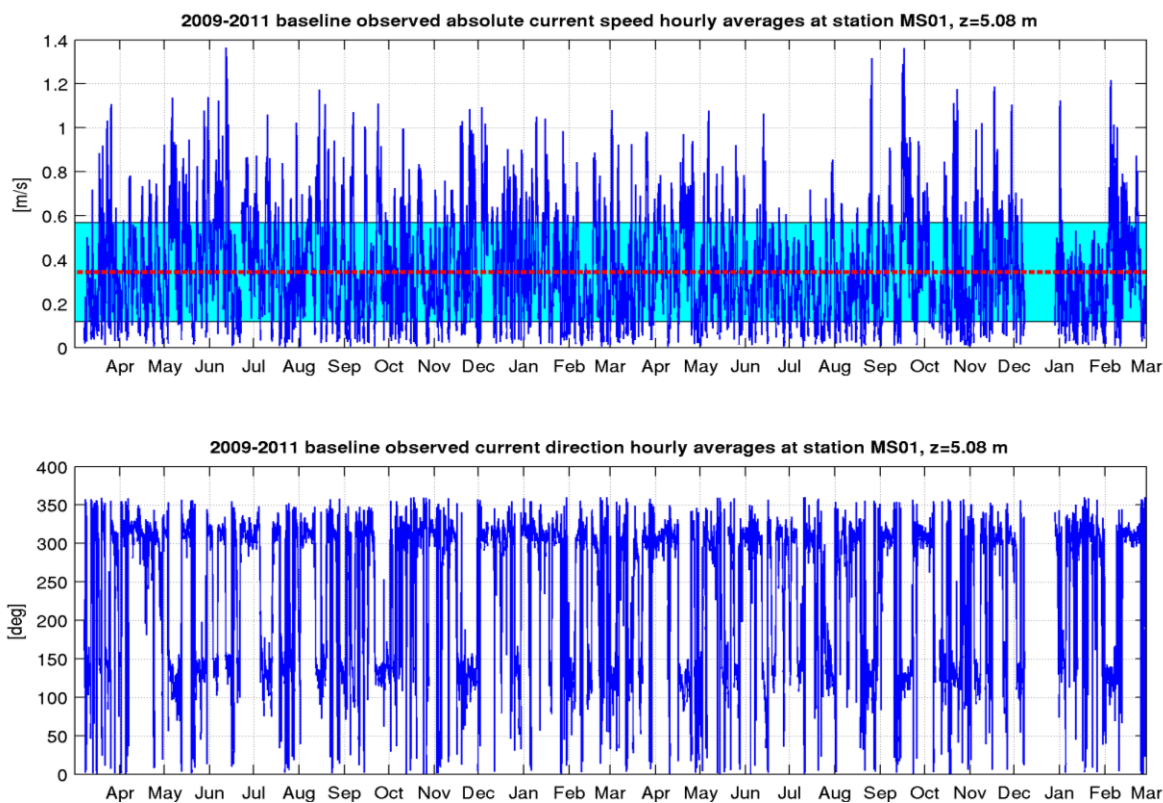


Fig. 6.18 Hourly averages of current speed (upper panel) and direction (lower panel) at MS01 in the surface layer with mean speed (red line) and standard deviation of current speed.

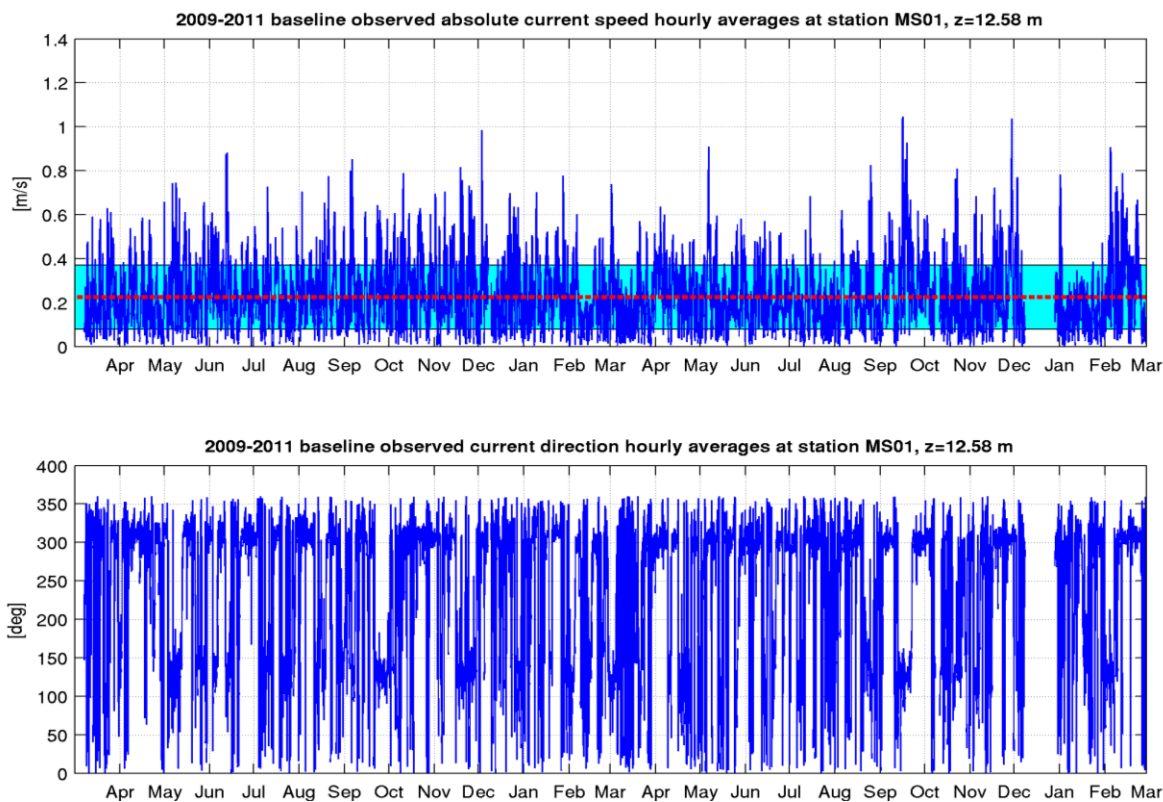


Fig. 6.19 Hourly averages of current speed (upper panel) and direction (lower panel) at MS01 at intermediate depth (12.58 m) with mean speed (red line) and standard deviation of current speed.

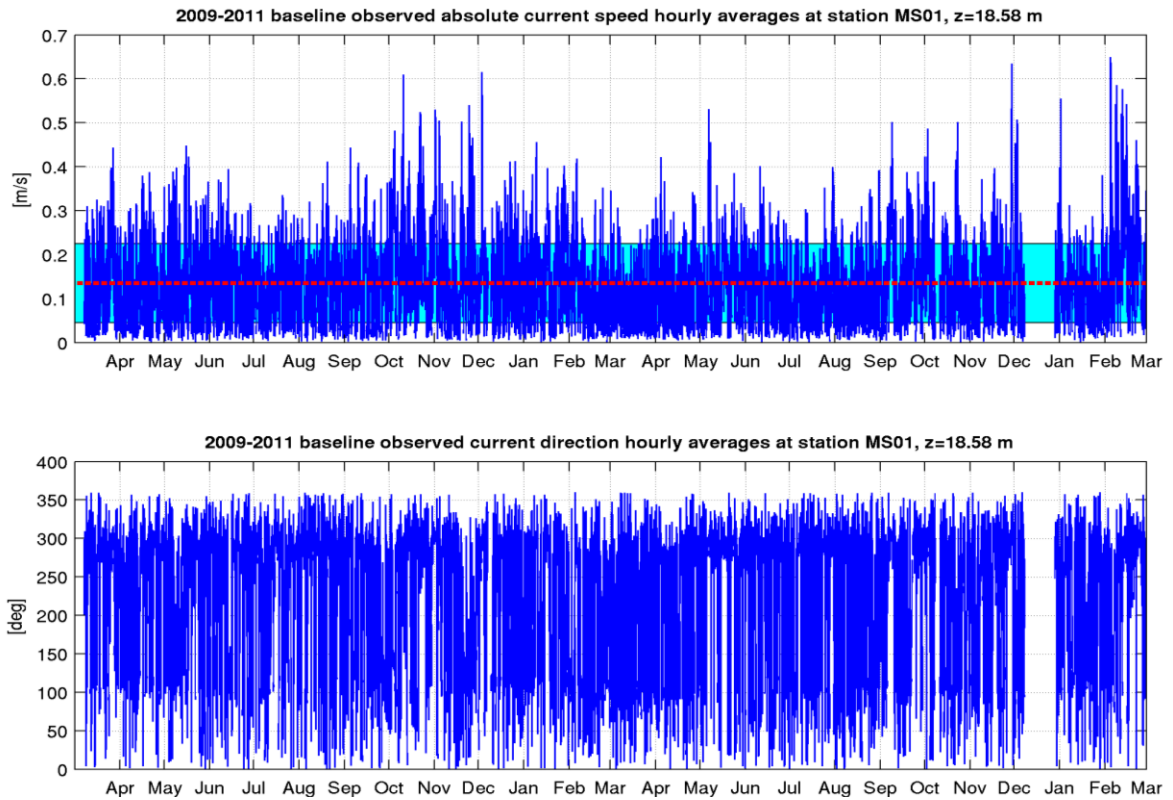


Fig. 6.20 Hourly averages of current speed (upper panel) and direction (lower panel) at MS01 near the bottom with mean speed (red line) and standard deviation of current speed.

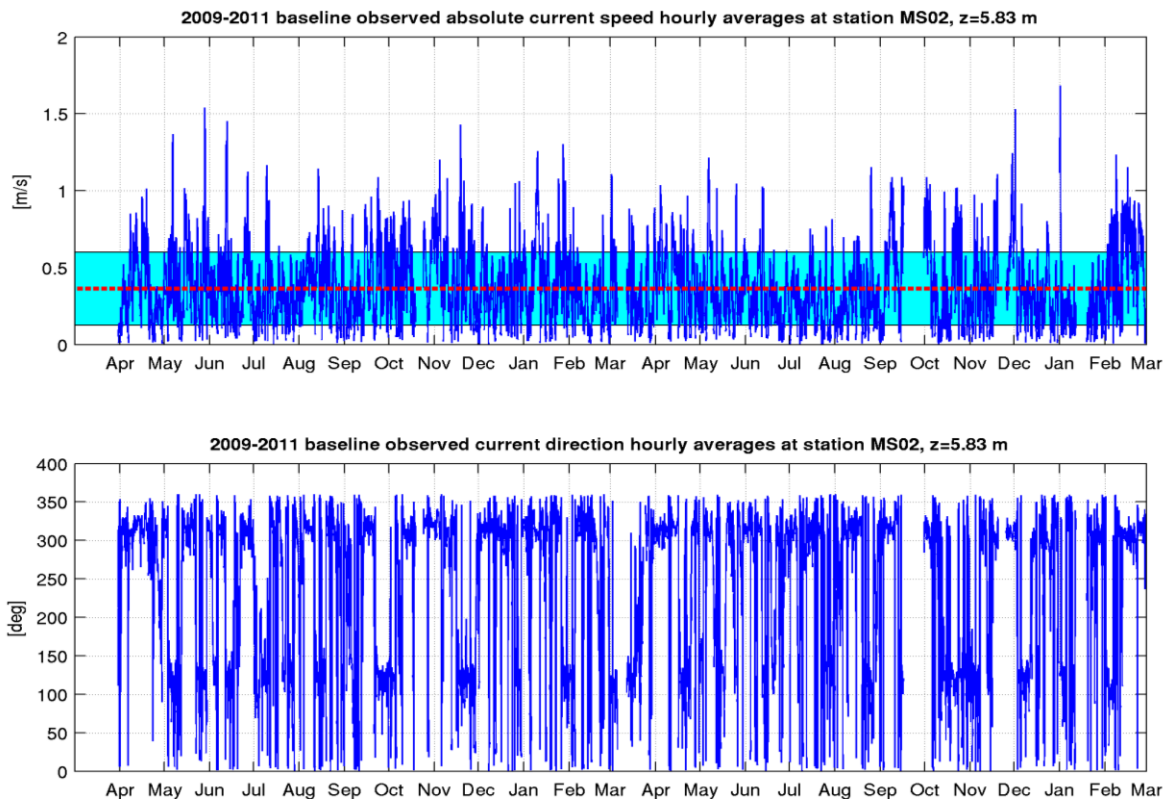


Fig. 6.21 Hourly averages of current speed (upper panel) and direction (lower panel) at MS02 in the surface layer with mean speed (red line) and standard deviation of current speed.

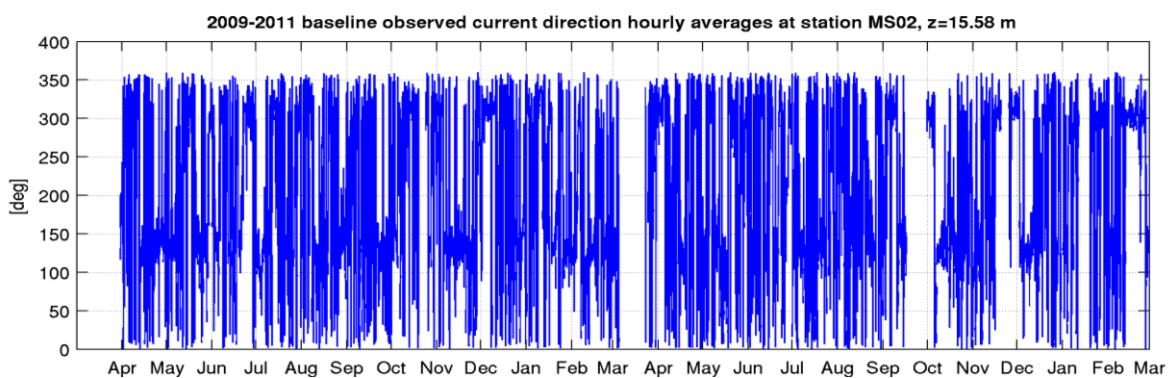
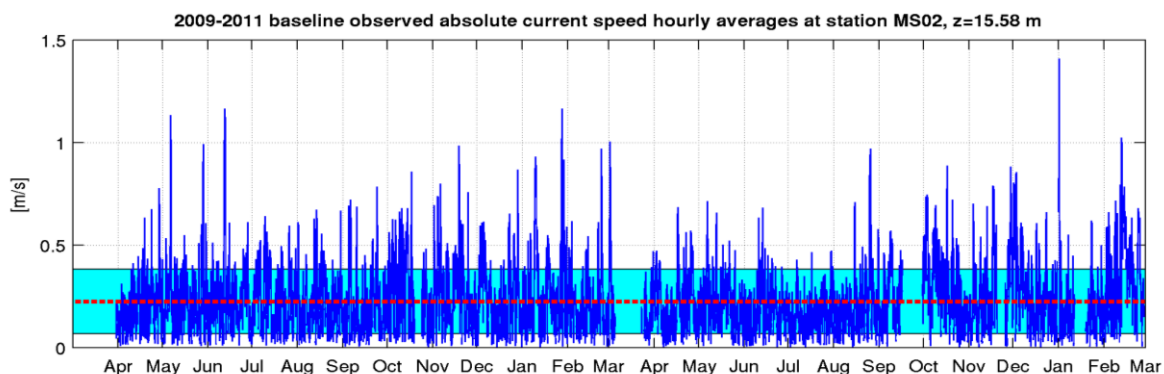


Fig. 6.22 Hourly averages of current speed (upper panel) and direction (lower panel) at MS02 at intermediate depth (15.58 m) with mean speed (red line) and standard deviation of current speed.

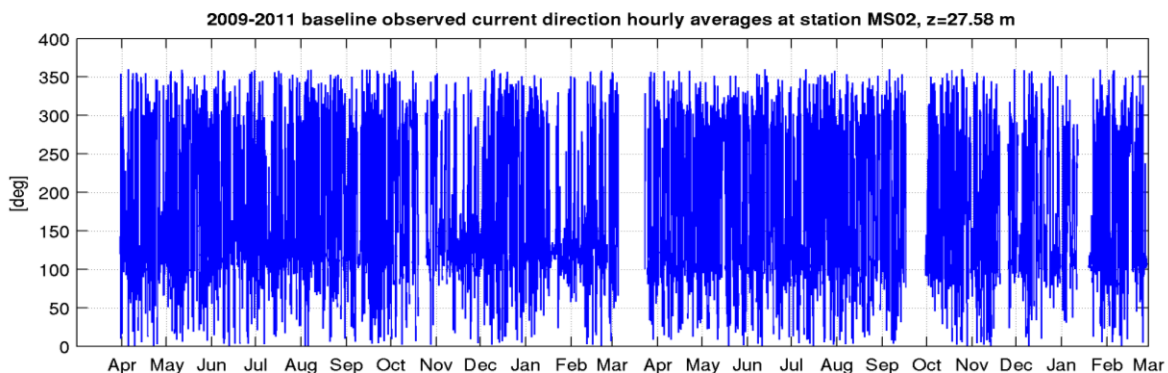
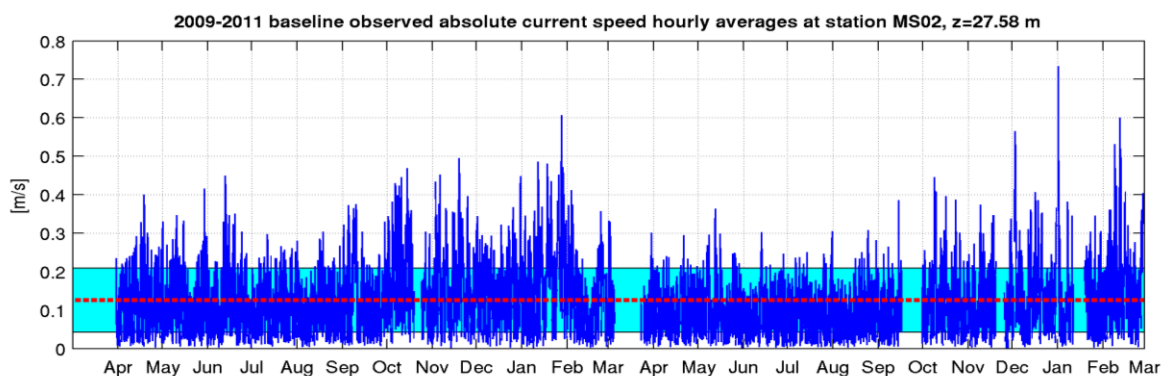


Fig. 6.23 Hourly averages of current speed (upper panel) and direction (lower panel) at MS02 near the bottom with mean speed (red line) and standard deviation of current speed.

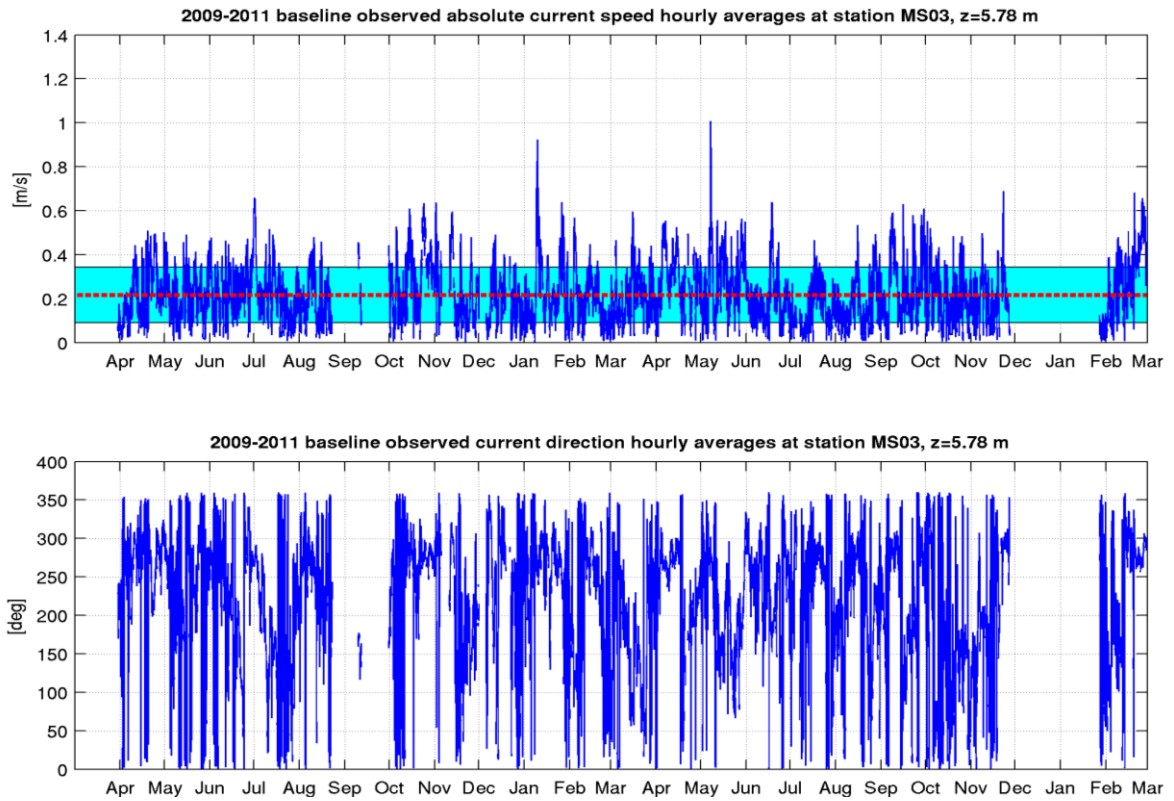


Fig. 6.24 Hourly averages of current speed (upper panel) and direction (lower panel) at MS03 in the surface layer with mean speed (red line) and standard deviation of current speed.

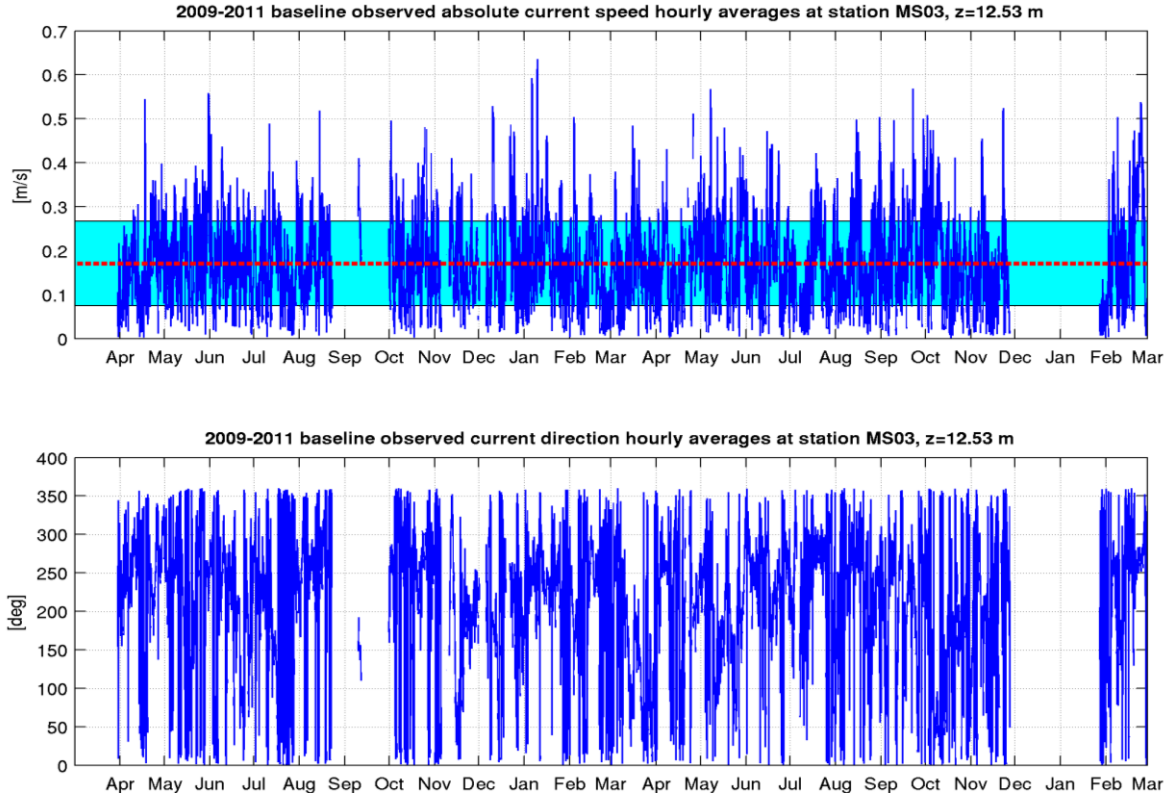


Fig. 6.25 Hourly averages of current speed (upper panel) and direction (lower panel) at MS03 at intermediate depth (12.53 m) with mean speed (red line) and standard deviation of current speed.

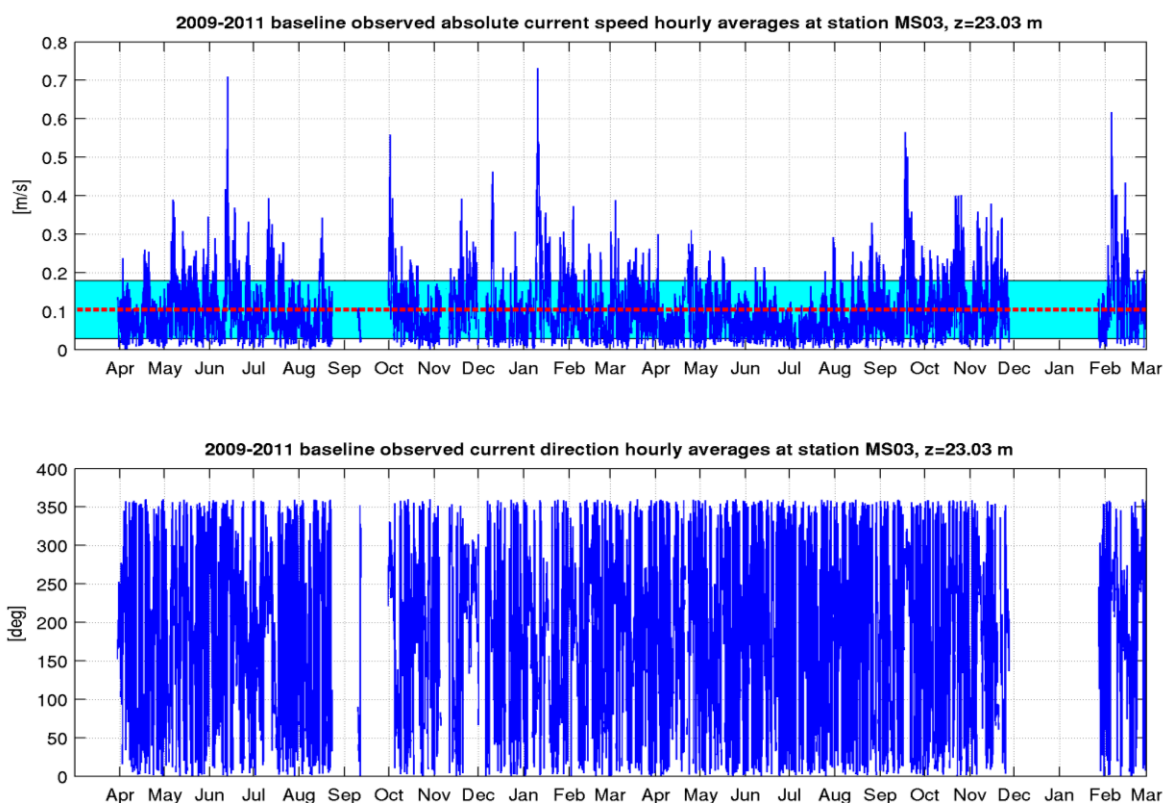


Fig. 6.26 Hourly averages of current speed (upper panel) and direction (lower panel) at MS03 near the bottom with mean speed (red line) and standard deviation of current speed.

Detailed variation of currents at MS01 in the Fehmarnbelt is shown in Fig. 6.27 and Fig. 6.28. In the upper layer first the last one day of an outflow is identified. It is followed by 4 days inflow event and a five days outflow event. At the end a situation with current reversal towards inflow is found.

The currents are driven partly by a water level difference between the Arkona Basin and the Kattegat and partly by tides from Kattegat. The tides are especially pronounced in the lower layer. In the upper layer the tides are superimposed on top of a stronger water level driven current with local wind stress causing highly frequent shifts.

The tidal signal is delayed in the lower layer compared to the upper layer.

The average current profile (Fig. 6.28) shows that inflowing water masses were in fact dominating but despite high singular current speeds of up to ± 1 m/s at the surface the net speed of the inflow was very weak with less than 0.1 m/s.

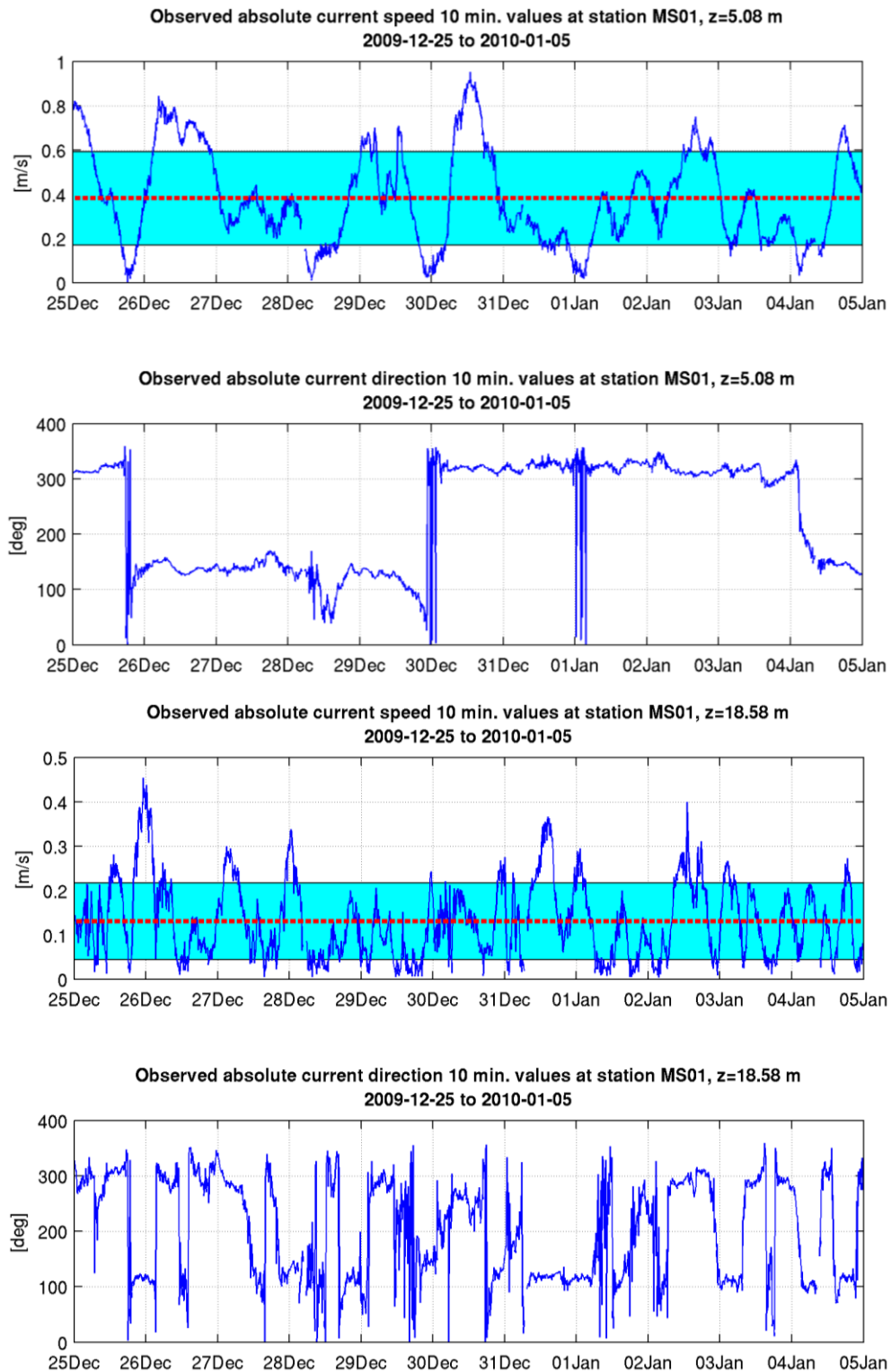


Fig. 6.27 Observed current speed and direction at MS01 from 2009-12-25 to 2010-01-05 at $z=5.08$ m (upper panel) and $z=18.58$ m (lower panel) with mean speed (red lines) and standard deviation of current speed.

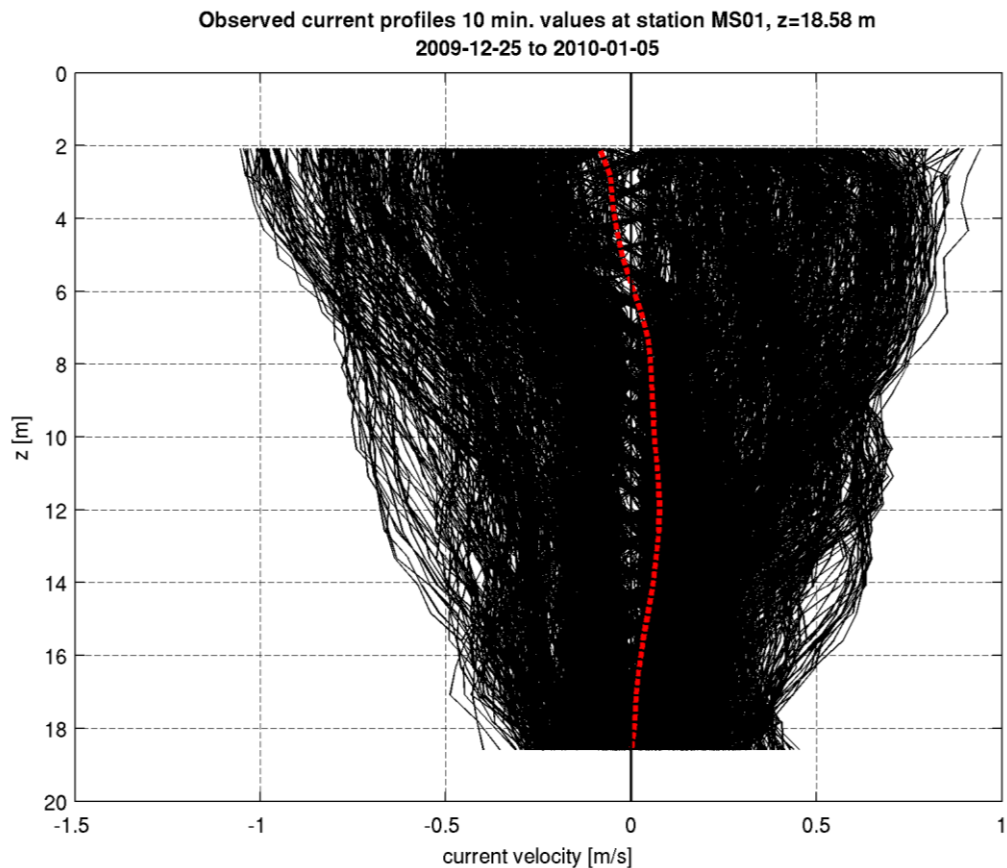


Fig. 6.28 Observed current speed profiles at MS01 from 2009-12-25 to 2010-01-05 with mean profile (red line). Positive values indicate eastward inflow, negative values indicate westward outflow.

Examples of different salinity, temperature, density and current profiles at MS02 are provided. The selected flow cases are:

- Outflow all over the water column – barotropic current dominates (high water level in the Arkona Basin and low in the Kattegat);
- Outflow at surface and inflow at bed – both barotropic and baroclinic flow are important. This is the most frequent situation at this station occurring in ca. 50% of all observed cases;
- Inflow all over the water column - barotropic current dominates (low water level in the Arkona Basin and high in the Kattegat);
- Inflow at surface and outflow at bed – rapid change of flow conditions;
- Three-layer flow case – intrusion between upper and low layer; and
- Continuous density (salinity) gradient from surface to bed – strong wind conditions for example during winter.

The examples are shown in Fig. 6.29 to Fig. 6.34 below.

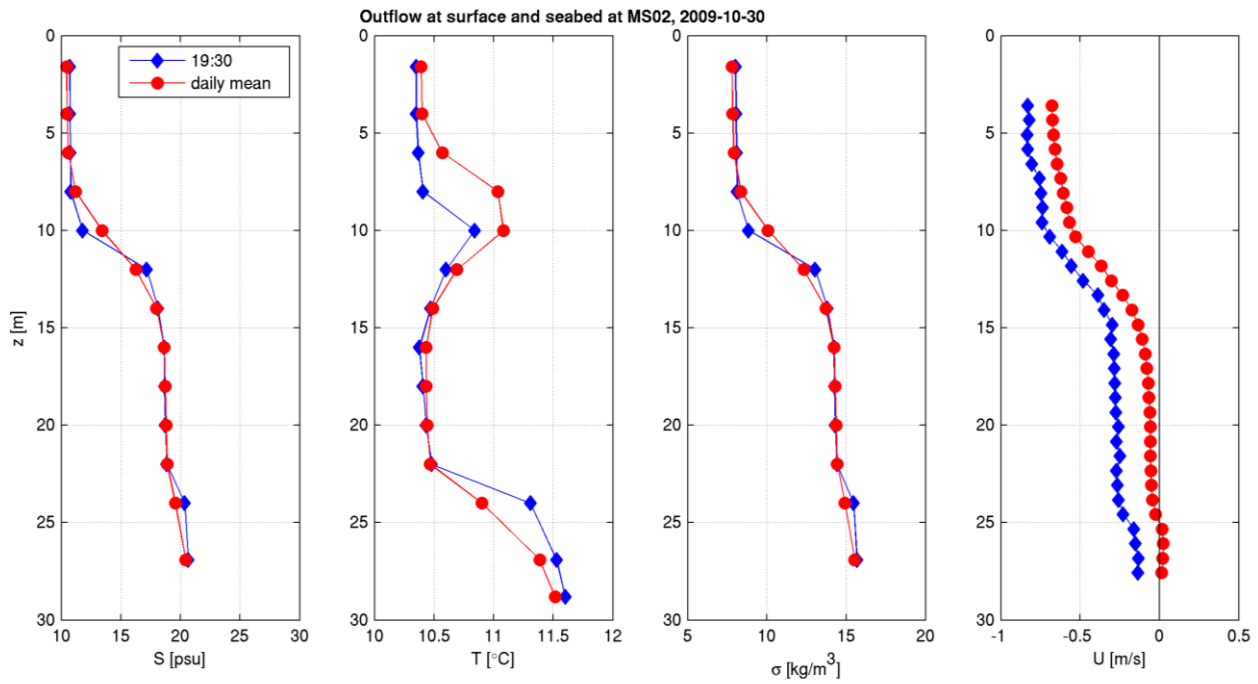


Fig. 6.29 Outflow all over the water column at MS02 on 2009-10-20 at 19:30 (blue line) and daily mean (red line). Note how the daily mean does still show a slight inflow near the seabed.

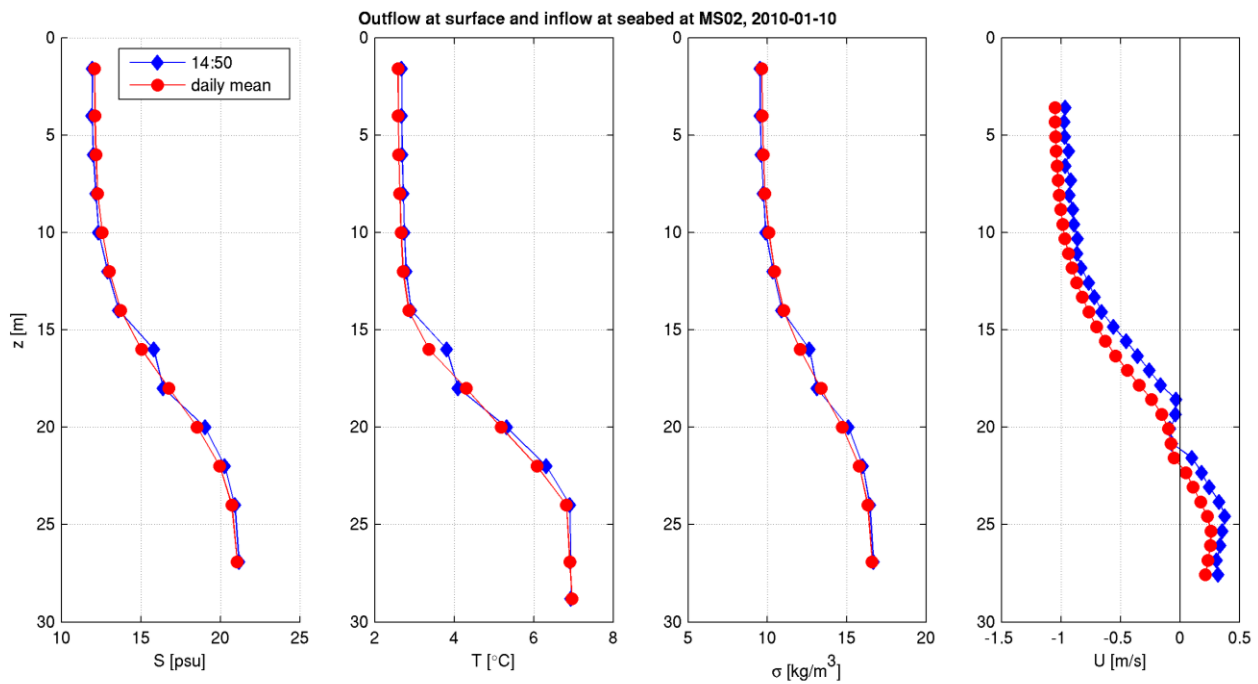


Fig. 6.30 Outflow at surface and inflow at bed at MS02 on 2010-01-10 at 14:50 (blue line) and daily mean (red line). On this day the daily average does not differ significantly from an instantaneous profile which indicates a stable stratification.

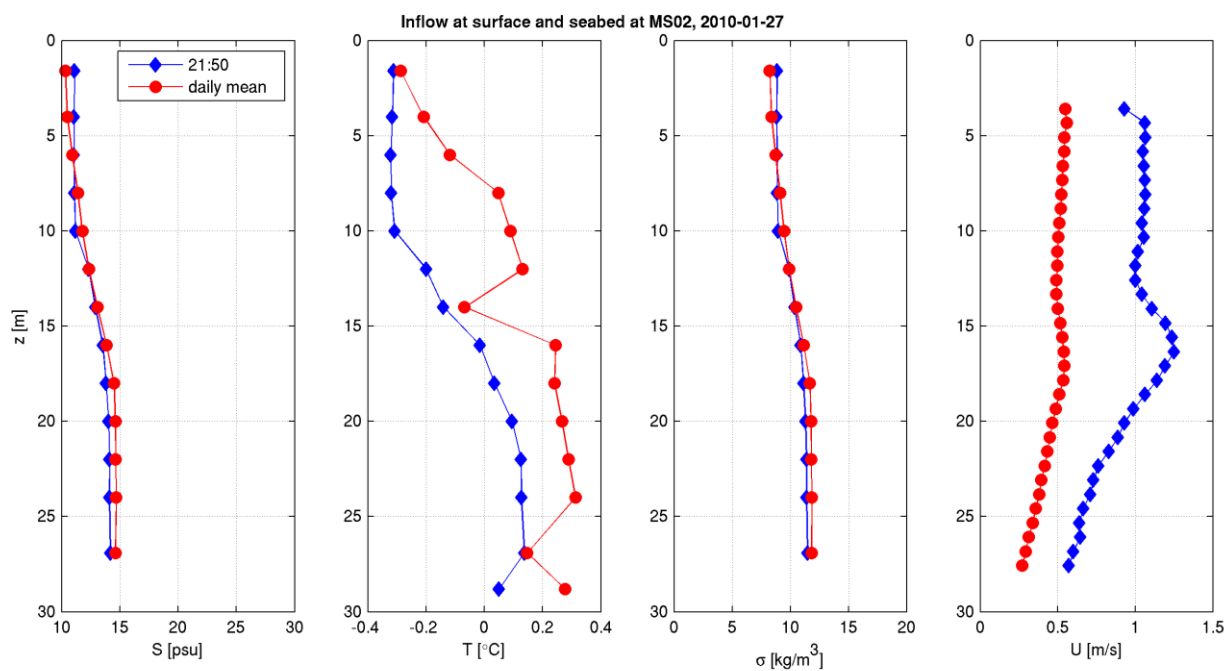


Fig. 6.31 Inflow all over the water column at MS02 on 2010-01-27 at 21:50 (blue line) and daily mean (red line). The temperature stratification is more pronounced on the daily average than in the instantaneous profile. This does however not affect the density.

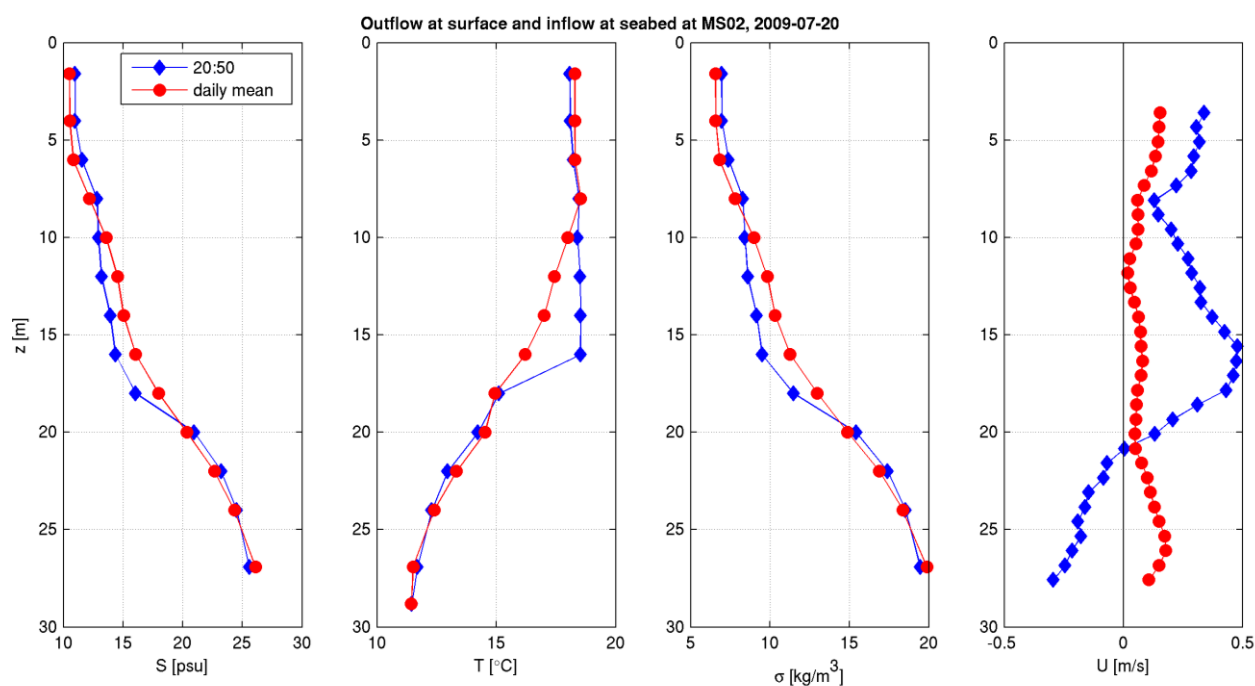


Fig. 6.32 Inflow at surface and outflow at bed at MS02 on 2009-07-20 at 20:50 (blue line) and daily mean (red line). The daily mean current speed is much lower than the instantaneous values that include highly frequent signals like tides and possibly internal waves, and it only shows inflow throughout the water column. The density stratification however remained stable on that day indicating two oscillating water masses in the respective layers.

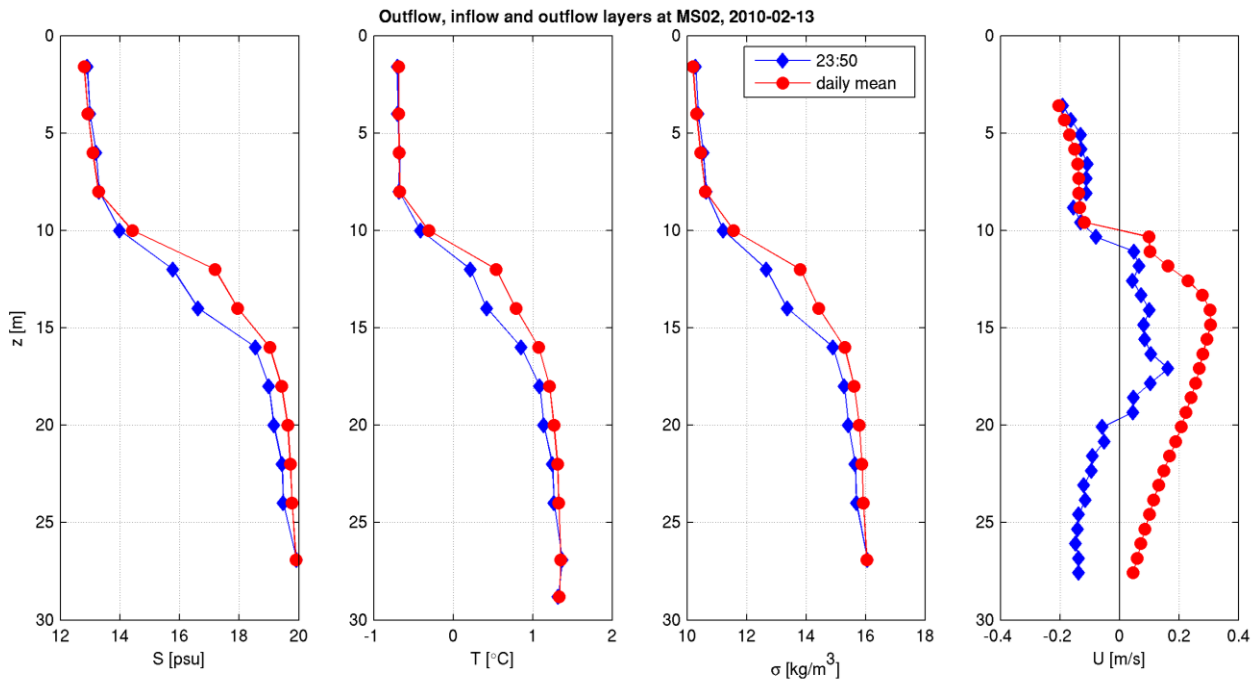


Fig. 6.33 Three-layer flow case at MS02 on 2010-02-13 at 23:50 (blue line) and daily mean (red line). The instantaneous current profile shows three layers while on average there were only two layers on this particular day. This is reflected in the stable density stratification.

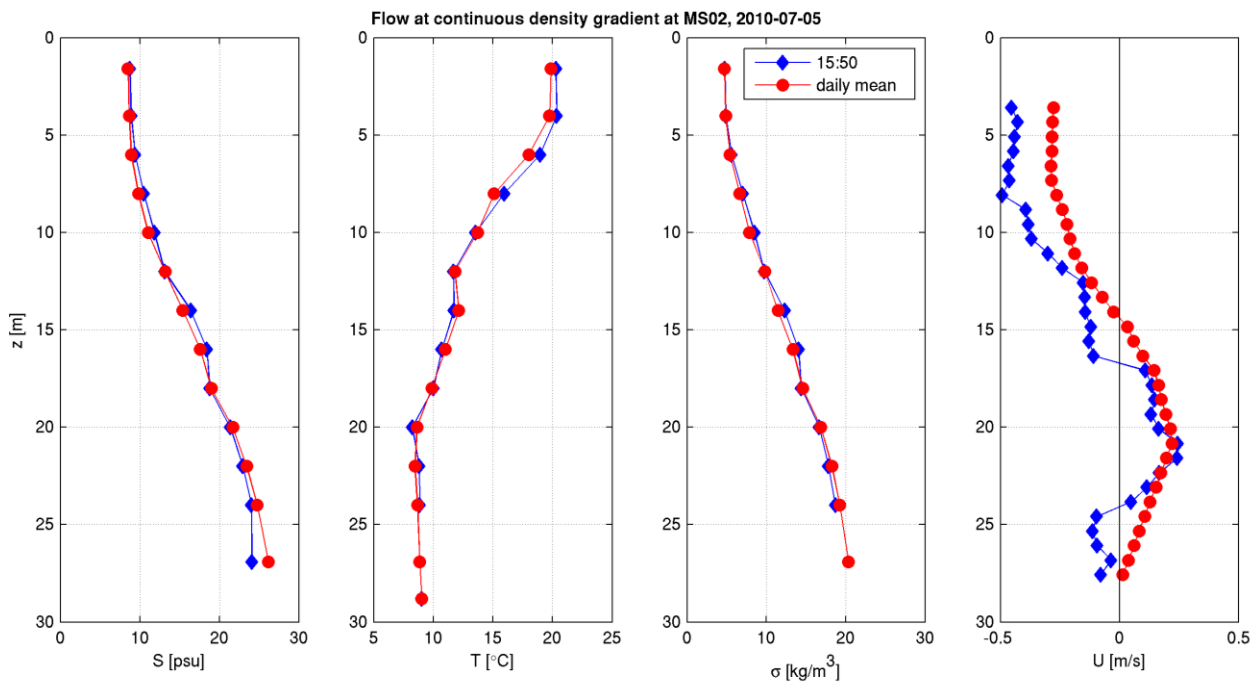


Fig. 6.34 Continuous density (salinity) gradient from surface to bed at MS02 on 2010-07-05 at 15:50 (blue line) and daily mean (red line). In contrast to the case in Fig. 6.33 there is an instantaneous three-layer flow but a constant density gradient. The daily mean current profile shows only two layers though with outflow dominating the upper layer to $z = 15$ m and inflow in the lower layer.



6.4 Salinity and Temperature

The salinity and its variation are related to the current conditions. Long-term outflow results in low salinities in the Fehmarnbelt, while long-term inflow results in high salinities. But the salinities have to be transported from either Kattegat or the Arkona Basin to cause a change. And that takes time. Hence the salinity variation is slower than the current variation.

Fig. 6.35 shows current and salinity variation at station MS02 during a five day period. The current varies rapidly on a daily time scale. The salinity variation cannot follow this rapid variation of the currents. Only if an in- or outflow event last more than a day it will cause the salinity to decrease or increase, respectively.

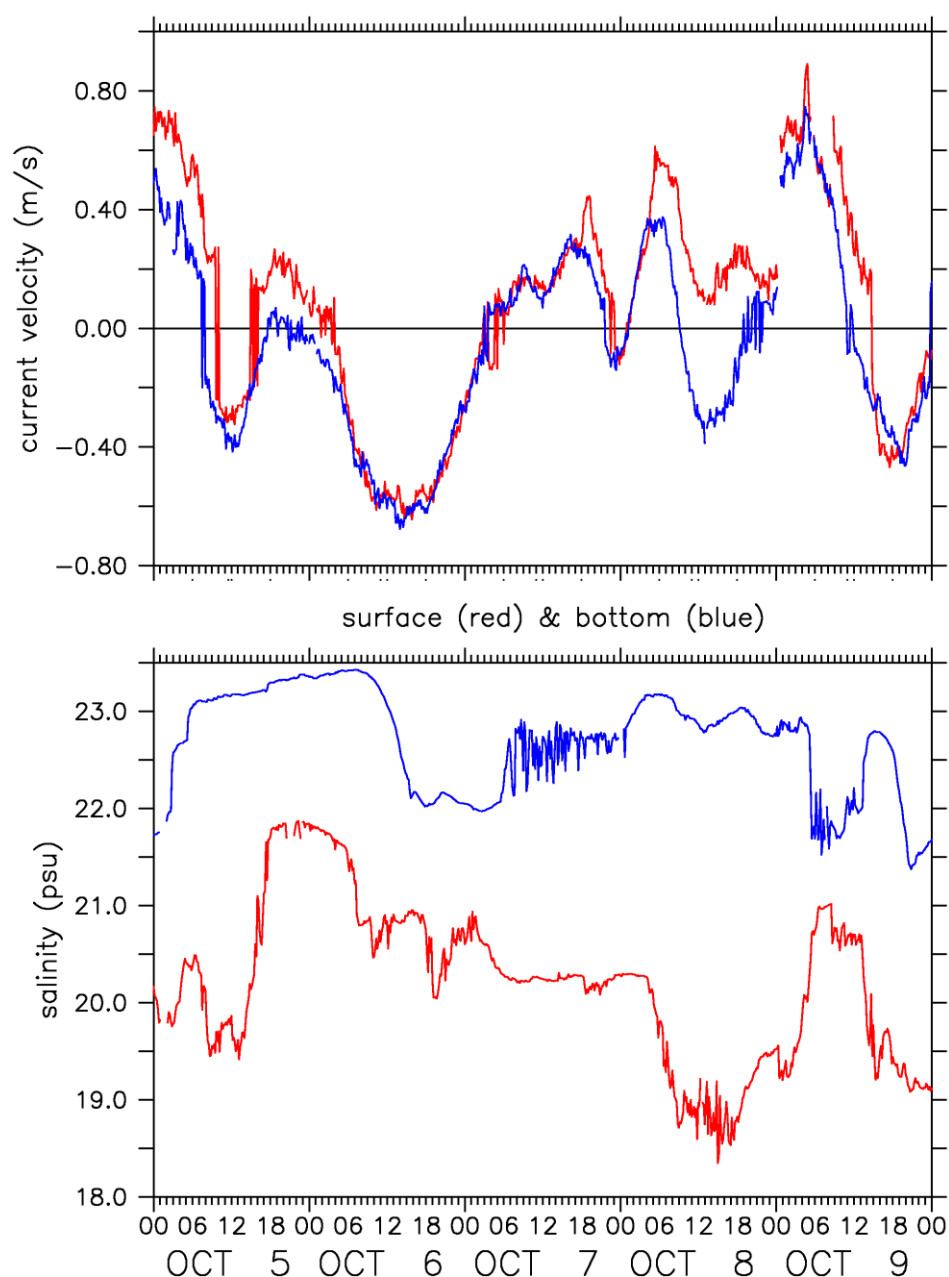
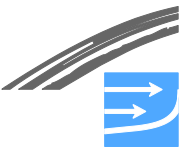


Fig. 6.35 Measured current and salinity close to surface and bottom at MS02 during a five days period in October 2009.



Distribution of salinity and temperature at the stations are shown in Fig. 6.36, Fig. 6.37 and Fig. 6.38.

The depth of temperature and salinity sensors at station MS02 in July 2009 was changed and data from this station only presented after 14 July 2009. In this quickly changing area with a high temporal and spatial variability, singular depth levels are required to present proper statistics of time-series.

A medium saline inflow through Fehmarnbelt was detected in October 2009 with salinities around 22 psu over the entire water column.

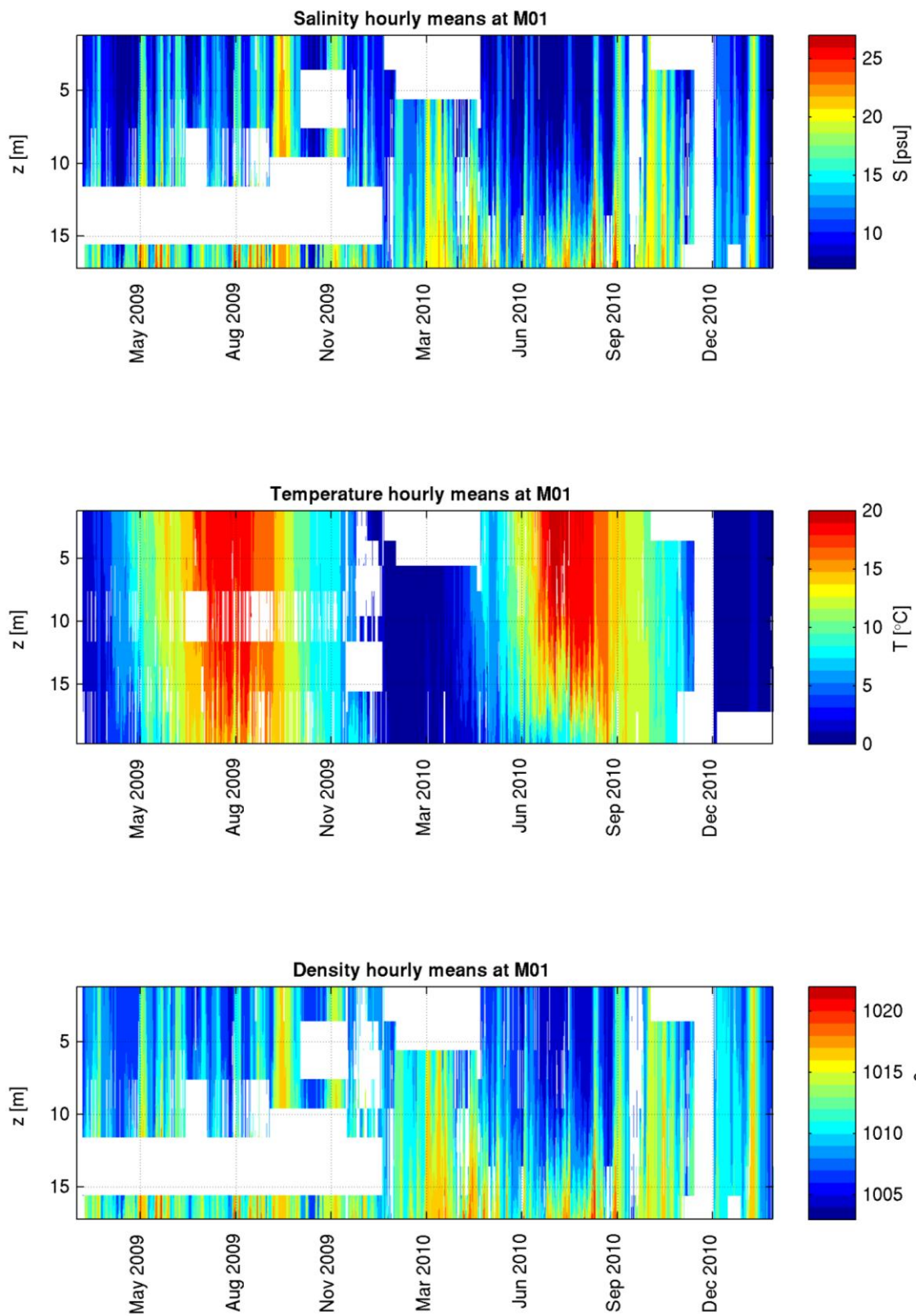


Fig. 6.36 Measured salinity, temperature and density (kg/m^3) at MS01 in Fehmarnbelt during the baseline monitoring.

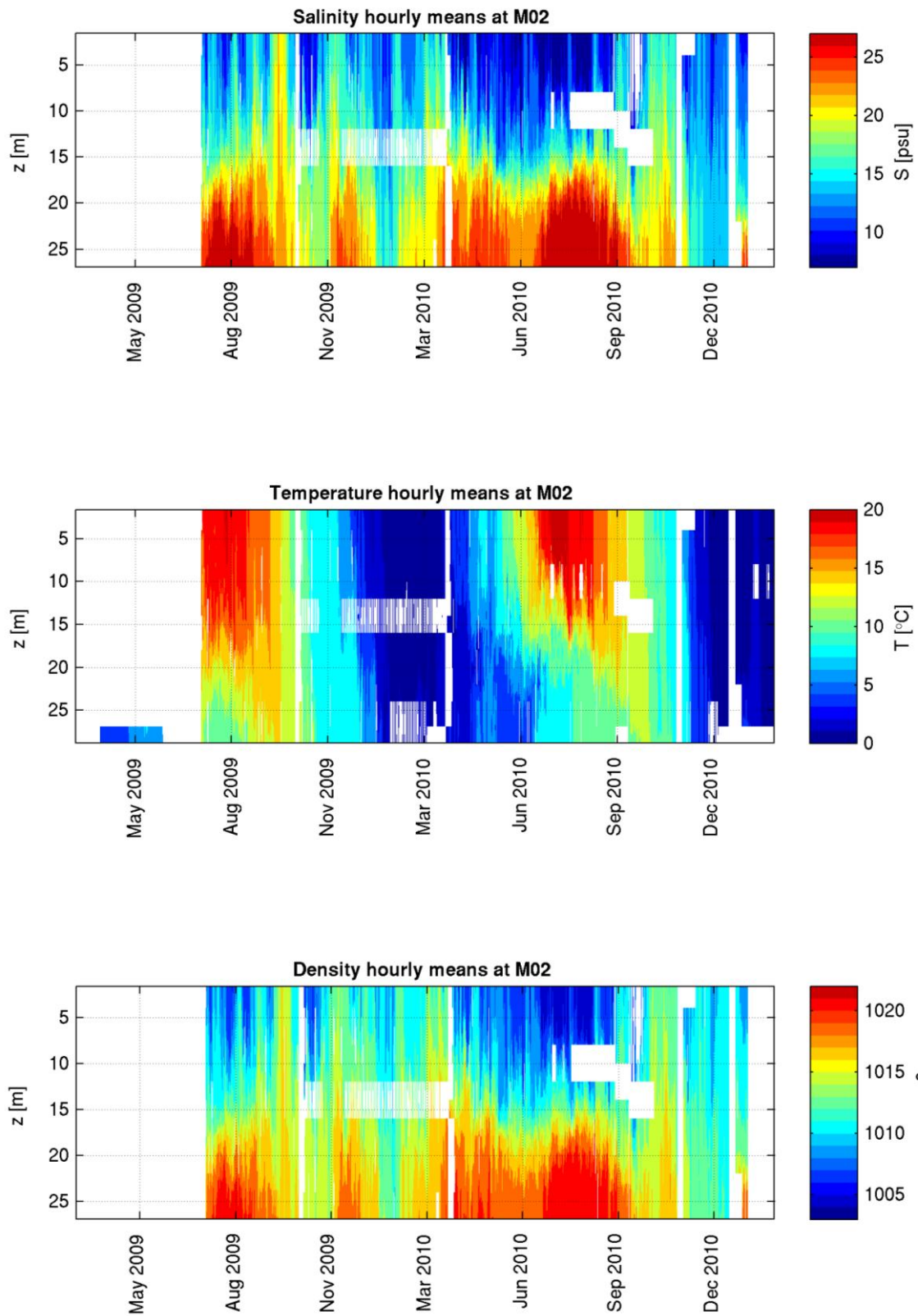


Fig. 6.37 Measured salinity, temperature and density (kg/m^3) at MS02 in Fehmarnbelt during the baseline monitoring.

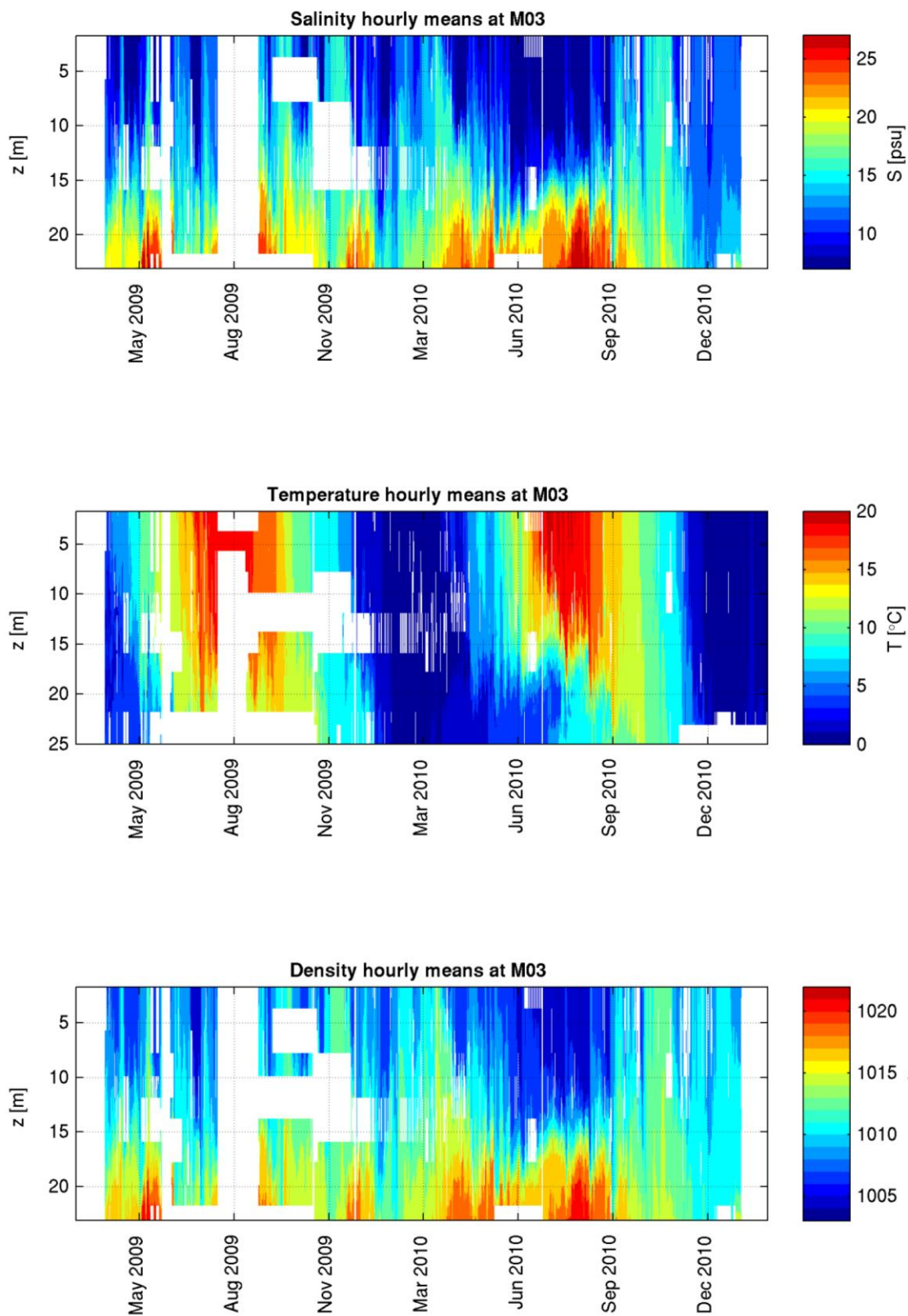


Fig. 6.38 Measured salinity, temperature and density (kg/m^3) at MS03 in Fehmarnbelt during the baseline monitoring.

The increased saline inflow in October is recorded at MS02 as a more or less continuous highly saline layer of $S > 22$ psu at depths below 15 m.



The bottom flow of saline North Sea water through Fehmarnbelt follows the southern slope of the Fehmarnbelt channel.

An example of the typical stratification in the Fehmarnbelt is presented in Fig. 6.39. It depicts temperature and salinity time-series in the Fehmarnbelt during summer 2009. The pycnocline depth is between 15 and 20 m with wind driven short term excursions of up to 5 m. The wind speed during this period is about 5 to 8 m/s. The onset of a strong westerly wind (max 15 m/s) on 5 September 2009 changed the stratification because of the enhanced mixing. The vertical gradients are smoothed and the former two layer stratification is transformed into one layer with a nearly constant vertical gradient in both temperature and salinity.

Well mixed conditions throughout the water column are rarely found in the Fehmarnbelt, but were observed during the baseline period.

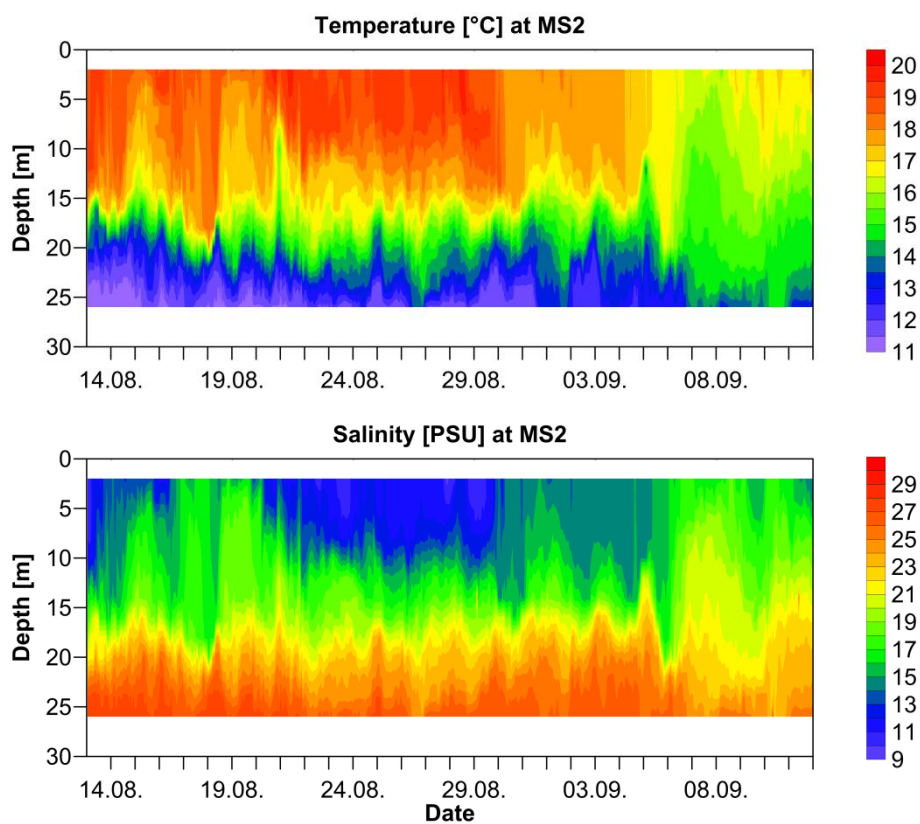


Fig. 6.39 Temperature and salinity variation at MS02 in late August and start of September 2009.

During winter the temperature stratification in the Fehmarnbelt often vanishes (see Fig. 6.40), since the initial temperatures of saline North Sea waters and brackish surface water of the Baltic have nearly the same value. However, the salinity stratification persists almost throughout the year. The only exception is the rare major Baltic inflow events, which were not covered in the baseline monitoring.

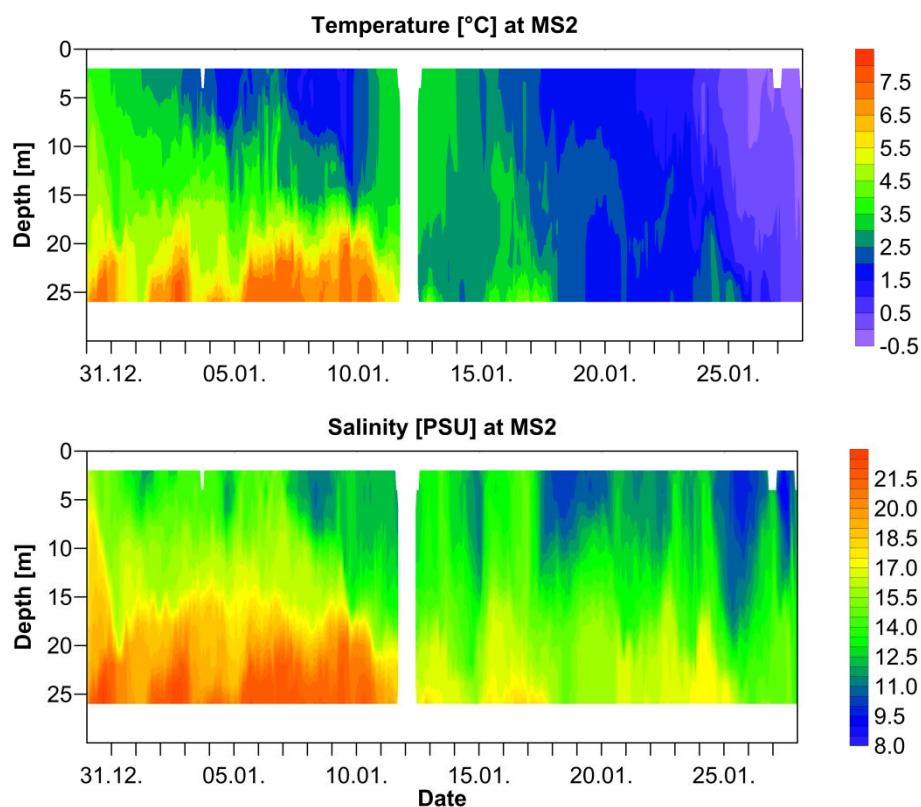


Fig. 6.40 Temperature and salinity variation at MS02 in January 2010.

Salinity profiles and salinity variation at the main stations in Fehmarnbelt are shown in Fig. 6.41 to Fig. 6.49. The salinity variation typically shows higher salinity during winter than during summer.

The salinity profiles are divided into inflow (eastward flow in the upper layer) and outflow (westward flow in the upper layer) conditions. Except for MS02 in the southern Fehmarnbelt channel they show higher salinity during inflow than during outflow. These features can be explained as follows:

- At station MS01 in the northern Fehmarnbelt outflowing water masses from the Baltic Sea are predominant throughout the water column, so that inflowing water from the North Sea will cause a shift to higher salinities in all levels.
- The water column at station MS02 in the southern Fehmarnbelt is divided into an outflowing upper layer and a lower layer where the compensation flow of saline North Sea water into the Baltic Sea takes place. Outflowing water below 15 m depth is mainly recirculating North Sea water so that the average salinity profiles of inflowing and outflowing water masses differ only in the upper layer.
- At Station MS03 in the Mecklenburg Bight a salinity shift of 1 psu between the inflowing and outflowing salinity profiles is found.

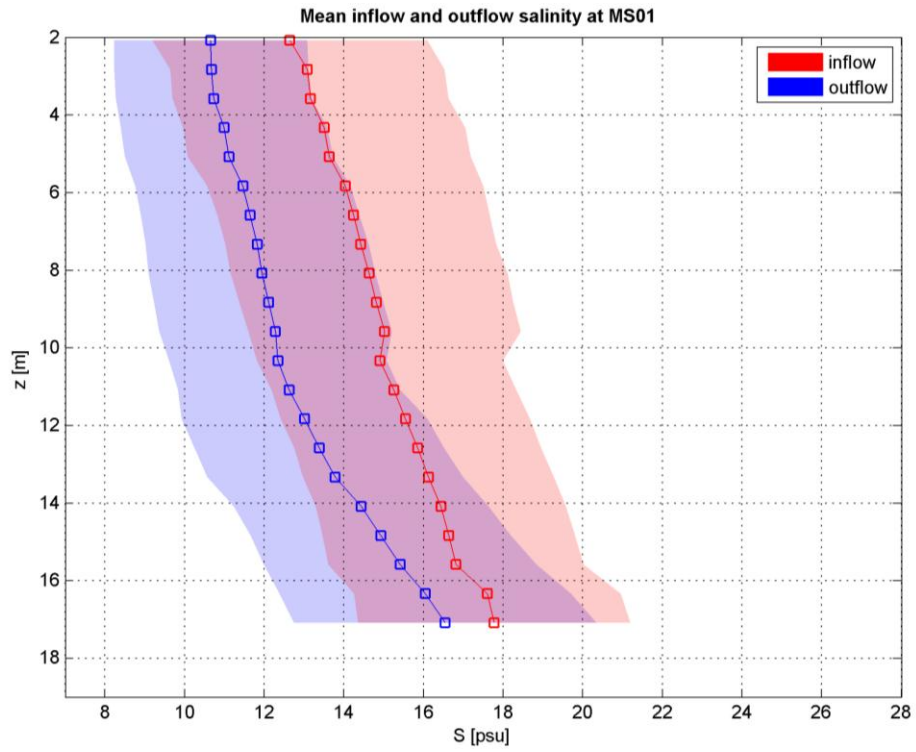


Fig. 6.41 Measured salinity profiles at MS01 during the baseline period divided into inflow or outflow conditions. Mean profile with standard deviation indicated.

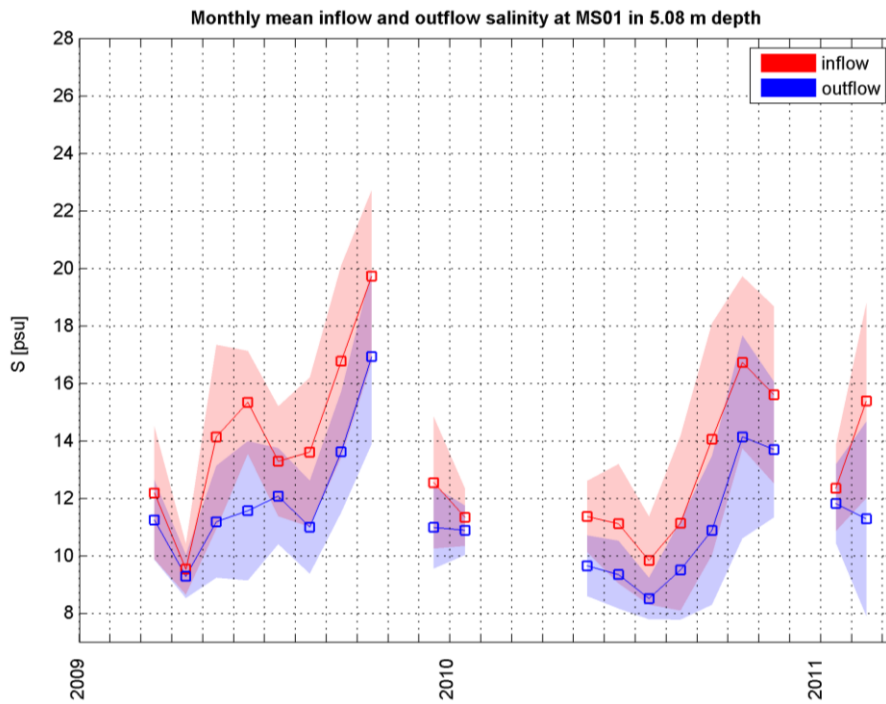


Fig. 6.42 Measured monthly salinity at MS01 in 5 m depth during the baseline period divided into inflow or outflow conditions.

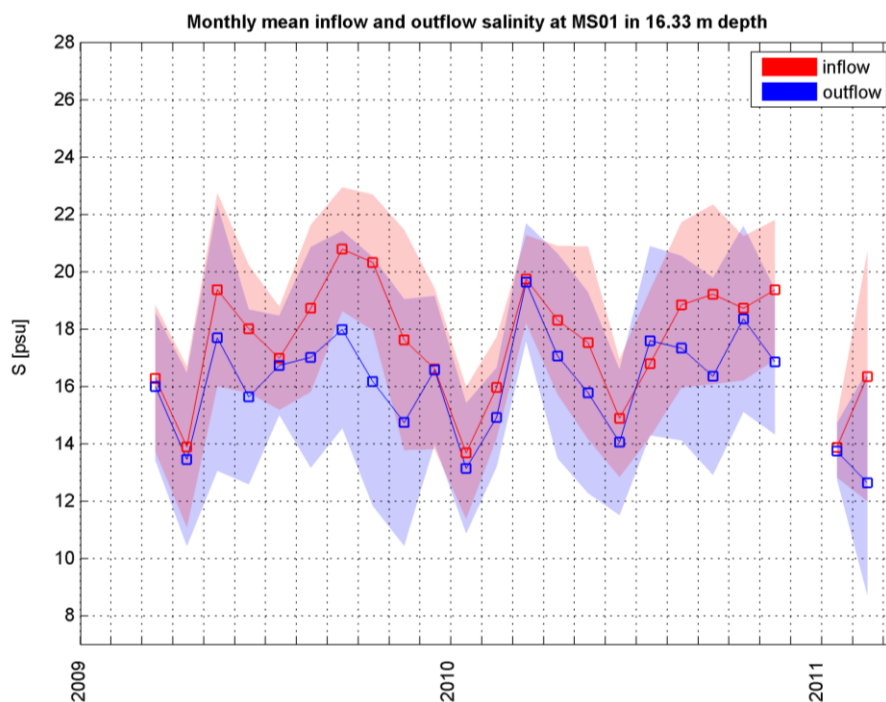


Fig. 6.43 Measured monthly salinity at MS01 in 16 m depth during the baseline period divided into inflow or outflow conditions.

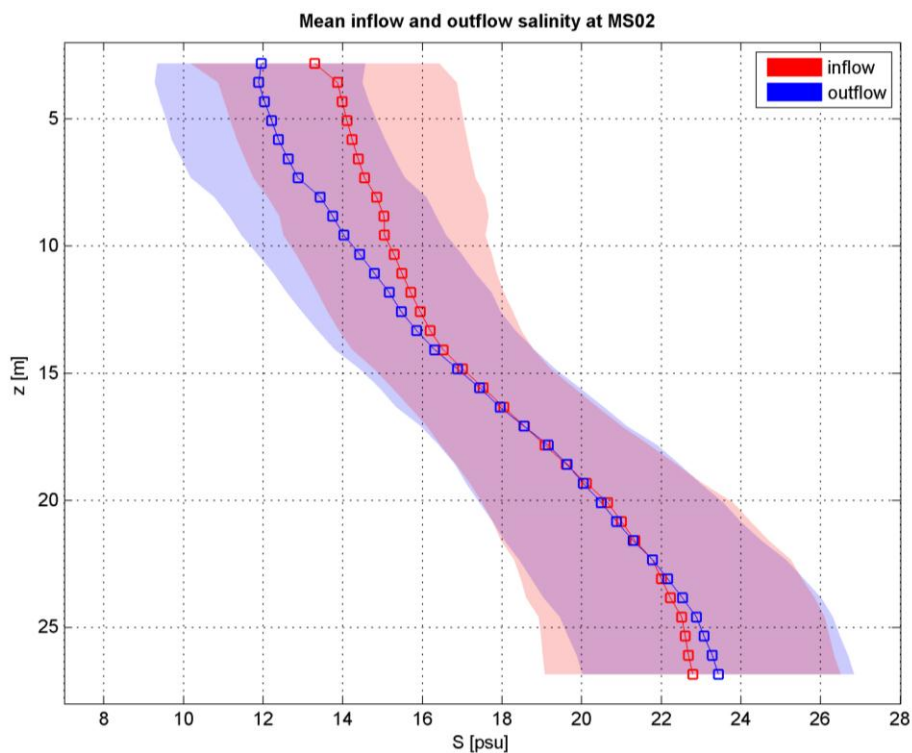


Fig. 6.44 Measured salinity profiles at MS02 during the baseline period divided into inflow or outflow conditions. Mean profile with standard deviation indicated.

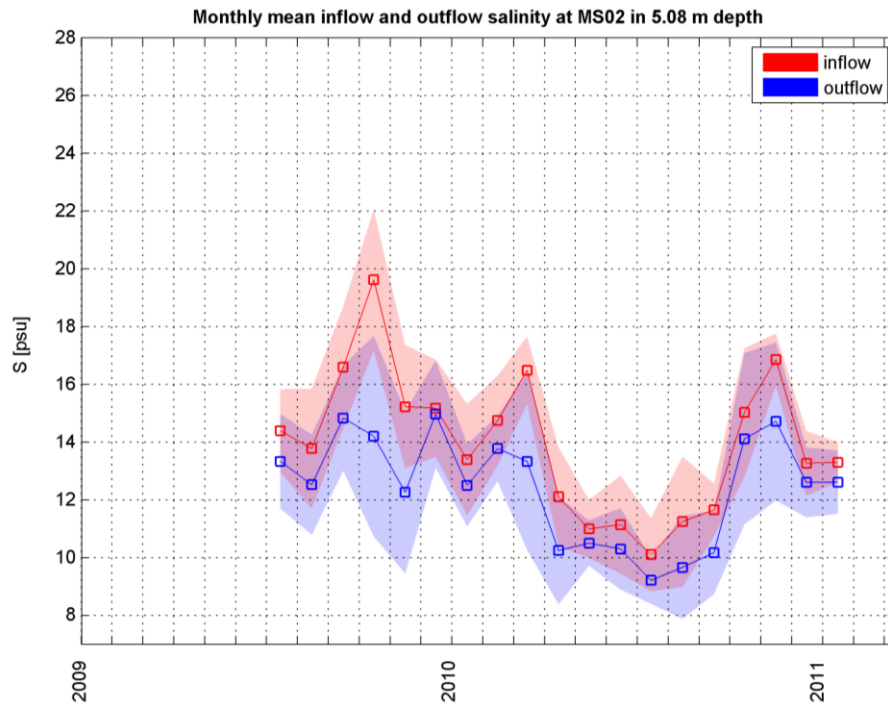


Fig. 6.45 Measured monthly salinity at MS02 in 5 m depth during the baseline period divided into inflow or outflow conditions.

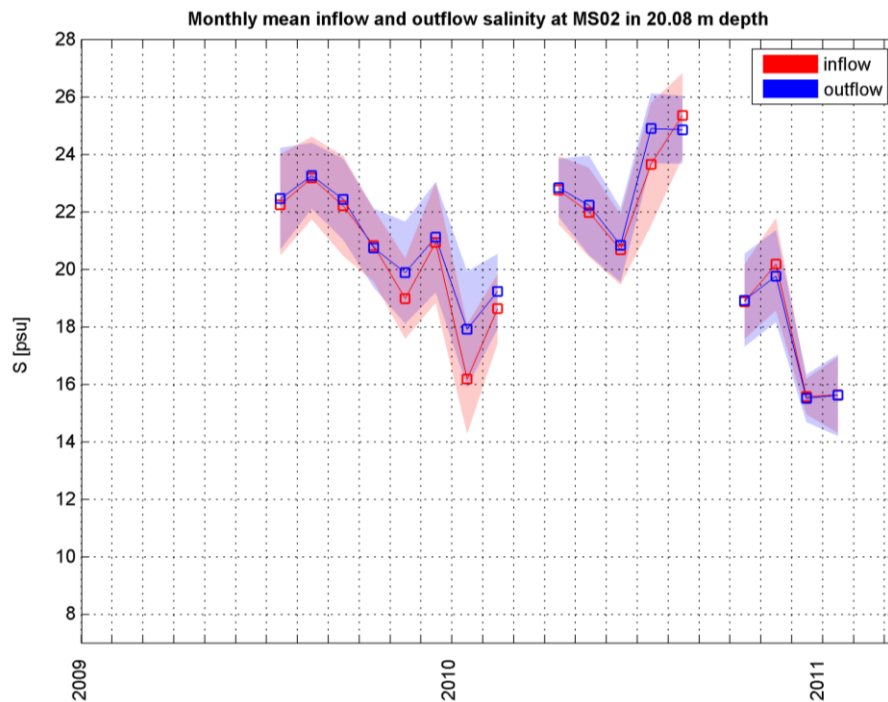


Fig. 6.46 Measured monthly salinity at MS02 in 20 m depth during the baseline period divided into inflow or outflow conditions.

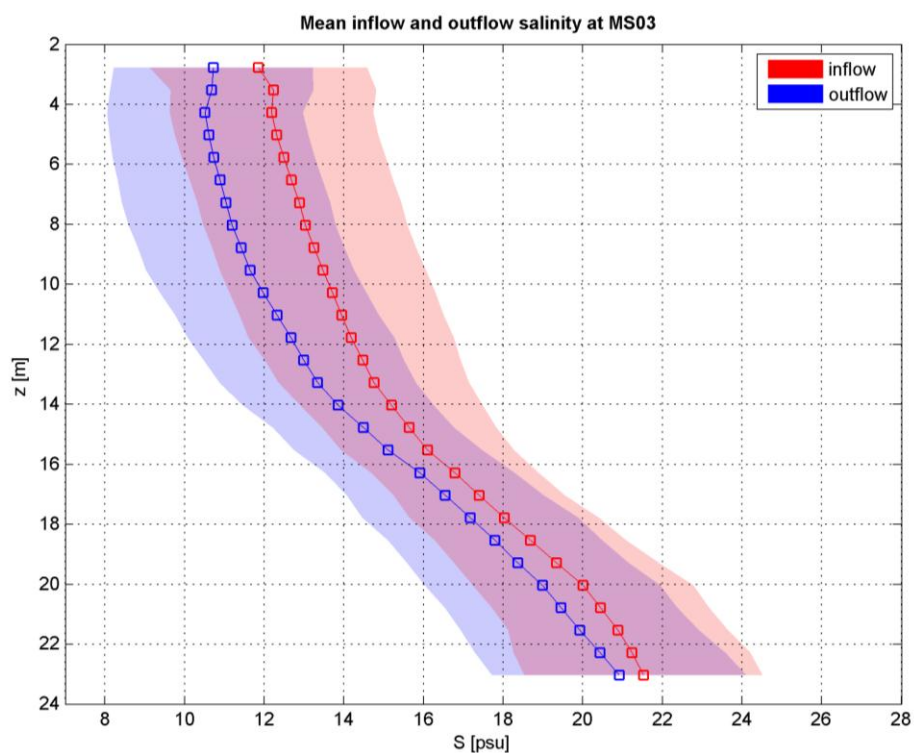


Fig. 6.47 Measured salinity profiles at MS03 during the baseline period divided into inflow or outflow conditions. Mean profile with standard deviation indicated.

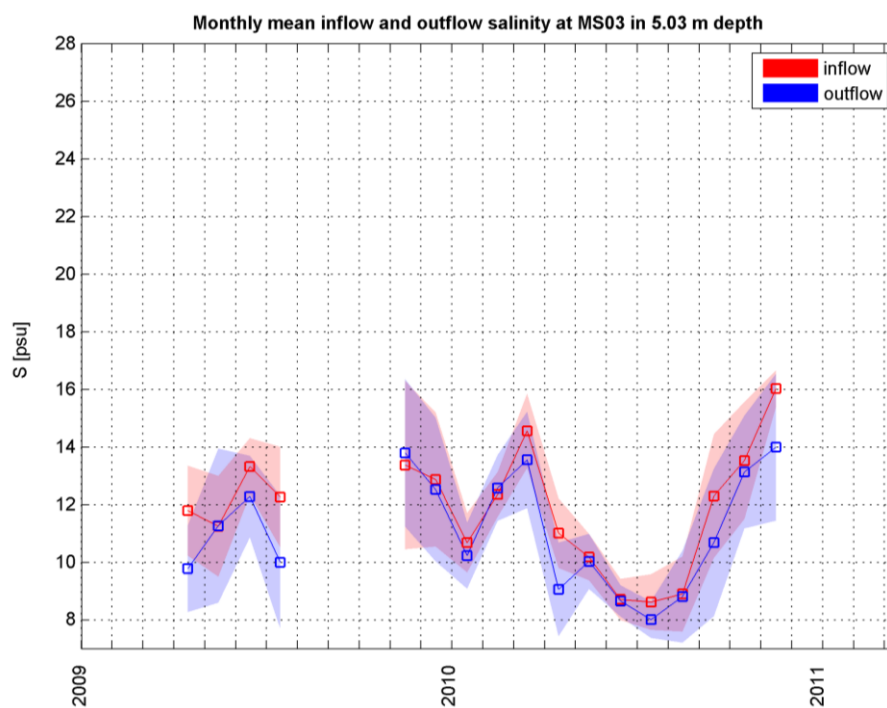


Fig. 6.48 Measured monthly salinity at MS03 in 5 m depth during the baseline period divided into inflow or outflow conditions.

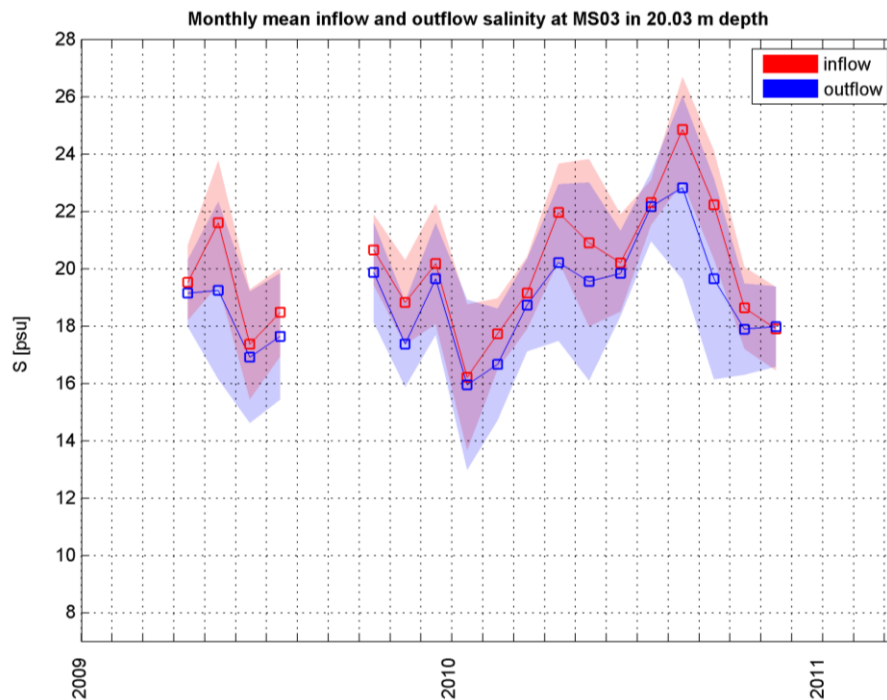


Fig. 6.49 Measured monthly salinity at MS03 in 16 m depth during the baseline period divided into inflow or outflow conditions.

The spatial distribution of surface and bottom salinity in the greater Fehmarnbelt area is shown in Fig. 6.50.

Compared to long-term observations (1902-2010) at HELCOM stations the baseline period is less saline at the surface in the Fehmarnbelt, but matched the long-term average of bottom and surface values in the western Mecklenburg Bight.

A gradient in surface and bottom salinity can be seen with salinity decreasing from the Fehmarnbelt towards the Darss Sill. Due to barotropic pulses of inflowing North Sea water the surface salinity at the southern edge of the Fehmarnbelt channel is also higher than in the northern part of the channel.

Mean sea surface and bottom temperatures during the baseline monitoring surveys show that the mean baseline surface temperature matches that of the long-term averages given by HELCOM observations (Fig. 6.51). The average bottom temperatures observed in the Fehmarnbelt are up to 1°C higher though than the long-term mean and bottom temperature at BMP M02 in the Mecklenburg Bight matches the long-term mean of the HELCOM data. A section across the entrance to the Bay of Lubeck was mainly worked during the summer and autumn seasons of 2009 and 2010 so it appears warmer than the rest of the stations.

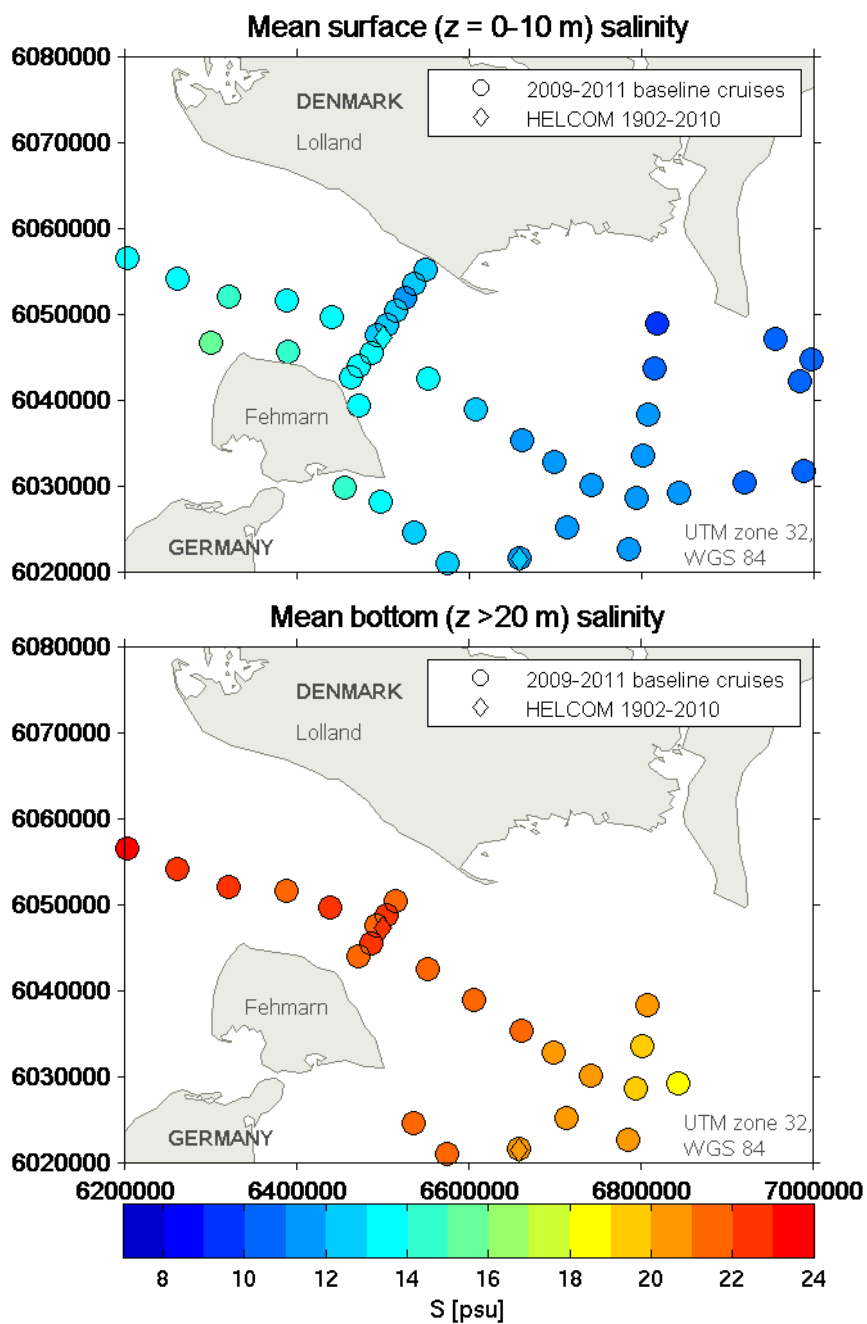


Fig. 6.50 Mean surface (upper panel) and bottom (lower panel) salinity observed during the 2009-2011 baseline cruises.

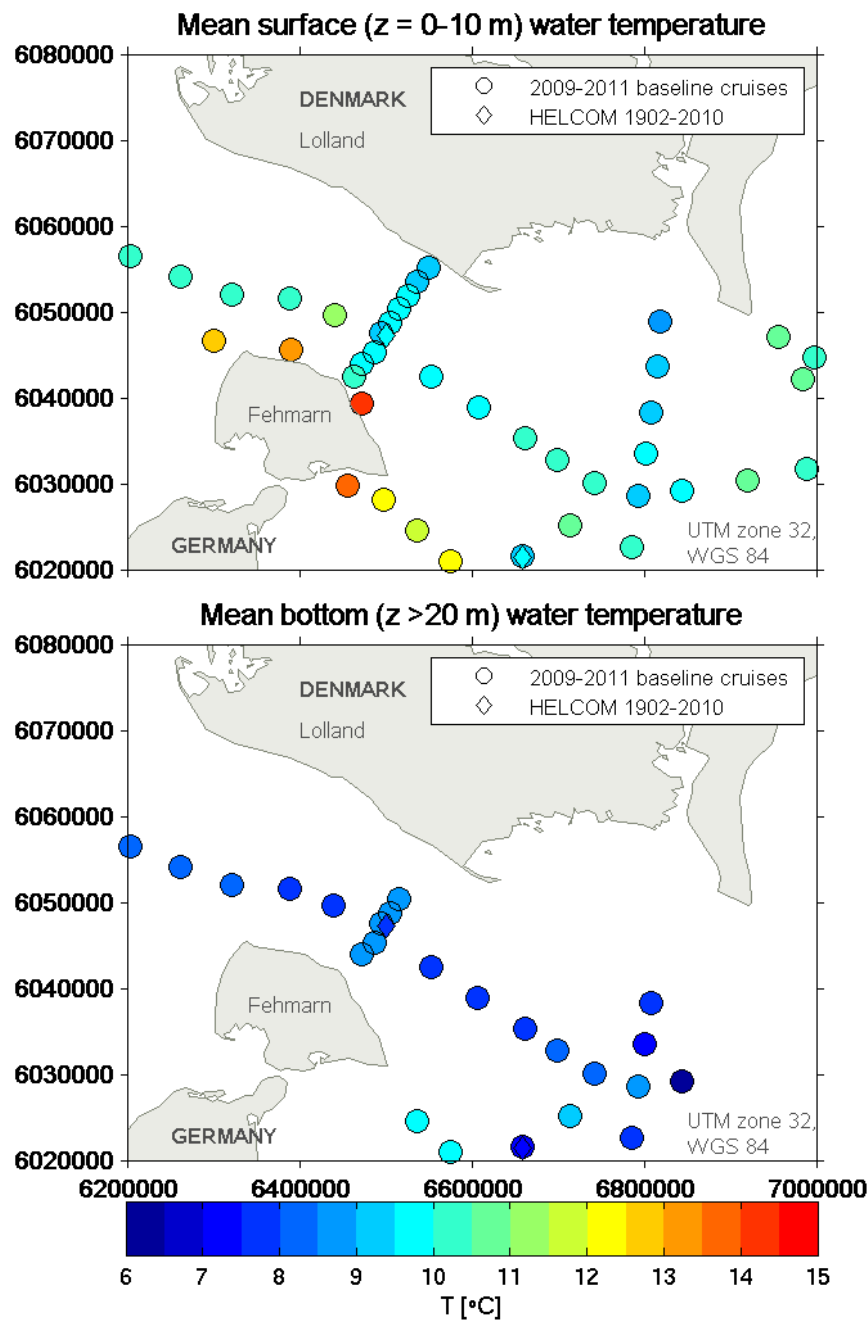


Fig. 6.51 Mean surface (upper panel) and bottom (lower panel) water temperature observed during the 2009-2011 baseline cruises. The warm transect across the entrance to the Bay of Lubeck was mainly sampled in summer.

A satellite image of sea surface temperature depicted in Fig. 6.52 shows that the central channels in Great Belt and Fehmarnbelt may still have colder water masses ($\Delta T \approx 2^\circ\text{C}$) in spring while the coastal areas and parts of the surrounding basins have already been warmed.

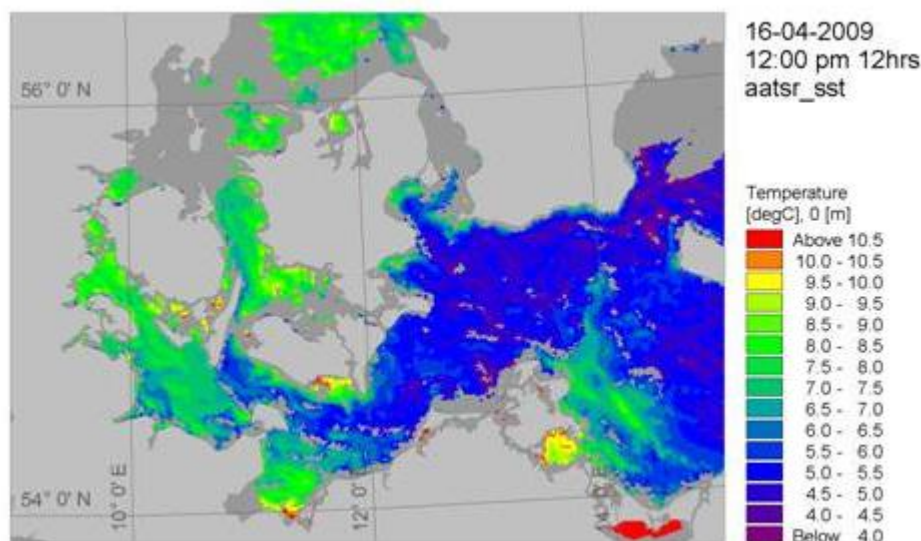


Fig. 6.52 Sea surface temperature on 16 April 2009 in the Belt Sea and Arkona Sea as observed by the ENVISAT satellite (ESA 2010).

To highlight the seasonal differences in temperature and salinity and the resulting stratification, we have furthermore analyzed the frequency of occurrence for temperature, salinity and the buoyancy frequency N^2 in summer (June-August) and winter (December-February) for the Main Stations in the Fehmarnbelt and Mecklenburg Bight.

The buoyancy frequency of a water parcel, also called the Brunt-Väisälä frequency, is defined as:

$$N^2 = -\frac{g}{\rho} \frac{\partial \rho}{\partial z} \quad (6-2)$$

where

- g is the gravitational acceleration
- ρ is the water density
- z is the depth of the water parcel in question.

If N^2 is positive a water parcel will oscillate back into its former position when it is perturbed from its initial position, i.e. the stratification is stable. For negative values the water stratification is statically unstable and convection or overturning will occur.

The southern Fehmarnbelt (MS02) shows a distinct stratification in summer with a mixed layer down to 17 ± 2 m depth. The average salinity is around 11.5 psu at the surface and 26 psu at the bottom. Temperatures are frequently above the average throughout the water column with temperatures of 18°C to 20°C at the surface and about 11°C at the bottom. Below 20 m depth a minimum temperatures of 6°C is common even in summer (Fig. 6.53).

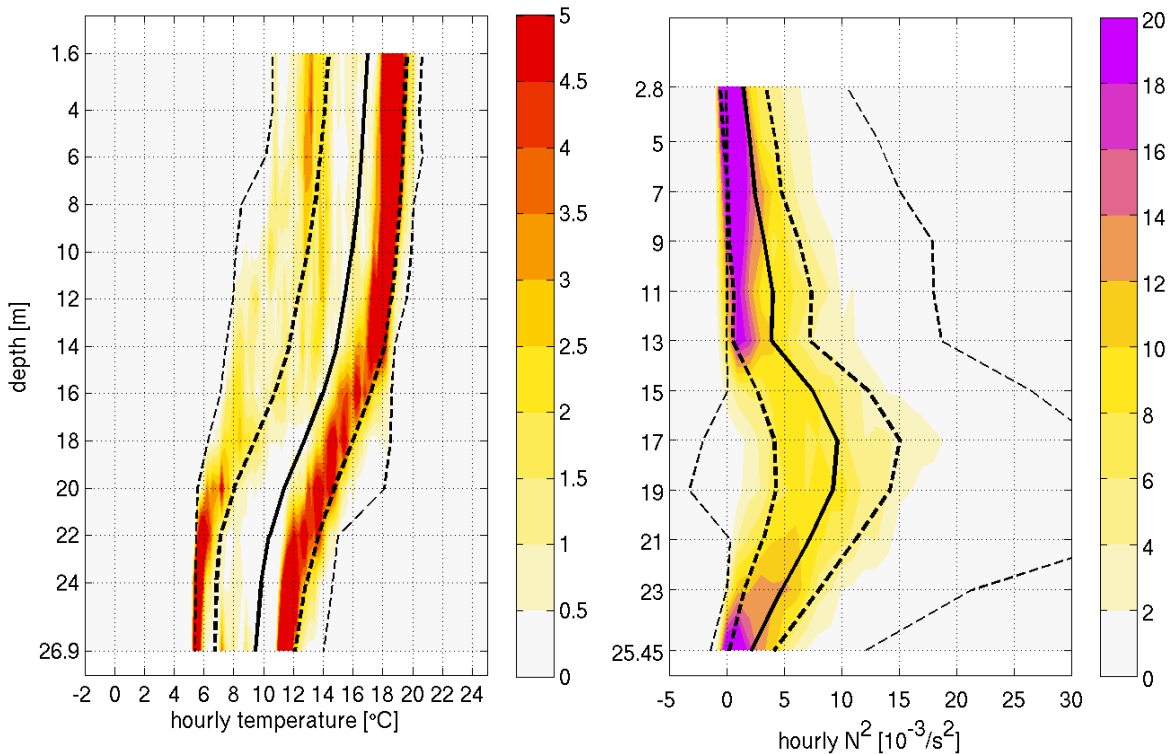
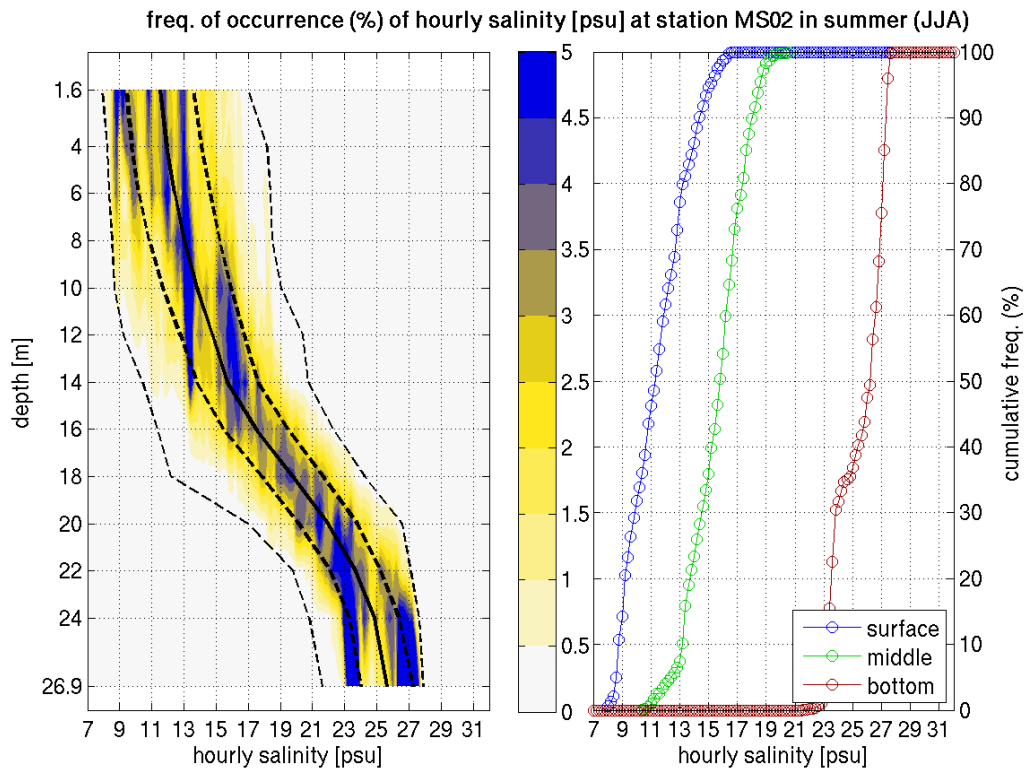


Fig. 6.53 Frequency of occurrence (in % of time) of salinity (colour), temperature and buoyancy frequency at MS02 in summer. Bold lines: averaged profile, bold dashed lines: averaged profile \pm standard deviation, simple dashed lines: all-time minimum and maximum salinity at depth level, -o- : cumulative frequency of occurrence of salinity at uppermost, central and lowest observed depth levels (temperature and salinity interval when calculating percentage is 0.2 °C or psu)

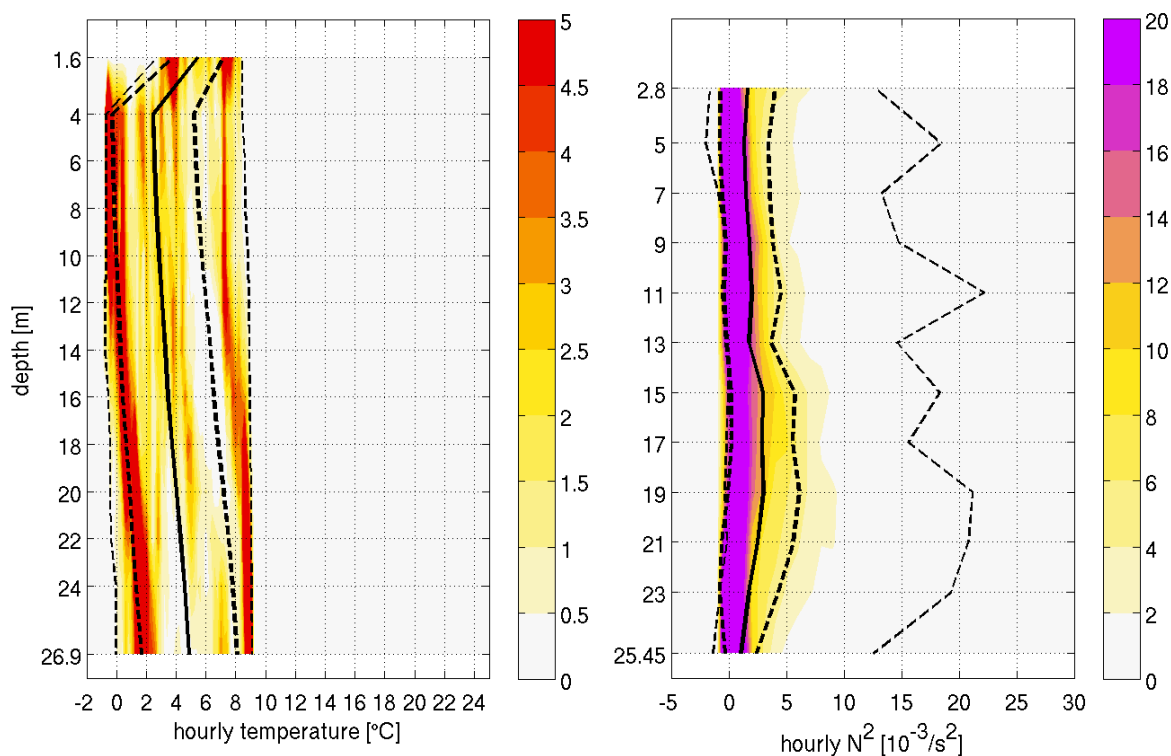
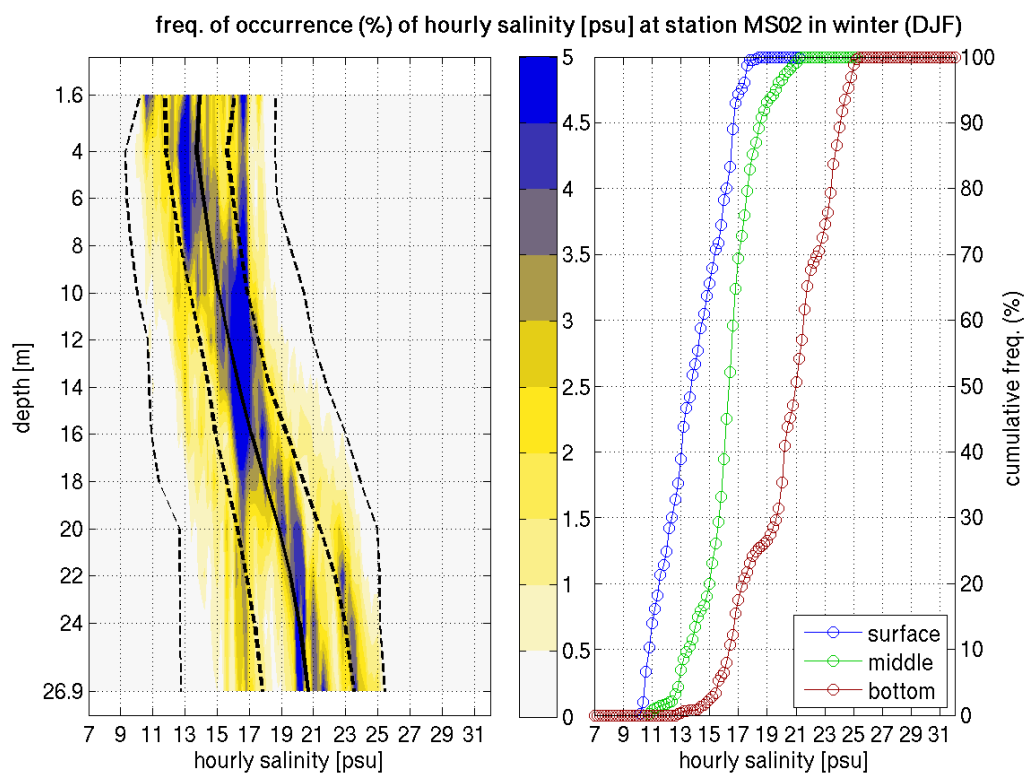


Fig. 6.54 Frequency of occurrence (in % of time) of salinity (colour), temperature and buoyancy frequency MS02 in winter. Bold lines: averaged profile, bold dashed lines: averaged profile \pm standard deviation, simple dashed lines: all-time minimum and maximum salinity at depth level, -o- : cumulative frequency of occurrence of salinity at uppermost, central and lowest observed depth levels (temperature and salinity interval when calculating percentage is 0.2 °C or psu)

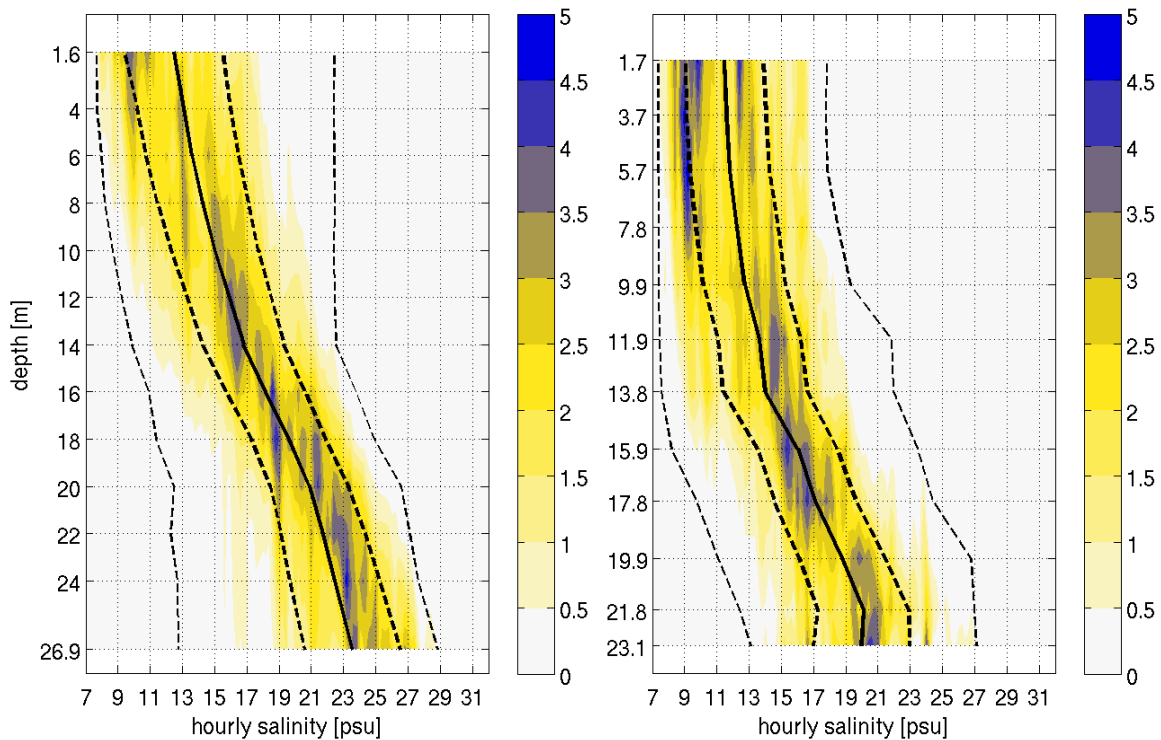


Fig. 6.55 Frequency of occurrence (colour) of salinity at MS02 (left) and MS03 (right) in the baseline period. Bold lines: averaged profile, bold dashed lines: averaged profile \pm standard deviation, simple dashed lines: all-time minimum and maximum salinity at depth level (temperature and salinity interval when calculating percentage is 0.2 °C or psu)

In winter there is no apparent halocline even the salinity increases from surface to bottom (14 psu to 20 psu), see Fig. 6.54. The homogenous temperature does not contribute to stratify the water column. A buoyancy frequency beyond its standard deviation occurs only in less than 4% of all cases and mostly stays below the average value.

Another common oceanographic tool applied to present properties of water masses is the so-called T-S diagram where temperature is plotted against salinity and corresponding isolines of density are added. The clusters displayed in such diagrams mark pools of water with similar characteristics.

In connection with the T-S diagram it is noted that in general:

- X-axis: The highest salinities are measured close to the bottom and the lowest salinities close to the surface; and
- Y-axis: The highest temperatures are measured during the summer and the lowest temperatures during winter.

The Mecklenburg Bight (MS03) shows features that are very similar to MS02 in the southern Fehmarnbelt since it is the inflowing water that supplies the lower layers in the central Mecklenburg Bight, but the salinity is lower at MS03 because of mixing of the downwards mixing. The average bottom salinity is 19.5 psu at MS03 and 23.5 psu at MS02, see Fig. 6.55 and Fig. 6.56.

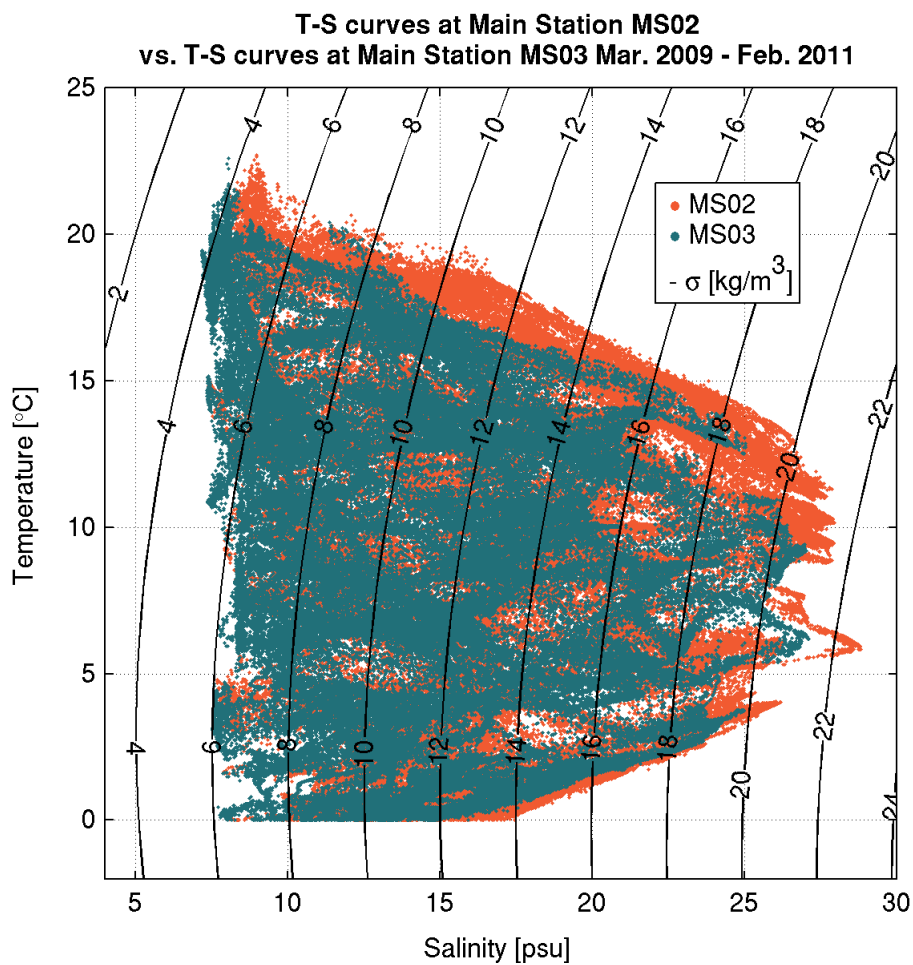


Fig. 6.56 T-S diagram based on measurements collected at MS02 and MS03. Black lines represent the oceanographic water density, $\sigma = \rho - 1000 \text{ kg/m}^3$.

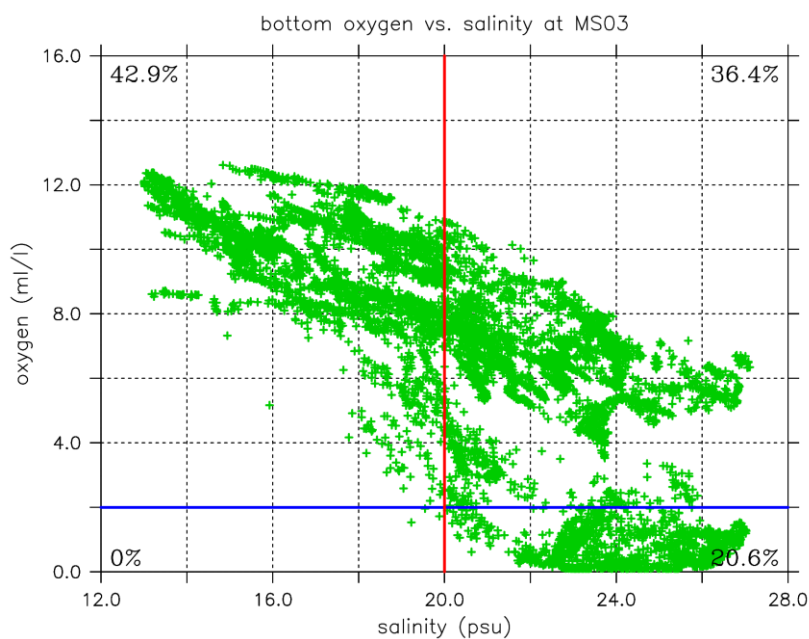


Fig. 6.57 Bottom oxygen and salinity at station MS03 observed during the 2009-2011 baseline period. The four quadrants denote the frequency of occurrence for water masses within the given salt/oxygen limits.



In the central Mecklenburg Bight at station MS03 hypoxic (concentration of oxygen less than 2 ml/l) and anoxic (occurrence of hydrogen sulphide) conditions is often found for water masses with salinities greater than 20 psu (see Fig. 6.57). Only in 36.4% of time the water masses with $S > 20$ psu are sufficiently ventilated, and show oxygen concentrations of 2 ml/l or more. Low saline water masses have the highest concentrations of oxygen with a maximum of 13 ml/l.

Similar relationship is found at MS02.

The time-series show (see Fig. 6.58) that both oxygen and salinity at the bottom of station MS03 have a pronounced annual cycle. In winter, due to convection and wind-induced stirring, the salinity reaches a minimum, because low-saline, oxygenated surface water is mixed down into the deep layer. In summer, when the winds are weak, inflowing saline water from the Fehmarnbelt can reside in the Mecklenburg Bight for longer periods. In this period low oxygen concentrations are found that are further reduced by the decomposition of spring and summer blooms of algae. Consequently, hypoxic conditions occur from July to October.

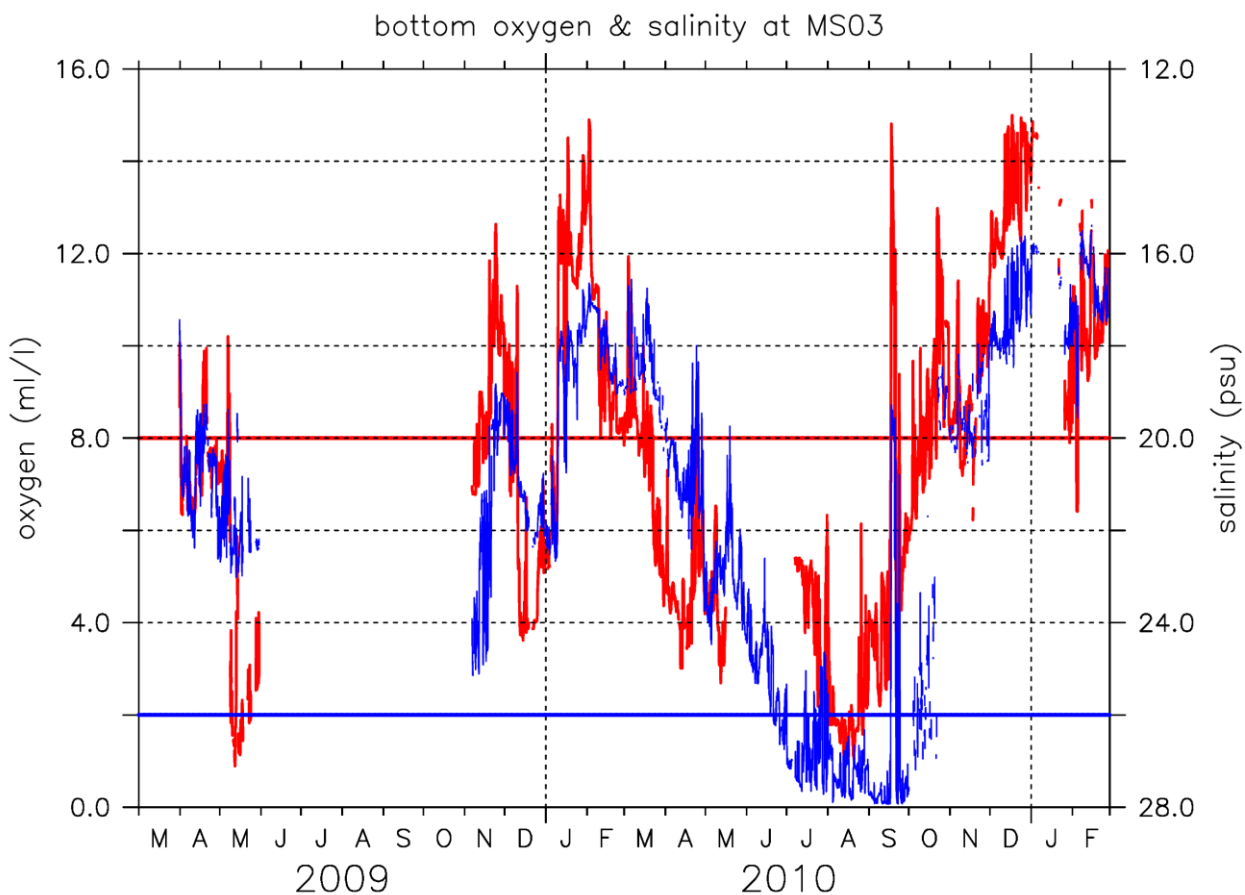


Fig. 6.58 Bottom oxygen (blue) and salinity (red) at station MS03 observed during the 2009-2011 baseline period. Note the opposed direction of scales for salinity and oxygen.

Conditions with low oxygen at the bottom were also observed during the baseline surveys. The horizontal distributions show that the hypoxic areas typically are found in deeper areas with high salinity. Fig. 6.59 and Fig. 6.60 show examples of oxygen minima in the Fehmarnbelt area as observed in summer of 2009 and autumn 2010. In August 2009 (Fig. 6.59) an extended hypoxic area of roughly 600 km² was found in the Mecklenburg Bight and another small area in Fehmarn-

belt. Also in October 2010 there was a continuous hypoxic area of approximately 700 km² extending from the Fehmarnbelt into the central Mecklenburg Bight (Fig. 6.60).

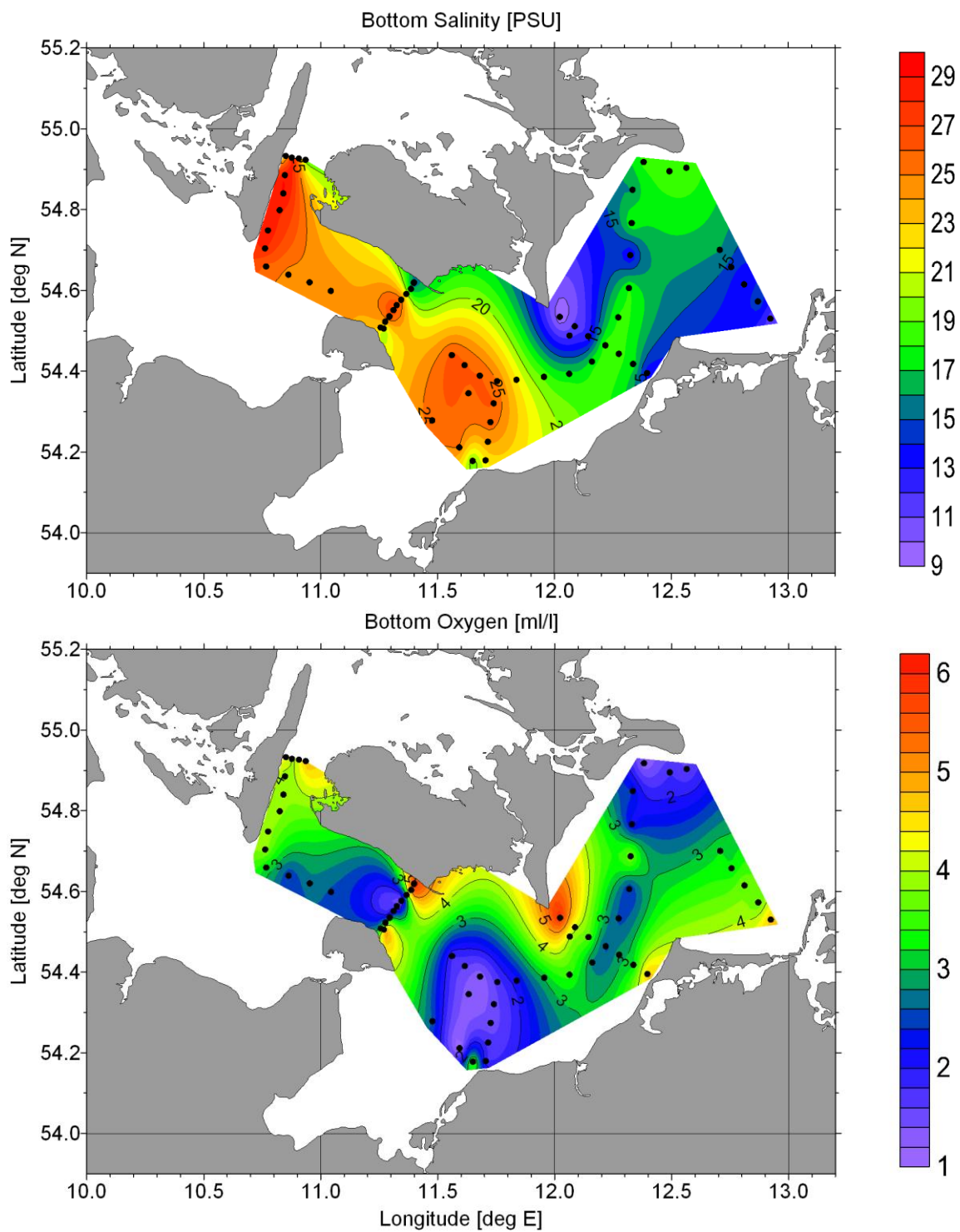


Fig. 6.59 Bottom salinity and oxygen concentration observed in August 2009 during the monitoring surveys from 2009-08-24 to 2009-08.

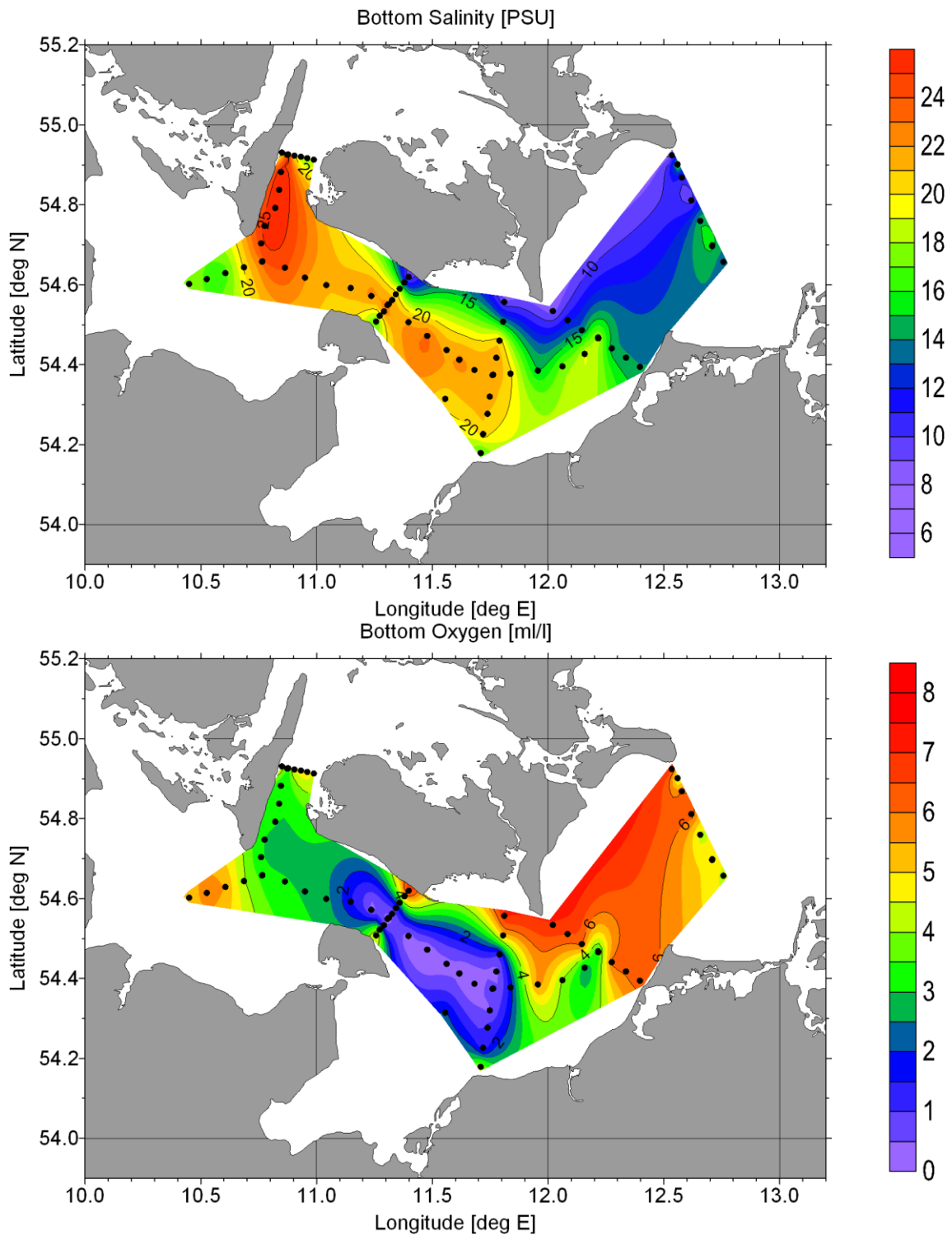


Fig. 6.60 Bottom salinity and oxygen concentration observed in October 2010 during the monitoring surveys from 2010-10-12 to 2010-10-13.

6.5 Sea Ice

The winters 2009-2010 and 2010-2011 were both cold. The frost index during the winter 2009-2010 is 162.8 and it was an ice-winter (SOK 2010). The frost index data can be found in Fig. 8.19 (definition of frost index is provided in Chapter 8.5).

The frost index for the winter 2010-2011 is not yet published or available from SOK.

Despite the strong winter of 2009-2010 not much ice was found in Fehmarnbelt. The observations at Rødbyhavn are shown in Fig. 6.61. Only 11 days of ice occurred off Westermønsø in the period from 26 January 2010 to 18 February 2010 and 10 days of ice were recorded at Marienleuchte from 26 January 2010 to 17 February 2010.

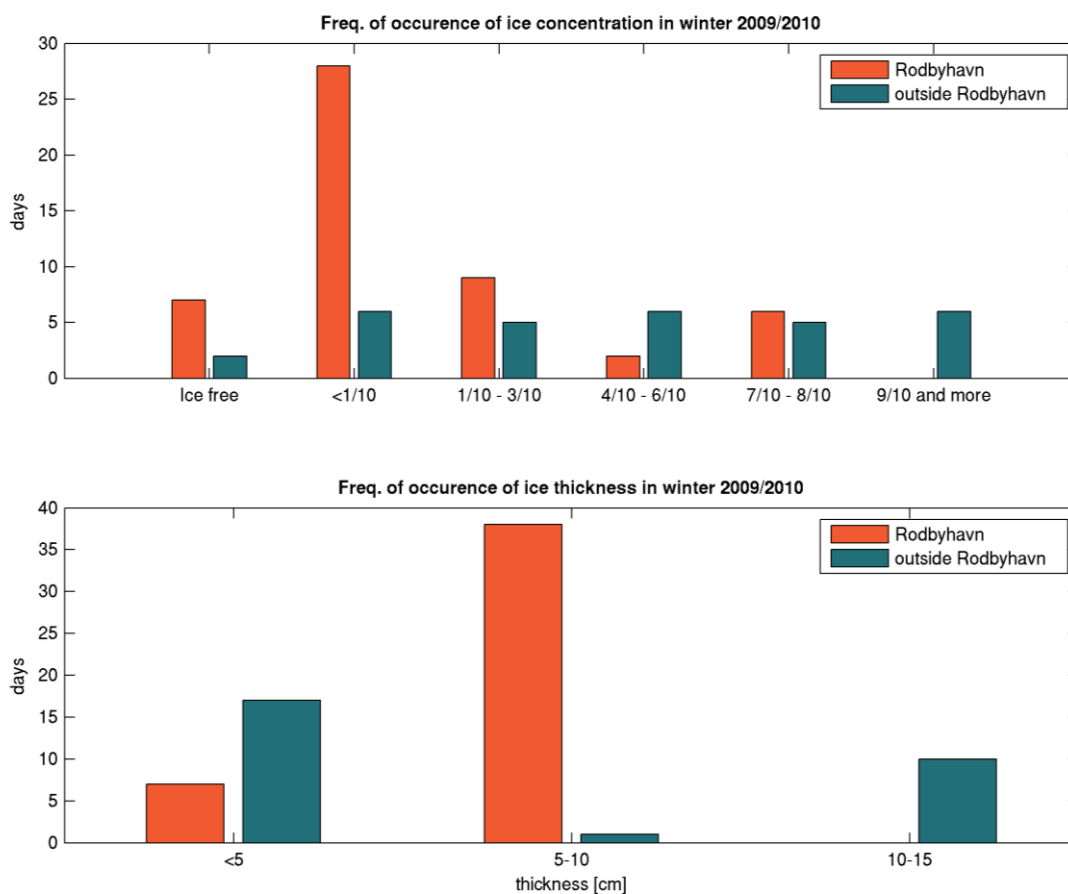


Fig. 6.61 Observed ice at Rødbyhavn (SOK 2010).



7 SELECTED FLOW FEATURES IN BASELINE OBSERVATIONS

In the following some selected hydrographic phenomena of importance in the Fehmarnbelt area are selected and described on the basis of data from the monitoring programme. In these presentation parameters are also related to one another.

7.1 Outflow and Inflow Conditions in the Belt Sea

Three maps resolving simulated currents and salinities in the Belt Sea in about 5 m depth are selected to illustrate inflow and outflow situations, see Fig. 7.1 to Fig. 7.3. The figures show:

- Water masses flowing out of the Central Baltic Sea that follows the northern coastline in Fehmarnbelt, see Fig. 7.1. The outflow has widened and occupies most of the width of Fehmarnbelt. The current speeds have a tendency to be higher close to the salinity front. An anti-cyclonic circulation takes place in the Kiel Bight;
- A situation where the flow changes from outflow to inflow. The low saline water masses flows from the Langelands Belt into the Kiel Bight, see Fig. 7.2. This flow pattern continues until the water level inside the Kiel Bight is lifted and able to turn the flow from Langelands Belt directly into the Fehmarnbelt; and
- Water masses flowing into the Central Baltic Sea, see Fig. 7.3. The water masses flows from Langelands Belt more or less directly into the Fehmarnbelt. The main current passes by the Kiel and Mecklenburg Bights. An anti-cyclonic circulation takes place in the Mecklenburg Bight.

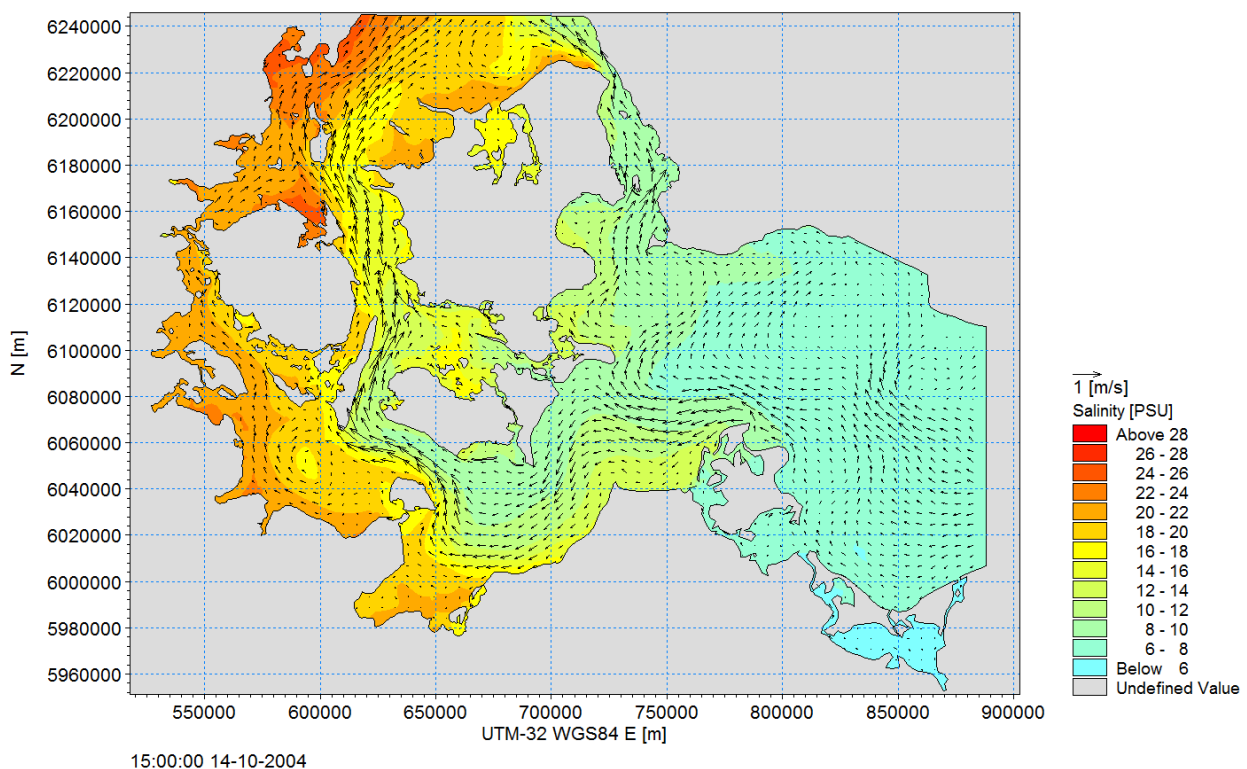


Fig. 7.1 Map of simulated current and salinity in 5m depth on the 14 October 2004 at 15:00 UTC.

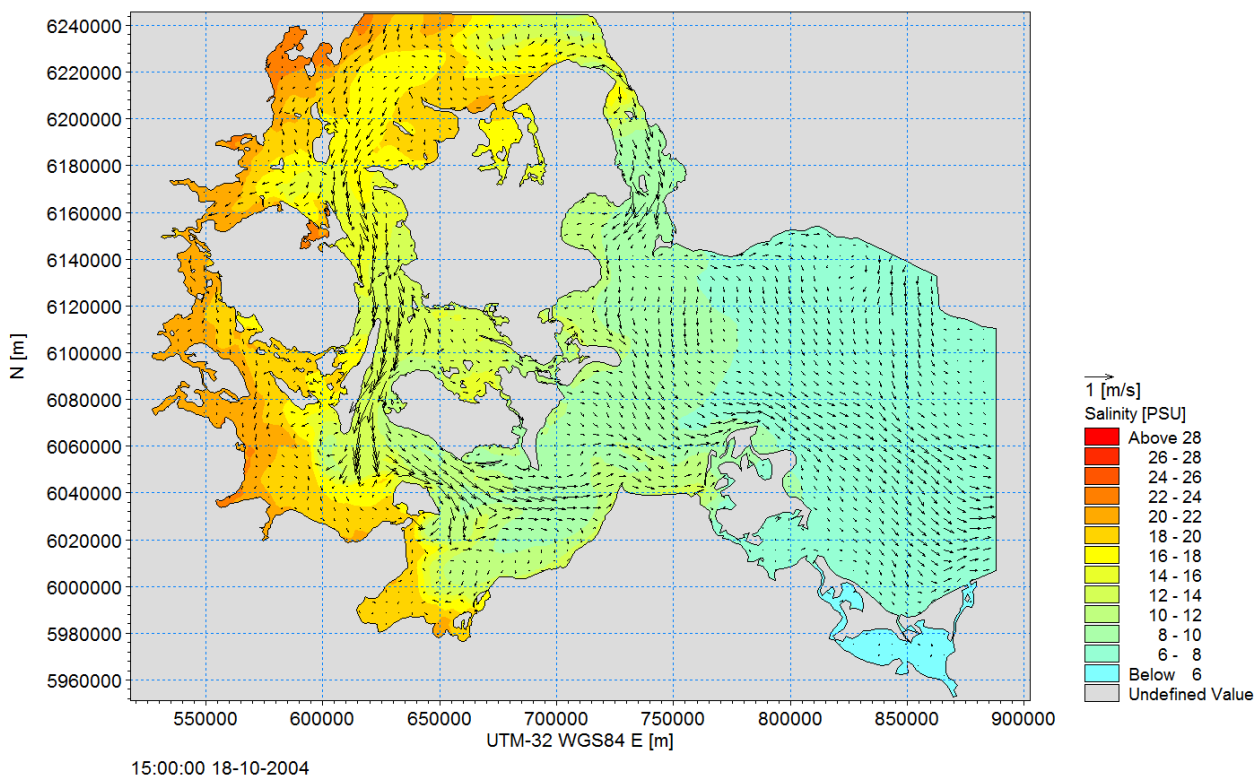


Fig. 7.2 Map of simulated current and salinity in 5m depth on the 18 October 2004 at 15:00 UTC.

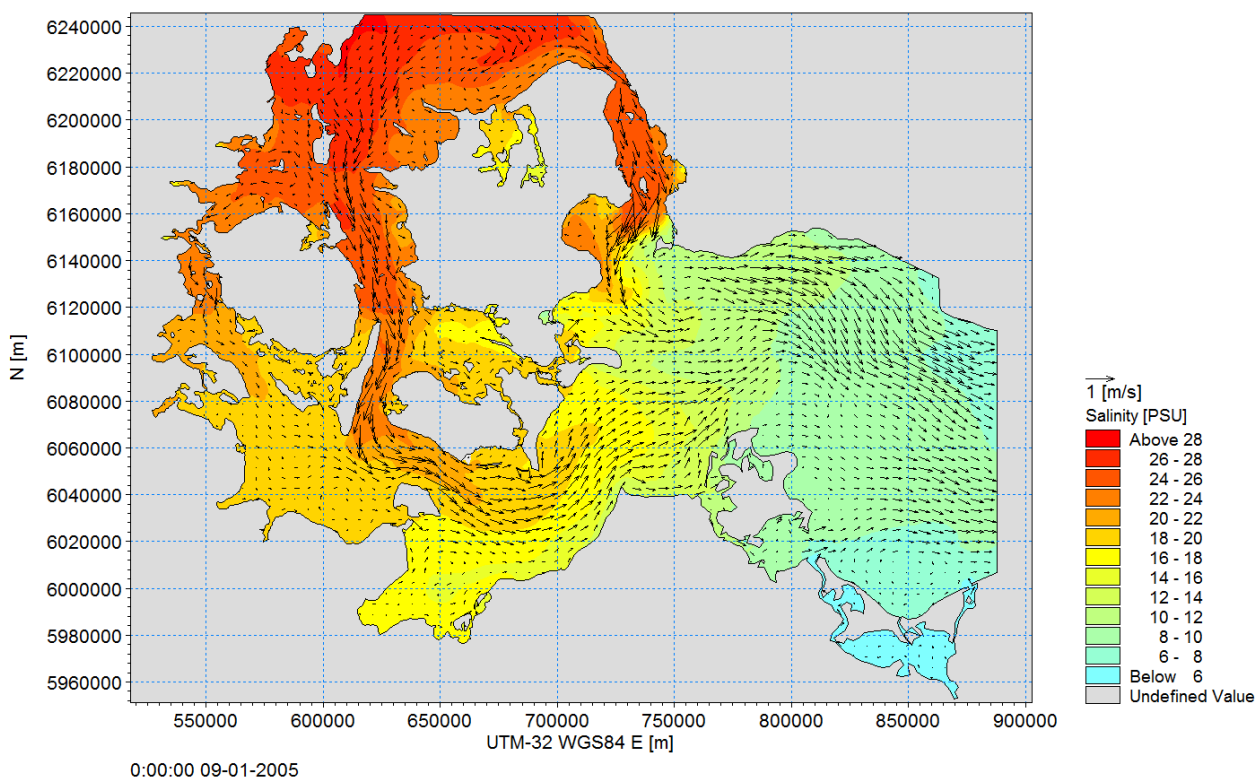


Fig. 7.3 Map of simulated current and salinity in 5m depth on the 9 January 2005 at 00:00 UTC.



7.2 Horizontal Distribution of Water Masses in Fehmarnbelt

In the Fehmarnbelt area the overall salinity distribution depicts a west–east gradient at all depth levels, which is maintained by the large scale saline gradient between the North Sea and the Baltic Sea.

Inflowing saline water advances through the Fehmarnbelt into the Mecklenburg Bight. There, a certain amount of saline water is buffered in the bowl shaped topography west of the Darss Sill.

The level of the halocline separating the saline bottom water from the brackish surface water must be above the minimum depth of the Darss Sill (18 m) to force an overflow of saline bottom water into the Arkona Basin.

Fig. 7.4 depicts two typical examples of the estuarine circulation in the greater Fehmarnbelt area.

First a horizontal distribution of measured salinity in the Fehmarnbelt region during an outflow situation is shown in the upper panel. While passing the Mecklenburg Bight, the outflowing surface water, which mainly propagates along the Danish coastline, shows an increasing salinity. Outflow prevails at all ADCP lines, and only in the central Mecklenburg Bight a small counter-current is observed, which may be due to an eddy.

The lower panel of Fig. 7.4 depicts a small inflow event that passes the Fehmarnbelt and reaches the area of the Darss Sill. Bottom salinities are well above 20 psu, whereas the upper layer is covered by brackish surface waters. Due to Coriolis force the core of inflowing saline waters spread out along the southern rim of the belt until it reaches the Darss Sill.

During the survey prevailing southeast winds intensified the southward shift of saline waters due to upwelling at the Fehmarn side of the channel.

Only the Fehmarnbelt ADCP survey measurements show a clear inflow signal because the plume had just passed through the channel when measurements were taken.

All other transects show outflowing or circulating water. This illustrates that a period of 6 days does not provide a synoptic view.

Also (Schmidt et al. 1998) have shown by a synchronized comparison of measurements and simulations of currents that reverse flow can occur at different locations in the area within 2 or 3 days.

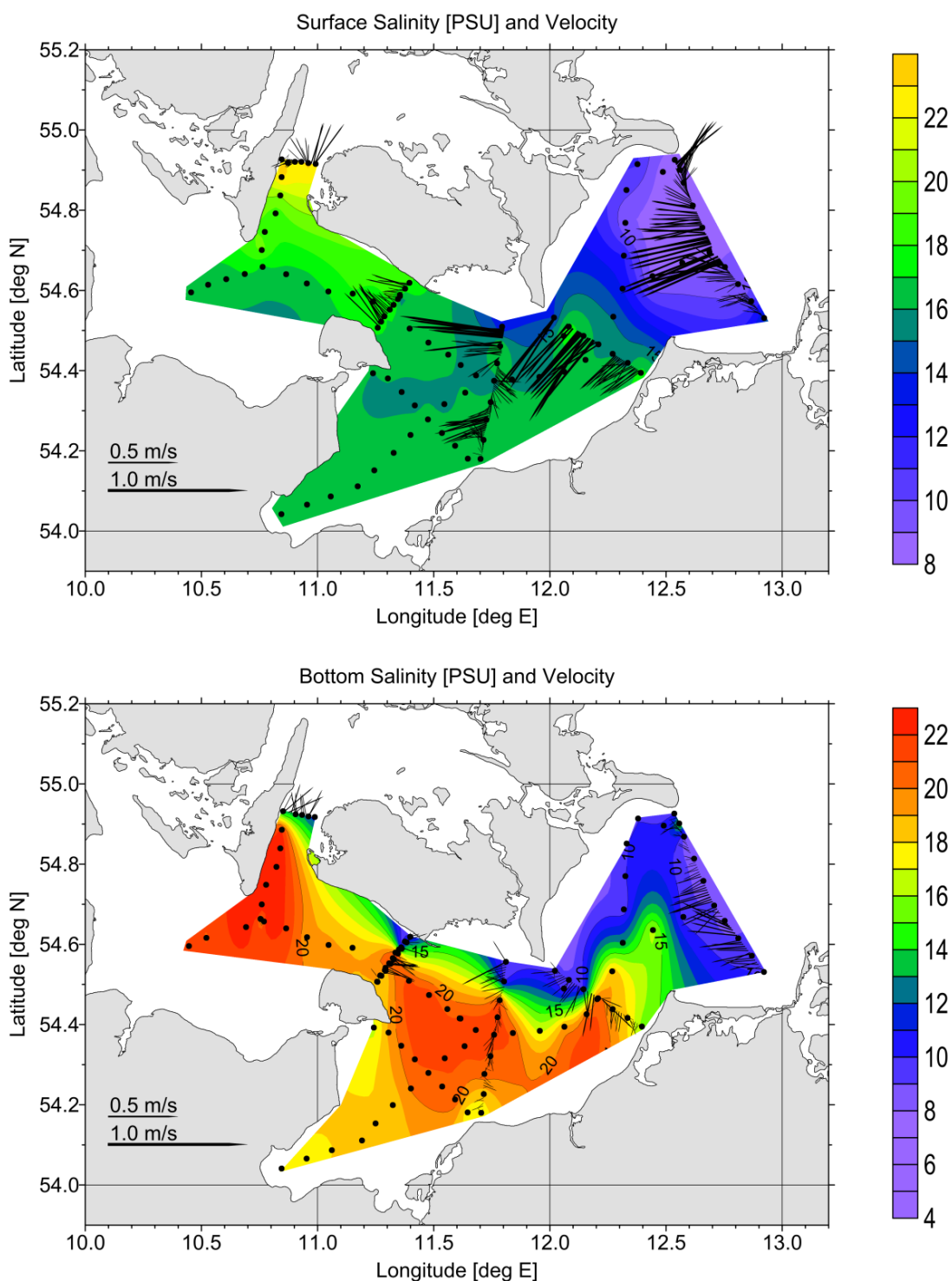


Fig. 7.4 Measured surface salinity and current in the Fehmarnbelt area during monitoring survey from 30 November 2009 to 6 December 2009 (top panel), while outflow took place. Measured bottom salinity and current in the Fehmarnbelt area during monitoring survey from 27 October 2009 to 3 November 2009 (bottom panel), while pulsating inflow took place.

7.3 Velocity Distribution in the Link Corridor

Velocity distributions in the Fehmarnbelt cross-section are shown in Fig. 7.5 (more distributions can be found in Appendix A). The red and yellow colours refer to inflow



and the blue colours refer to outflow. The current is not homogeneous, but varies over the cross-section.

The observed patterns depict uniform flow, two and three layer flow, dipole and quadrupole structures. The actual flow pattern depends on a complex superposition of wind forcing, remote driven barotropic and baroclinic pressure gradients and on local stratification. Additionally, it will be modified by tides. The isohalines (not shown) indicate geostrophic balance of currents and cross-channel pressure field. The current has a spatial cross channel structure and varies in both the vertical and horizontal direction. The speed ranges from -80 to +80 cm/s.

The changes of the flow patterns are rather quick, so a covering of sections with a moving research vessel implies a substantial aliasing.

7.4 Mesoscale Eddies

Several times mesoscale eddies were observed in the Fehmarnbelt. A prominent example is presented in Fig. 7.6. The observed anticyclonic eddy covered the southern half of the link corridor in the Fehmarnbelt. The maximum current velocities were about 0.3 m/s which is a typical value for mesoscale eddies in the western Baltic.

The eddy covered the entire water column. Its geostrophic adjustment caused an uplift of the dense bottom water, forming a dome like structure in the centre of the eddy. This indicates that an eddy life time is significantly longer than the inertial period (>14.4 hours). However, the same transect worked on 16 June 2009 at 12:35, 18 hours earlier, did not reveal any eddy like structure.

The link corridor transect was repeated several times on the 17 June, and an eastward movement of the eddy with the mean flow was observed. The eddy has passed the link corridor completely at 22 UTC.

The eddy has passed the link corridor from west to east. The available measurements cannot provide any information about how the eddy was formed or how its later pathway looked like.

A possible location for the formation of eddies in the Fehmarnbelt might be the deep and narrow valley in the bottom topography along the survey line at 11°0.0'E, close to the western edge of the bowl like Fehmarnbelt (cf. Fig. 7.7). At this constriction an eastward directed inflow can generate jet like currents (Fig. 7.8) that are injected in the slowly moving water body of the Fehmarnbelt and may cause the formation of mesoscale eddies.

7.5 Upwelling

The current distribution in the Fehmarnbelt is strongly modified by local wind forcing, but also by the Coriolis force. Upwelling is often found at the northern or southern rim of the belt and is forced by along channel winds.

In January 2010 a strong upwelling event was observed during the monitoring survey. From 12 to 18 January upwelling favourable winds, varying between 5 and 12 m/s, blew over the Fehmarnbelt (Fig. 7.9).

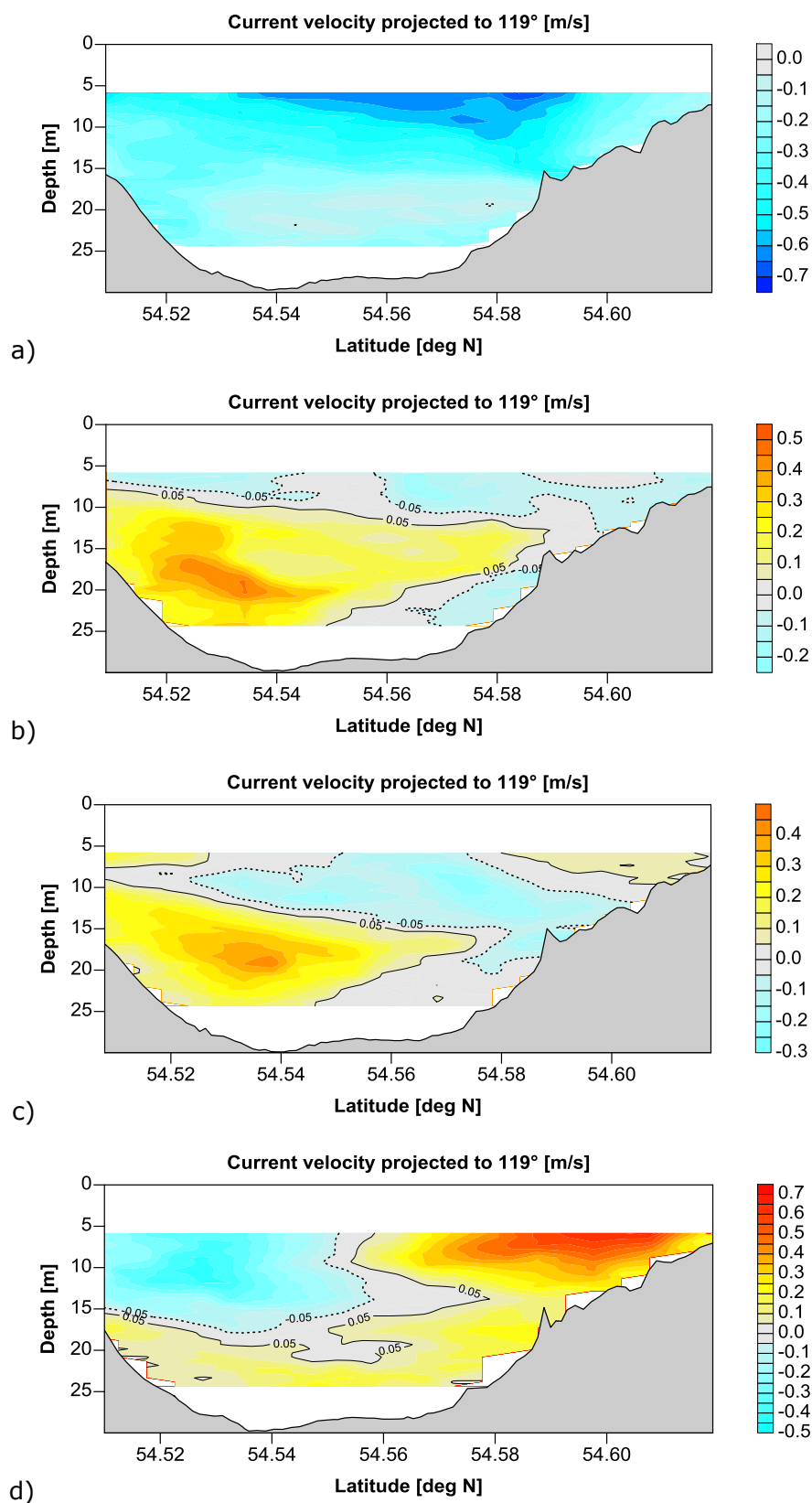


Fig. 7.5 Along-channel current velocity in the link corridor during the survey in August 2009. The current pattern changed rapidly. The data were collected within a week: a) 24 August 2009; b) 27 August 2009; c) 28 August 2009; and d) 31 August 2009. The 119° is clockwise from north: inflow is positive and outflow is negative.

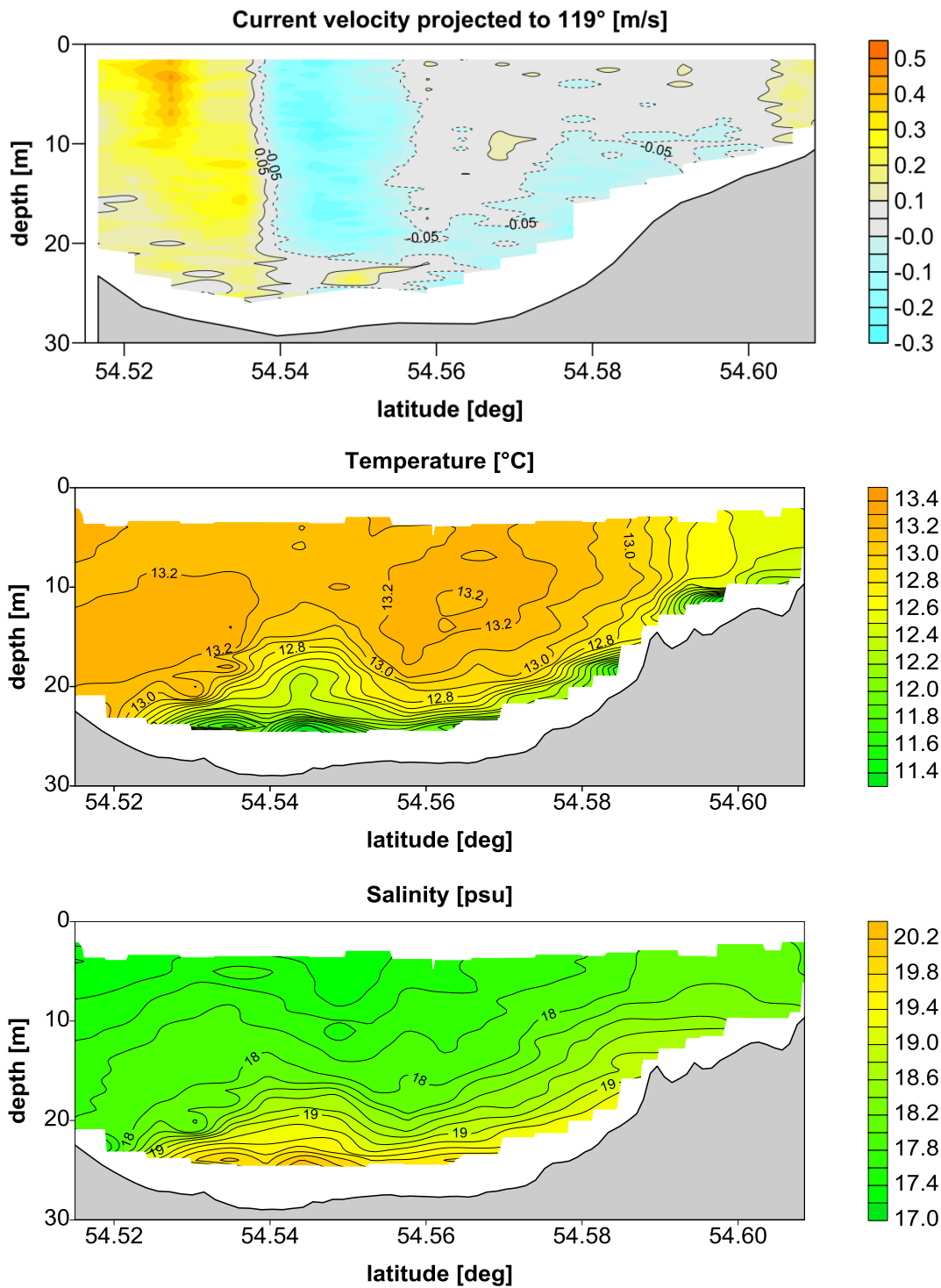
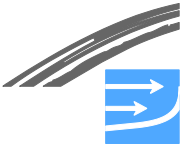


Fig. 7.6 Cross channel current velocity (top), temperature (middle) and salinity (lower panel) along a transect through a mesoscale eddy in the link corridor on 17 June 2009 05:00 UTC. An eddy is clearly indicating by the velocity distribution around the doming of temperature and salinity stratification.

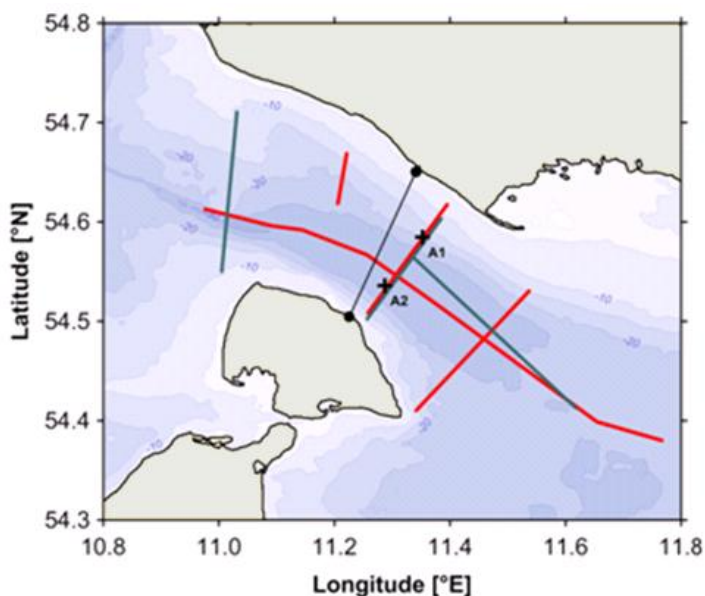


Fig. 7.7 Map of high resolution survey at the Fehmarnbelt Link. Red lines indicate the combined ScanFish T-CTD)/T-ADCP/VM-ADCP transects and green lines the combined MSS/VM-ADCP transects. The black crosses depict the mooring positions.

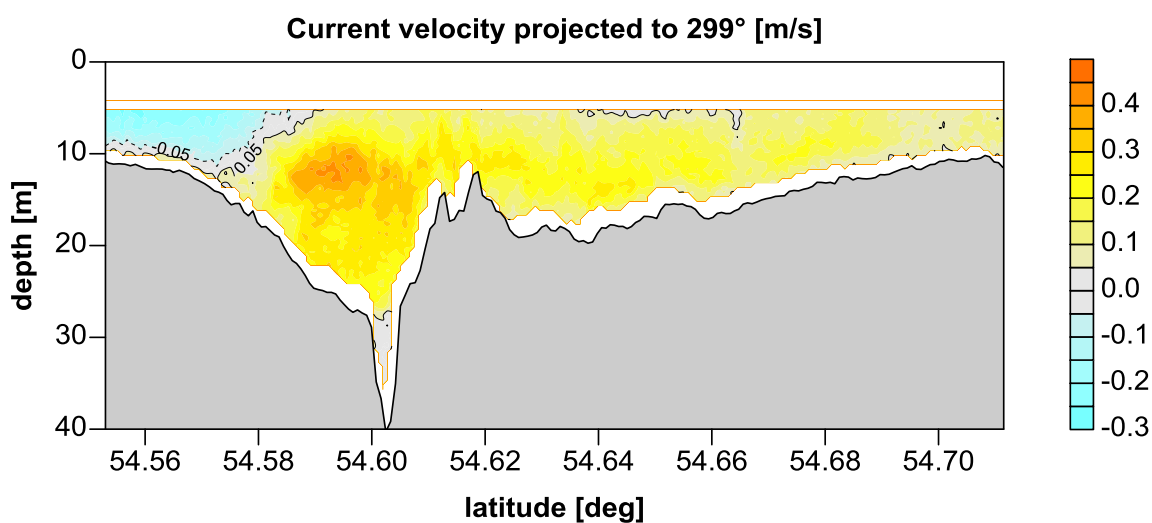


Fig. 7.8 Jet-like eastward flow in the narrow section west of the Fehmarnbelt, see Fig. 7.7, westernmost green line (18 June 2009 09:00 UTC).

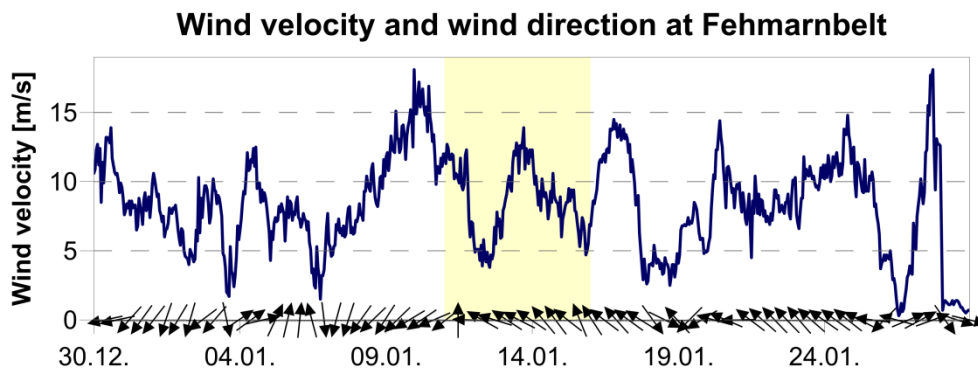


Fig. 7.9 Time-series of wind in the Fehmarnbelt during January 2010.



The south-east wind caused a cross channel Ekman transport towards north-east in the surface layer of about 10 m thickness. Below the surface layer a compensating flow is found (Fig. 7.10). Whereas the saline bottom layer depicts no cross channel current component. The along channel current shows a strong inflow signal at the southern rim of the Fehmarnbelt with a slight increase of current velocity towards the bottom. This current pattern coincides with an upward lifted belt of inflowing saline bottom water.

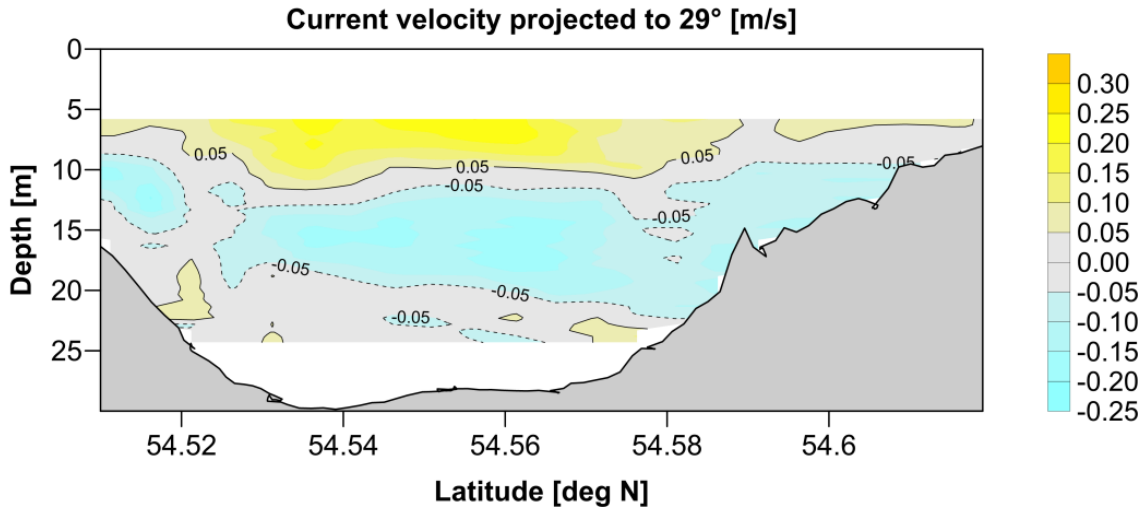


Fig. 7.10 Cross channel flow with a northward surface current and a southward directed compensation flow in mid water layer. Date: 11 January 2010.

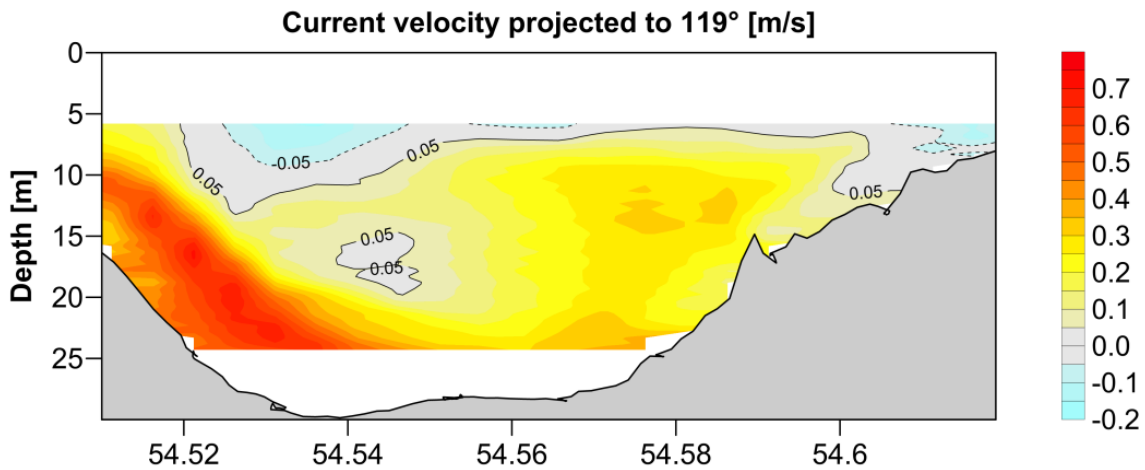


Fig. 7.11 The along channel current shows a situation with strong inflow at the southern flank. Date: 11 January 2010.

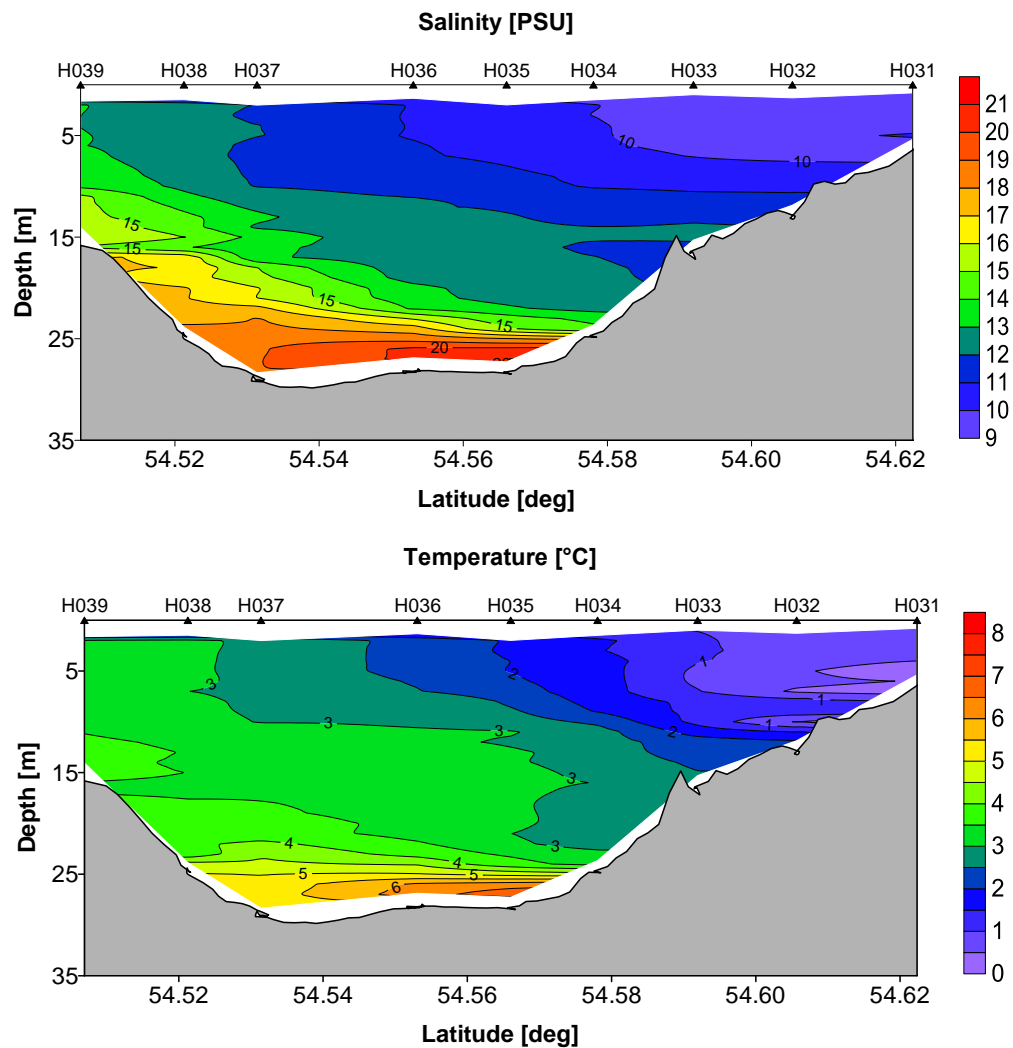


Fig. 7.12 The salinity (top) and temperature (bottom) pattern refers to upwelling in the south and downwelling in the north of the Fehmarnbelt channel. Date: 11 January 2010.

A simulated small inflow event is depicted in Fig. 7.13 (extracted from MIKE local model), revealing a case of strong stratification with inflowing saline bottom water of $S > 22$ psu filling the deep central channel below a depth of 22 m. Limited upwelling of colder water is observed in the distributions.

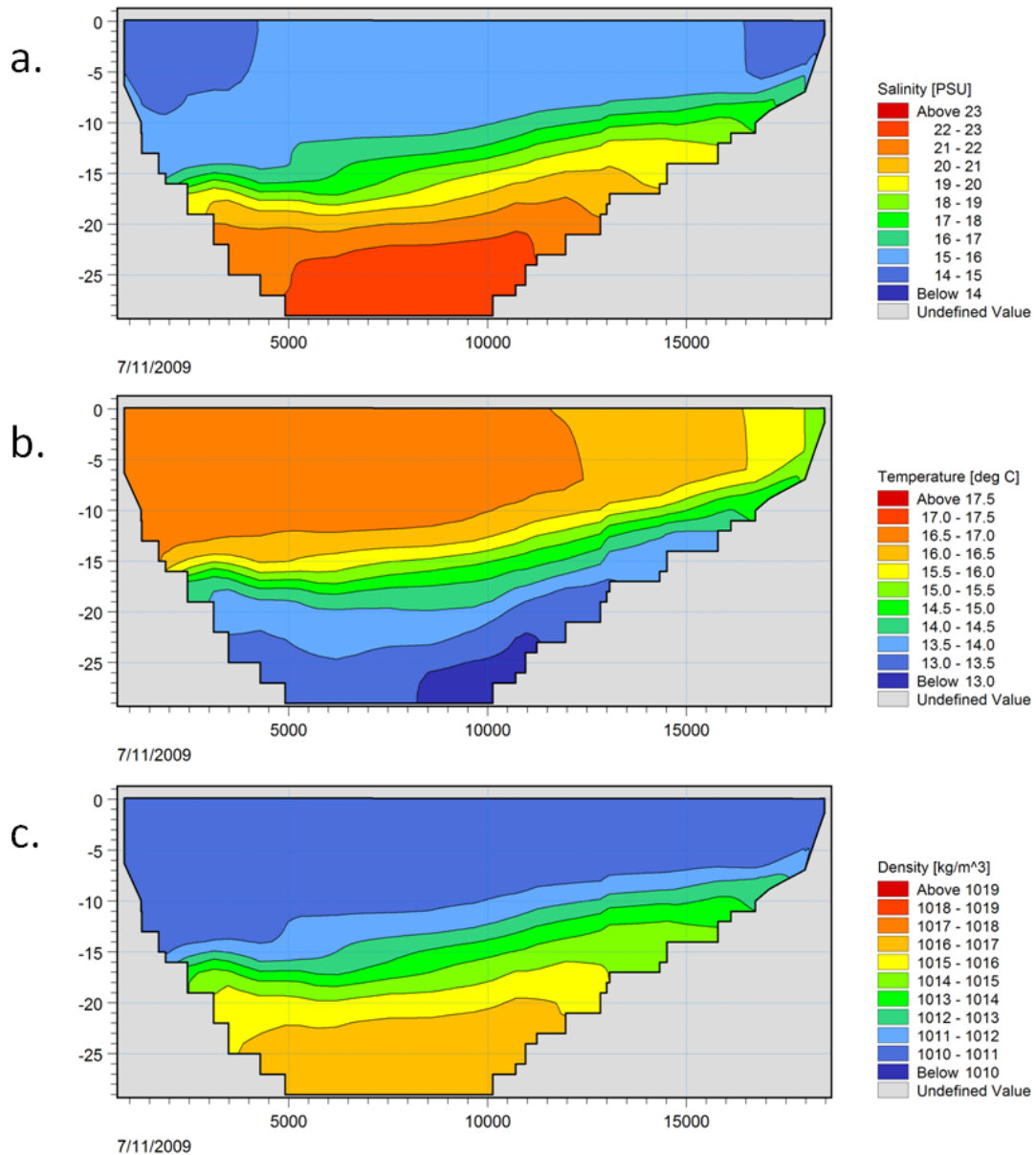


Fig. 7.13 Simulated parameters: a) salinity and b) temperature; in the Puttgarden-Rødbyhavn cross-section during an inflow event. Date: 11 July 2009.

7.6 Comparisons of Flow Distributions across Fehmarnbelt

In the following measured and simulated currents in the upper 10 m across the Fehmarnbelt are shown, see Fig. 7.14 and Fig. 7.15.

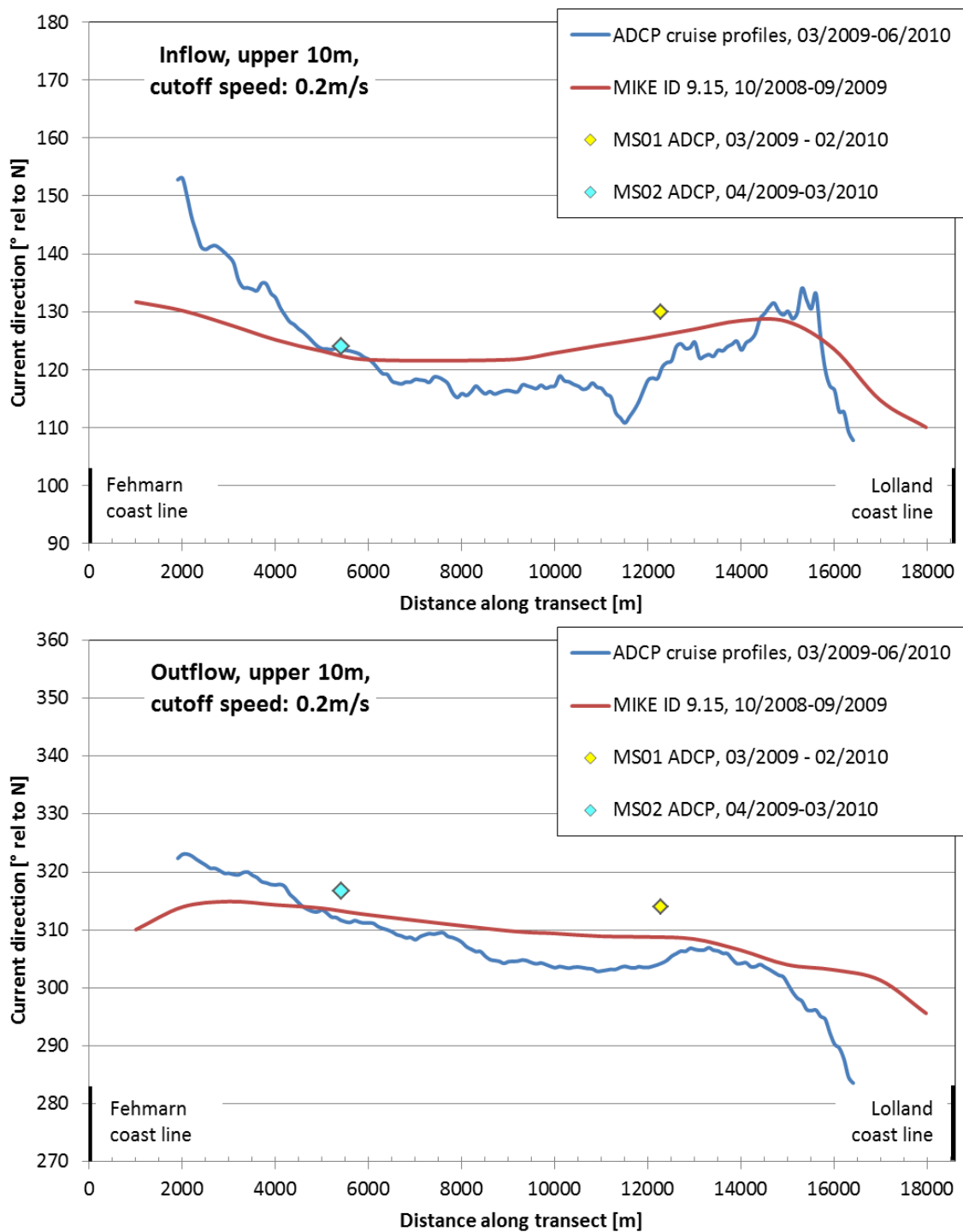


Fig. 7.14 Mean current direction (relative to north) within the 10 m surface layer across Fehmarn-belt along the alignment as observed with ship mounted ADCP (monthly cruises) and at the main stations MS01 and MS02. The red lines depict current directions simulated with the local MIKE model. The upper panel refers to inflow in south-easterly direction and the lower panel to north-western outflow.

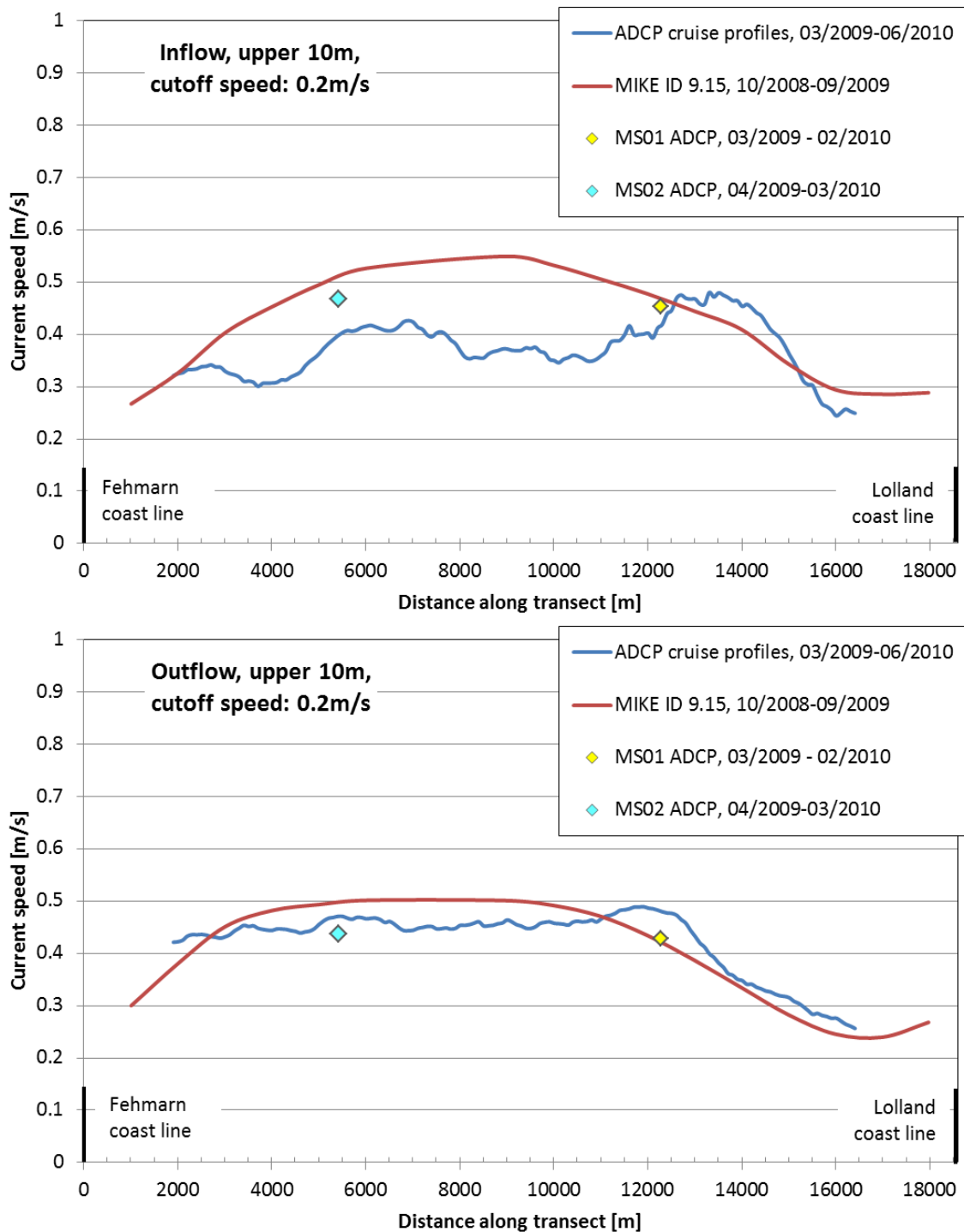


Fig. 7.15 Mean current speed (m/s) within the 10 m surface layer across Fehmarnbelt along the alignment as observed with ship mounted ADCP (monthly cruises) and at the main stations MS01 and MS02. The red lines depict current speeds simulated with the local MIKE model. The upper panel refers to inflow and the lower panel to outflow.

The flow distributions are divided into inflow and outflow conditions. The following is observed:

- The cruise measured distributions are less uniform than the simulated ones, but are also based on much fewer data;
- The current direction and speed distributions are more varying during inflow than during outflow. Two local maximum speeds are found in the cruise

measured speed distributions during inflow, but it should be noted that the measured cruise distribution is based only on limited measurement and hence uncertain. The more complicated distributions measured during inflow can be because of the adjustment process: the turning from the Langelands Belt and the exchange with the Kiel Bight; and

- During outflow the lowest currents speeds are found close to Lolland. It is because the highest flow speeds will be along the salinity fronts (and partly the bed friction) which moves southwards in the Fehmarnbelt as the outflow develops, see also Fig. 7.1.
- Observed mean current directions in the upper 10 meters of the water column at the period of March 2009 to February 2010 vary in ± 5 degrees from the all-time average of the entire baseline period at the sea surface ($z = 5$ m) (see Chapter 6.3).

7.7 Water level difference and velocity

Correlation between water level difference Hornbæk-Gedser and velocity in main direction on a 10 minutes, 1 hour time and 1 day time scale is shown in Fig. 7.16, Fig. 7.17 and Fig. 7.18, respectively:

- The correlations show that the flow in the upper layer in the Fehmarnbelt to a considerably extent is driven by the water level difference, while in the lower layer in Fehmarnbelt and at MS03 it is not so; and
- The longer the integration period the higher the correlation in the upper layer at MS01 and MS02, because for example tidal flow is averaged out.

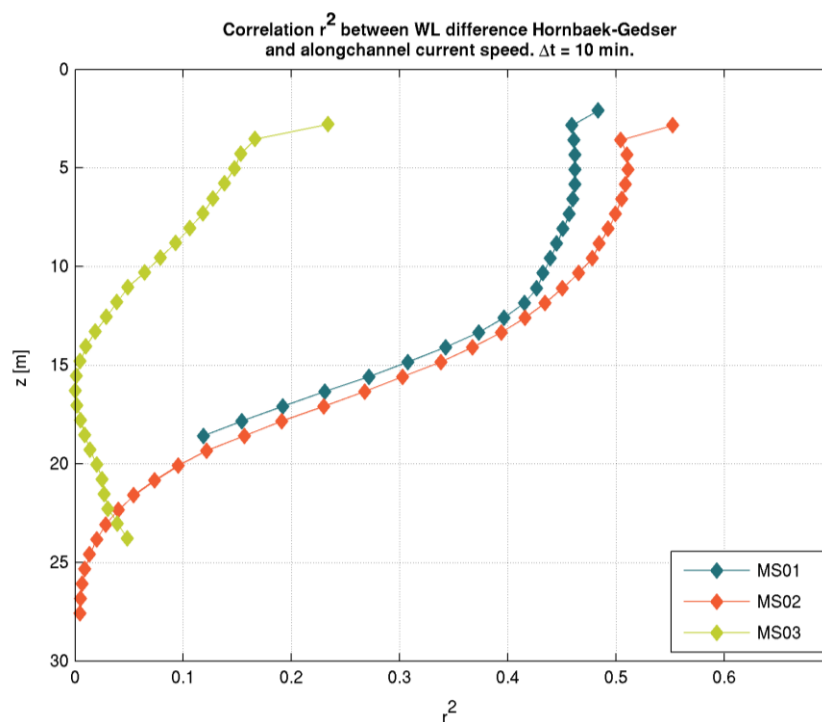


Fig. 7.16 Correlation over local water depth between water level difference Hornbæk-Gedser and velocity in main direction on a 10 minutes time scale.

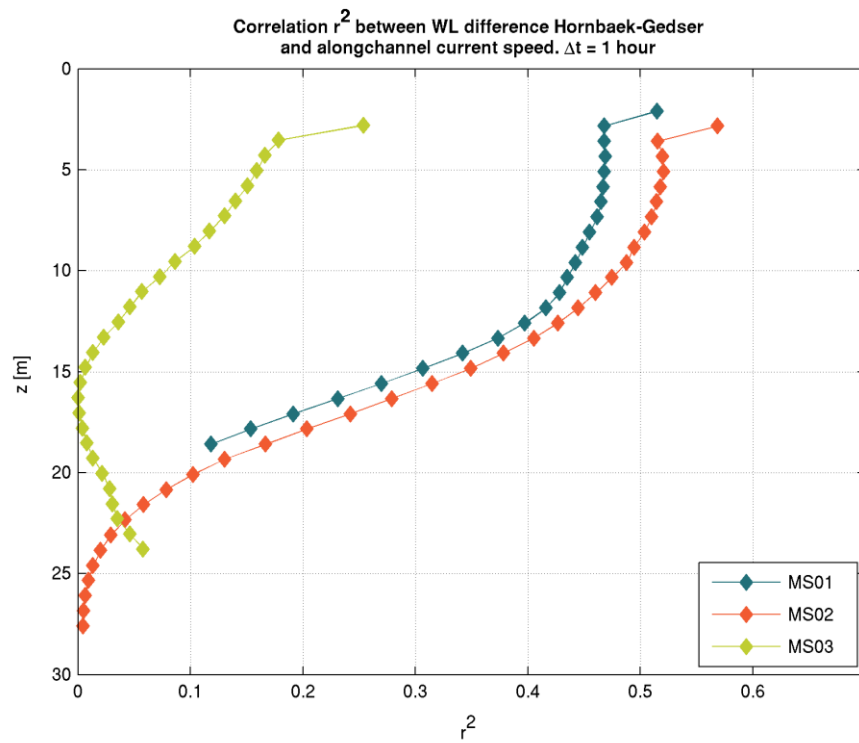


Fig. 7.17 Correlation over water depth between water level difference Hornbæk-Gedser and velocity in main direction on a 1 hour time scale.

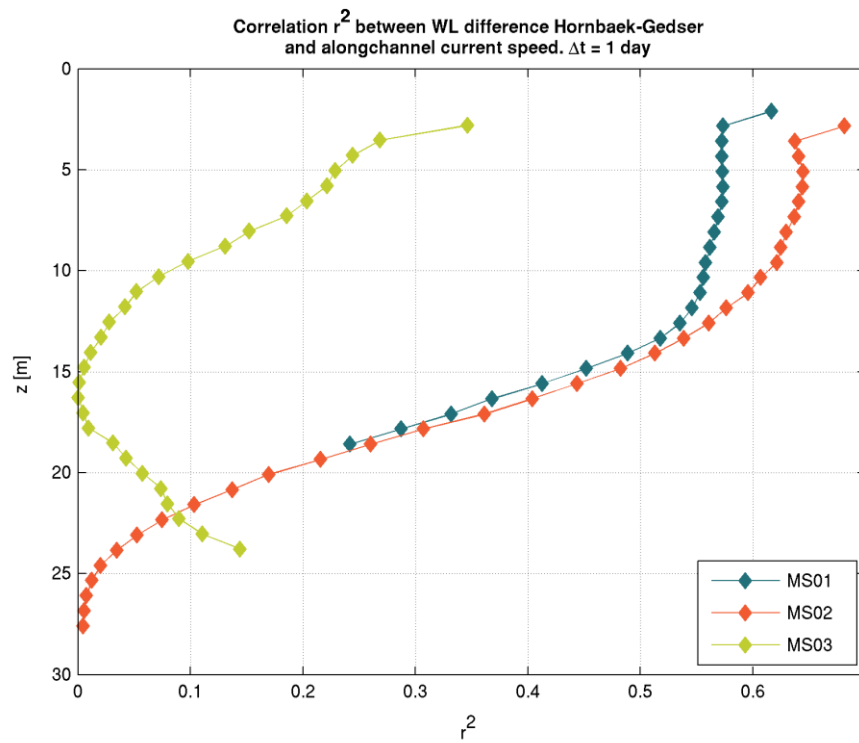


Fig. 7.18 Correlation over water depth between water level difference Hornbæk-Gedser and velocity in main direction on a 1 day time scale.



7.8 Volume and Salt Transports

In general, estimations of transports through the Danish Straits are based on measurements, simplified models or primitive ocean models.

Observations are often based on current measurements at moorings along a given section but to obtain a better temporal and spatial coverage, numerical models can be used.

The MIKE local and regional model runs resolves the water exchange through the Fehmarnbelt and that enables one to analyse the discharge as function of the salinity of the water mass, see Fig. 7.19 and Fig. 7.20:

- The discharge is varying on time scales from hours to months, but an average outflow of 12,700 m³/s is observed; and
- The salinity of the outflowing water masses is from 7 psu to 14.5 psu, while the salinity of the inflowing water masses is from 14.5 psu to 31 psu (and a relatively flat distribution).

These numbers are in good agreement with expectations.

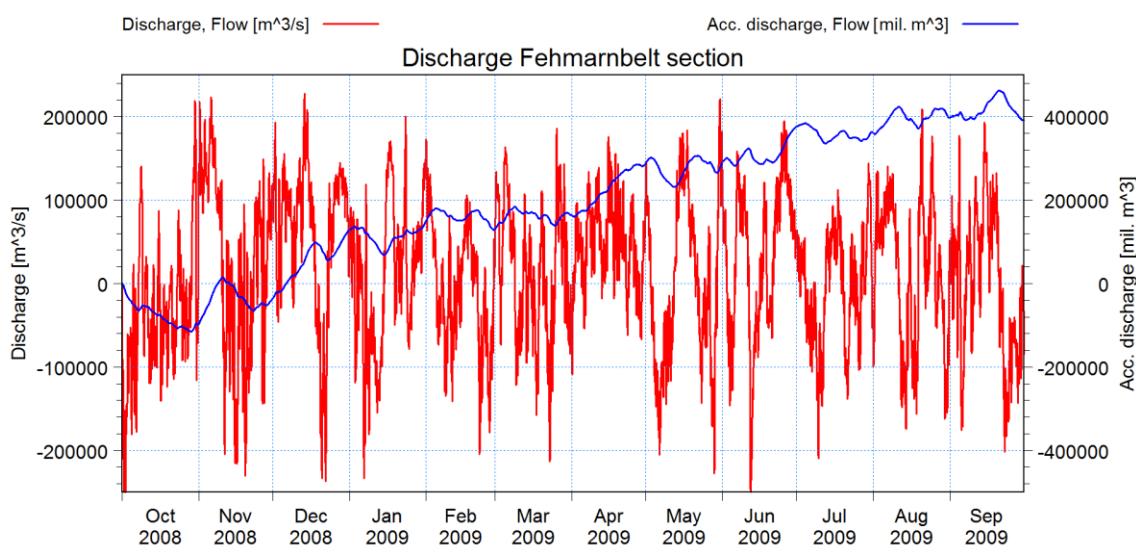


Fig. 7.19 Simulated discharge through the Fehmarnbelt during the period Distribution of salinity classes in Fehmarnbelt water volume exchange (net exchange volumes for each salt class), long-term simulation. MIKE local model, run 9.15. Positive values indicate outflow from the Baltic Sea.

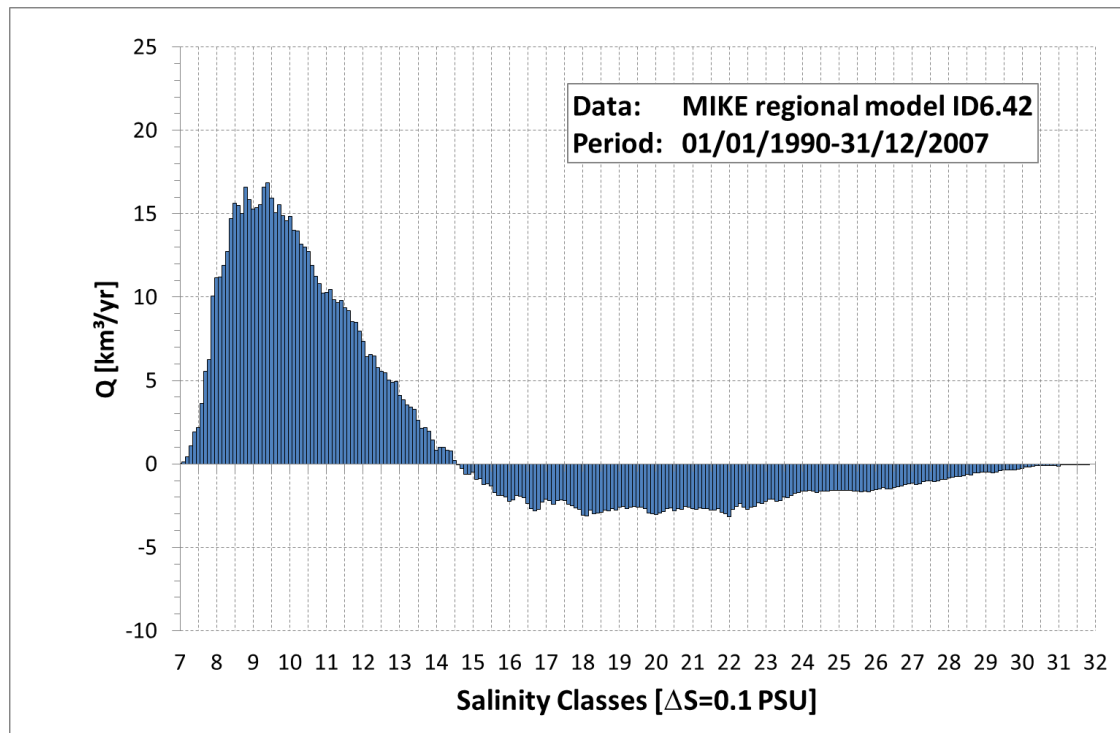


Fig. 7.20 Distribution of salinity classes in Fehmarnbelt water volume exchange (net exchange volumes for each salt class), long-term simulation. MIKE regional model, run 6.24. Positive values indicate outflow from the Baltic Sea.



8 HISTORICAL OBSERVATIONS OF HYDROGRAPHY

The historical observations of hydrography include long-term time-series of:

- Water level – it is noted that water level measurements are influenced by datum uncertainty of typically some centimetres;
- Waves;
- Current;
- Salinity and temperature; and finally
- Sea ice.

These time-series are crucial when calculating statistical values for the hydrographic parameters. Such values are for example of importance when evaluating the representativeness of the baseline period.

8.1 Water Level

Observed water level time-series at stations close to Fehmarnbelt are shown in Fig. 8.1 to Fig. 8.3. The observations cover the period from 2004 to 2010. Rapid variations caused by changing wind fields and seiching are observed in the data.

Storms cause extreme water level in the transition area. One such event occurred in the period 12-14 November 1872 (Colding 1881). The maximum water levels in the Fehmarnbelt during this storm are about 9 feet (2.7 m), see Fig. 8.4.

Detailed statistical analysis of water level variation, especially the occurrence and return period of extreme events has been investigated.

The analysis is based on both irregular historical observations extracted from literature and regular water level measurements collected at Rødbyhavn during the years 1955 to 2007 (source: Danish Coastal Authority) and at Puttgarden (source: Bundesamt für Seeschifffahrt und Hydrographie, Germany (BSH)).

The results from the analysis of water levels at Rødbyhavn are presented in Fig. 8.5. The data are fitted by a logarithmic distribution. The 'short period' is the high-resolution data from 1955 to 2007. The 'long period' is an analysis of the historical observations extracted literature and is much more uncertain, because the reported values are uncertain and because storms are missing. It is also found that the analysis of the historical observations leads to lower extreme water levels. Hence the analysis of the measurements from 1955 to 2007 is most reliable.

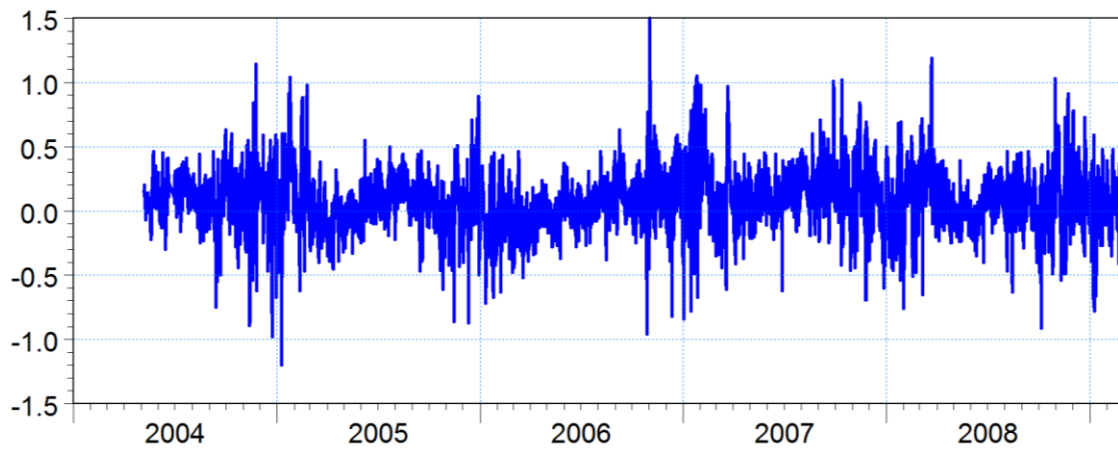


Fig. 8.1 Measured water level (m) at Warnemünde station.

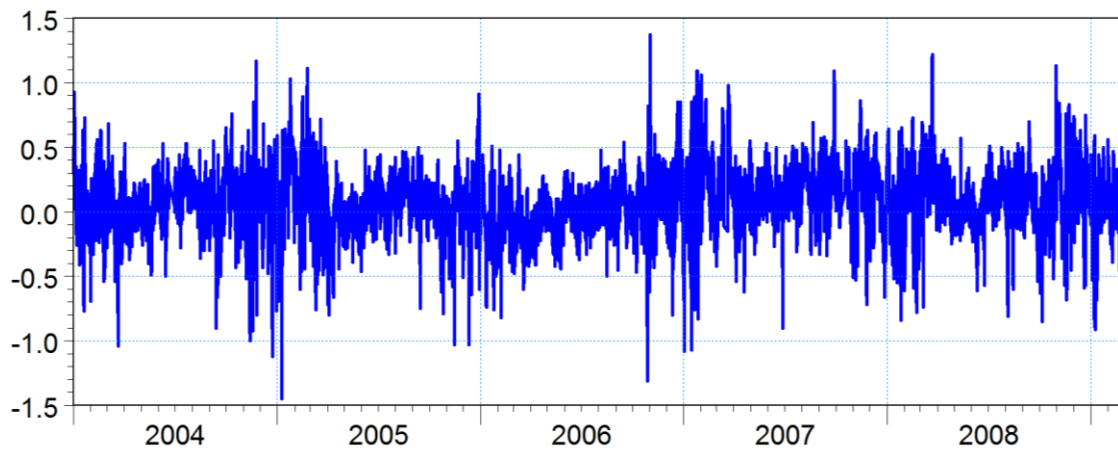


Fig. 8.2 Measured water level (m) at Gedser station.

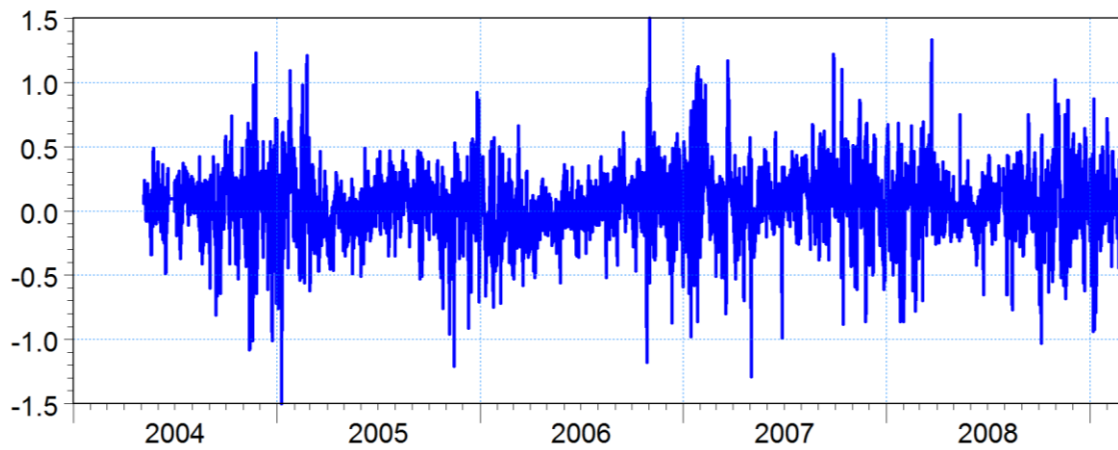


Fig. 8.3 Measured water level (m) at Kiel-Holtenau station.

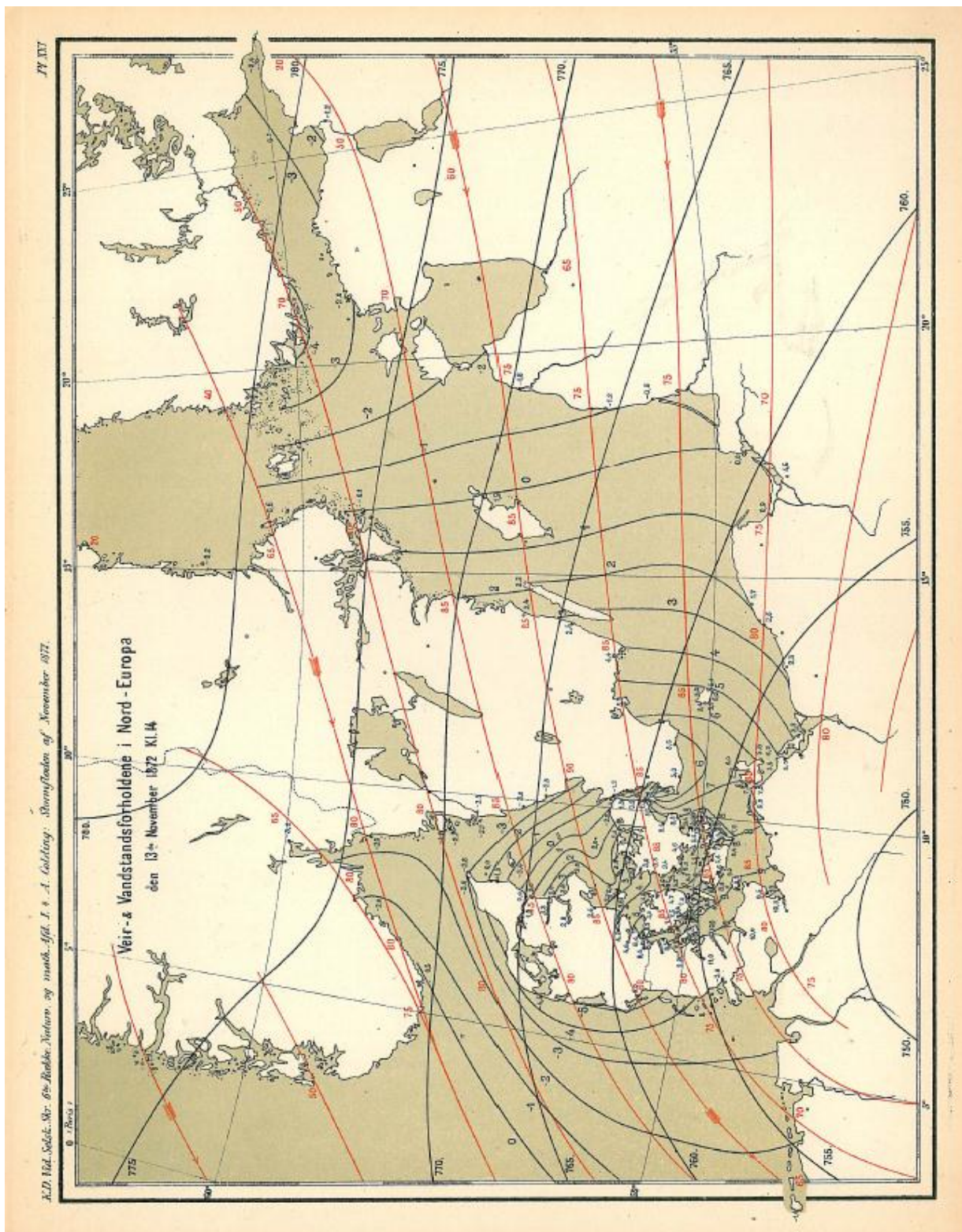


Fig. 8.4 Storm surge in the Baltic Sea on the 13 November 1872 at 14:00 (Colding 1881).

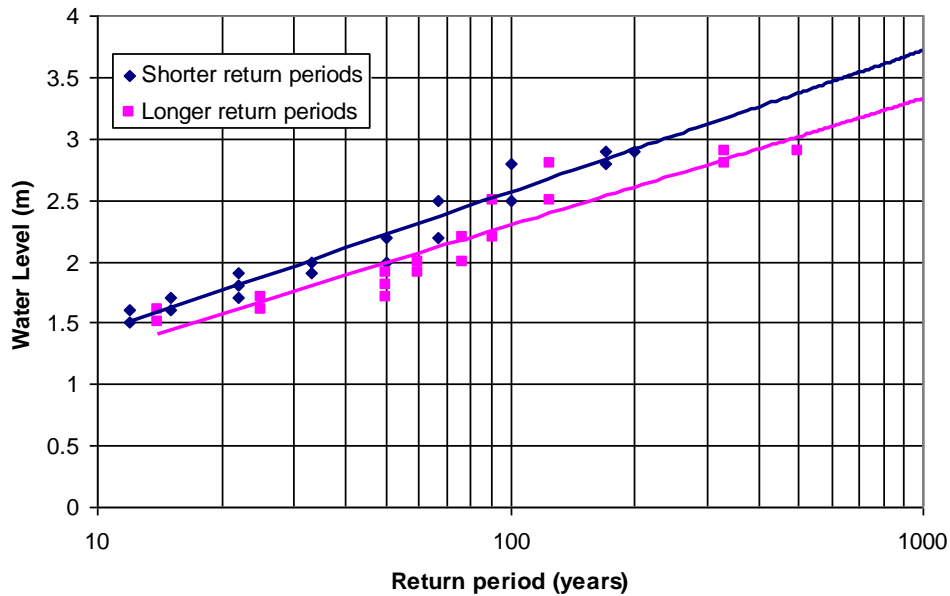


Fig. 8.5 High water statistics for Rødbyhavn based on extreme events. Threshold level is 1.5m. The water levels are relative to the present mean sea level.

8.2 Waves

Wave height and period observations was collected at Fehmarn Belt light-vessel, but not wave direction. The wave direction is in the following substituted by the wind direction. The resulting wave rose is shown in Fig. 8.6.

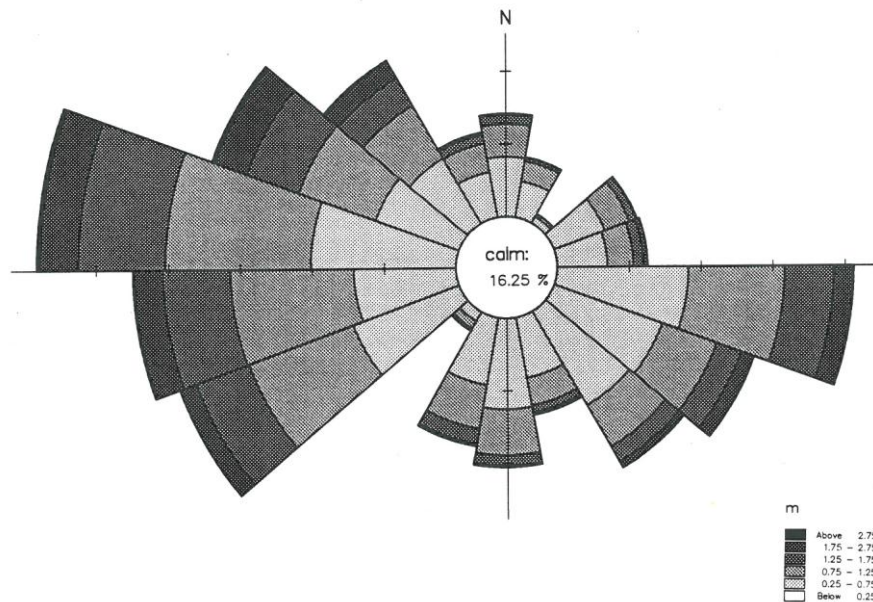


Fig. 8.6 Wave rose based on wave height and wind direction at Fehmarn Belt light-vessel during the period 1970 to 1984. From Fehmarn Belt Feasibility Study (1996).

In Table 8.1 the number of wave measurements in different wave heights and wave period classes are given. The table clearly shows that the higher the wave the longer the period. The connection can be written as:

$$T = 2.96s \cdot \left(\frac{H}{1m} \right)^{0.47} \quad (8-1)$$

Table 8.1 Wave observations at Fehmarn Belt light-vessel during the period 1970 to 1984 divided into different wave classes.

T (s)	H (m)									
	0	0.5	1	1.5	2	2.5	3	3.5	4	Sum
0	8512	855	449	279	90	20	7	1		10213
1	419	119	10	2						550
2	1034	13769	324	109	26	1				15263
3	8	6131	14033	1749	26	1				21948
4		9	320	4957	1939	136	10			7371
5				8	420	282	127	6		843
6					1	8	5	12	2	28
7							3			3
Sum	9973	20883	15136	7104	2502	448	152			56219

An atlas of wave heights in the southern Baltic Sea shows that maximal wave heights of 4.5 to 5 m can occur in the greater Fehmarnbelt area at wind speeds of 10 Bft. (24 m/s to 28 m/s), see Fig. 8.7.

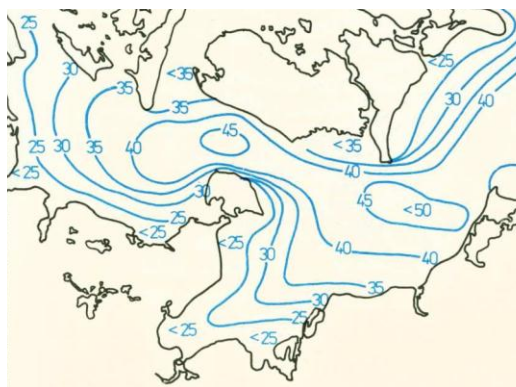


Fig. 8.7 Maximal wave height (dm) in the greater Fehmarnbelt area at 10 Bft (24 m/s to 28 m/s) west wind (Schmager 1979).

8.3 Current

In Lange et al. (1991) current measurements are analysed and treated statistically:

- Current measurements from Kiel Bight, Fehmarnbelt, Mecklenburg Bight and Lübeck Bight during the years 1982 to 1986; and
- Surface current observations and stratification measurements from the Fehmarn Belt light-vessel during the years 1950 to 1986.

The surface current at Fehmarn Belt light-vessel shows a typical 100 degrees direction during inflow, while 300 degrees during outflow, see Fig. 8.8. This confirms the



results by (Thiel 1938) and (Krauss 1966) and is refined by the FEHY current observations in Fehmarnbelt next to the link alignment during the baseline period.

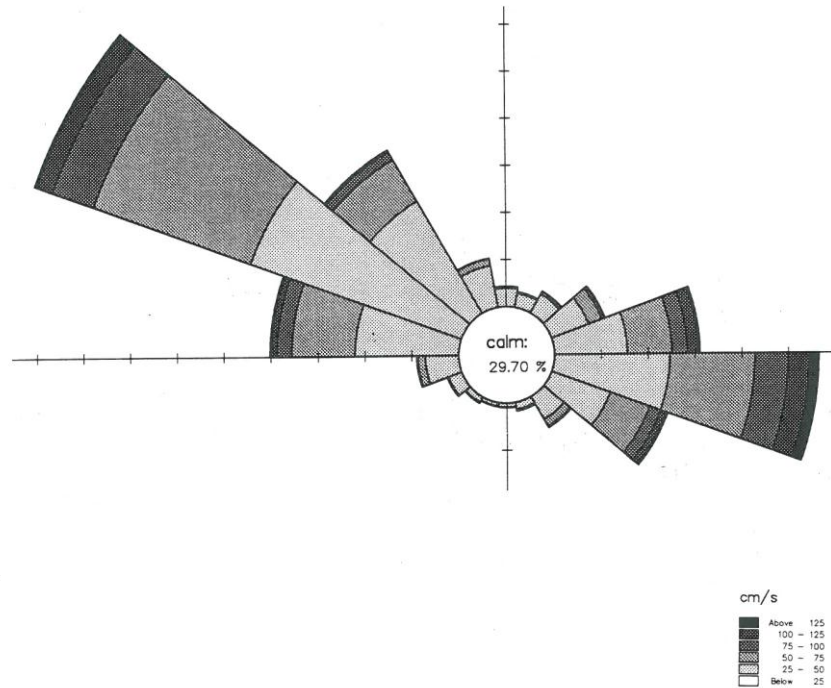


Fig. 8.8 Current rose based on surface observations collected at Fehmarn Belt light-vessel in the period 1970 to 1984 (extracted from Fehmarn Belt Feasibility Study 1996 or (Jakobsen et al. 1996).

At station 6 in the Fehmarnbelt (see Fig. 3.8) the current near the surface (6 to 10 m depth) shows inflow during 47% of time and outflow during 54% of time, while the current near the bottom (24 m to 28 m depth) show inflow during 67% of time and outflow during 33% of time, see Table 8.2 and Fig. 8.2. The inflow is thus more frequent in the lower layer.

Most inflow situations at the surface at station 6 have durations of less than 3 to 5 days, while outflow situations tend to last 1 or 2 days longer. The longest inflow situation lasted 14 days, and the longest outflow 17 days. Near the bottom the inflow has a typical duration of 3 to 5 days, with the longest situation observed lasted 21 days. Outflow is rare but has occurred with duration up to 5 to 7 days.



Table 8.2 Surface velocity scatter diagram at station 6 in Fehmarnbelt (Lange et al. 1991).

Direction (degrees)	Speed					
	0-20 (cm/s)	20-40 (cm/s)	40-60 (cm/s)	60-80 (cm/s)	80-100 (cm/s)	Sum (cm/s)
0-30	2.3	0.4				2.9
30-60	6.4	3.6	1.3	0.6	0.2	12.3
60-90	2.7	2.9	1.0	0.2		7.0
90-120	3.3	5.9	3.8	1.4		14.8
120-150	2.0	1.9	1.1	0.2		5.6
150-180	1.4	0.8	0.1			2.7
180-210	1.0	0.1				1.3
210-240	1.5	0.2				1.8
240-270	1.9	1.3	0.2			3.5
270-300	4.1	7.0	4.7	1.2	0.1	17.1
300-330	6.9	11.9	4.7	0.7	0.1	24.7
330-360	4.0	2.2	0.2			6.5
Sum	37.6	38.9	17.5	4.8	1.1	~100

Table 8.3 Near-bottom velocity scatter diagram at station 6 in Fehmarnbelt (Lange et al. 1991).

Direction (degrees)	Speed						Sum (cm/s)
	0-10 (cm/s)	10-20 (cm/s)	20-30 (cm/s)	30-40 (cm/s)	40-50 (cm/s)	>50 (cm/s)	
0-30	1.0	0.4					1.5
30-60	2.7	1.3					4.4
60-90	3.4	2.9	1.2	0.3			8.3
90-120	6.8	14.1	8.3	3.6	1.3		35.4
120-150	3.7	5.4	2.5	0.7	0.1	0.6	12.7
150-180	2.0	1.2	0.1				3.5
180-210	1.7	0.5					2.3
210-240	2.6	1.5	0.1				4.4
240-270	2.8	2.8	1.4	0.5	0.1		7.8
270-300	4.0	4.8	2.3	0.9	0.1		12.7
300-330	1.9	1.7	0.4				4.5
330-360	1.0	0.5					1.7
Sum	33.6	37.5	17.2	7.0	2.5	1.4	~100

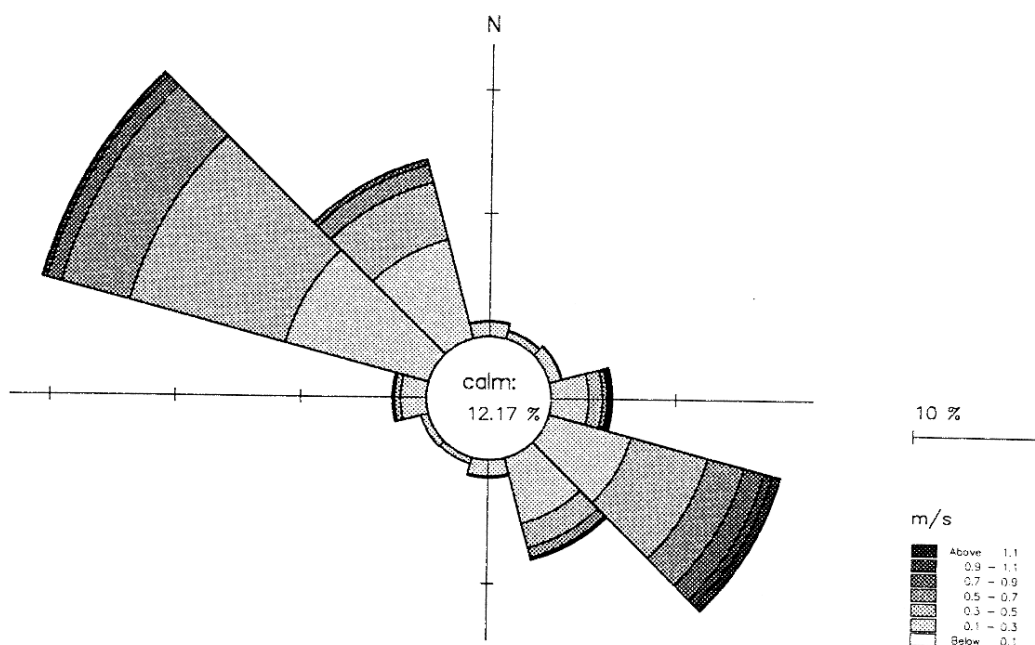
Comparison of the current at Fehmarn Belt light-vessel and at 7 m depth at station 528 (see Fig. 3.8) shows, that the current magnitudes and directions are highly correlated (secondary flow seems not too important), see Fehmarn Belt Feasibility Study (1997).

Results from (Fehmarn Belt Feasibility Study 1998) are extracted and presented in the following (locations of stations are shown in Fig. 3.9):

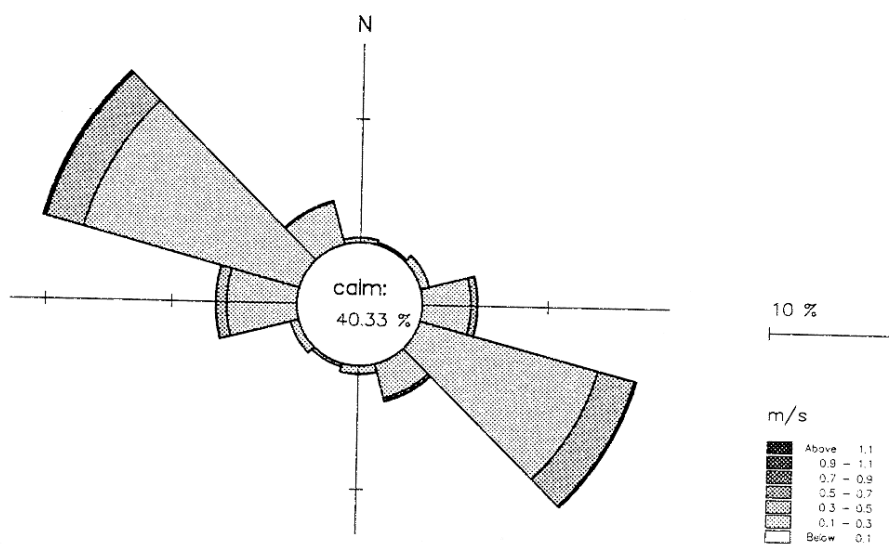
- Fig. 8.9 shows the current roses for the depths 5 m and 20 m, respectively, for Fehmarn Belt South. At the uppermost level (2 m depth) the maximum and mean speeds are 2.04 m/s and 0.35 m/s, resp. For the lowermost level (20 m depth) the corresponding numbers are 0.86 m/s and 0.14 m/s.



- Fig. 8.10 shows the current roses for the depths 5 m and 12 m, respectively, for Fehmarn Belt North. At the uppermost level (1 m depth) the maximum and mean speeds are 1.66 m/s and 0.33 m/s, respectively. For the lower-most level (13 m depth) the corresponding numbers are 0.72 m/s and 0.16 m/s.
- In Fig. 8.11 the comparison of the instantaneous and 25 hour moving averaged current in the main direction 5 m below the surface at station Fehmarn Belt South and Darss Sill is shown. As in the case of the comparison between the current at Fehmarn Belt South and Fehmarn Belt North, if the correlation is good it indicates that the velocities are, to a large extent, determined by the same dynamics. The correlation shows a good relation for both the instantaneous and the 25 hour moving average values and, as the stations are far apart, good relations are important. The current velocity at the station Darss Sill is approximately half the current velocity at the station Fehmarn Belt South. Thus we expect that the current speeds in the main direction are, to a large extent, determined by the water exchange, i.e. the discharge can be estimated by the current measurements.

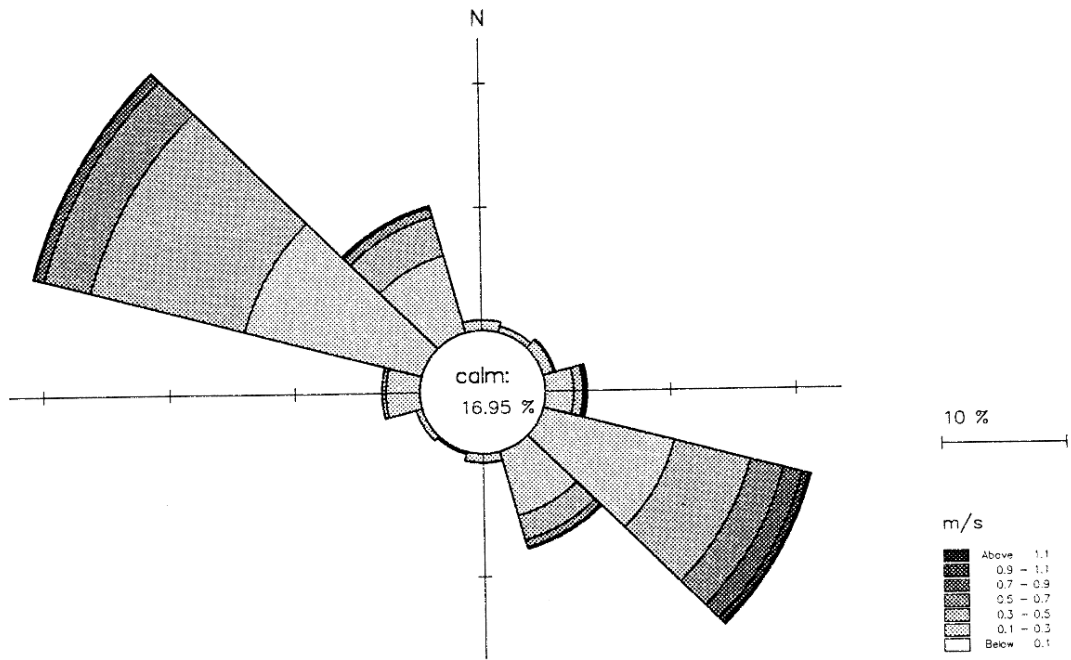


a)

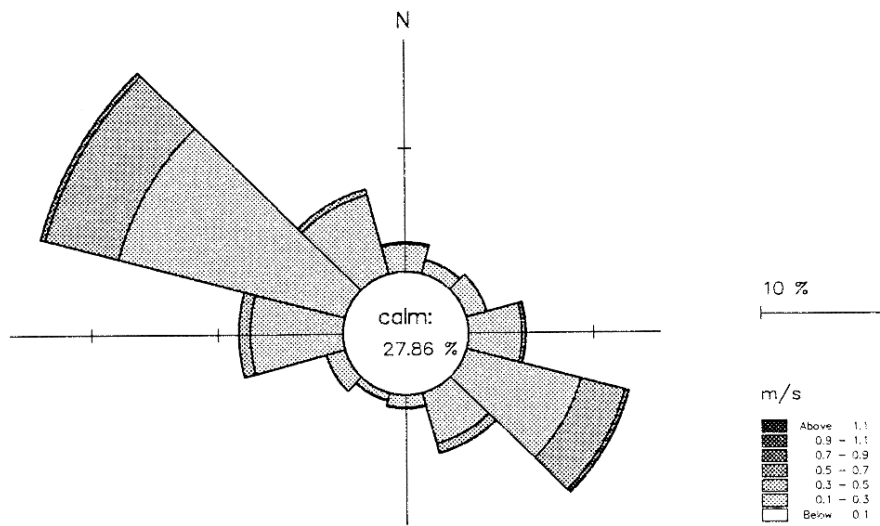


b)

Fig. 8.9 Current roses from the station Fehmarn Belt South for the depths 5 m and 20 m respectively (Fehmarn Belt Feasibility Study 1998).

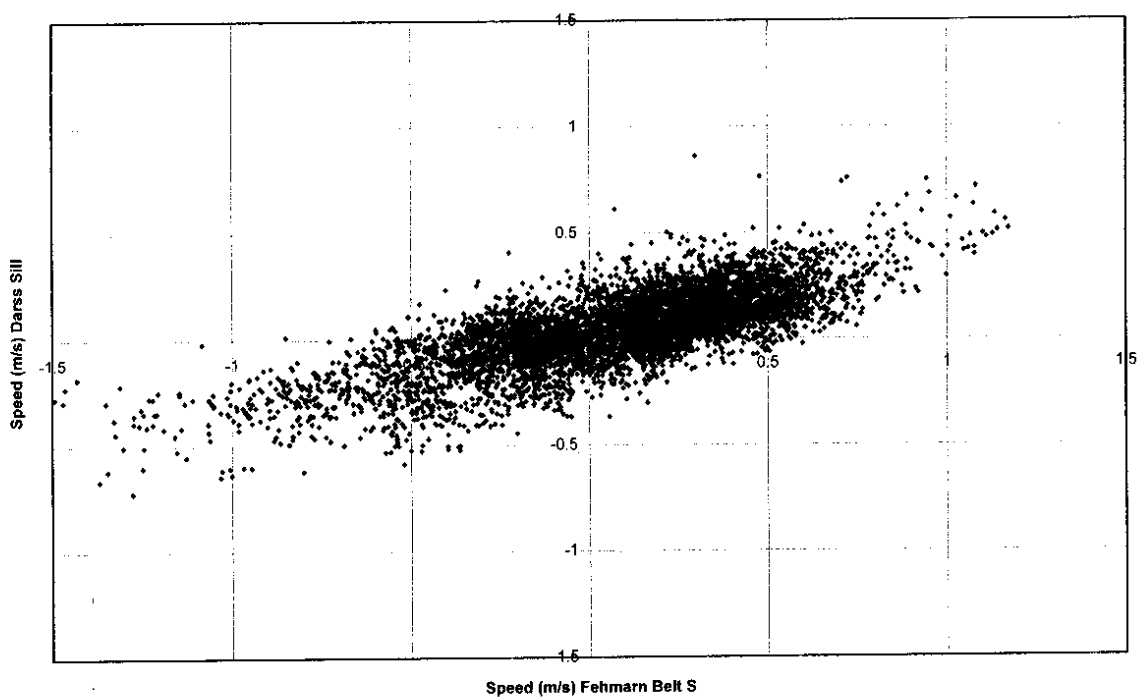


a)

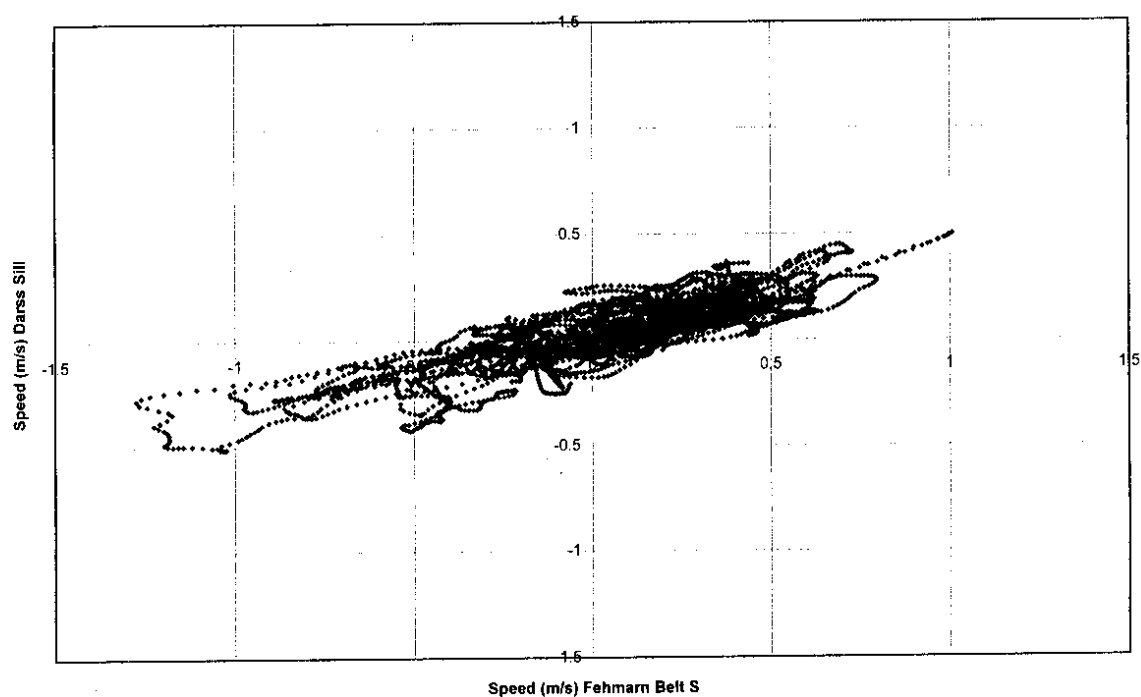


b)

Fig. 8.10 Current roses from the station Fehmarn Belt North for the depths 5 m and 12 m respectively (Fehmarn Belt Feasibility Study 1998).



a)



b)

Fig. 8.11 Comparison of the current speed in the main direction 5 m below surface at Fehmarn Belt South versus at Darss Sill: A) instantaneous values; and B) 25 hour moving average values (Fehmarn Belt Feasibility Study 1998).



8.4 Salinity and Temperature

The yearly salinity variation at Fehmarn Belt light-vessel is shown in Fig. 8.12 and Fig. 8.13. In December, the wind conditions are strong whereby the stratification is destroyed by mixing of the water masses.

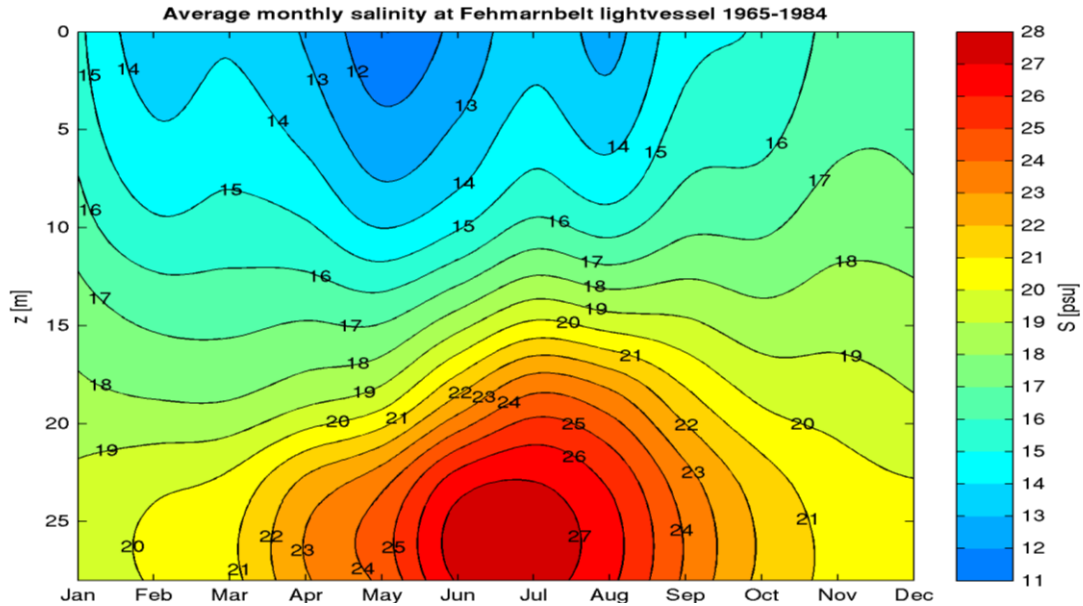


Fig. 8.12 The yearly salinity variation at Fehmarn Belt light-vessel redrawn after Lange et al. (1991).

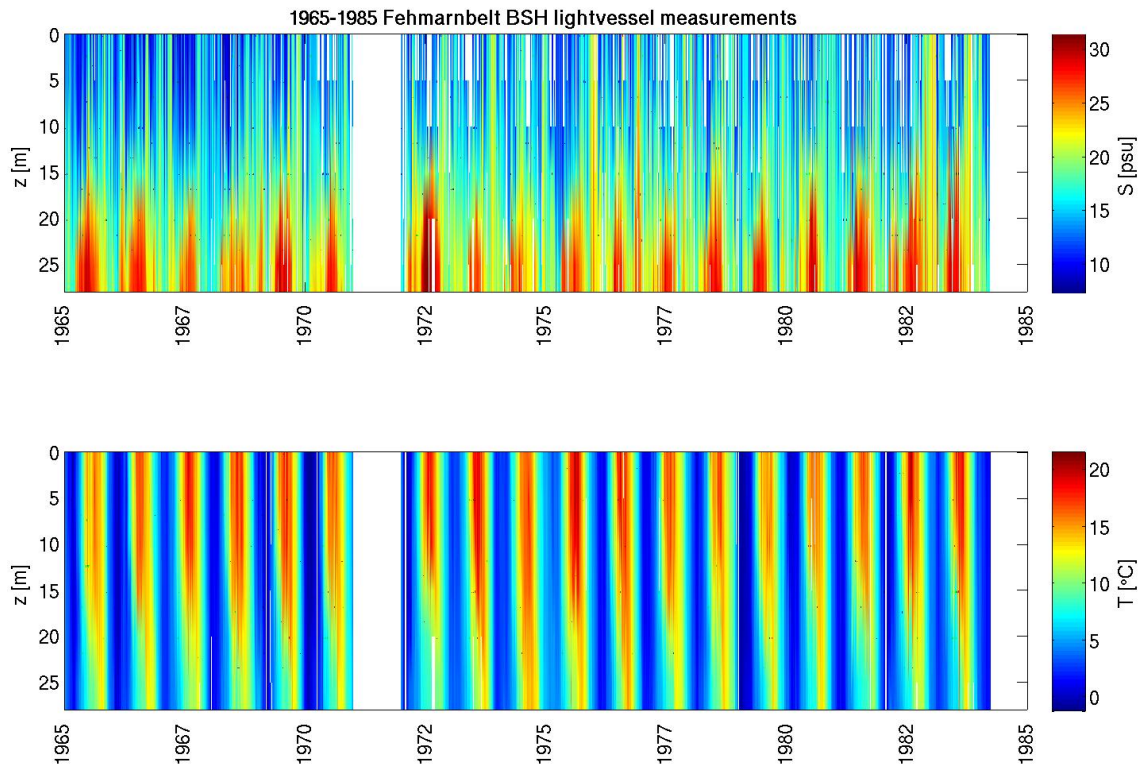


Fig. 8.13 Measured salinity and temperature variation at the Fehmarnbelt light-vessel from 1965 to 1984. Note the cyclic nature of bottom salinity with infrequent inflows of saline North Sea water.

Salinity and temperature variation at Fehmarn Belt light-vessel is shown in Fig. 8.13. The original data collected at Fehmarn Belt light-vessel have undergone a

post-processing that clipped off salinity values below 10 psu from 1970 and onwards. Salinities below 10 psu do occur in the Fehmarnbelt, especially at depths less than 10 m. Because such low-saline water is rare at depths below 20 m, we will still use the full light-vessel time-series in such depths for assessment of salinity and for overall T-S diagrams, while we restrict salinity statistics of single depths at less than 15 m to the period of 1965-1969.

Time-series of salinity and temperature are shown in Fig. 8.14 and Fig. 8.15. Surface temperature shows a trend near zero ($+0.007^{\circ}\text{C}/\text{year}$) that equals a rise of 1°C in 143 years. The trends are nearly zero in this historical period and not important for our purpose.

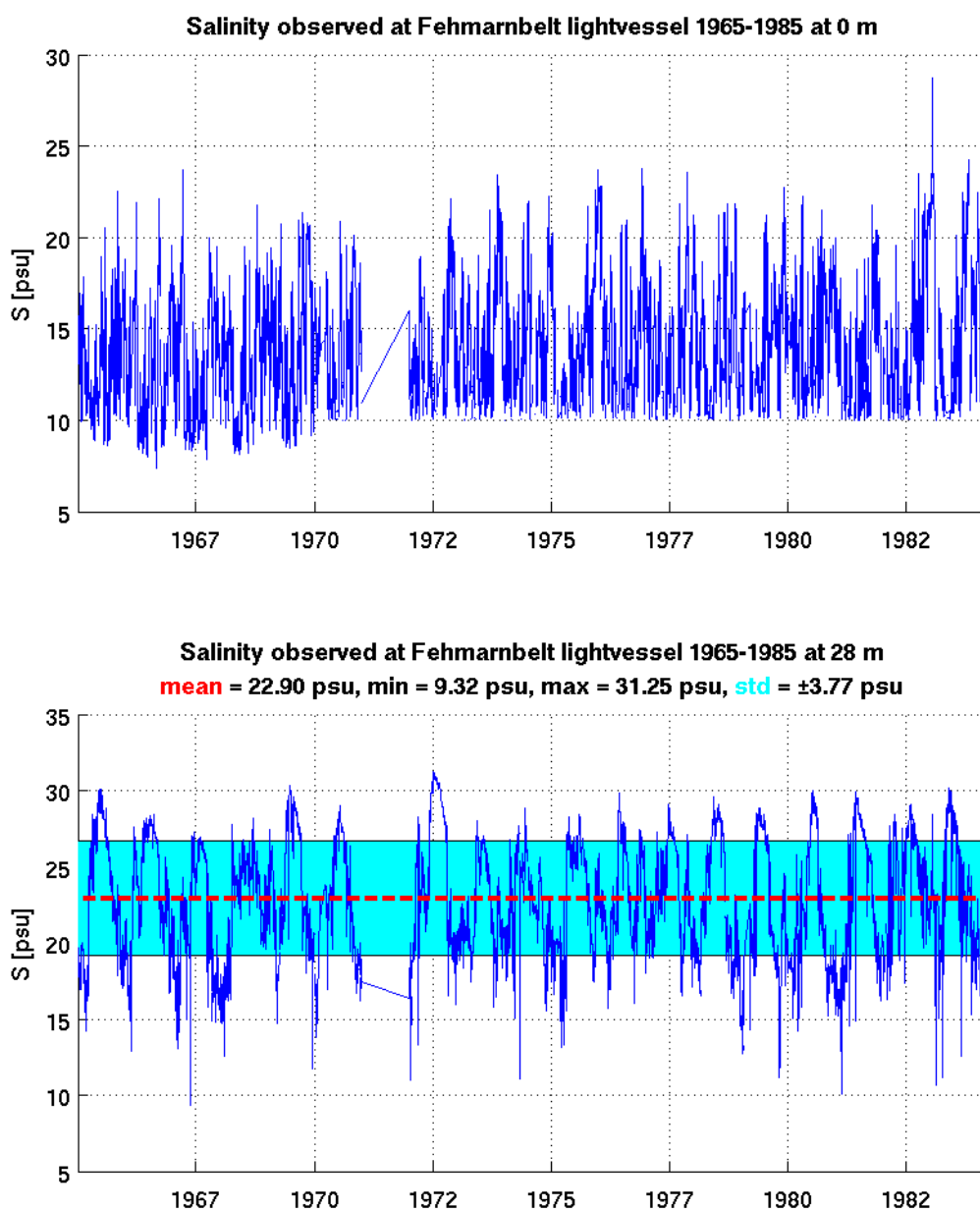


Fig. 8.14 Measured salinity at Fehmarnbelt light-vessel in 0 m and 28 m depth during the period 1965-1985. Note the cut-off in salinity below 10 psu after 1970 in the basic data.

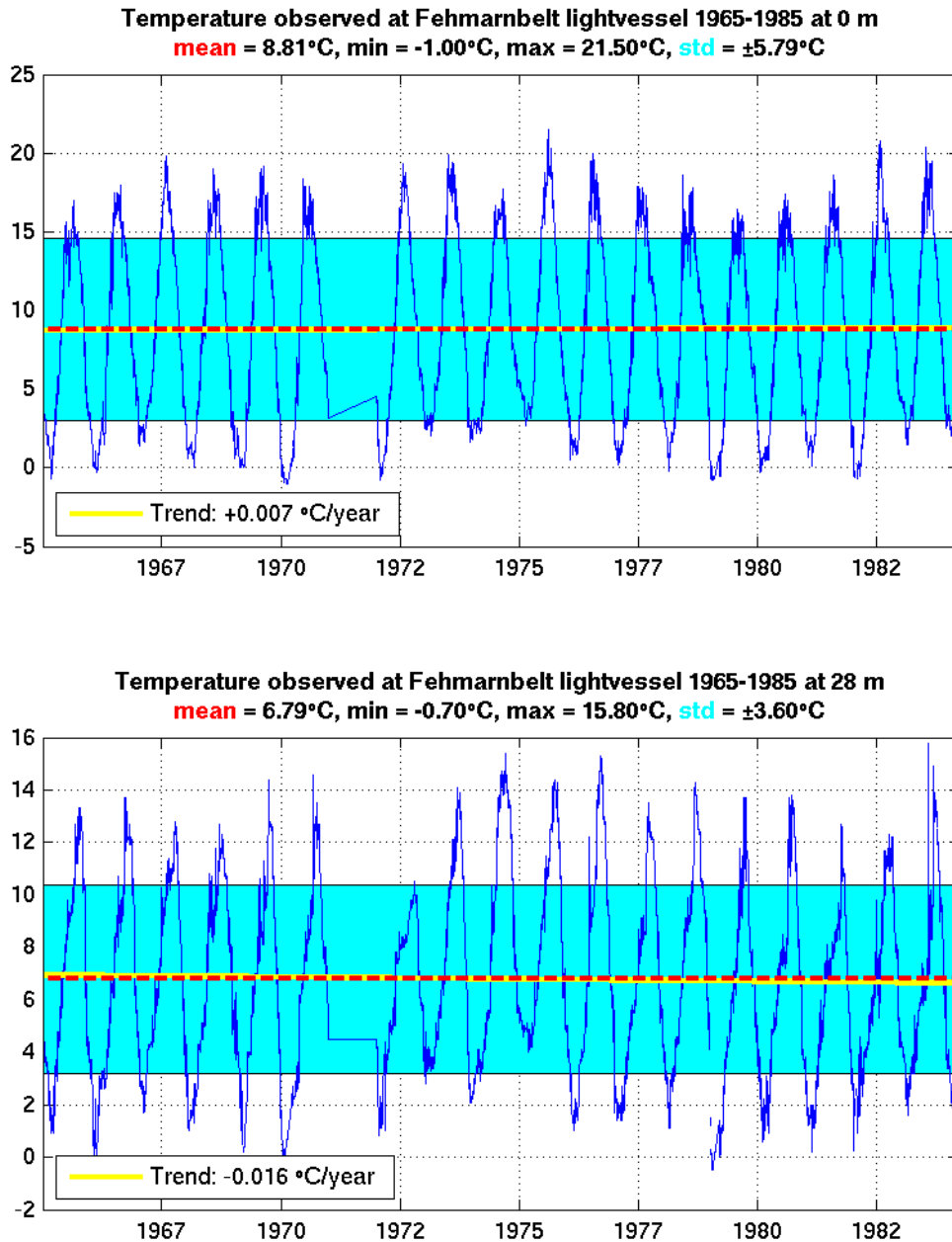


Fig. 8.15 Measured temperature at Fehmarnbelt light-vessel in 0 m and 28 m depth during the period 1965-1985.

Surface salinity at BMP M02 (Fig. 8.16) in Mecklenburg Bight shows an average salinity of 11.8 psu with a standard deviation of ± 2.5 psu (NO1 was not considered, because nearby light-vessel data with much better resolution in time has been analyzed). High salinities frequently exceed the upper boundary of mean plus standard deviation, reaching an absolute maximum of 19.3 psu in the resolved period. This represents stronger saline inflows that deviate from the average surface salinity due to vertical mixing of highly saline bottom water. Minimum values along the lower boundary (mean minus standard deviation) are more stable, i.e. they do not exceed the boundary as often as the high salinities. The all-time minimum at the surface was 7.9 psu.

Salinity at 25 m shows that again the highly saline inflow from the Fehmarnbelt dominates the range above the upper standard deviation boundary, reaching an overall maximum of 29.5 psu.

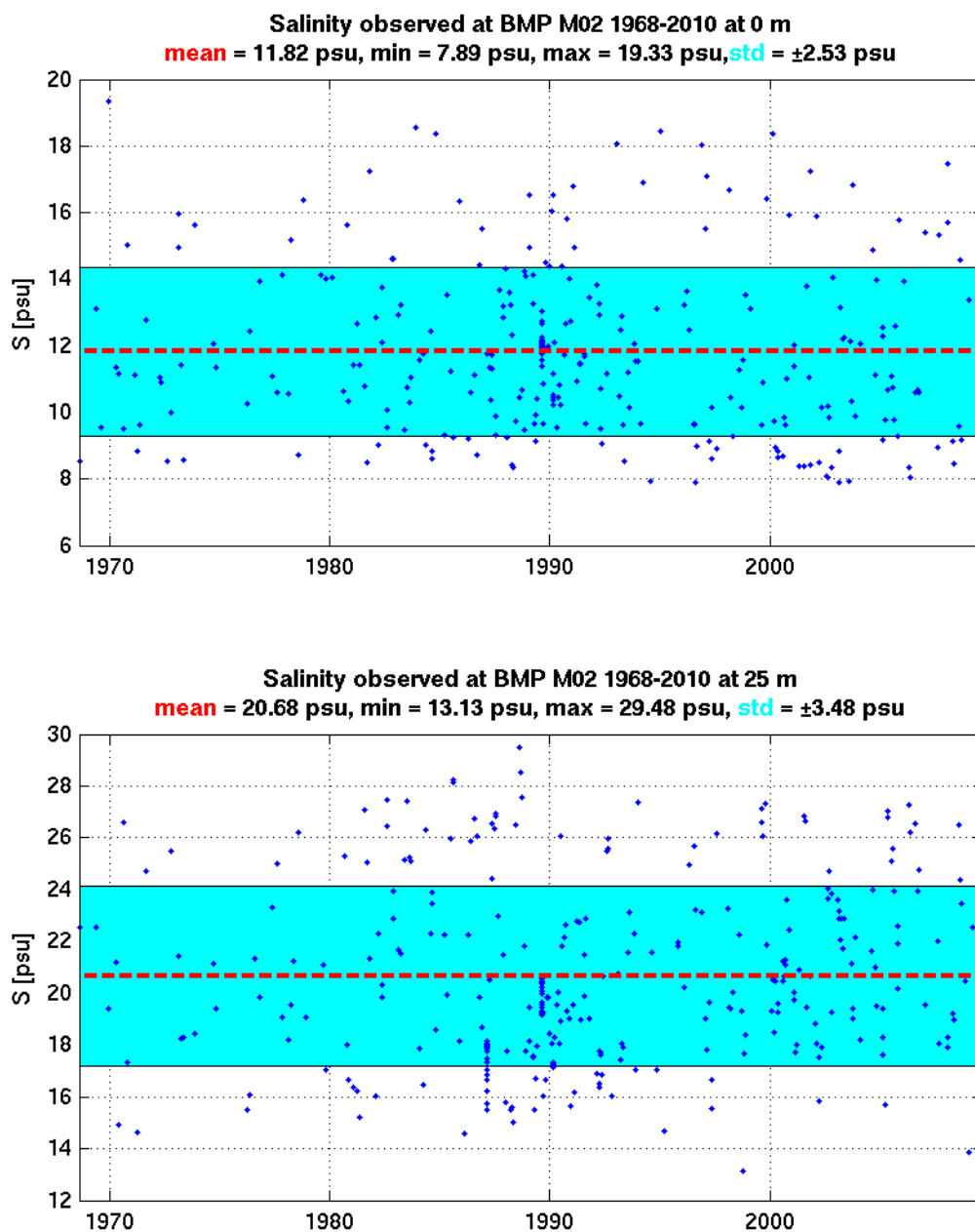


Fig. 8.16 Measured salinity in 0 m and 25 m depth at HELCOM station BMP M02 in Mecklenburg Bight during 1960-2010.

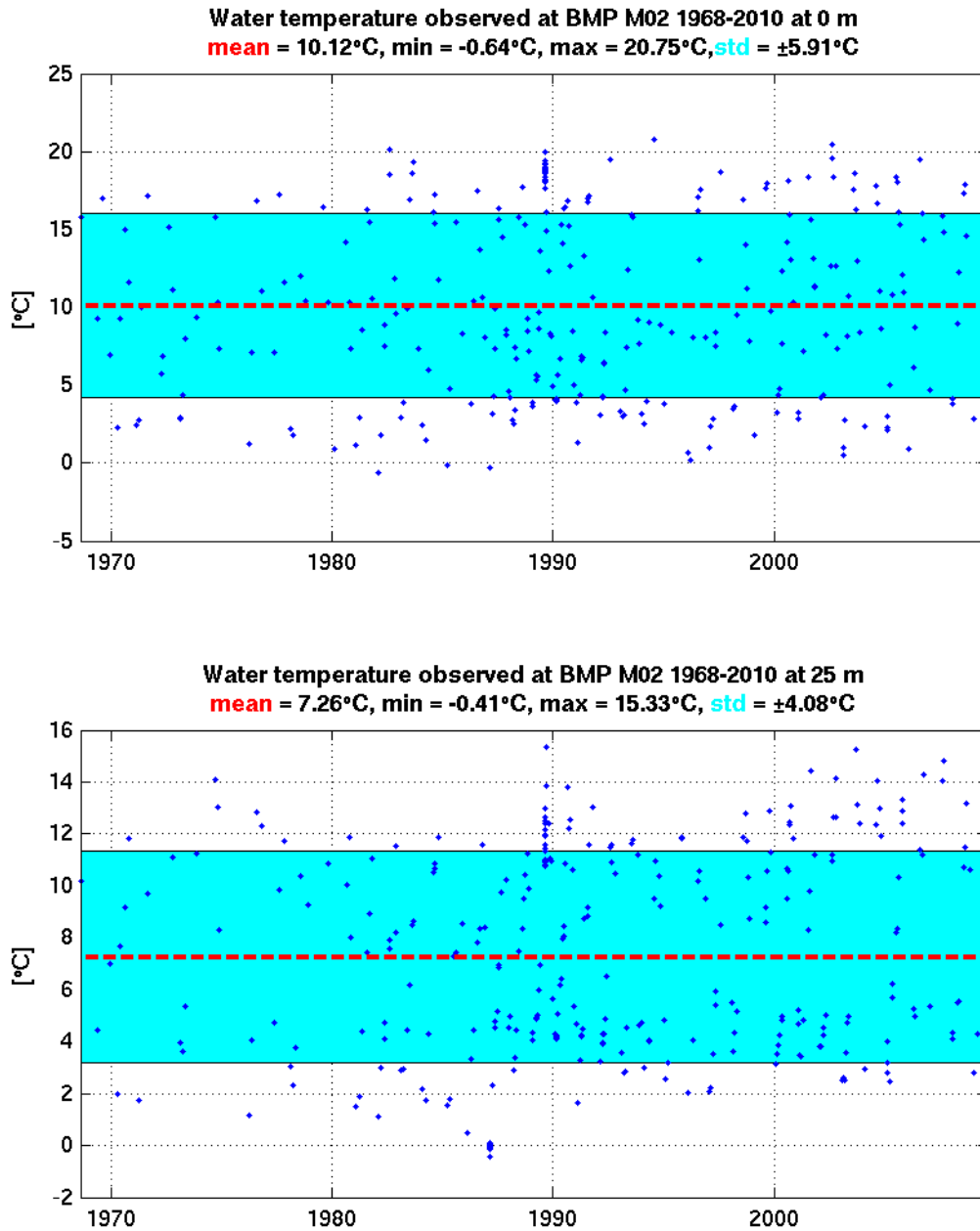


Fig. 8.17 Measured temperature in 0 m and 25 m depth at HELCOM station BMP M02 in Mecklenburg Bight during 1968-2010.

The bottom salinity in the Fehmarnbelt shows a pronounced annual cycle and it can be linked to lower wind speeds during summer than during winter, see Fig. 8.18. During periods with low wind speeds the upwards and downwards mixing of water masses is low and the surface salinity is low and the bottom salinity high. During periods with high wind speeds the upwards and downwards mixing of water masses is high and the surface salinity is not so low and the bottom salinity not so high.

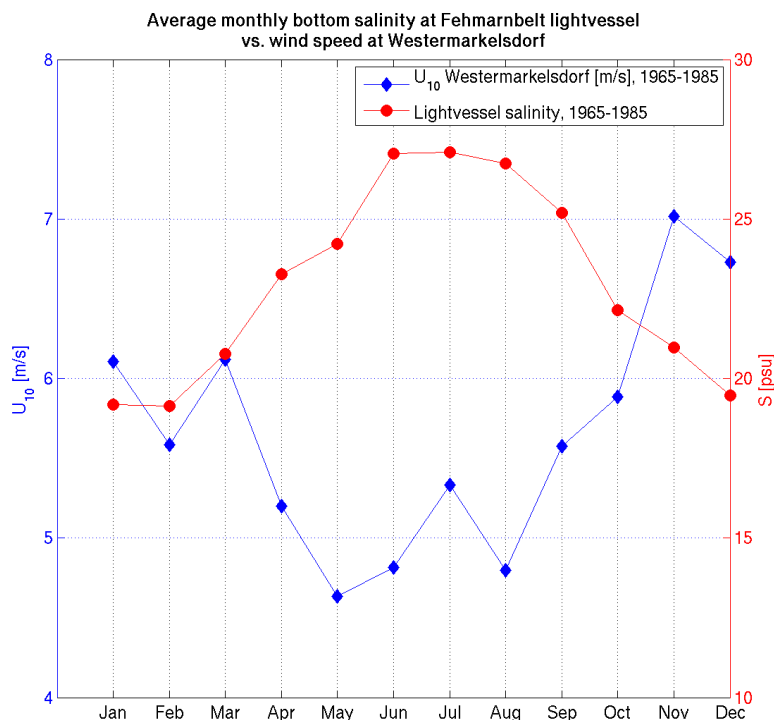


Fig. 8.18 Climatological monthly means of bottom salinity ($z = 28\text{ m}$) at Fehmarnbelt light-vessel and wind speed at Westermarkelsdorf/Fehmarn.

8.5 Sea Ice

Ice formation depends on local cooling (frost index) and salinity of surface water. The frost index is calculated by (it is also sometimes referred to as accumulated freezing-degree-days):

$$K = \sum_{i=1}^N \max(-T_{mi} \cdot 1\text{day}; 0) \quad (8-2)$$

Where

- K : frost index (°C-days)
- N : number of days in period
- T_{mi} : daily mean temperature (°C)

The frost index from the winter 1906-07 to the winter 2009-2010, or in total 104 winters is presented in Fig. 8.19. The bigger the frost index is, the colder the winter is. An especially cold period from year 1939 to year 1942 is identified in the time-series.

There are 20 winters in this period that are referred to as "ice-winters". The ice-winter 1906-07 has the lowest frost index value of these and the frost index value that year is 121 °C-days. Hence a winter with a frost index value above 120 °C-days will be an ice-winter. The average frost index is 93.1.

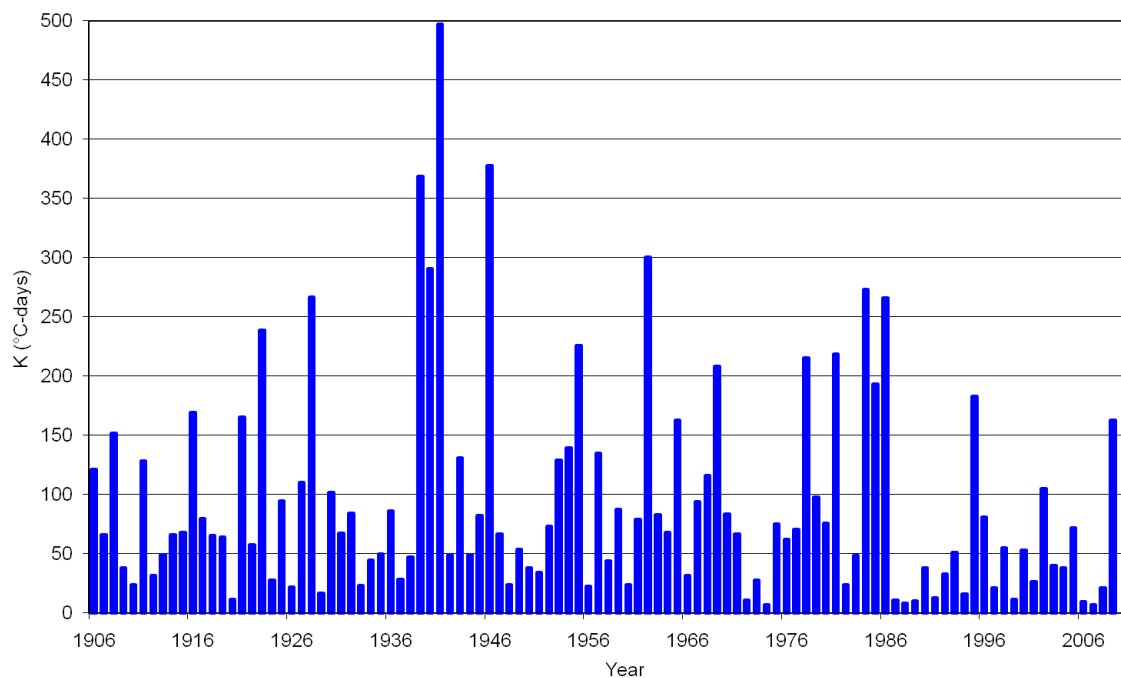


Fig. 8.19 Time-series of frost index for Baltic transition area (data are extracted from SOK 2010).

The Belt Sea area is only ice covered during severe winters or “ice-winters”, except for some shallow and semi-enclosed areas that can also be ice covered during normal winters. Based on 14 ice-winters from year 1906 to year 1955 Fehmarnbelt is in average ice covered in 50 days per ice-winter, see Fig. 8.20.

The measured development in ice sheet thickness in Danish waters during the ice winter 1940/41 is shown in Fig. 8.21. The measured development during the ice winters 1939/40 and 1941/42 is very similar to the one measured during ice-winter 1940/41.

Note that the measurement locations are all located close to the coastline, for example in harbours or fiords. Only very few measurements are observed from ships in the Baltic transition area far from land.

In general the ice cover in the more open and deeper sea areas is build-up later and destroyed earlier than the ice cover close to land. And for that reason the sheet is also in general thinner than measured close to land.

The development of ice cover in the Baltic transition area during the strong ice winter 1940/41 was analyzed by (DONG 2010). Exemplarily it can be used to describe the build-up of ice cover in the Belt Sea as follows:

- The ice starts to build up along the coastlines in January and in this period also mainly locally generated drifting ice floes is present;
- By end of January the Baltic transition area are completed ice covered and the ice cover is land-locked. The ice thickness at the coastal stations is about 20-40 cm;
- In the first half of February the ice starts to break-up in the deeper open sea areas and again mainly locally generated drifting ice floes are present. The ice cover at the coastal stations reaches its maximum thickness of about 30-50 cm; and

- By the end of February the ice starts to break-up closer to land. The ice thickness at the coastal stations is about 20-40 cm.

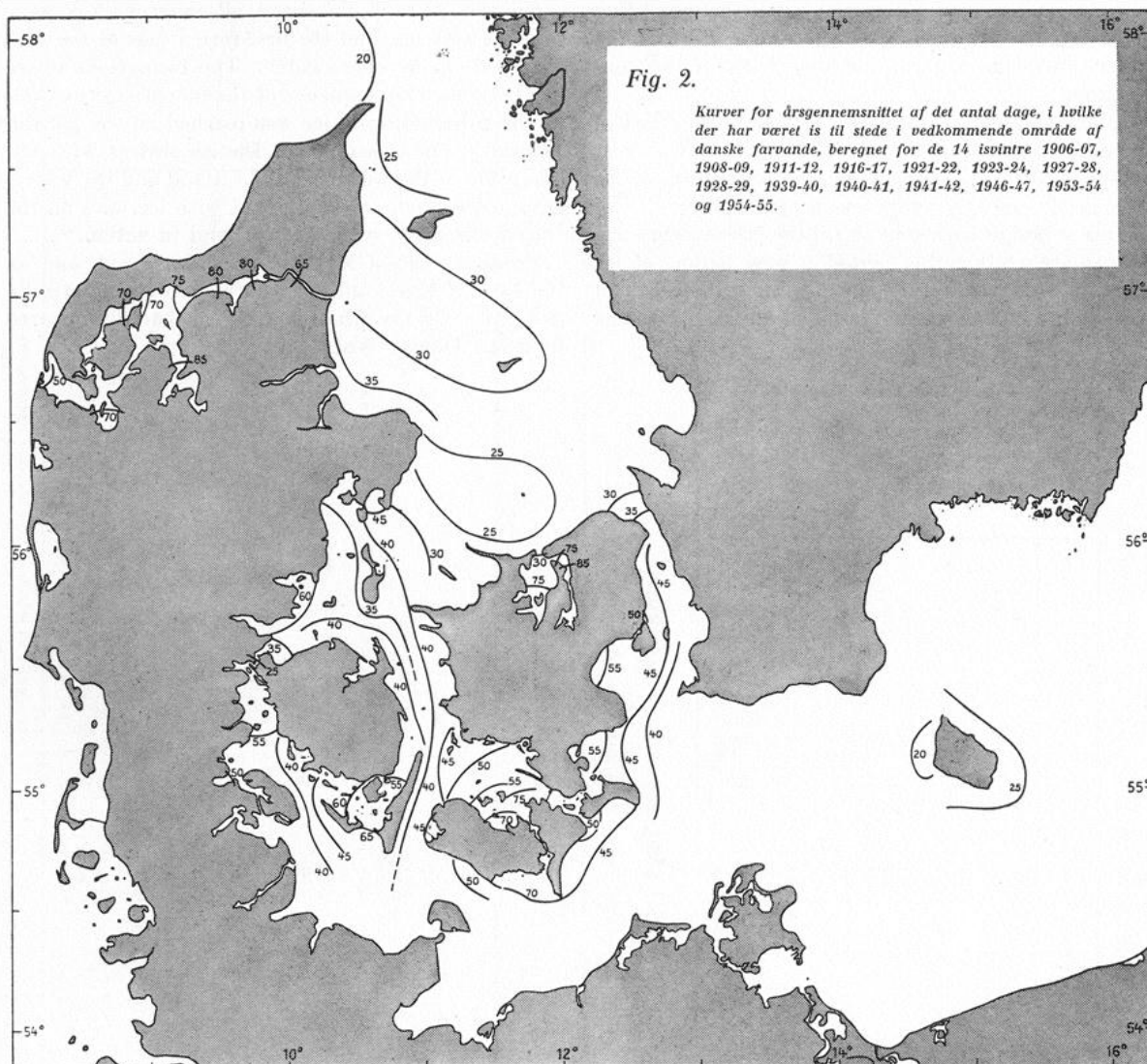


Fig. 8.20 Average number of days with ice per ice winter. Based on 14 ice-winters. From (Statens Istjeneste 1954-1955).

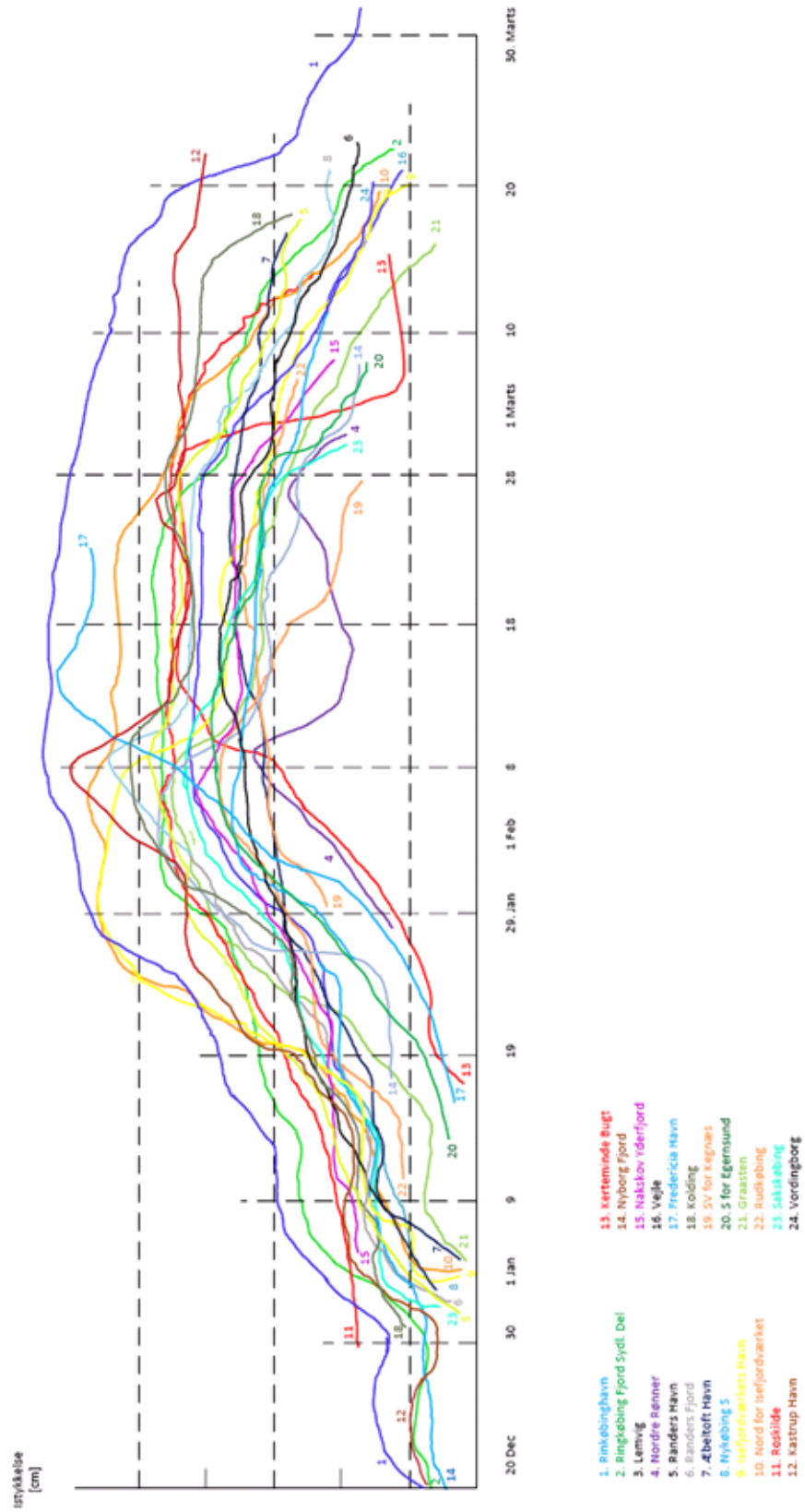


Fig. 8.21 Development of ice sheet thickness in Danish waters during the 1940/41 winter season (redrawn from SII 1942).



In Table 8.4 the occurrence of ice-winters, durations, number of ice-days and the ice thickness are presented. In general sea ice is present every 3 – 4 years (winters) in the trace area. The thickness of the sea ice during severe winters is 10-30 cm. In very severe winters 30-50 cm, and in extremely severe winters (the last occurred in 1962/63) more than 50 cm can occur. See also Fig. 8.25 to Fig. 8.28.

Table 8.4 Sea ice conditions in the Fehmarnbelt during ice-winters. Locations are shown in Fig. 3.7.

Location	Winters		Freezing data		Break-up date		Days with ice		Thickness (cm)	
	total	ice	earliest	median	median	latest	mean	max	mean	max
Sea station 3 (light-vessel)	42	12	01.01.	25.01.	05.03.	19.04.	24	87	21	50
Westermarkelsdorf	72	22	31.12	22.Jan	11.03.	18.04.	35	89	38	120
Marienleuchte	71	18	05.01.	21.01.	16.03.	20.04.	40	90	46	120
Fehmarnbelt, east	40	14	31.12.	21.01.	08.03.	31.03.	20	82	22	60

The sheet ice thickness (h_o) can be calculated by the following relationship (see e.g. Christensen and Skourup 1991):

$$h_o = 0.032 \frac{m}{\sqrt{^\circ\text{C} - \text{days}}} \cdot \sqrt{k \cdot K - 50^\circ\text{C} - \text{days}} \quad (8-3)$$

Where

h_o : Ice sheet thickness (m)
 K : frost index ($^\circ\text{C} - \text{days}$)
 k : parameter

On the basis of data from the Danish Straits the relation was improved to give (DONG 2010):

$$h_N = 0.032 \frac{m}{\sqrt{^\circ\text{C} - \text{days}}} \cdot \sqrt{k \cdot K - T_+ \cdot (n - n_f) - T_f \cdot n} \quad (8-4)$$

Where

h_N : Ice sheet thickness (m)
 T_+ : 0.5°C
 n : number of days with frost (function of K)
 n_f : $3.6K^{1/2}$
 T_f : -0.56°C

The sheet ice thickness as function of frost index is shown in Fig. 8.22. The comparison between Equation (8-4) and the measurement from the Fehmarnbelt area are satisfactory.

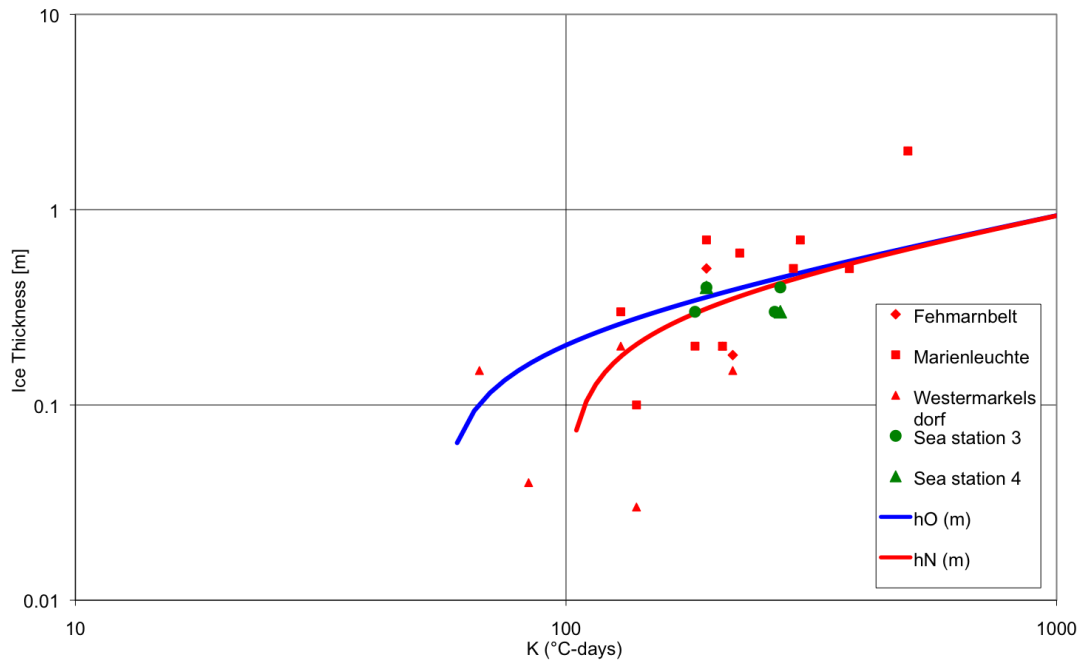


Fig. 8.22 Sheet ice thickness as function of frost index. Data are from German stations.

Ice formation from Kiel Bay to Mecklenburg Bight in the open sea occurs only in about 25% of winters, in the period from mid-January to about mid-April. Schmelzer et al. (2008) write: "During this period, the time of occurrence and extent of ice fields as well as the intensity of ice formation (ice thickness, drift ice concentration, etc.) are highly variable—and often only ice floes that hardly impede navigation are observed for a short time ranging from 1 to 3 [monthly] decades. The probability of ice formation in November or in mid-December is low for inner waters and zero for sea areas". The ice coverage in open sea areas of the Western Baltic has its highest value in strong winters in the last decade of February.

In 1947/48, the reduced ice sum was introduced for the evaluation of ice winter severity in the German coastal regions (Büdel 1947 and Nusser 1948). It constitutes the arithmetic mean of days with ice recorded at currently 13 climatological stations along the German Baltic Sea coast and characterises the extent and duration of ice occurrence. In the time since 1897, the reduced ice sum computed for the Baltic Sea coast has fluctuated between zero and a maximum of 98 days. The arithmetic mean is 21 days, and the median value 11 days (see Fig. 8.23).

In 1989 the accumulated areal ice volume was introduced by Koslowski (initially only for the coastal area of the western Baltic) as a new way of classifying ice winters. Apart from the duration of ice cover, also ice concentration and thickness is included in the calculation, thus taking into account interruptions of freezing periods during each winter season. The daily areal ice volume data at the 13 ice climatological stations along the German Baltic shore are summed up, and the accumulated areal ice volume is obtained by computing the average of the 13 stations, with:

$$V_{A\Sigma} = \frac{1}{n} \sum_j \sum_k (NH)_{jk}, \quad (8-5)$$

where

n	=	number of stations (13)
N	=	ice concentration in tenth
j	=	index of station
k	=	index of days with ice.



A time-series of the accumulated areal ice volume for the German Baltic Sea coast from 1899 to 2008 is shown in Fig. 8.24. While the general ice volume is below 5 m, frequent extreme winters occurred during the middle of the 20th century. With an exception of 1995, these severe winters seem to be missing past 1987. Although the reduced ice sum for the German Baltic Shore in the winter of 2009/2010 shows the strongest ice coverage for the last ten years (Fig. 8.23), the decreasing trend is continued in the Fehmarnbelt according to the statistical analysis of the ice coverage off Fehmarn island by BSH. Despite the strong winter, only 11 days of ice occurred off Westermarkelsdorf in the period from 26 January 2010 to 18 February 2010 and 10 days of ice were recorded at Marienleuchte from 26 January 2010 to 17 February 2010, an unusually short period compared to the long-term mean (see Table 8.5 and Table 8.6).

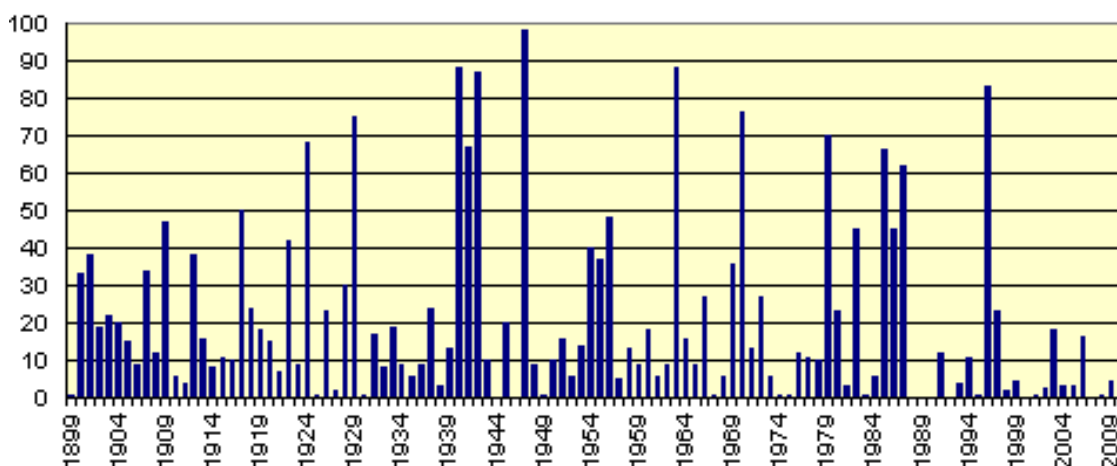


Fig. 8.23 Reduced ice sum: the arithmetic mean of days with ice recorded at 13 stations along the German Baltic Sea coast from 1897 to 2010, from (BSH 2010).

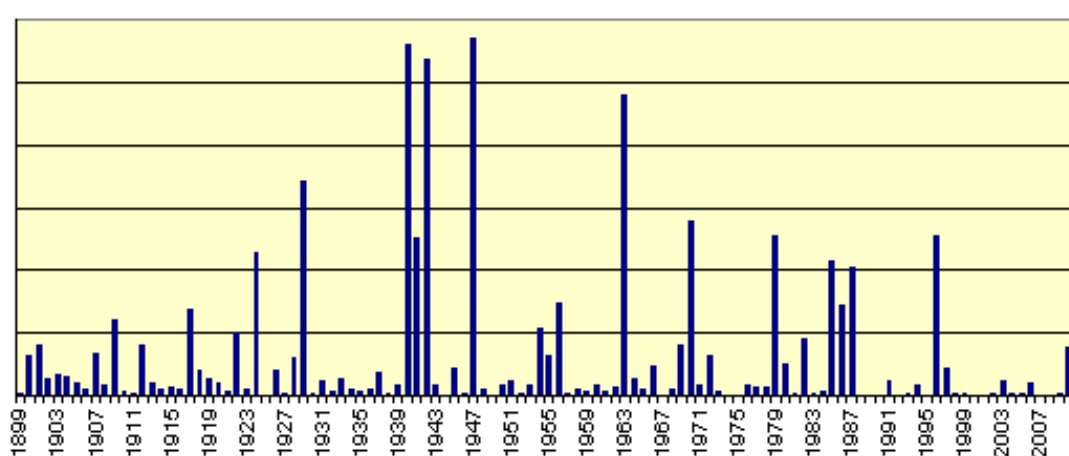


Fig. 8.24 Accumulated areal ice volume for the German Baltic Sea coastline. (BSH 2010).



Table 8.5 Statistical parameters for sea ice off **Westermarkelsdorf** on the north-western Fehmarn island. The ice winter 2009/10 is compared to long-term observations from 1961-2000. While sea ice in the Fehmarnbelt in 2009/10 started to form in mid- January which is the normal period, ice occurrence lasted only until 18 February, which is a rather short period. Ice was spotted only on 11 days during the whole season, which is less than half the long-term mean period. Data from (BSH 2010).

Mean and extreme values of ice parameters for the period 1961-2000 *(representative only for winter seasons with ice)										
Number of years total with ice		Frequency of ice occurrence	Start of ice occurrence*			End of ice occurrence*			Number of days with ice	
			early	median	late	early	median	late	mean	max.
40	12	30%	5 Jan	20 Jan	7 Mar	5 Feb	13 Mar	1 Apr	34	84
Ice winter 2009/10			26 Jan			18 Feb			11	

Table 8.6 Statistical parameters for sea ice off **Marienleuchte** on the south-eastern shore of Fehmarn island. The ice winter 2009/10 is compared to long-term observations from 1961-2000. While sea ice in the Fehmarnbelt in 2009/10 started to form in mid- January which is the normal period, ice occurrence lasted only until 18 February, which is a rather short period. Ice was spotted only on 11 days during the whole season, which is less than half the long-term mean period. Data from (BSH 2010).

Mean and extreme values of ice parameters for the period 1961-2000 *(representative only for winter seasons with ice)										
Number of years total with ice		Frequency of ice occurrence	Start of ice occurrence*			End of ice occurrence*			Number of days with ice	
			early	median	late	early	median	late	mean	max.
40	10	25%	5 Jan	18 Jan	12 Feb	28 Jan	17 Mar	2 Apr	35	84
Ice winter 2009/10			26 Jan			17 Feb			10	

The ice winter 2008/2009 was however very mild with less than 10 days of ice at the German Baltic coast (Fig. 8.23) and an accumulated areal volume near zero (Fig. 8.24), a state that matches the last 20 years of observations except for 1995/96.

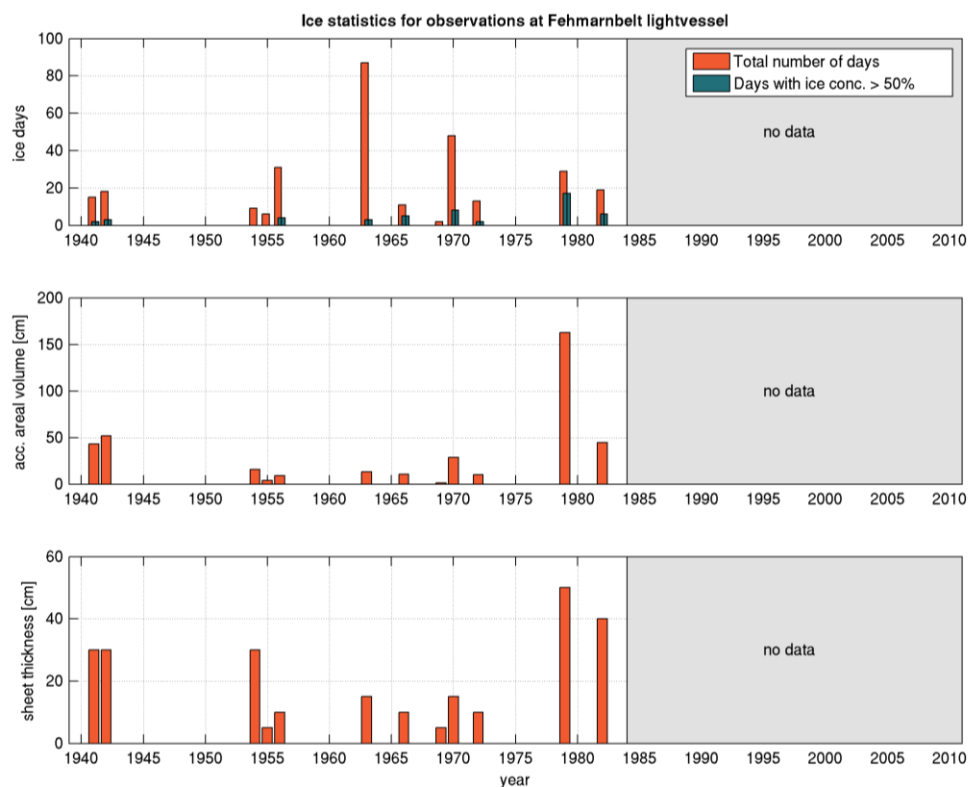


Fig. 8.25 Number of ice days (upper panel), accumulated ice volume (central panel) and maximum sheet thickness (lower panel) as observed at the Fehmarnbelt light-vessel 1941-1982.

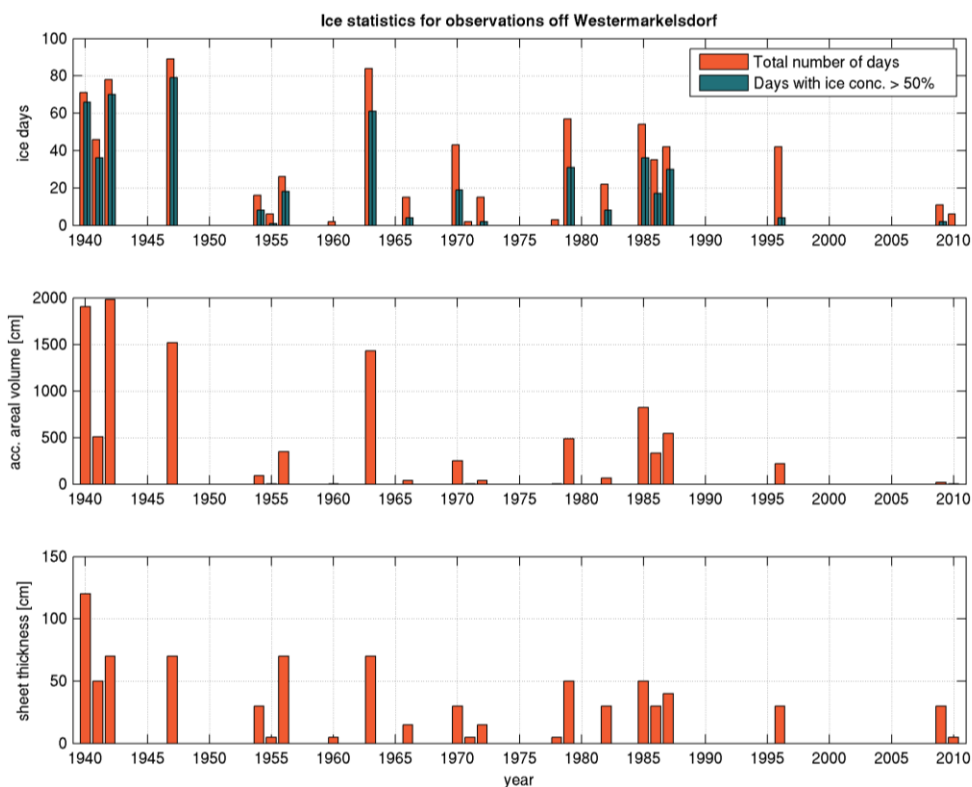


Fig. 8.26 Number of ice days (upper panel), accumulated ice volume (central panel) and maximum sheet thickness (lower panel) as observed off Westermarkelsdorf 1940-2010/2011.



Fig. 8.27 Number of ice days (upper panel), accumulated ice volume (central panel) and maximum sheet thickness (lower panel) as observed off Marienleuchte 1940-2010/2011.

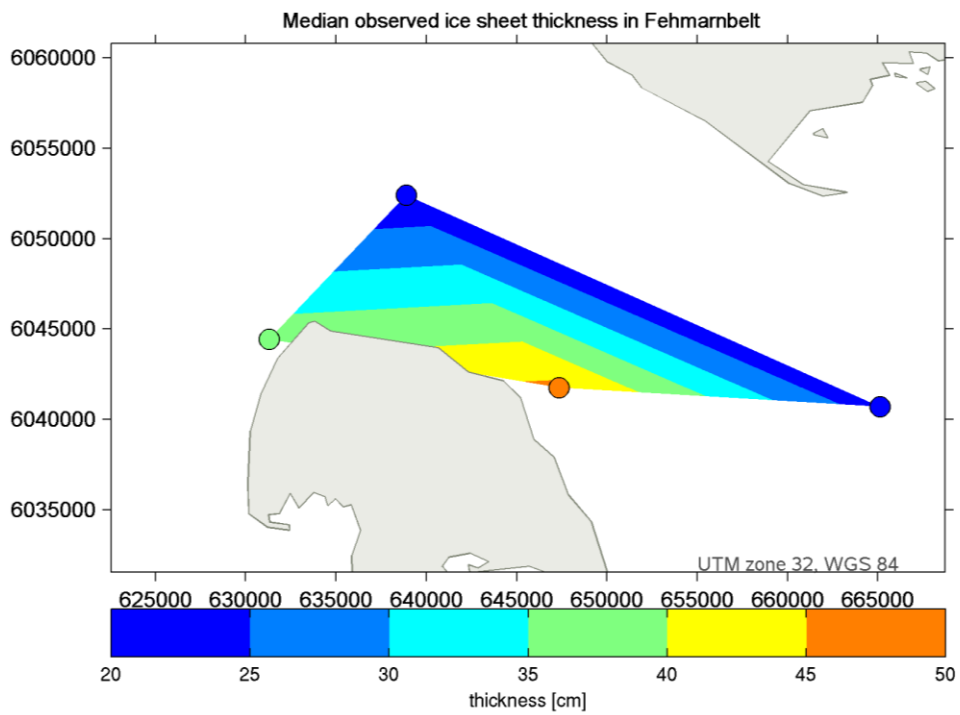


Fig. 8.28 Long-term median ice sheet thickness as observed in Fehmarnbelt (cf. Table 8.4).



9 REPRESENTATIVENESS OF BASELINE PERIOD

The monitoring period is compared to long-term statistics for the following parameters:

- Meteorology;
- Water level;
- Current;
- Salinity and temperature; and
- Sea ice.

9.1 Meteorology

The analyses of meteorological data presented in Chapter 5.2 conclude that most meteorological conditions did not differ significantly from average during the baseline period. The only obvious deviations from the long-term averages were the cold and snowy winters in 2009/10 and 2010/11. An enhanced number of days with strong wind occurred in May, November and December 2010. July 2009 was the warmest month in the baseline exceeding the long-term average by 3°C. High precipitation was observed in May, August and November 2009.

Simulated wind speed and temperature are extracted at MS02 from the meteorological forcing data for the oceanographic models. These time-series enables one to perform a comparison of the representativeness of the baseline period conditions from one uniform and consistent data set. The comparisons are shown in Fig. 9.1 and Fig. 9.2. Slightly low winds are found in February and Marts, and slightly high in September and October. But overall the wind conditions do not deviate significantly from the long-term mean. Both winters are found to be cold.

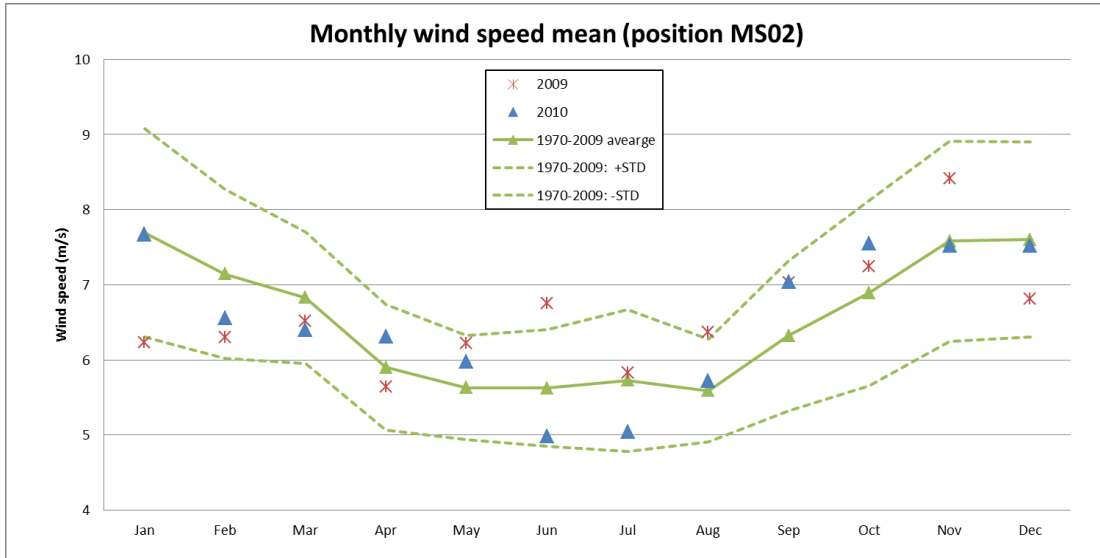


Fig. 9.1 Simulated monthly mean wind speed at position MS02 (compilation of SN-REMO and STORM data).

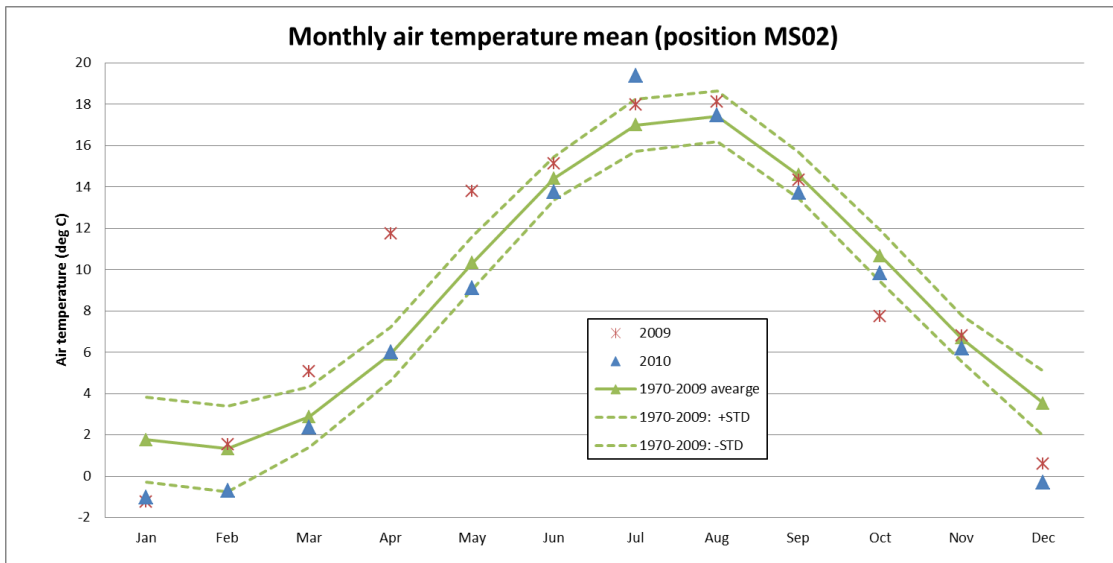


Fig. 9.2 Simulated monthly mean air temperature at position MS02 (compilation of SN-REMO and STORM data).

9.2 Water Level

Water level time-series are shown in Fig. 6.1 to Fig. 6.3 and Fig. 8.1 to Fig. 8.3 that can be compared. A statistical analysis of the measurements is presented in Table 9.1. The mean and standard deviation do not differ much between the two periods. The minimum and maximum values are lower and higher, respectively, in the longer period than in the shorter baseline period as expected.

Based on the figures it is found that the variation during the baseline period do not differ importantly from the other years covered.



Table 9.1 Statistical parameters for water level measurements The parameters are mean, standard deviation, minimum and maximum.

Station	Period	Water level [m]			
		mean	STD	min	max
Gedser	Jan 2004 - Feb 2009	0.080	0.240	-1.45	1.37
	Mar 2009 - Feb 2011	0.088	0.240	-1.38	1.24
Warnemuende	Jan 2004 - Feb 2009	0.079	0.220	-1.20	1.62
	Mar 2009 - Feb 2011	0.064	0.219	-1.15	1.17
Kiel	Jan 2004 - Feb 2009	0.046	0.238	-1.57	1.71
	Mar 2009 - Feb 2011	0.053	0.245	-1.29	1.36

9.3 Current

The historical long-term data and the current observations in on-going baseline monitoring can be compared by evaluating the following statistical measures, which describe magnitude, direction and stability of the currents:

- Mag: the magnitude is the scalar mean of all recorded current velocities;
- Max: the maximum current velocity observed in the record;
- Speed: vector averaged velocity;
- Sf: stability factor, speed/mag x 100, a measure for the directional stability of the flow (Middelstaedt et al. 2008); sf=100% implies a constant flow direction; and
- Dir: vector averaged current direction.

Table 9.2 and Table 9.3 below show that magnitudes and maxima at the northern edge of the Fehmarnbelt in the baseline period are slightly lower than the long-term average in the central channel. It is noted that the stations compared are separated in space, see Fig. 3.8, and therefore the currents should not be identical even if collected during the same period.

Current stability is generally stronger at the bottom than at the surface, where wind-induced changes in current direction are more prominent.

Table 9.2 Current statistics at Fehmarnbelt light-vessel (FB) 1982-86 compared to baseline measurements at MS01 March 2009 - February 2011. Both statistics are derived from hourly values. Fehmarnbelt light-vessel values are from Middelstaedt et al. 2008. Note the big difference for the deeper levels.

Z [m]		mag [cm/s]		max [cm/s]		speed [cm/s]		sf [%]		dir [deg.]	
FB	MS01	FB	MS01	FB	MS01	FB	MS01	FB	MS01	FB	MS01
8-12	10.33	29	27	118	112	8	6	28	22	347	314
26	18.58	16	14	93	62	7	5	44	40	114	286

Table 9.3 Current statistics at Fehmarnbelt light-vessel (FB) 1982-86 compared to baseline measurements at MS02 March 2009 to February 2011. Both statistics are derived from hourly values. Fehmarnbelt light-vessel values are from Middelstaedt et al. 2008.



Z [m]		mag [cm/s]		max [cm/s]		speed [cm/s]		sf [%]		dir [deg.]	
FB	MS02	FB	MS02	FB	MS02	FB	MS02	FB	MS02	FB	MS02
8-12	10.33	29	30	118	136	8	7	28	25	347	323
26	27.58	16	19	93	64	7	5	44	40	114	118

Simulated current speed and direction in two levels are extracted at MS02 from the simulations of the oceanographic conditions. These time-series enables one to perform a comparison of the representativeness of the baseline period conditions from one uniform and consistent data set. The comparisons are shown in Fig. 9.3 to Fig. 9.6. The current in the two levels do not deviate from the long-term mean in any systematic manner.

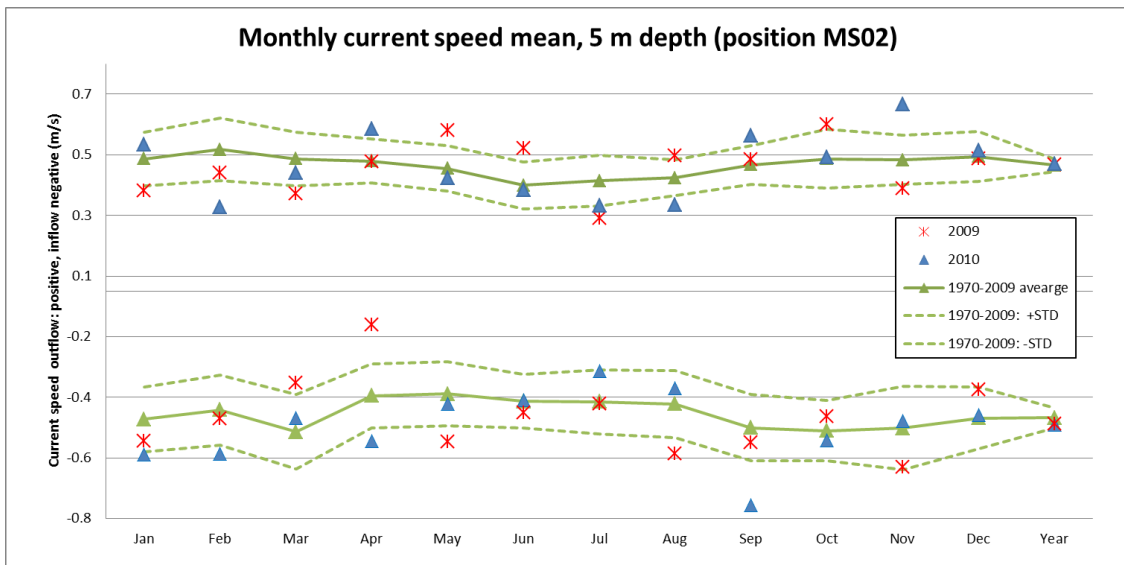


Fig. 9.3 Simulated monthly mean current speed at position MS02 in 5 m depth.

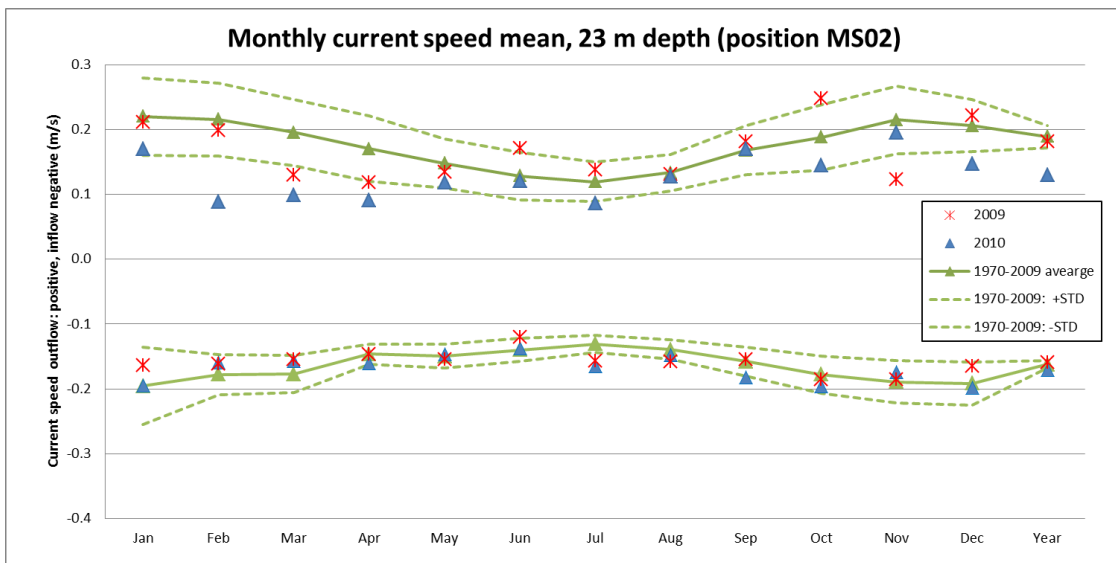


Fig. 9.4 Simulated monthly mean current speed at position MS02 in 23 m depth.

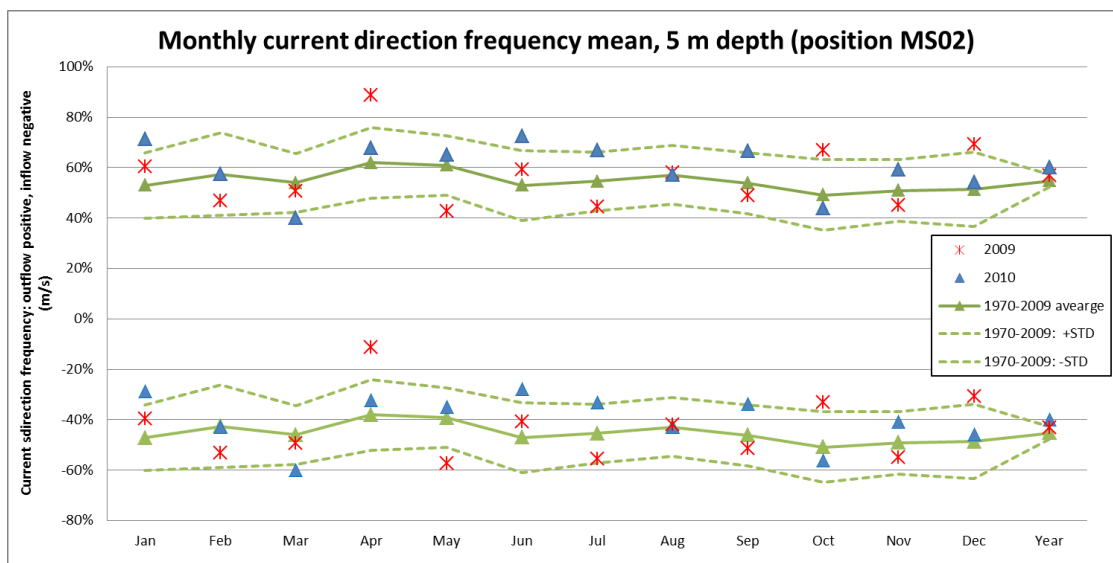


Fig. 9.5 Simulated monthly current direction frequency at position MS02 in 5 m depth.

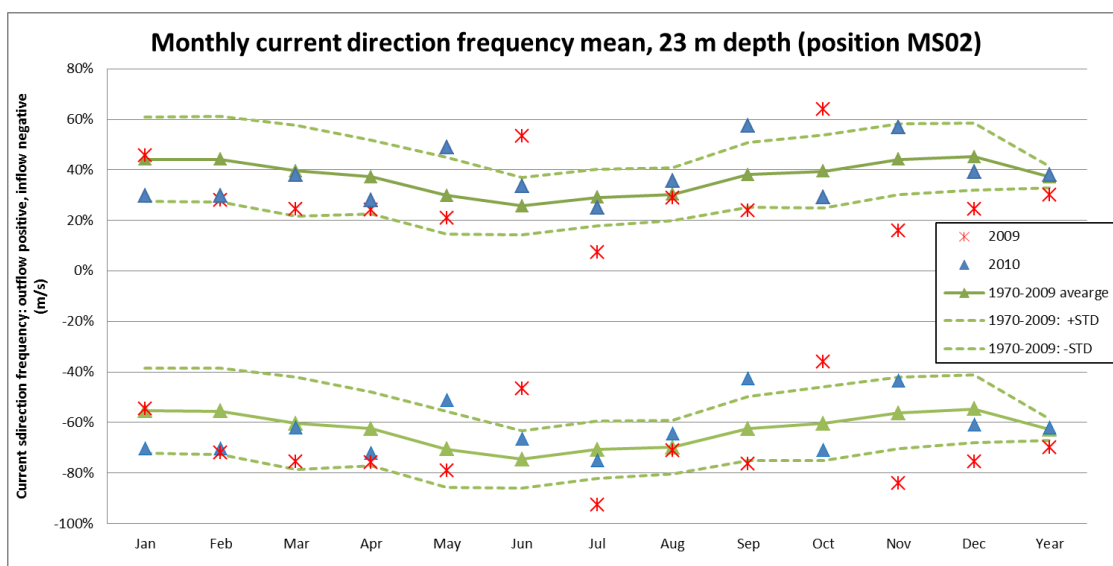


Fig. 9.6 Simulated monthly current direction frequency at position MS02 in 23 m depth.

9.4 Salinity and Temperature

The variation of the monthly mean salinity and temperature at MS01 and MS02 during the baseline period are compared to the 6-years means at Fehmarnbelt light-vessel, see Fig. 9.7 and Fig. 9.8.

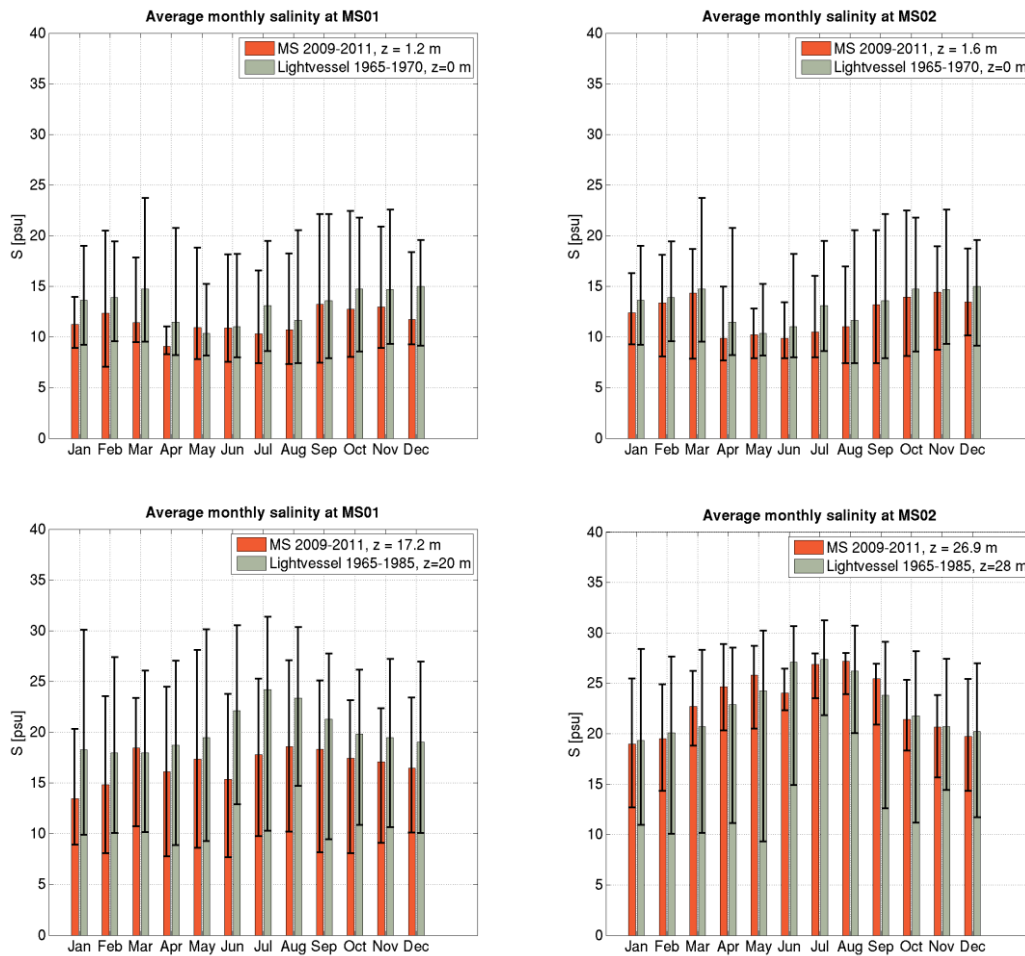


Fig. 9.7 Monthly means of salinity at MS01 (left hand row) and MS02 (right hand row) at surface (upper panels) and bottom (lower panels) layers compared to corresponding 6-years means at surface and long-term at bottom at Fehmarnbelt light-vessel. Black range bars indicate monthly all-time minima and maxima.

In Fig. 9.7 it is found that in the Fehmarnbelt:

- Surface salinity is in general lower during the baseline period than in the 6-year average. The winter months shows a difference of up to 4 psu between the baseline and the 6-year average; and
- Bottom salinity at MS01 is lower in the baseline period than in the 20-year average with the biggest difference of 5 psu occurring during summer. At MS02 the bottom salinity only deviates slightly from the 20-year average.

It is noted that the different locations of the main stations and the light-vessel and in the lower levels will also influence the comparison and therefore some difference in salinities should be expected. Another factor is the relative absence of Major Baltic Inflows since 1984 while the light-vessel records include 14 moderate to strong MBIs with inflowing highly saline water, see (Matthäus et al. 2008).

The ranges of monthly minima and maxima measured at both stations are generally well within the 6-year averages for surface and bottom layers.

It is in this connection noted that MS01 do not cover the deepest of the bottom layer as the lowest sensor is at 17.2 m depth while light-vessel measurements were taken at 20 m depth. Another point is that the light-vessel records represent the

central Fehmarnbelt channel while the main stations are located of the northern and southern channel edges respectively.

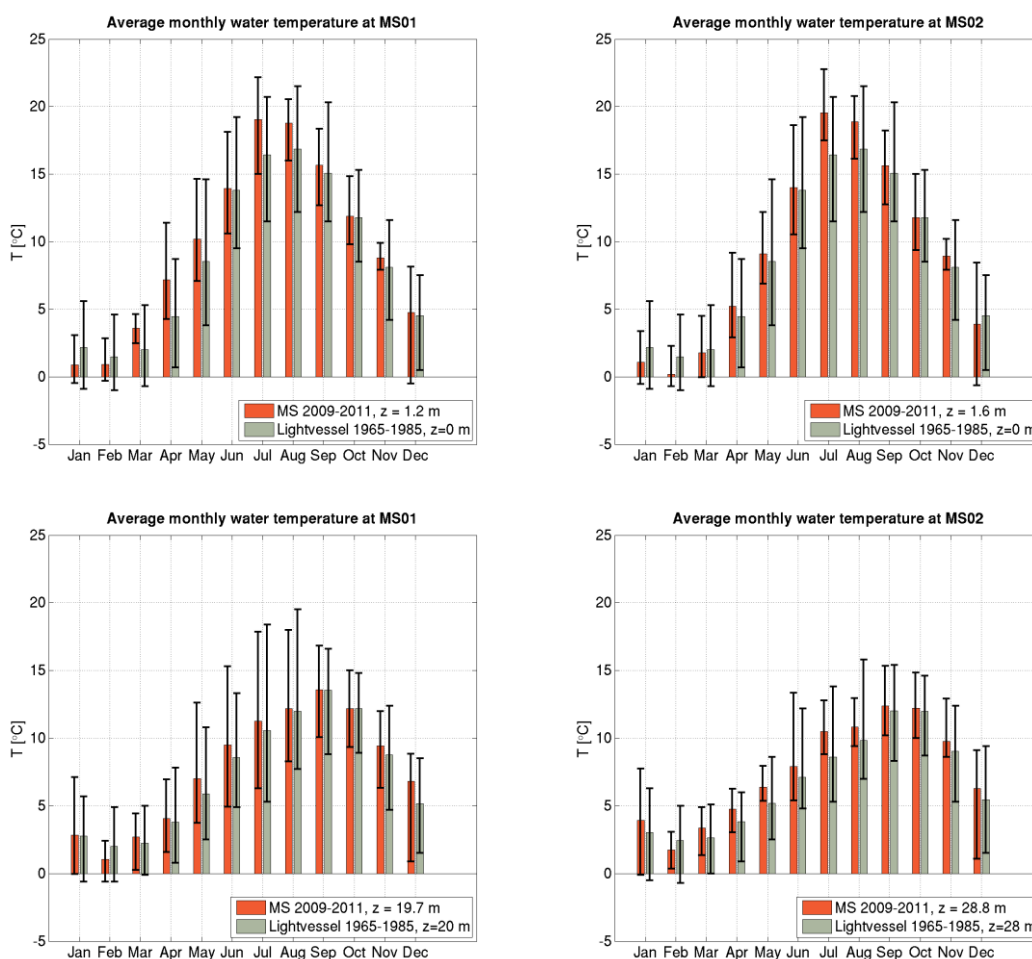


Fig. 9.8 Monthly means of water temperature at MS01 (left hand row) and MS02 (right hand row) at surface (upper panels) and bottom (lower panels) layers compared to corresponding 6-year means from Fehmarnbelt light-vessel. Black range bars indicate monthly all-time minima and maxima.

Water temperatures in the Fehmarnbelt during the baseline period are characterized by some extremes. The main stations records show an unusually cold winter 2009-2010 from January to March with water temperatures below 0°C in February near the surface at station MS02. At MS01 the February data is missing due to impact of drift ice. Also MS02 was affected by ice close to the sea surface in February.

While the winter season was colder than average, the rest of the year appears warmer than the 6-year record and both close to the surface and the bottom. While still within the all-time maximum range, bottom temperature in the summer months was up to 2°C higher at MS01 than the 20-year average. Also the bottom temperature at the southern channel slope, which is normally influenced by cold inflowing North Sea water, was up to 2°C higher in summer than the 20-year average.

The salinity variation is more important for the density than the temperature. Based on the comparison of salinities it is concluded that the baseline period can be applied to assess the hydrographic impacts of the different considered link solutions.



Fig. 9.9 shows T-S diagrams for the two Main Stations in the Fehmarnbelt compared to long-term records from Fehmarnbelt light-vessel.

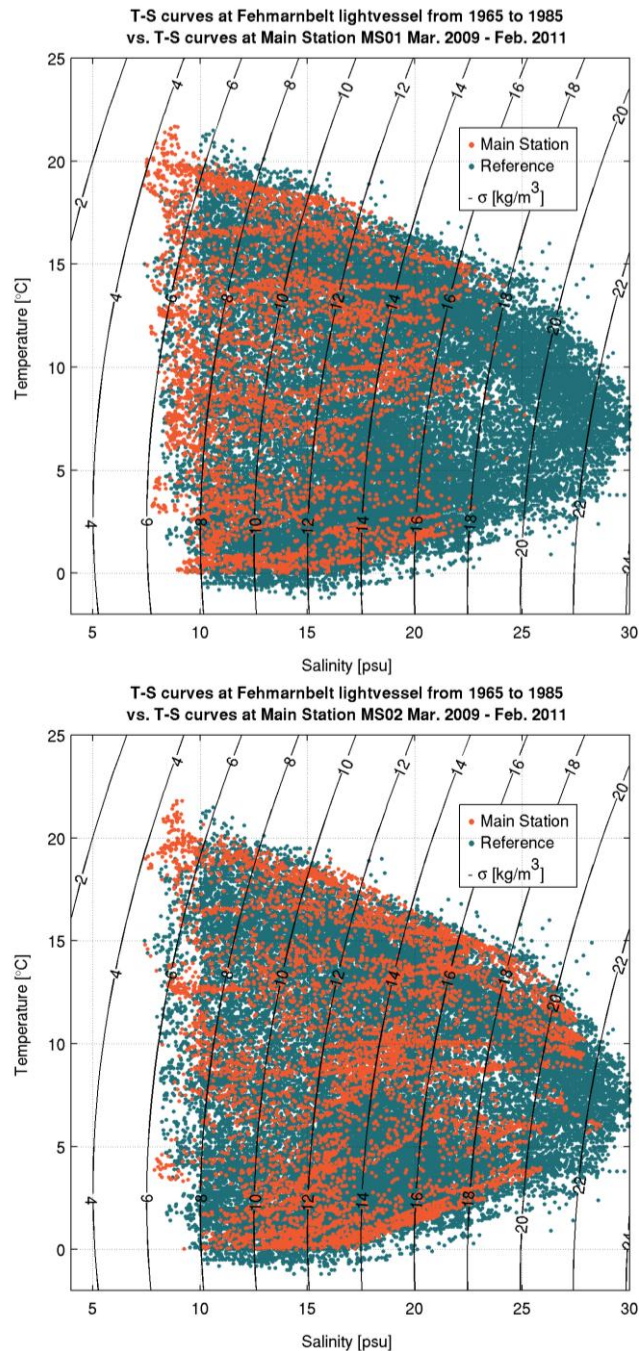


Fig. 9.9 T-S diagrams based on measurements collected at MS01 and MS02 compared to long-term measurements from Fehmarnbelt light-vessel. MS01 in particular shows a concentration of low saline water. MS02 displays two extremes in temperature along the upper and lower edges of the reference cloud. Black lines represent the oceanographic water density, $\sigma = \rho - 1000 \text{ kg/m}^3$. It is noted that the lack of high salinities at MS01 is caused by that the dense inflow follows the southern bed slope in the Fehmarnbelt and hence do not impact MS01.

The findings extracted in the monthly means above are also observed in these plots. At MS01 off the northern shore one can observe that the baseline period are shifted toward less saline and warmer waters which also bring about an observed density maximum for the baseline near 1020 kg/m^3 while densities above 1022 kg/m^3 are not uncommon in general. Main Station MS02 at the southern slope

shows three main bodies of water. At the lower edge of the cluster, a cold winter water covers the entire water column, as indicated by the range of salinities from 10 psu to above 25 psu. The other distinct water mass occurs in summer when the entire water column is warmed to temperatures between 15°C and 20°C; this can be seen at the upper edge of the cluster. The third water mass is spread between these two extremes and represents the spring and fall seasons. While the baseline values for MS02 stay within the frame of the long-term observations, the clear dipole between summer and winter waters seems unusual.

Main Station MS03 in the Mecklenburg Bight has no such direct long-term observational reference station like the Fehmarnbelt Main Stations since the nearest long-term station BMP MS02 has only irregularly been probed. Therefore not all months of the year are represented equally in the samples and the observations are only snapshots of a highly variable water body. Notably only 3 sampling surveys were made in December during the last 40. BMP MS02 is still suited for providing general statistics like all-time standard deviation, minima and maxima of parameters and for calculation of long term means from months with more than 30 samples to compare these with observations from MS03.

A T-S diagram (Fig. 9.10) reveals a well-mixed water body with almost no distinct water masses although a weak seasonal stratification can be found in the long-term records with temperatures between -1°C and 5°C in winter and 15°C to 20°C in summer. It also shows that the baseline observations fit well into the long-term salinity and temperature measurements taken at BMP M02 although the difference between summer and winter water masses is less obvious. The thin plume of cold winter water at the lower edge of the plot cloud fits the pattern of inflowing North Sea water at Main Station MS02 in the Fehmarnbelt (Fig. 9.9) but due to mixing in the Mecklenburg Bight, a density maximum in winter is reached at 1020 kg/m³ compared to more than 1025 kg/m³ in the southern Fehmarnbelt.

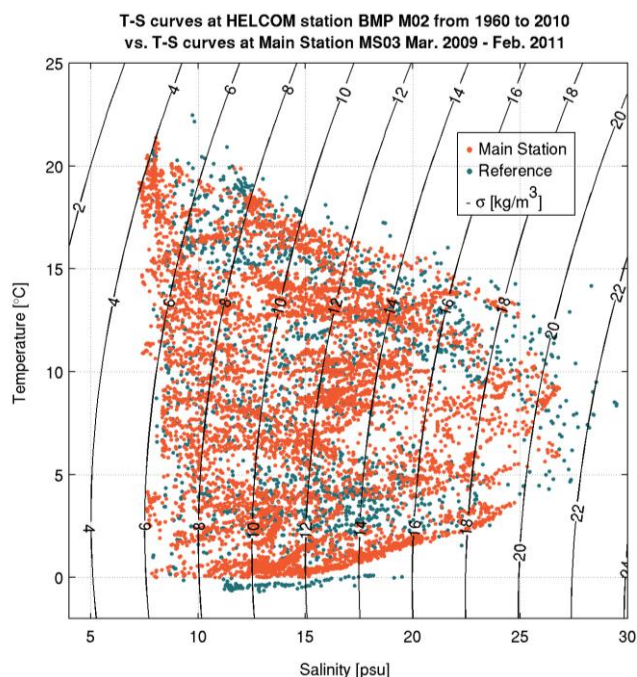


Fig. 9.10 T-S diagram based on measurements collected at MS03 compared to long-term measurements from BMP M02 (blue). The baseline observations fit well into the multitude of long-term salinity and temperature records, the spring months of 2010 are missing though in the MS03 samples. Black lines represent the oceanographic water density, $\sigma = \rho - 1000 \text{ kg/m}^3$.



Simulated salinity and temperature in two levels are extracted at MS02 from the simulations of the oceanographic conditions. These time-series enables one to perform a comparison of the representativeness of the baseline period conditions from one uniform and consistent data set. The comparisons are shown in Fig. 9.11 to Fig. 9.14. The salinities in the two levels do not deviate from the long-term mean in any systematic manner. The temperature in 5 m depth is low during year 2010 and the temperature in 23 m depth is high during year 2009.

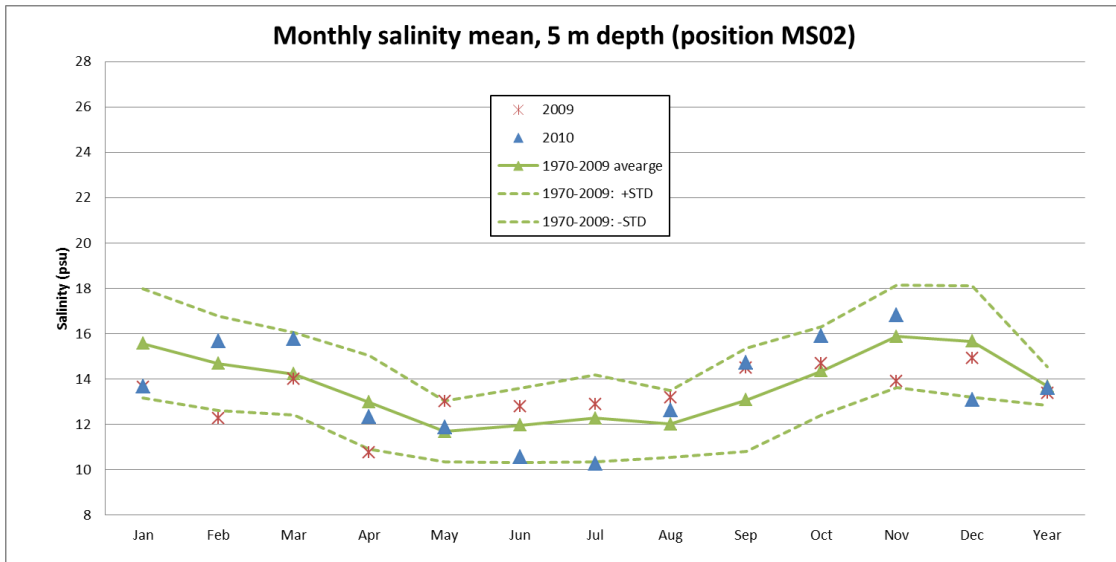


Fig. 9.11 Simulated monthly mean salinity at position MS02 in 5 m depth.

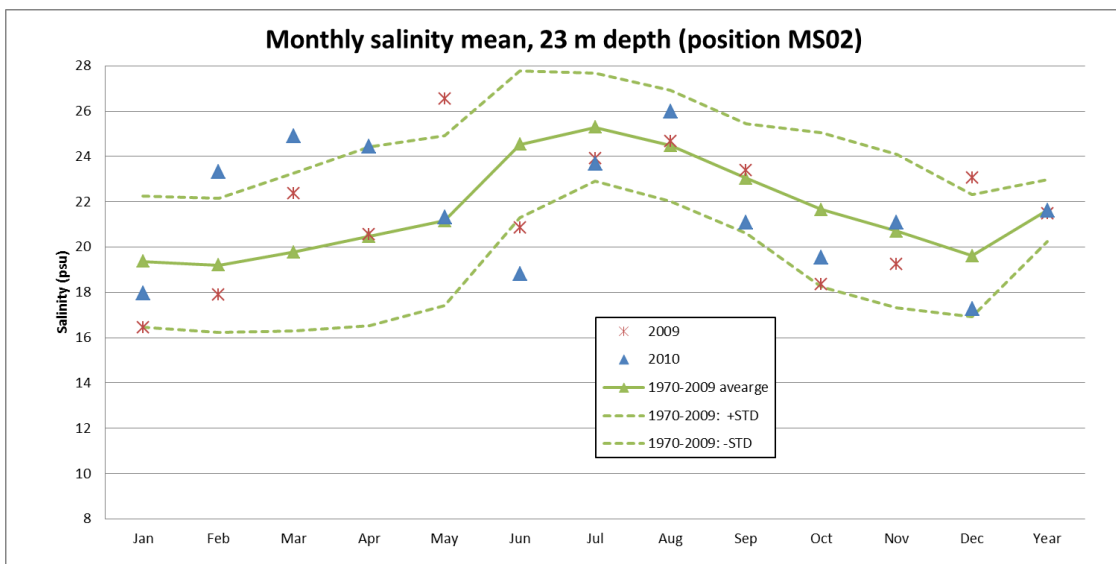


Fig. 9.12 Simulated monthly mean salinity at position MS02 in 23 m depth.

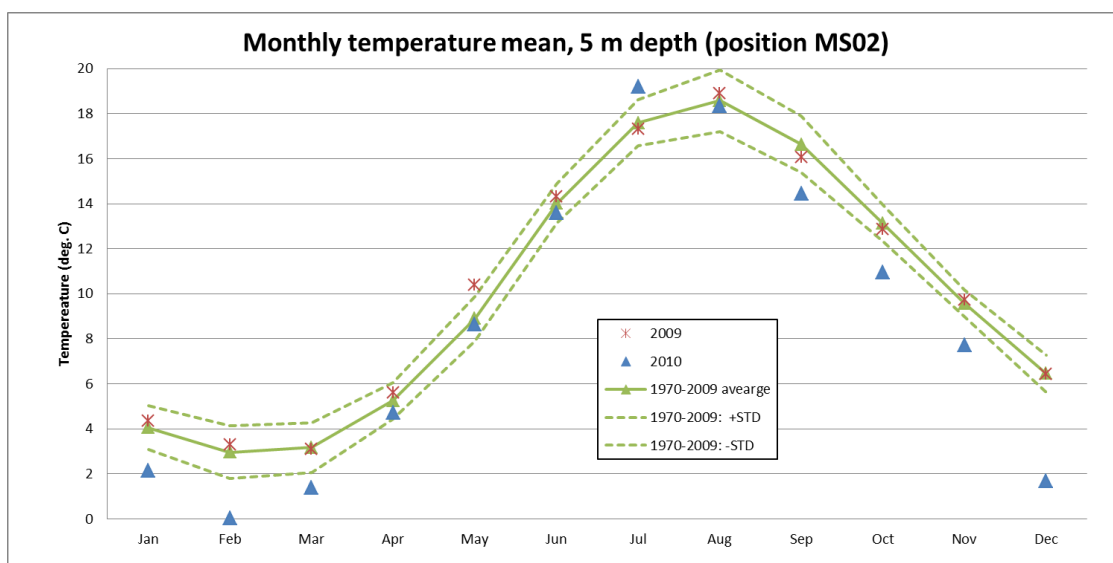


Fig. 9.13 Simulated monthly mean temperature at position MS02 in 5 m depth.

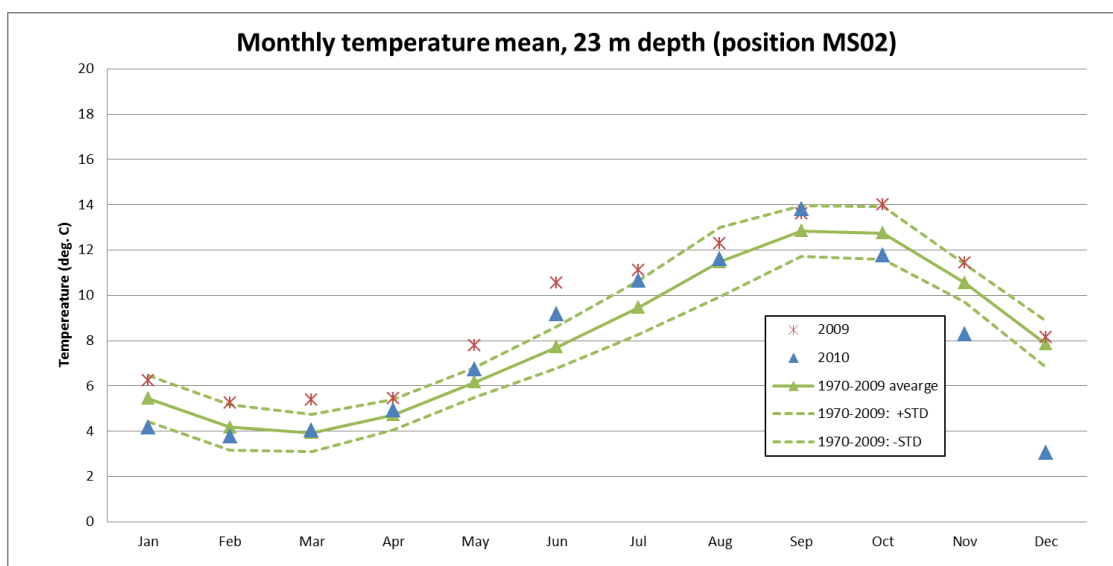


Fig. 9.14 Simulated monthly mean temperature at position MS02 in 23 m depth.

9.5 Sea Ice

The winter 2009-2010 was an ice-winter, see Fig. 8.19. Hence it is colder than normal.

A comparison of winter of 2009-2010 with long-term values is shown in Table 9.4.

While sea ice in the Fehmarnbelt in 2009-2010 started to form in mid- January which is the normal period, ice occurrence lasted only until 18 February, which is a rather short period. Ice was spotted only on 11 days during the whole season, which is less than half the long-term mean period.



Table 9.4 Statistical parameters for sea ice off Marienleuchte on the south-eastern shore of Fehmarn island. The ice winter 2009-2010 is compared to long-term observations from 1961-2000. Data from (BSH 2010).

Mean and extreme values of ice parameters for the period 1961-2000 *(representative only for winter seasons with ice)										
Number of years total with ice		Frequency of ice occurrence	Start of ice occurrence*			End of ice occurrence*			Number of days with ice	
			early	median	late	early	median	late	mean	max.
40	10	25%	5 Jan	18 Jan	12 Feb	28 Jan	17 Mar	2 Apr	35	84
Ice winter 2009-10			26 Jan			17 Feb			10	

9.6 Partial Conclusion

2009:

- June wind speed and spring air temperature above normal;
- Spring bottom temperature higher than typically, else normal;
- April 2009 more surface outflow than normally. June+Oct more bottom outflow and July+Nov+Dec more bottom inflow than normally; and
- Inflow of high salinity to Baltic Sea in November (not a major Baltic inflow).

2010:

- Wind speed normal, winter air temperature below normal – July above normal;
- Surface salinities normal, bottom salinities high Feb-Mar and low June;
- Surface temperatures low Jan-Mar and Sep-Dec, bottom temperatures low Jan + Nov-Dec; and
- Weak bottom level outflow speed Feb-Apr and lower inflow frequency in May and September than normally.

No major inflows happen in the baseline period. Major inflows are rare and should not be expected in a limited baseline period. On the other hand several minor inflows occur during the monitoring period.



10 PRESENT PRESSURES

The present pressures include:

- Major constructions;
- Ship and ferry traffic; and
- Expected Climate change.

10.1 Major Constructions

The bridges across the Danish Straits are hydrographically implemented as zero solutions, designed to not affect the Baltic Sea after their implementation. Hence they should not impact the Fehmarnbelt.

The breakwaters of the Rødbyhavn and Puttgarden harbours extend up to 600 m offshore, which has a blocking effect on the flow. The size of this effect has not been documented.

Offshore wind farms have been constructed in Danish waters and a number of locations along the German coastline have been approved by German authorities for the construction of further wind farms. Some of these wind farms are located close to Fehmarnbelt.

Existing offshore wind parks at Nysted (Rødsand) together with planned new offshore installations also have an impact on the hydrography. They tend to block the exchange flow through the Belt Sea and create mixing of the stratified water masses unless compensating dredging is carried out as for the fixed links.

The mixing efficiency of the turbulence production by a Wind Turbine Generator (WTG) foundation is close to the mixing efficiency of the turbulence production by a bridge pier. But often the offshore wind farms are located in shallower water with homogenous water column.

10.2 Ship Traffic and Its Effects

On the Great Belt – Fehmarnbelt route the number and size of ships is increasing and especially the traffic of oil tankers is ever more increasing, see Fig. 10.1. HELCOM (2009) predicts an increase of 40% by the year 2015 in the amount of oil that is transported through the Great Belt (Fig. 10.2). Likewise they expect an increasing number of large tankers with capacities above 100,000 t which is however not yet specified. Collisions or grounding of oil tankers pose a threat and may cause oil spills that will affect the local ecosystem for several years. A 2006 analysis by the European Union's Baltic Master II programme estimated a general increase of 180% by the year 2020 in vessels navigating the Danish Straits based on 2005 values (Baltic Master 2006).

An investigation on the mixing of water masses caused by ferries on the Rødby-Puttgarden route showed that the mixing in the ferries wakes is limited. Hence their environmental impact is only of minor importance. None the less if the number of ferries increases or their size increases then their impact will increase.

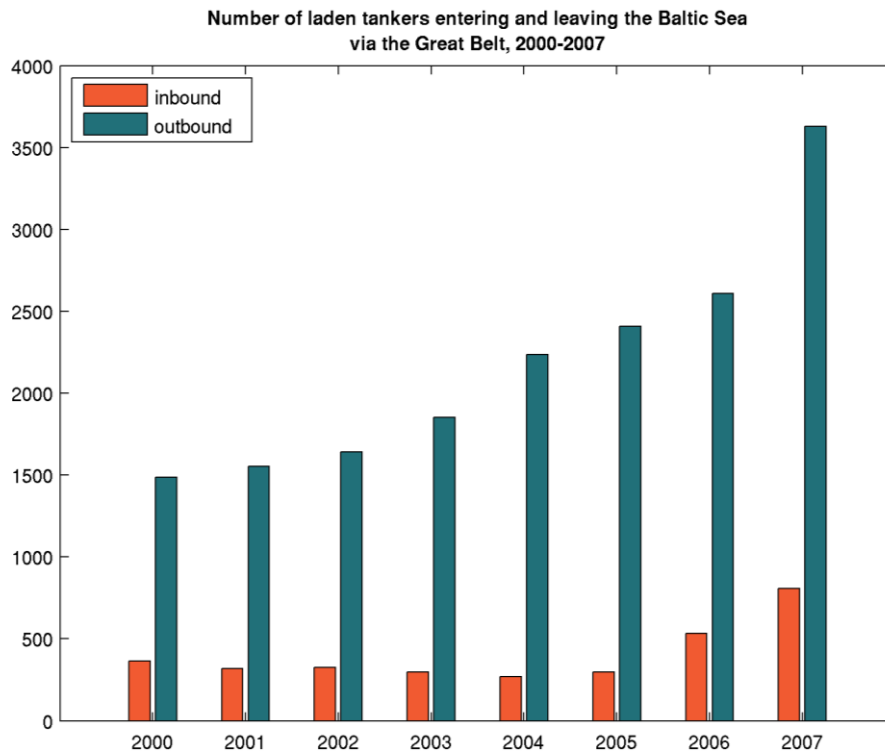


Fig. 10.1 Number of laden tankers entering and leaving the Baltic Sea via the Great Belt. Figure re-drawn with data from HELCOM (2009).

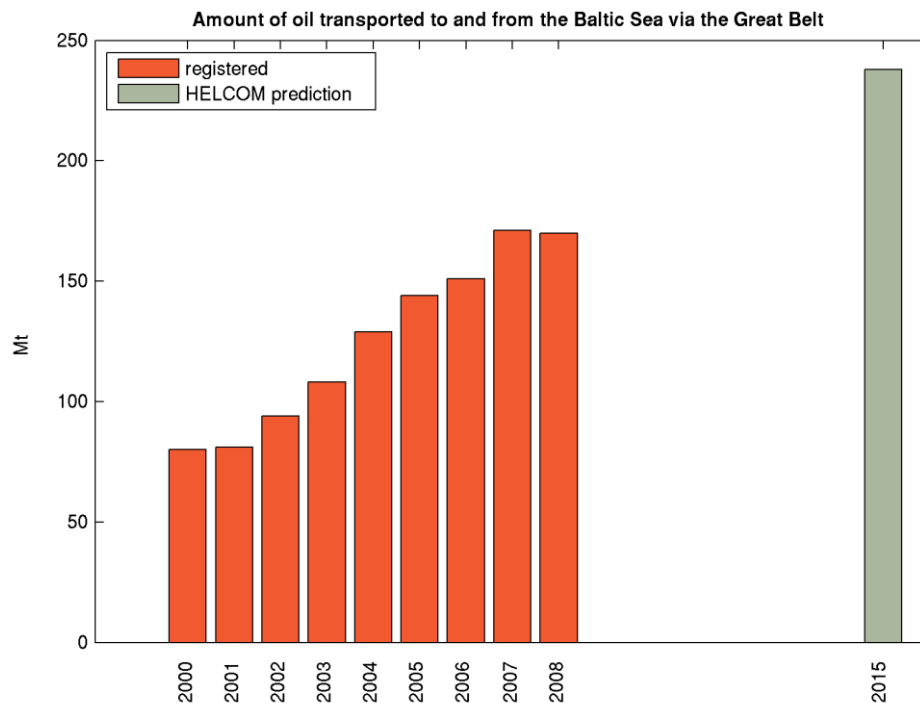


Fig. 10.2 Amount of oil transported to and from the Baltic Sea via the Great Belt (million tonnes). Figure based on data from HELCOM (2009).



10.3 Expected Climate Change

It is anticipated that climate change will raise water levels and increase extreme storm wind speeds in the future. For example +1 m and + 3 m/s by year 2100 (Fehmarnbelt Fixed Link 2009). Both effects will lead to higher water levels in the Belt Sea:

- If the water levels in the world oceans are raised by 1 m then it will cause the water levels in the Belt Sea to be permanently raised by 1 m; and
- If extreme storm wind speeds are increased, then storm surge levels will go up. If storm wind speed for example is increased from 27 m/s to 30 m/s, then the storm surge set-up is increased by roughly 23%.

The higher water level will reduce the resistance of the Belt Sea; see (Jakobsen and Trébuchet 2000) and (Jakobsen et al. 1996 and 2010).

The mesoscale local dynamics of the Fehmarnbelt are mainly driven by local wind forcing and remote pressure gradients. These forcing factors are highly sensitive to interannual and climate changes. It is not quite obvious how a change in mesoscale dynamics will impact the ecosystem as a whole.

An increase in strength of wind forcing will also increase the intensity of mesoscale current patterns. This may cause an enhanced mixing between in- and outflowing water masses of the Baltic Sea. However, this will affect only small and medium in-flow events by lowering the salinity of the inflowing water.



11 ASSESSMENT OF IMPORTANCE

The hydrography of the Fehmarnbelt has been assigned importance categories for use in the impact assessment. The importance categories are established by the individual consortia (FEHY, FEMA, etc.) and are presented jointly in a note on environmental criteria (Femern 2011).

The hydrography belongs under the subfactor seawater. The subfactor sea water is special as in the sense that the water constantly moves around. It has been decided to apply a two level importance scale for the hydrography (special and general class).

The conditions within the special importance class of hydrography relate to Fehmarnbelt being one of the two main connections for the water exchange of the Baltic Sea, thus determining the hydrographical conditions in the Baltic Sea with its brackish waters and the stratification, particularly in salinity and dissolved oxygen, see the Baltic Sea baseline description (FEHY 2011a). Changes in the Fehmarnbelt hydrography due to structures partially blocking the water exchange or effecting the local stratification by changed mixing in Fehmarnbelt will risk affecting the water exchange with the Baltic and thus the Baltic Sea conditions.

In addition local stratification in Fehmarnbelt is of special importance for the risk of creating conditions for eutrophication conditions in Fehmarnbelt and surrounding water bodies in adjacent bays. The frequently seen oxygen depletion events in for example Mecklenburg Bight etc. are thus dependent on the strength of the density stratification.

The two above concerns are relevant for water depths of more than 10 m and it is only these areas that are considered for importance assessment.

Finally changes in current conditions at beach areas and in front of harbours have been assigned special importance due to the potential impact from changed currents and waves on bathers and safe approach of harbours. Technically the beach zone is defined as extending 200m offshore and the harbour access area to be within 1500 m from the harbour entrance.

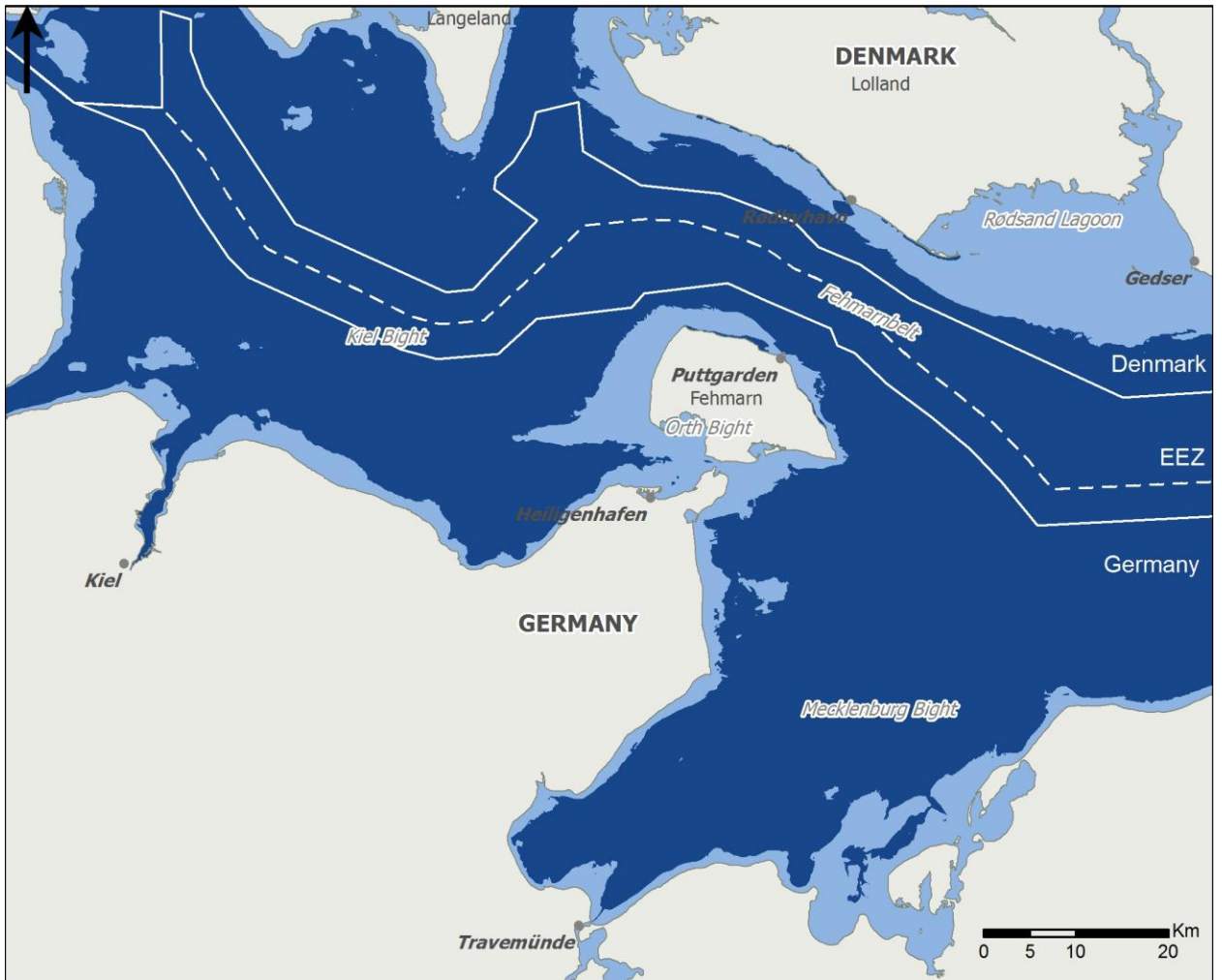
The remaining sea area is characterised as having a general importance category in relation to hydrography specifically.

Similar importance categories are developed for other subfactors such as seawater quality, morphology benthic fauna etc., see the respective baseline reports.

The hydrographic importance classification is summarised in Table 11.1 and the areas of special and general importance identified in Figure 11.1.

Table 11.1 Importance categories for subfactor seawater hydrography.

Importance level	Description
Special	Areas sensitive to overall water exchange in Fehmarnbelt and stratified areas (defined as minimum 10m water depth). Areas around harbors (1500m radius) and beaches (200m zone) (in relation to effects of changed currents and waves).
General	Other areas (and hydrographical parameters).



Importance level for seawater hydrography

- Special** Areas sensitive for water exchange and mixing (depth below 10m),
 harbour areas (1500m radius) and sand beaches (down to 3m water depth)
- General** Other areas

Fig. 11.1 Importance map for subfactor seawater hydrography.



12 REFERENCES

- Aarup T. (2002): Transparency of the North Sea and Baltic Sea – a Secchi depth data mining study. *Oceanologia*, 44 (3), 323–337.
- Bergström S. (1976): Development and application of a conceptual runoff model for Scandinavian catchments. Doctoral thesis, Department of Water Resources Engineering, Lund Institute of Technology, Lund University, Lund, Sweden, 134pp.
- Brasseur O. (2001): Development and Application of a Physical Approach to Estimating Wind Gusts. *Monthly Weather Review*, 129, 5–25.
- BSH (2010): Statistical Data – Westermarkelsdorf.
http://www.bsh.de/en/Marine_data/Observations/Ice/Westermarkelsdorf.jsp
- Christensen F.T. and Skourup J. (1991): Extreme Ice Properties. *ASCE Journal of Cold Regions Engineering* 5(2), 51-68.
- Christiansen C., Emilyanov E. (1995): Nutrients and Organic Matter in Southern Kattegat - Western Baltic Sea Sediments: Effects of Resuspension. *Geografisk Tidsskrift*, 95, 19-27.
- Baltic Master (2006): General Assumption of the Ship Safety in the Western and Southern Baltic Sea. Baltic Master Report MII part 2/4. Maritime University of Szczecin.
- DONG (2010): Design ice loads for Anholt Offshore Wind Farm. Memoranda by LIC-engineering for DONG energy. Project No.: 1012. Can be obtained by contacting DONG energy.
- ESA (2010): Envisat. European Space Agency
<http://envisat.esa.int/earth/www/area/index.cfm?fareaid=6>
- Fehmarn Belt Feasibility Study (1996): Hydrographic data collection and review Fehmarn Belt Feasibility Study, Phase 1, Technical note by FEC.
- Fehmarn Belt Feasibility Study (1997): Determination of cross sectional velocity Fehmarn Belt Feasibility Study, Phase 2, Technical note by Prof. Fl. Bo Pedersen & FEC.
- Fehmarn Belt Feasibility Study (1998): Hydrography Baseline Investigation, Phase 2, Technical note by FEC.
- Fehmarnbelt Fixed Link (2009): Climate Change and the Fehmarnbelt Fixed Link. Report on the Workshop on Climate Scenarios. 13 and 14 May 2009. September 2009.
- FEHY (2013a): Fehmarnbelt Fixed Link. Marine Water - Baseline. Hydrography, water quality and plankton of the Baltic Sea. DHI/IOW Consortium in association with LICEngineering, Bolding & Burchard and Risø DTU. E1TR0057 Volume I.
- FEHY (2013b): Fehmarnbelt Fixed Link. Marine Soil - Baseline. Coastal Morphology along Fehmarn and Lolland, E1TR0056 Volume II.



- FEHY (2013c): Fehmarnbelt Fixed Link. Marine Water – Impact Assessment. Hydrography of the Fehmarnbelt Area. DHI/IOW Consortium in association with LICEngineering, Bolding & Burchard and Risø DTU. E1TR0058 Volume II.
- Feistel R., Nausch G. and Wasmund N. (Eds., 2008): State and evolution of the Baltic Sea, 1925-2005. John Wiley & Sons.
- Femern (2011): Miljøkriterier, Work in progress, draft version March 2011. Femern A/S.
- Fennel W. and Sturm M. (1992): Dynamics of the western Baltic. *Journal of Marine Systems* 3(1-2), 183–205.
- Graham P. (2000): Large-scale hydrologic modeling in the Baltic Basin. Doctoral thesis, Division of Hydraulic Engineering, Department of Civil and Environmental Engineering, Royal Institute of Technology, Stockholm, Sweden, 55 pp. and 5 reprinted papers.
- HELCOM (1986): Water balance of the Baltic Sea. *Baltic Sea Environment Proceedings* No.16.
- HELCOM (2009): Overview of the Shipping Traffic in the Baltic Sea. http://www.helcom.fi/stc/files/shipping/Overview%20of%20ships%20traffic_updateApril2009.pdf
- ICES (2010): HELCOM data. ICES Oceanographic Database and Services, <http://www.ices.dk/Ocean/index.asp>
- ICOADS (2010): International Comprehensive Ocean-Atmosphere Data Set. <http://dss.ucar.edu/datasets/ds540.0>
- Jacobsen T.S. (1980): Sea water exchange of the Baltic, measurements and methods. The Belt project. The National agency of Environmental Protection, Denmark, 106 pp.
- Jakobsen Fl. (1991): The Bornholm Basin—Estuarine Dynamics. Technical University of Denmark, Institute of Hydrodynamics and Hydraulic Engineering, Series Paper 52, 199 pp.
- Jakobsen Fl. (1997): Hydrographic investigation of the Northern Kattegat front. *Continental Shelf Research*, 17 (5), 533-554.
- Jakobsen Fl., Hansen I.S., Hansen N.-E.O. and Østrup-Rasmussen F. (2010): Flow resistance in the Great Belt, the biggest strait between the North Sea and The Baltic Sea. *Estuarine, Coastal and Shelf Science* 87, 325-332.
- Jakobsen Fl., Petersen N.H., Petersen H.M., Møller J.S., Schmidt T. and Siefert T. (1996): Hydrographic investigations in the Fehmarn Belt in connection with the planning of the Fehmarn Belt link. *Proceedings of the Baltic Marine Science Conference 1996 (Rønne, Denmark)*, 10 pp. Published in ICES Cooperative Research Report 257, 2003, 179-189.
- Jakobsen Fl. and Trébuchet C. (2000): Observations of the transport through the Belt Sea and an investigation of the momentum balance. *Continental Shelf Research* 20, 293-311.



- Jun S., Berg P. and Berg J. (2007): Bathymetry impacts on water exchange modeling through the Danish Straits. *Journal of Marine Systems* 65, 450-459.
- Krauss W. (1966): Die Spektren der Temperaturschwankungen und der Strömung im Gebiet nordwestlich von Fehmarn. *Kieler Meeresforschungen XXII*, 35-38.
- Kruse H.H., Jacobsen T.S. and Nielsen P.B. (1980): Physical Measurements in the Open Danish Waters 1974-77, and their storage. *The Belt Project*, 161 pp.
- Kuhrts C., Fennel W., Seifert T. (2004): Model studies of transport of sedimentary material in the western Baltic. *Journal of Marine Systems*, 52, 167-190.
- Lange W., Mittelstaedt E. and Klein H. (1991): Strömungsdaten aus der Westlichen Ostsee. *Deutsche Hydrographische Zeitschrift, Ergänzungsheft Reihe B*, 24.
- Lehmann A. and Myrberg K. (2008): Upwelling in the Baltic Sea - a review. *Journal of Marine Systems* 74 (S1), S3-S12.
- Leppäranta M. and Myrberg K. (2009): *Physical Oceanography of the Baltic Sea*. Springer.
- Lindau R. (2002): Energy and water balance of the Baltic Sea derived from merchant ship observations. *Boreal Environment Research*, 7, 417-424.
- Matthäus W., Nehring D., Feistel R., Nausch G., Mohrholz V., Lass H.U. (2008): The Inflow of Highly Saline Water into the Baltic Sea. In: Feistel R., Nausch G., Wasmund N. (Eds.): *State and evolution of the Baltic Sea, 1925-2005*. John Wiley & Sons, 265-309.
- Middelstaedt E., Klein H. and König P. (2008): Current Observations in the Western Baltic Sea. In: Feistel R., Nausch G., Wasmund N. (Eds.): *State and evolution of the Baltic Sea, 1952-2005*. John Wiley & Sons, Inc. Hoboken, New Jersey, 121-141.
- Miętus M. (1998): *The Climate of the Baltic Sea Basin*. World Meteorological Organization, Report No. 41, 64 pp.
- Sayin E. and Krauss W. (1996): A numerical study of the water exchange through the Danish Straits. *Tellus* 48A, 324-341.
- Schmager G. (1979): *Atlas zur Ermittlung der Wellenhöhen in der südlichen Ostsee*. Seehydrographischer Dienst der Deutschen Demokratischen Republik, 115 pp.
- Schmager G., Fröhle P., Schrader D., Weisse R., Müller-Navarra S. (2008): Sea State, Tides. In: Feistel R., Nausch G., Wasmund N. (Eds.): *State and evolution of the Baltic Sea, 1925-2005*. John Wiley & Sons, 143-198.
- Schmelzer N., Seinä A., Lundqvist J.-E., Sztobryn M. (2008): Ice. In: Feistel R., Nausch G., Wasmund N. (Eds.): *State and evolution of the Baltic Sea, 1925-2005*. John Wiley & Sons, 199-240.
- Schmidt M., Seifert T., Lass H.-U. and Fennel W. (1998): Patterns of Salt Propagation in the southwestern Baltic Sea. *Deutsche Hydrographische Zeitschrift* 50(4), 345-364.



- SOK (2010): Ice and Navigational Conditions in Danish Waters during the Winter 2009-2010. Søværnets Operative Kommando, Istjenesten.
- Sparre A. (1982): Waves and currents at the surface. The Climate of Denmark, Summaries of observations from lighthvessels II, No. 9.
- Sparre A. (1984a): Salinity A; means, extremes and frequency. The climate of Denmark, Summaries of observations from light-vessels IV, No. 11.
- Sparre A. (1984b): Salinity B; Day to day changes; Relations between values at the surface and at the bottom. The climate of Denmark, Summaries of observations from light-vessels IV, No. 12.
- Statens Istjeneste (1954-55). The state of the ice and the navigational conditions in the Danish Waters during the winter 1954-55. Published by Statens Istjeneste, Denmark.
- Thiel G. (1938): Strombeobachtungen in der westlichen Ostsee im Juli 1936. Archiv de Deutschen Seewarte 58(7), 28 pp.
- Tiesel R. (2008): Weather of the Baltic Sea. In: Feistel R., Nausch G., Wasmund N. (Eds.): State and evolution of the Baltic Sea, 1925-2005. John Wiley & Sons, 65-92.
- Ærtebjerg Nielsen G., Jacobsen T.S., Gargas E. and Buch E. (1981): Evaluation of the Physical, Chemical and Biological Measurements. The Belt Project, 122 pp.



Table of figures

Fig. 1.1	Map with the monitoring stations MS01, MS02 and MS03.	2
Fig. 1.2	Instrumentation at one of the three main stations (all three station have in principle the same instrumentation, but the precise instrumentation depends on the local water depth).	2
Fig. 1.3	Map with survey lines applied in monthly surveys. The hydrochemical/water quality stations are marked with green and yellow symbols.....	3
Fig. 1.4	Location of meteorological stations used for analysis: Fehmarnbelt buoy (FB), Westernmarkelsdorf (WD), Nysted (NY), Warnemünde (WM), and Darss Sill (DS). The background shows mean wind speed derived from ship observations in 1961-1990 compiled by Mietus (1998).	4
Fig. 1.5	Bathymetry of the Belt Sea: southern Kattegat (KG), Little Belt (L), Great Belt (G), Sound (S), Fehmarnbelt (F), Kiel Bight (K), Mecklenburg Bight (M), Lübeck Bight (B), Darss Sill (D) and Drogden Sill (R).....	5
Fig. 1.6	Simulated water levels and current velocities in Belt Sea during strong inflow event.	7
Fig. 1.7	Simulated water levels and current velocities in Belt Sea during strong outflow event.	7
Fig. 1.8	Wave roses at MS01 (top, $H_m0 > 0.60$) and MS02 (bottom, $H_m0 > 0.80$).....	9
Fig. 1.9	Measured mean current profile at MS02 during the baseline period. Inflow with a south-westerly current dominates below 15 m depth. Maximum current speeds are reached at the surface while bottom friction reduces current speed near the bottom.....	10
Fig. 1.10	Current roses based on measured current at MS01. The roses are shown in the three levels 5.08 m, 12.58 m and 18.58 m.	11
Fig. 1.11	Current roses based on measured current at MS02. The roses are shown in the three levels 5.08 m, 15.58 m and 27.58 m.	12
Fig. 1.12	Current rose based on measured current at MS03. The roses are shown in the three levels 5.03 m, 12.53 m and 23.53 m.	13
Fig. 1.13	Observed current speed and direction at MS01 from 2009-12-25 to 2010-01-05 at $z=5.08$ m (upper panel) and $z=18.58$ m (lower panel) with mean speed (red lines) and standard deviation of current speed.	14
Fig. 1.14	Measured salinity and temperature variation at the Fehmarnbelt light-vessel from 1965 to 1984. Note the cyclic nature of bottom salinity with infrequent inflows of saline North Sea water.	15
Fig. 1.15	Measured salinity, temperature and density (kg/m^3) at MS01 in Fehmarnbelt (southeast of Rødbyhavn) during the baseline monitoring.	16
Fig. 1.16	Measured salinity, temperature and density (kg/m^3) at MS02 (north of Puttgarden) during the baseline monitoring.....	17
Fig. 1.17	Measured salinity profile at MS01 during the baseline period divided into inflow or outflow conditions. Mean profile with standard deviation indicated.	18
Fig. 1.18	Along-channel current velocity in the link corridor during the survey in August 2009. Positive values indicate flow in the direction of the Central Baltic Sea. The current pattern changed rapidly. The data were collected within a week: a) 24 August 2009; b) 27 August 2009; c) 28 August 2009; and d) 31 August 2009.	19
Fig. 1.19	Measured salinity (PSU) distribution in the Fehmarnbelt. Upwelling is observed at the southern coastline.	20
Fig. 1.20	Monthly means of salinity at MS01 (left hand row) and MS02 (right hand row) at surface (upper panels) and bottom (lower panels) layers compared to corresponding 6-years means at surface and long-term at bottom at Fehmarnbelt light-vessel. Black range bars indicate monthly all-time minima and maxima.	21



Fig. 1.21	Annual cycle of air temperature (°C). Coloured lines with small symbols indicate climatological monthly means at Warnemünde (green), Westermarkelsdorf (red), and Darss Sill. The shaded region corresponds to ± 1 standard deviation. Triangles denote conditions in baseline years 2009 (upward) and 2010 (downward).	23
Fig. 1.22	Annual cycle of magnitude of wind speed (m/s). Coloured lines with small symbols indicate climatological monthly means at Warnemünde (green), Westermarkelsdorf (red) and Darss Sill (cyan). Shaded regions correspond to ± 1 standard deviation. Triangles denote conditions in baseline years 2009 (upward) and 2010 (downward) and star the monthly means at Nysted from June 2004 to November 2005.	23
Fig. 3.1	Map with the monitoring stations MS01, MS02 and MS03.	27
Fig. 3.2	Instrumentation of one of the three main stations. The instrumentation at the three main stations are very similar, but depends on the actual water depth.....	27
Fig. 3.3	Map with survey lines applied in monthly surveys. The hydrochemical/water quality stations are marked with green and yellow symbols.....	28
Fig. 3.4	Location of meteorological stations used for analysis: Fehmarnbelt buoy (FB), Westermarkelsdorf (WD), Nysted (NY), Warnemünde (WM), and Darss Sill (DS). The background shows mean wind speed derived from ship observations in 1961-1990 compiled by (Mietus 1998).	31
Fig. 3.5	Water level gauges in the Fehmarnbelt area that have been evaluated in this report.....	33
Fig. 3.6	Rivers considered are indicated by blue dots and the river identification number. Coloured polygons show sub-basins of Belt Sea according to HELCOM (polygons taken from Feistel et al. 2008a). Acronyms denote: southern Kattegat (KG), Little Belt (L), Great Belt (G), Sound (S), Kiel Bight (K), Mecklenburg Bight (M), Arkona Basin (A).	33
Fig. 3.7	Map of area with the four monitoring stations (red points). Data are provided by Bundesamt für Seeschifffahrt und Hydrographie: Ice Data Bank.	34
Fig. 3.8	Map with stations in the Fehmarnbelt: Fehmarn Belt light-vessel, Belt Project stations (station 6,528, 529 and 952) and HELCOM COMBINE monitoring stations (BMP NO1 and MO2).	35
Fig. 3.9	Map with Fehmarn Belt Feasibility Study monitoring stations.....	36
Fig. 4.1	Bathymetry and geographical structures of the Baltic Sea. Water depths refer to (Seifert et al. 2001). Water depth is cut off at 200m. Acronyms indicate some basins and connecting channels: Arkona Basin (AB), Bornholm Channel (BC), Bornholm Basin (BB), Stolpe Channel (SC, also called Slupsk Furrow), Gdansk Depression (GD), Eastern Gotland Basin (EGB), Landsort Deep (LD), Fårö Deep (FD), Karlsö Deep (KD) and Aland Deep (AD).	37
Fig. 4.2	Bathymetry and geographical structures in the Belt Sea. Acronyms indicate some basins, connecting channels, and sills: southern Kattegat (KG), Little Belt (L), Great Belt (G), Sound (S), Fehmarnbelt (F), Kiel Bight (K), Mecklenburg Bight (M), Lübeck Bight (B), Darss Sill (D), and Drogden Sill (R).....	38
Fig. 4.3	Major rivers contributing to the Baltic Sea water budget. Dark blue arrows indicate specific river runoff, light blue arrows show accumulated diffuse sources. The Göta Älv is shown for although it empties into the Kattegat. Torneälv and Kemijoki have been summed up as their mouths are located only 15 km apart. Values from (Mikulski 1970) and (Bergström & Carlsson 1994).	40
Fig. 4.4	Cross-section showing simulated longitudinal salinity distribution as monthly means from Great Belt through Fehmarnbelt and into the Baltic Proper, where the vertical line shows the position of the planned link (FEHY MOM model, version v06_r01).....	43
Fig. 4.5	Cross-section showing the longitudinal salinity distribution as monthly means from Skagerrak through Fehmarnbelt and into the Central Baltic Sea (the vertical link shows the position of the planned link). Drawn by data given in (Sparre 1984a), (Lange et al. 1991) and (Jakobsen 1991).	44
Fig. 4.6	Main tidal constituents for Hornbæk gauge.	46



Fig. 4.7	Main tidal constituents for Gedser gauge.	46
Fig. 4.8	Annual river discharge (km ³ /year) into the sub-basins of Belt Sea.	47
Fig. 4.9	Simulated water levels and current velocities in Belt Sea during strong inflow event.	48
Fig. 4.10	Simulated water levels and current velocities in Belt Sea during strong outflow event. ..	49
Fig. 4.11	Wind rose at Westermarkelsdorf.	49
Fig. 4.12	Sketch of wind-driven cross circulation in Fehmarnbelt in case of along channel wind, coastal upwelling and downwelling, surface Ekman transport and deep cross-channel compensation flow.	51
Fig. 5.1	Rose plot of daily mean wind observed in 2000-2010 at open sea station Darss Sill (see Fig. 3.4). Slices show the frequency of wind directions and colours correspond to wind speed.	55
Fig. 5.2	Rose plot of daily mean wind observed in 1947-2010 at coastal station Westermarkelsdorf on island Fehmarn (see Table 3.3). Slices show the frequency of wind directions and colours correspond to wind speed.	55
Fig. 5.3	Frequency of occurrence of daily mean air temperature in bins of 1°C, observed at Westermarkelsdorf on island Fehmarn by Deutscher Wetterdienst (DWD). The bold vertical line indicates the median mean value.	56
Fig. 5.4	Annual cycle of air temperature (°C). Coloured lines with small symbols indicate climatological monthly means at Warnemünde (green), Westermarkelsdorf (red), and Darss Sill, see Table 3.3 and Fig. 3.4 The shaded region corresponds to ±1 standard deviation. Triangles denote conditions in baseline years 2009 (upward) and 2010 (downward).	59
Fig. 5.5	Annual cycle of the daily variation of air temperature (°C) at Westermarkelsdorf. Lines with symbols show monthly minimum (blue), mean (black), and maximum values. Simple lines indicate one standard deviation from the monthly means.	60
Fig. 5.6	Daily mean air temperature observed at Westermarkelsdorf during the baseline period 2009-2010. Symbols indicate the measurements taken at Warnemünde (black and Darss Sill (blue).	60
Fig. 5.7	Annual cycle of magnitude of wind speed (m/s) in upper panel, and number of days with strong wind (daily mean > 10 m/s) in lower panel. Coloured lines with small symbols indicate climatological monthly means at Warnemünde (green), Westermarkelsdorf (red) and Darss Sill (cyan), see Table 3.3 and Fig. 3.4. Shaded regions correspond to ±1 standard deviation. Triangles denote conditions in baseline years 2009 (upward) and 2010 (downward) and star the monthly means at Nysted from June 2004 to November 2005.	61
Fig. 5.8	Daily mean wind speed observed at Westermarkelsdorf (red curve). Symbols indicate the measurements taken at Warnemünde (black) and Darss Sill (blue). The limit of 10 m/s, used for identifying strong wind events, is indicated.	62
Fig. 5.9	Rose plot of daily mean wind observed in 2009/2010 at coastal station Westermarkelsdorf on Fehmarn island (see Fig. 3.4). Slices show the frequency of wind directions and colours correspond to wind speed.	63
Fig. 5.10	Rose plot of daily wind observed in 2009/2010 at open sea station Darss Sill (see Fig. 3.4). Slices show the frequency of wind directions and colours correspond to wind speed.	63
Fig. 5.11	Annual cycle of cloudiness (0-8). Coloured lines indicate climatological monthly means at Warnemünde (green) and Westermarkelsdorf (red), see Table 3.3 and Fig. 3.4. Triangles denote conditions at Westermarkelsdorf in baseline years 2009 (upward) and 2010 (downward).	64
Fig. 5.12	Monthly mean of daily sunshine duration (hours). Coloured lines indicate climatological monthly means at Warnemünde (green) and Westermarkelsdorf (red), see. Table 3.3 and	



	Fig. 3.4. Triangles denote conditions at Westermarkelsdorf in baseline years 2009 (upward) and 2010 (downward).	64
Fig. 5.13	Daily precipitation (mm) observed at Westermarkelsdorf (red curve) and Warnemünde (black symbols) during the baseline period 2009/2010.	65
Fig. 5.14	Annual cycle of relative humidity (%). Coloured lines with small symbols indicate climatological monthly means observed at Warnemünde (green), Westermarkelsdorf (red) and Darss Sill (cyan), see Table 3.3 and Fig. 3.4. Triangles denote conditions at Westermarkelsdorf in baseline years 2009 (upward) and 2010 (downward).	66
Fig. 6.1	Measured water level (m) at Warnemünde station.	68
Fig. 6.2	Measured water level (m) at Gedser station.	68
Fig. 6.3	Measured water level (m) at Kiel-Holtenau station.	69
Fig. 6.4	Mean simulated water levels in the Belt Sea in the period 1 January 2009 to 30 September 2009.	70
Fig. 6.5	Maximal simulated water levels in the Belt Sea in the period 1 January 2009 to 30 September 2009.	70
Fig. 6.6	Simulated water level time-series close to Puttgarden and Rødbyhavn.	71
Fig. 6.7	Histogram based on simulated water levels at Puttgarden and Rødbyhavn in the period 1 January 2009 to 30 September 2009.	71
Fig. 6.8	Time-series of Hm0, Tp, T01 and MWD at MS01 (top) and MS02 (bottom).	73
Fig. 6.9	Wave roses at MS01 (top, Hm0 > 0.60) and MS02 (bottom, Hm0 > 0.80).	74
Fig. 6.10	Scatter diagrams of Hm0 vs. Tp T01 and U10 at MS01 (left, Hm0 > 0.25) and MS02 (right, Hm0 > 0.30).	75
Fig. 6.11	Exceedance diagrams of Hm0, Tp and T01 at MS01 (left, Hm0 > 0.25) and MS02 (right, Hm0 > 0.30).	76
Fig. 6.12	Example of westerly wave pattern in Fehmarnbelt. Date: 08.01.2005.	77
Fig. 6.13	Example of easterly wave pattern in Fehmarnbelt. Date: 28.12.2005.	77
Fig. 6.14	Measured mean current profile at MS02 during the baseline period. Inflow with a south-westerly current dominates below 15 m depth. Maximum current speeds are reached at the surface while bottom friction reduces current speed near the bottom.	78
Fig. 6.15	Current roses based on measured current at MS01. The roses are shown in the three levels 5.08 m, 12.58 m and 18.58 m.	79
Fig. 6.16	Current roses based on measured current at MS02. The roses are shown in the three levels 5.08 m, 15.58 m and 27.58 m.	80
Fig. 6.17	Current rose based on measured current at MS03. The roses are shown in the three levels 5.03 m, 12.53 m and 23.53 m.	81
Fig. 6.18	Hourly averages of current speed (upper panel) and direction (lower panel) at MS01 in the surface layer with mean speed (red line) and standard deviation of current speed... ..	83
Fig. 6.19	Hourly averages of current speed (upper panel) and direction (lower panel) at MS01 at intermediate depth (12.58 m) with mean speed (red line) and standard deviation of current speed.	83
Fig. 6.20	Hourly averages of current speed (upper panel) and direction (lower panel) at MS01 near the bottom with mean speed (red line) and standard deviation of current speed.	84
Fig. 6.21	Hourly averages of current speed (upper panel) and direction (lower panel) at MS02 in the surface layer with mean speed (red line) and standard deviation of current speed... ..	84
Fig. 6.22	Hourly averages of current speed (upper panel) and direction (lower panel) at MS02 at intermediate depth (15.58 m) with mean speed (red line) and standard deviation of current speed.	85
Fig. 6.23	Hourly averages of current speed (upper panel) and direction (lower panel) at MS02 near the bottom with mean speed (red line) and standard deviation of current speed.	85



Fig. 6.24	Hourly averages of current speed (upper panel) and direction (lower panel) at MS03 in the surface layer with mean speed (red line) and standard deviation of current speed. .	86
Fig. 6.25	Hourly averages of current speed (upper panel) and direction (lower panel) at MS03 at intermediate depth (12.53 m) with mean speed (red line) and standard deviation of current speed.	86
Fig. 6.26	Hourly averages of current speed (upper panel) and direction (lower panel) at MS03 near the bottom with mean speed (red line) and standard deviation of current speed.	87
Fig. 6.27	Observed current speed and direction at MS01 from 2009-12-25 to 2010-01-05 at z=5.08 m (upper panel) and z=18.58 m (lower panel) with mean speed (red lines) and standard deviation of current speed.	88
Fig. 6.28	Observed current speed profiles at MS01 from 2009-12-25 to 2010-01-05 with mean profile (red line). Positive values indicate eastward inflow, negative values indicate westward outflow.	89
Fig. 6.29	Outflow all over the water column at MS02 on 2009-10-20 at 19:30 (blue line) and daily mean (red line). Note how the daily mean does still show a slight inflow near the seabed.	90
Fig. 6.30	Outflow at surface and inflow at bed at MS02 on 2010-01-10 at 14:50 (blue line) and daily mean (red line). On this day the daily average does not differ significantly from an instantaneous profile which indicates a stable stratification.	90
Fig. 6.31	Inflow all over the water column at MS02 on 2010-01-27 at 21:50 (blue line) and daily mean (red line). The temperature stratification is more pronounced on the daily average than in the instantaneous profile. This does however not affect the density.	91
Fig. 6.32	Inflow at surface and outflow at bed at MS02 on 2009-07-20 at 20:50 (blue line) and daily mean (red line). The daily mean current speed is much lower than the instantaneous values that include highly frequent signals like tides and possibly internal waves, and it only shows inflow throughout the water column. The density stratification however remained stable on that day indicating two oscillating water masses in the respective layers.	91
Fig. 6.33	Three-layer flow case at MS02 on 2010-02-13 at 23:50 (blue line) and daily mean (red line). The instantaneous current profile shows three layers while on average there were only two layers on this particular day. This is reflected in the stable density stratification.	92
Fig. 6.34	Continuous density (salinity) gradient from surface to bed at MS02 on 2010-07-05 at 15:50 (blue line) and daily mean (red line). In contrast to the case in Fig. 6.33 there is an instantaneous three-layer flow but a constant density gradient. The daily mean current profile shows only two layers though with outflow dominating the upper layer to z = 15 m and inflow in the lower layer.	92
Fig. 6.35	Measured current and salinity close to surface and bottom at MS02 during a five days period in October 2009.	93
Fig. 6.36	Measured salinity, temperature and density (kg/m ³) at MS01 in Fehmarnbelt during the baseline monitoring.	95
Fig. 6.37	Measured salinity, temperature and density (kg/m ³) at MS02 in Fehmarnbelt during the baseline monitoring.	96
Fig. 6.38	Measured salinity, temperature and density (kg/m ³) at MS03 in Fehmarnbelt during the baseline monitoring.	97
Fig. 6.39	Temperature and salinity variation at MS02 in late August and start of September 2009.	98
Fig. 6.40	Temperature and salinity variation at MS02 in January 2010.	99
Fig. 6.41	Measured salinity profiles at MS01 during the baseline period divided into inflow or outflow conditions. Mean profile with standard deviation indicated.	100



Fig. 6.42	Measured monthly salinity at MS01 in 5 m depth during the baseline period divided into inflow or outflow conditions.....	100
Fig. 6.43	Measured monthly salinity at MS01 in 16 m depth during the baseline period divided into inflow or outflow conditions.....	101
Fig. 6.44	Measured salinity profiles at MS02 during the baseline period divided into inflow or outflow conditions. Mean profile with standard deviation indicated.	101
Fig. 6.45	Measured monthly salinity at MS02 in 5 m depth during the baseline period divided into inflow or outflow conditions.....	102
Fig. 6.46	Measured monthly salinity at MS02 in 20 m depth during the baseline period divided into inflow or outflow conditions.....	102
Fig. 6.47	Measured salinity profiles at MS03 during the baseline period divided into inflow or outflow conditions. Mean profile with standard deviation indicated.	103
Fig. 6.48	Measured monthly salinity at MS03 in 5 m depth during the baseline period divided into inflow or outflow conditions.....	103
Fig. 6.49	Measured monthly salinity at MS03 in 16 m depth during the baseline period divided into inflow or outflow conditions.....	104
Fig. 6.50	Mean surface (upper panel) and bottom (lower panel) salinity observed during the 2009-2011 baseline cruises.....	105
Fig. 6.51	Mean surface (upper panel) and bottom (lower panel) water temperature observed during the 2009-2011 baseline cruises. The warm transect across the entrance to the Bay of Lubeck was mainly sampled in summer.	106
Fig. 6.52	Sea surface temperature on 16 April 2009 in the Belt Sea and Arkona Sea as observed by the ENVISAT satellite (ESA 2010).	107
Fig. 6.53	Frequency of occurrence (in % of time) of salinity (colour), temperature and buoyancy frequency at MS02 in summer. Bold lines: averaged profile, bold dashed lines: averaged profile \pm standard deviation, simple dashed lines: all-time minimum and maximum salinity at depth level, -o- : cumulative frequency of occurrence of salinity at uppermost, central and lowest observed depth levels (temperature and salinity interval when calculating percentage is 0.2 °C or psu).....	108
Fig. 6.54	Frequency of occurrence (in % of time) of salinity (colour), temperature and buoyancy frequency MS02 in winter. Bold lines: averaged profile, bold dashed lines: averaged profile \pm standard deviation, simple dashed lines: all-time minimum and maximum salinity at depth level, -o- : cumulative frequency of occurrence of salinity at uppermost, central and lowest observed depth levels (temperature and salinity interval when calculating percentage is 0.2 °C or psu).....	109
Fig. 6.55	Frequency of occurrence (colour) of salinity at MS02 (left) and MS03 (right) in the baseline period. Bold lines: averaged profile, bold dashed lines: averaged profile \pm standard deviation, simple dashed lines: all-time minimum and maximum salinity at depth level (temperature and salinity interval when calculating percentage is 0.2 °C or psu).....	110
Fig. 6.56	T-S diagram based on measurements collected at MS02 and MS03. Black lines represent the oceanographic water density, $\sigma = \rho - 1000 \text{ kg/m}^3$	111
Fig. 6.57	Bottom oxygen and salinity at station MS03 observed during the 2009-2011 baseline period. The four quadrants denote the frequency of occurrence for water masses within the given salt/oxygen limits.	111
Fig. 6.58	Bottom oxygen (blue) and salinity (red) at station MS03 observed during the 2009-2011 baseline period. Note the opposed direction of scales for salinity and oxygen.	112
Fig. 6.59	Bottom salinity and oxygen concentration observed in August 2009 during the monitoring surveys from 2009-08-24 to 2009-08.	113
Fig. 6.60	Bottom salinity and oxygen concentration observed in October 2010 during the monitoring surveys from 2010-10-12 to 2010-10-13.	114



Fig. 6.61	Observed ice at Rødbyhavn (SOK 2010).....	115
Fig. 7.1	Map of simulated current and salinity in 5m depth on the 14 October 2004 at 15:00 UTC.	116
Fig. 7.2	Map of simulated current and salinity in 5m depth on the 18 October 2004 at 15:00 UTC.	117
Fig. 7.3	Map of simulated current and salinity in 5m depth on the 9 January 2005 at 00:00 UTC.	117
Fig. 7.4	Measured surface salinity and current in the Fehmarnbelt area during monitoring survey from 30 November 2009 to 6 December 2009 (top panel), while outflow took place. Measured bottom salinity and current in the Fehmarnbelt area during monitoring survey from 27 October 2009 to 3 November 2009 (bottom panel), while pulsating inflow took place.....	119
Fig. 7.5	Along-channel current velocity in the link corridor during the survey in August 2009. The current pattern changed rapidly. The data were collected within a week: a) 24 August 2009; b) 27 August 2009; c) 28 August 2009; and d) 31 August 2009. The 119° is clockwise from north: inflow is positive and outflow is negative.....	121
Fig. 7.6	Cross channel current velocity (top), temperature (middle) and salinity (lower panel) along a transect through a mesoscale eddy in the link corridor on 17 June 2009 05:00 UTC. An eddy is clearly indicating by the velocity distribution around the doming of temperature and salinity stratification.	122
Fig. 7.7	Map of high resolution survey at the Fehmarnbelt Link. Red lines indicate the combined ScanFish T-CTD)/T-ADCP/VM-ADCP transects and green lines the combined MSS/VM-ADCP transects. The black crosses depict the mooring positions.	123
Fig. 7.8	Jet-like eastward flow in the narrow section west of the Fehmarnbelt, see Fig. 7.7, westernmost green line (18 June 2009 09:00 UTC).	123
Fig. 7.9	Time-series of wind in the Fehmarnbelt during January 2010.	123
Fig. 7.10	Cross channel flow with a northward surface current and a southward directed compensation flow in mid water layer. Date: 11 January 2010.	124
Fig. 7.11	The along channel current shows a situation with strong inflow at the southern flank. Date: 11 January 2010.	124
Fig. 7.12	The salinity (top) and temperature (bottom) pattern refers to upwelling in the south and downwelling in the north of the Fehmarnbelt channel. Date: 11 January 2010.	125
Fig. 7.13	Simulated parameters: a) salinity and b) temperature; in the Puttgarden-Rødbyhavn cross-section during an inflow event. Date: 11 July 2009.	126
Fig. 7.14	Mean current direction (relative to north) within the 10 m surface layer across Fehmarnbelt along the alignment as observed with ship mounted ADCP (monthly cruises) and at the main stations MS01 and MS02. The red lines depict current directions simulated with the local MIKE model. The upper panel refers to inflow in south-easterly direction and the lower panel to north-western outflow.	127
Fig. 7.15	Mean current speed (m/s) within the 10 m surface layer across Fehmarnbelt along the alignment as observed with ship mounted ADCP (monthly cruises) and at the main stations MS01 and MS02. The red lines depict current speeds simulated with the local MIKE model. The upper panel refers to inflow and the lower panel to outflow.....	128
Fig. 7.16	Correlation over local water depth between water level difference Hornbæk-Gedser and velocity in main direction on a 10 minutes time scale.....	129
Fig. 7.17	Correlation over water depth between water level difference Hornbæk-Gedser and velocity in main direction on a 1 hour time scale.	130
Fig. 7.18	Correlation over water depth between water level difference Hornbæk-Gedser and velocity in main direction on a 1 day time scale.	130



Fig. 7.19	Simulated discharge through the Fehmarnbelt during the period Distribution of salinity classes in Fehmarnbelt water volume exchange (net exchange volumes for each salt class), long-term simulation. MIKE local model, run 9.15. Positive values indicate outflow from the Baltic Sea.	131
Fig. 7.20	Distribution of salinity classes in Fehmarnbelt water volume exchange (net exchange volumes for each salt class), long-term simulation. MIKE regional model, run 6.24. Positive values indicate outflow from the Baltic Sea.	132
Fig. 8.1	Measured water level (m) at Warnemünde station.	134
Fig. 8.2	Measured water level (m) at Gedser station.	134
Fig. 8.3	Measured water level (m) at Kiel-Holtenau station.	134
Fig. 8.4	Storm surge in the Baltic Sea on the 13 November 1872 at 14:00 (Colding 1881).	135
Fig. 8.5	High water statistics for Rødbyhavn based on extreme events. Threshold level is 1.5m. The water levels are relative to the present mean sea level.	136
Fig. 8.6	Wave rose based on wave height and wind direction at Fehmarn Belt light-vessel during the period 1970 to 1984. From Fehmarn Belt Feasibility Study (1996).	136
Fig. 8.7	Maximal wave height (dm) in the greater Fehmarnbelt area at 10 Bft (24 m/s to 28 m/s) west wind (Schmager 1979).	137
Fig. 8.8	Current rose based on surface observations collected at Fehmarn Belt light-vessel in the period 1970 to 1984 (extracted from Fehmarn Belt Feasibility Study 1996 or (Jakobsen et al. 1996).	138
Fig. 8.9	Current roses from the station Fehmarn Belt South for the depths 5 m and 20 m respectively (Fehmarn Belt Feasibility Study 1998).	141
Fig. 8.10	Current roses from the station Fehmarn Belt North for the depths 5 m and 12 m respectively (Fehmarn Belt Feasibility Study 1998).	142
Fig. 8.11	Comparison of the current speed in the main direction 5 m below surface at Fehmarn Belt South versus at Darss Sill: A) instantaneous values; and B) 25 hour moving average values (Fehmarn Belt Feasibility Study 1998).	143
Fig. 8.12	The yearly salinity variation at Fehmarn Belt light-vessel redrawn after Lange et al. (1991).	144
Fig. 8.13	Measured salinity and temperature variation at the Fehmarnbelt light-vessel from 1965 to 1984. Note the cyclic nature of bottom salinity with infrequent inflows of saline North Sea water.	144
Fig. 8.14	Measured salinity at Fehmarnbelt light-vessel in 0 m and 28 m depth during the period 1965-1985. Note the cut-off in salinity below 10 psu after 1970 in the basic data.	145
Fig. 8.15	Measured temperature at Fehmarnbelt light-vessel in 0 m and 28 m depth during the period 1965-1985.	146
Fig. 8.16	Measured salinity in 0 m and 25 m depth at HELCOM station BMP M02 in Mecklenburg Bight during 1960-2010.	147
Fig. 8.17	Measured temperature in 0 m and 25 m depth at HELCOM station BMP M02 in Mecklenburg Bight during 1968-2010.	148
Fig. 8.18	Climatological monthly means of bottom salinity (z = 28 m) at Fehmarnbelt light-vessel and wind speed at Westermarkelsdorf/Fehmarn.	149
Fig. 8.19	Time-series of frost index for Baltic transition area (data are extracted from SOK 2010).	150
Fig. 8.20	Average number of days with ice per ice winter. Based on 14 ice-winters. From (Statens Istjeneste 1954-1955).	151
Fig. 8.21	Development of ice sheet thickness in Danish waters during the 1940/41 winter season (redrawn from SII 1942).	152
Fig. 8.22	Sheet ice thickness as function of frost index. Data are from German stations.	154



Fig. 8.23	Reduced ice sum: the arithmetic mean of days with ice recorded at 13 stations along the German Baltic Sea coast from 1897 to 2010, from (BSH 2010).	155
Fig. 8.24	Accumulated areal ice volume for the German Baltic Sea coastline. (BSH 2010).	155
Fig. 8.25	Number of ice days (upper panel), accumulated ice volume (central panel) and maximum sheet thickness (lower panel) as observed at the Fehmarnbelt light-vessel 1941-1982.	157
Fig. 8.26	Number of ice days (upper panel), accumulated ice volume (central panel) and maximum sheet thickness (lower panel) as observed off Westermarkelsdorf 1940-2010/2011.	157
Fig. 8.27	Number of ice days (upper panel), accumulated ice volume (central panel) and maximum sheet thickness (lower panel) as observed off Marienleuchte 1940-2010/2011.	158
Fig. 8.28	Long-term median ice sheet thickness as observed in Fehmarnbelt (cf. Table 8.4).	158
Fig. 9.1	Simulated monthly mean wind speed at position MS02 (compilation of SN-REMO and STORM data).	160
Fig. 9.2	Simulated monthly mean air temperature at position MS02 (compilation of SN-REMO and STORM data).	160
Fig. 9.3	Simulated monthly mean current speed at position MS02 in 5 m depth.	162
Fig. 9.4	Simulated monthly mean current speed at position MS02 in 23 m depth.	162
Fig. 9.5	Simulated monthly current direction frequency at position MS02 in 5 m depth.	163
Fig. 9.6	Simulated monthly current direction frequency at position MS02 in 23 m depth.	163
Fig. 9.7	Monthly means of salinity at MS01 (left hand row) and MS02 (right hand row) at surface (upper panels) and bottom (lower panels) layers compared to corresponding 6-years means at surface and long-term at bottom at Fehmarnbelt light-vessel. Black range bars indicate monthly all-time minima and maxima.	164
Fig. 9.8	Monthly means of water temperature at MS01 (left hand row) and MS02 (right hand row) at surface (upper panels) and bottom (lower panels) layers compared to corresponding 6-year means from Fehmarnbelt light-vessel. Black range bars indicate monthly all-time minima and maxima.	165
Fig. 9.9	T-S diagrams based on measurements collected at MS01 and MS02 compared to long-term measurements from Fehmarnbelt light-vessel. MS01 in particular shows a concentration of low saline water. MS02 displays two extremes in temperature along the upper and lower edges of the reference cloud. Black lines represent the oceanographic water density, $\sigma = \rho - 1000 \text{ kg/m}^3$. It is noted that the lack of high salinities at MS01 is caused by that the dense inflow follows the southern bed slope in the Fehmarnbelt and hence do not impact MS01.	166
Fig. 9.10	T-S diagram based on measurements collected at MS03 compared to long-term measurements from BMP M02 (blue). The baseline observations fit well into the multitude of long-term salinity and temperature records, the spring months of 2010 are missing though in the MS03 samples. Black lines represent the oceanographic water density, $\sigma = \rho - 1000 \text{ kg/m}^3$	167
Fig. 9.11	Simulated monthly mean salinity at position MS02 in 5 m depth.	168
Fig. 9.12	Simulated monthly mean salinity at position MS02 in 23 m depth.	168
Fig. 9.13	Simulated monthly mean temperature at position MS02 in 5 m depth.	169
Fig. 9.14	Simulated monthly mean temperature at position MS02 in 23 m depth.	169
Fig. 10.1	Number of laden tankers entering and leaving the Baltic Sea via the Great Belt. Figure redrawn with data from HELCOM (2009).	172
Fig. 10.2	Amount of oil transported to and from the Baltic Sea via the Great Belt (million tonnes). Figure based on data from HELCOM (2009).	172
Fig. 11.1	Importance map for subfactor seawater hydrography.	176

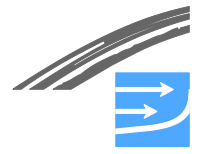


List of tables

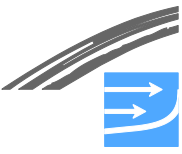
Table 3.1	Positions of the Main Stations.....	26
Table 3.2	List of instruments used in the FEHY baseline monitoring.....	29
Table 3.3	List of meteorological stations for which data of air pressure (P), air temperature (T), wind (W), cloudiness (C), relative humidity(R) and precipitation (N) were available. Frequency denotes basic time resolution.	31
Table 3.4	Positions of the gauge stations	32
Table 4.1	The ten largest rivers of the Baltic Sea system, including the Belt Sea, Sound and Kattegat, their approximate drainage area and mean annual runoff 1950-1999 (Bergström & Carlsson 1994).....	40
Table 4.2	Mean annual river discharges into Belt Sea and its sub-basins in 1999-2009 according to FEHY river data set. The local importance of river inputs is characterized by relation to the sea surface, yielding a hypothetical rise of the sea level (cm/year).	47
Table 5.1	Basic statistics of mean daily/hourly wind speed observed at meteorological stations, see Table 3.3 and Fig. 3.4. The second column specifies the overall mean value, the standard deviation and the absolute minimum and maximum values. The percentiles in the third column characterize rare events (below 1% or 99% probability, the 90% data range (between 5-95%), and the median of data (50%).	53
Table 5.2	Basic statistics of maximum daily wind speed observed at meteorological stations, see Table 3.3 and Fig. 3.4	54
Table 5.3	Basic statistics of mean daily/hourly air temperature observed at meteorological stations, see Table 3.3 and Fig. 3.4. The second column specifies the overall mean value, the standard deviation and the absolute minimum and maximum values. The percentiles in the third column characterize rare events (below 1% or 99% probability, the 90% data range (between 5-95%), and the median of data (50%).	56
Table 5.4	Daily range of air temperature, i. e. difference between daily minimum and maximum values, observed at meteorological stations, see Table 3.3 and Fig. 3.4.....	57
Table 5.5	Basic statistics of mean daily air pressure observed at meteorological stations, see Table 3.3 and Fig. 3.4. The average percentiles for probability levels 1, 5, 50, 95, 99% are 987, 996, 1014, 1029, 1036 hPa.	57
Table 5.6	Basic statistics of mean daily relative humidity observed at meteorological stations, see Table 3.3 and Fig. 3.4. The average percentiles for probability levels 1, 5, 50, 95, 99% are 60, 68, 85, 97, 99 % of relative humidity.....	58
Table 5.7	Basic statistics of mean daily cloudiness observed at meteorological stations, see Table 3.3 and Fig. 3.4. The average percentiles at 1, 5, 50, 95, 99% are 0, 1, 5.5, 8, 8 indicating 5% of probability for very bright and 5% for overcast cloud cover.....	58
Table 5.8	Basic statistics of mean daily precipitation observed at meteorological stations, see Table 3.3 and Fig. 3.4. The second column specifies the overall mean value, the standard deviation and the absolute minimum and maximum values. The percentiles in the third column characterize rare events(below 1% or 99% probability, the 90% data range (between 5-95%), and the median of data (50%).	58
Table 5.9	Monthly weather conditions observed at Westermønselv by Deutscher Wetterdienst (DWD) during baseline period 2009-2010. Besides wind events above 10 m/s only deviations from long-term averages are noted.	67
Table 6.1	Statistical parameters for simulated water levels at Puttgarden and Rødbyhavn in the period 1 January 2009 to 30 September 2009.	69
Table 8.1	Wave observations at Fehmarn Belt light-vessel during the period 1970 to 1984 divided into different wave classes.	137
Table 8.2	Surface velocity scatter diagram at station 6 in Fehmarnbelt (Lange et al. 1991).....	139
Table 8.3	Near-bottom velocity scatter diagram at station 6 in Fehmarnbelt (Lange et al. 1991).	139



Table 8.4	Sea ice conditions in the Fehmarnbelt during ice-winters. Locations are shown in Fig. 3.7.	153
Table 8.5	Statistical parameters for sea ice off Westermarkelsdorf on the north-western Fehmarn island. The ice winter 2009/10 is compared to long-term observations from 1961-2000. While sea ice in the Fehmarnbelt in 2009/10 started to form in mid- January which is the normal period, ice occurrence lasted only until 18 February, which is a rather short period. Ice was spotted only on 11 days during the whole season, which is less than half the long-term mean period. Data from (BSH 2010).	156
Table 8.6	Statistical parameters for sea ice off Marienleuchte on the south-eastern shore of Fehmarn island. The ice winter 2009/10 is compared to long-term observations from 1961-2000. While sea ice in the Fehmarnbelt in 2009/10 started to form in mid- January which is the normal period, ice occurrence lasted only until 18 February, which is a rather short period. Ice was spotted only on 11 days during the whole season, which is less than half the long-term mean period. Data from (BSH 2010).	156
Table 9.1	Statistical parameters for water level measurements The parameters are mean, standard deviation, minimum and maximum.	161
Table 9.2	Current statistics at Fehmarnbelt light-vessel (FB) 1982-86 compared to baseline measurements at MS01 March 2009 – February 2011. Both statistics are derived from hourly values. Fehmarnbelt light-vessel values are from Middelstaedt et al. 2008. Note the big difference for the deeper levels.	161
Table 9.3	Current statistics at Fehmarnbelt light-vessel (FB) 1982-86 compared to baseline measurements at MS02 March 2009 to February 2011. Both statistics are derived from hourly values. Fehmarnbelt light-vessel values are from Middelstaedt et al. 2008.	161
Table 9.4	Statistical parameters for sea ice off Marienleuchte on the south-eastern shore of Fehmarn island. The ice winter 2009-2010 is compared to long-term observations from 1961-2000. Data from (BSH 2010).	170
Table 11.1	Importance categories for subfactor seawater hydrography.	175



A P P E N D I C E S



A P P E N D I X A

ADCP transects across Fehmarnbelt during baseline years



ADCP transects across Fehmarnbelt during baseline years 2009-2010

This appendix provides an overview of the current distributions measured by Acoustic Doppler Current Profilers (ADCP) across Fehmarnbelt during the baseline monitoring surveys. The observations are listed chronologically. The figures depict the along-channel current component in the main inflow direction (119° clockwise from North). Colours from blue to red indicate current speeds from -1 to +1 m/s. Colour bars show only the actual data range within a plot. Inflow is positive and yellow-red, while outflow is shown in blue colours. If available, isopycnals derived from temperature and salinity measurements are shown (density-1000 kg/m³).

Processed data are currently available from June 2009 till February 2010. These measurements comprise 39 snapshots taken on 24 days within 8 campaigns. A list of tracks is presented in Table A.1. As a first step for a more detailed analysis, the table classifies current patterns roughly into horizontal and vertical distribution of inflow and outflow. In the typical case of an estuarine circulation, bottom inflow is overlaid by surface outflow, see O/I column in the table (first letter is for upper layer and second letter for lower and I=inflow and O=outflow). The reverse case is indicated by I/O. Due to the Coriolis force, inflow runs along the southern rim of Fehmarnbelt and outflow along the northern rim, expressed by IO, or OI for the reverse case. The main signals are also classified by suffixes H for horizontal and V for vertical current distribution. To characterize the wind forcing, the daily mean and maximum wind speed and wind direction observed at Westermarkelsdorf (Fehmarn) have been added.

The horizontal structure of the current patterns in June 2009 indicates a cyclonic eddy passing through Fehmarnbelt. Towards the end of this survey a complete outflow was established.

Measurements taken between July and September show some exceptional current patterns.

For example on 28 July 2009 a weak inflow on both sides of the channel is separated by a weak outflow core in the central channel which reaches down to the northern slope.

Another remarkable observation was taken on 31 August 2009, where a strong inflow (ca. 0.7 m/s) took place on the northern rim while an outflow of 0.5 m/s ran along the southern side of the Fehmarnbelt.

The lines taken during autumn and winter correspond to the estuarine circulation with outflow in the surface layer and inflow at the bottom, where different distribution of current cores may occur.

The distributions shown are measured by either:

- ADCP: measured by ship mounted ADCP; and
- TADCP: measured by ADCP mounted on towed catamaran. It resolves the flow closer to the surface but is also slightly influenced by the wave movement of the catamaran.



Table A.1 List of ADCP transects across Fehmarnbelt taken during baseline monitoring surveys.

figure	acronym	date	begin	end	pattern		daily wind at Westermärkelsdorf			
					horizontal	vertical	main signal	maximum	mean	direction
A.1	Juni_2009_ADCP_01	16.06.2009	12:35	13:48	OI*O	I*/O	I	14.3	9.4	W
A.2	Juni_2009_ADCP_02	17.06.2009	04:26	05:50	I*OI		IO_H			
A.3	Juni_2009_ADCP_03	17.06.2009	05:52	07:10	IOI		IO_H			
A.4	Juni_2009_ADCP_04	17.06.2009	07:17	08:49	I*OI		IO_H			
A.5	Juni_2009_ADCP_05	17.06.2009	08:54	10:19	I*OI		IO_H			
A.6	Juni_2009_ADCP_06	17.06.2009	10:20	11:47	IOI		IO_H			
A.7	Juni_2009_ADCP_07	17.06.2009	11:50	13:15	IO		IO_H			
A.8	Juni_2009_ADCP_08	17.06.2009	13:20	14:40	IOI		IO_H			
A.9	Juni_2009_ADCP_09	17.06.2009	14:44	16:04	OIO		IO_H			
A.10	Juni_2009_ADCP_10	17.06.2009	16:08	17:38	OIO	O/I	O			
A.11	Juni_2009_ADCP_11	17.06.2009	19:01	22:16	O*	O	O			
A.12	Juni_2009_ADCP_12	17.06.2009	23:17	01:24	O	O/I	O			
A.13	Juni_2009_ADCP_13	18.06.2009	01:30	04:49	O*	O/I	O			
A.14	Juni_2009_ADCP_14	18.06.2009	04:50	07:25	IO	I/O/I	O			
A.15	Juli-August_2009_1	25.07.2009	05:51	07:36	OI		I			
A.16	Juli-August_2009_2	28.07.2009	12:47	14:23	IOI	I/O	IO_HV			
A.17	Juli-August_2009_3	01.08.2009	03:55	05:18	I	I*/I	I			
A.18	Juli-August_2009_4 (d)	01.08.2009	05:20	18:43	OIO	O/I	O/V			
A.19	August-September_2009_1	24.08.2009	11:04	12:47	O	O*/O	O			
A.20	August-September_2009_2	27.08.2009	10:59	12:36	IO	O/I	O/V			
A.21	August-September_2009_3	28.08.2009	14:04	15:43	IOI	I/O/I	OI_HV			
A.22	August-September_2009_4 (d)	31.08.2009	15:14	19:11	O*I*	O*/I	OI_H			
A.23	September-Oktober_2009_1 (d)	28.09.2009	15:50	19:12	OI*	I*/O	I			
A.24	September-Oktober_2009_2	28.09.2009	13:50	15:20	OI*	I*/O	I			
A.25	September-Oktober_2009_3	30.09.2009	05:19	06:59	OIO	I/O	IO_V			
A.26	Oktober-November_2009_1 (d)	27.10.2009	15:34	19:13	OI*	O/I*	O/V			
A.27	Oktober-November_2009_2	30.10.2009	01:25	02:52		O/I*	O/V			
A.28	Oktober-November_2009_3	01.11.2009	03:50	07:14		O*/I	O/V			
A.29	November-Dezember_2009_1 (d)	30.11.2009	12:30	19:05	IO	O/I	O/V			
A.30	November-Dezember_2009_2	30.11.2009	19:16	21:06	IOI	O/I	O/V			
A.31	November-Dezember_2009_3	02.12.2009	05:12	06:42		O/I	O/V			
A.32	November-Dezember_2009_4	05.12.2009	17:10	18:52	IO*	O*/I	O/V			
A.33	Januar_2010_1 (d)	11.01.2010	20:58	00:28	I*O	O/I*	O/V			
A.34	Januar_2010_2	13.01.2010	04:49	06:55		O/I	O/V			
A.35	Januar_2010_3	16.01.2010	10:13	12:31	IO*	O*/I	O/V			
A.36	Februar_2010_1 (d)	16.02.2010	14:09	19:47	IO	O/I	O/V			
A.37	Februar_2010_2	16.02.2010	12:02	13:52	IO	O/I	O/V			
A.38	Februar_2010_3	18.02.2010	00:25	02:37		O*/I	O/V			
A.39	Februar_2010_4	19.02.2010	21:39	22:57	IO	O/I	O/V			

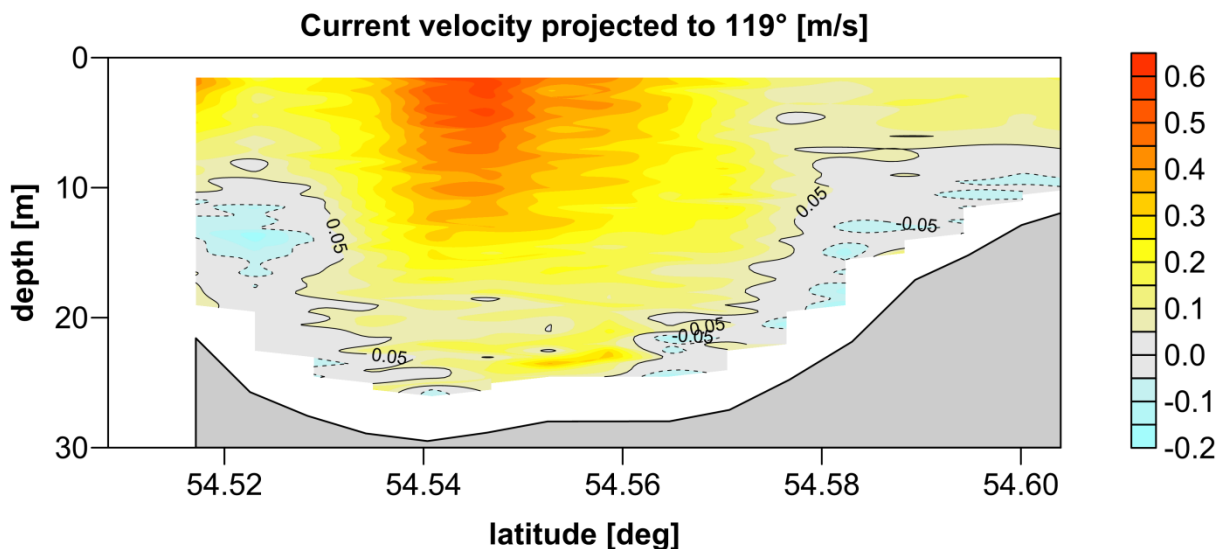


Fig. A.1.b Juni_2009_TADCP_01 16.06.2009 12:35 UTC - 16.06.2009 13:48 UTC.

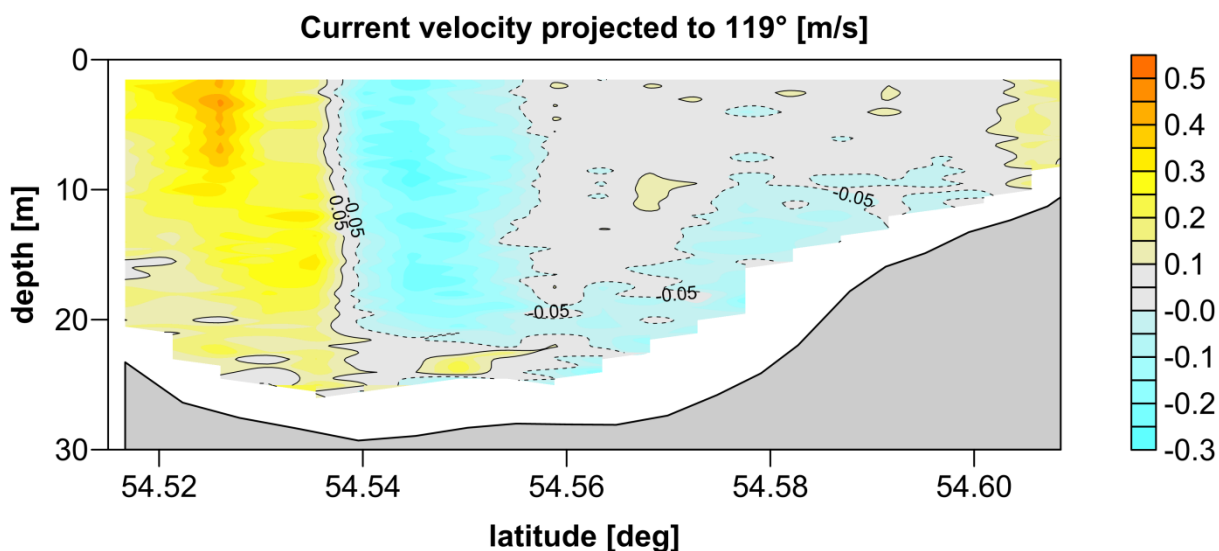


Fig. A.2.b Juni_2009_TADCP_02 17.06.2009 04:26 UTC - 17.06.2009 05:50 UTC.

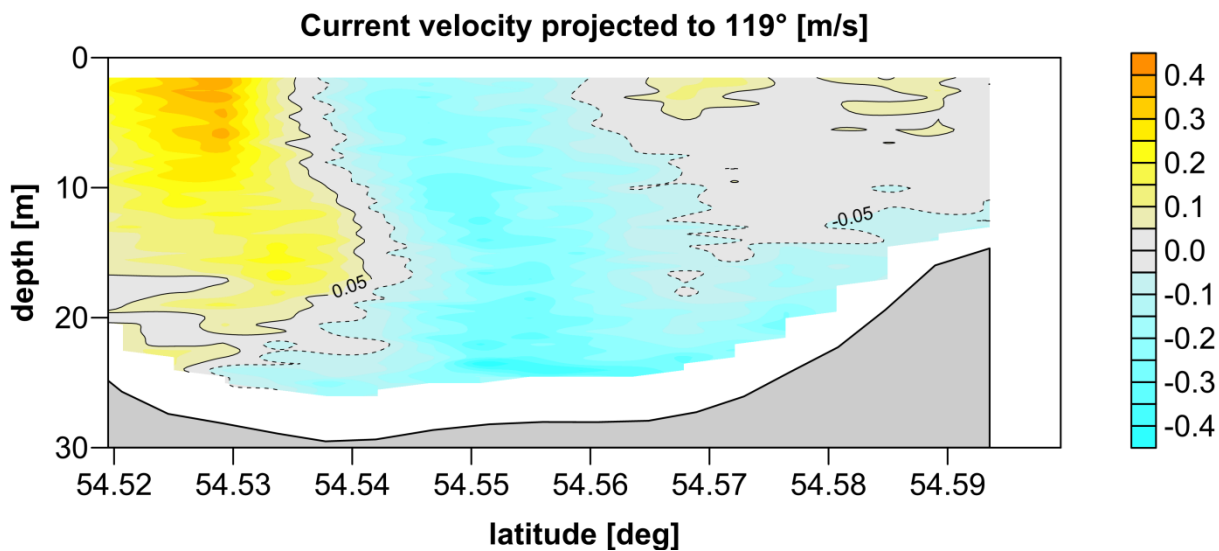




Fig. A.3.b Juni_2009_TADCP_03

17.06.2009 05:52 UTC - 17.06.2009 07:10 UTC.

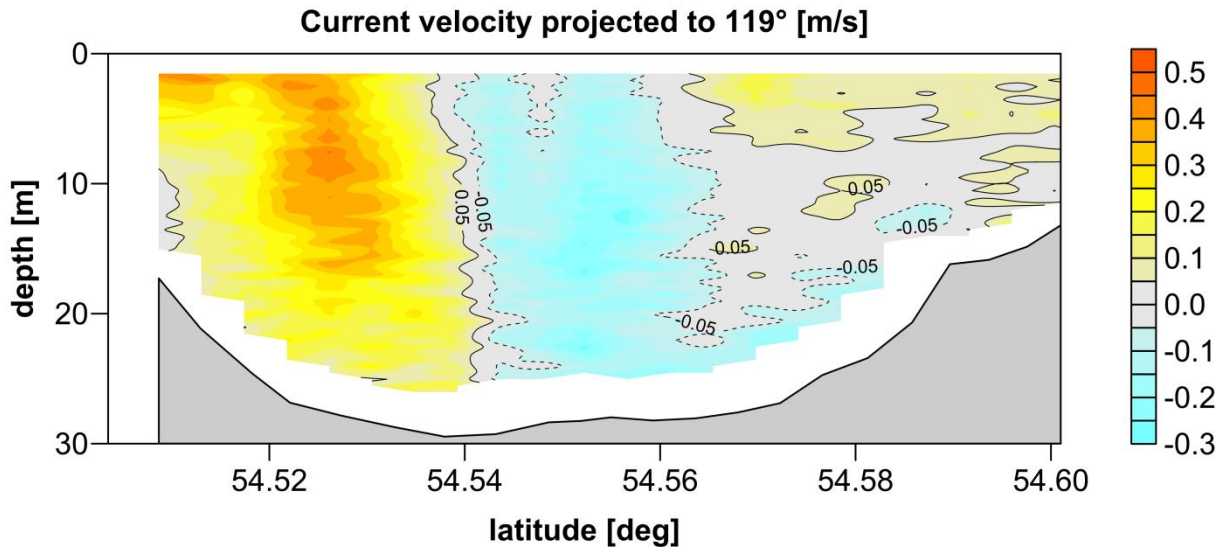


Fig. A.4.b Juni_2009_TADCP_04

17.06.2009 07:17 UTC - 17.06.2009 08:49 UTC.

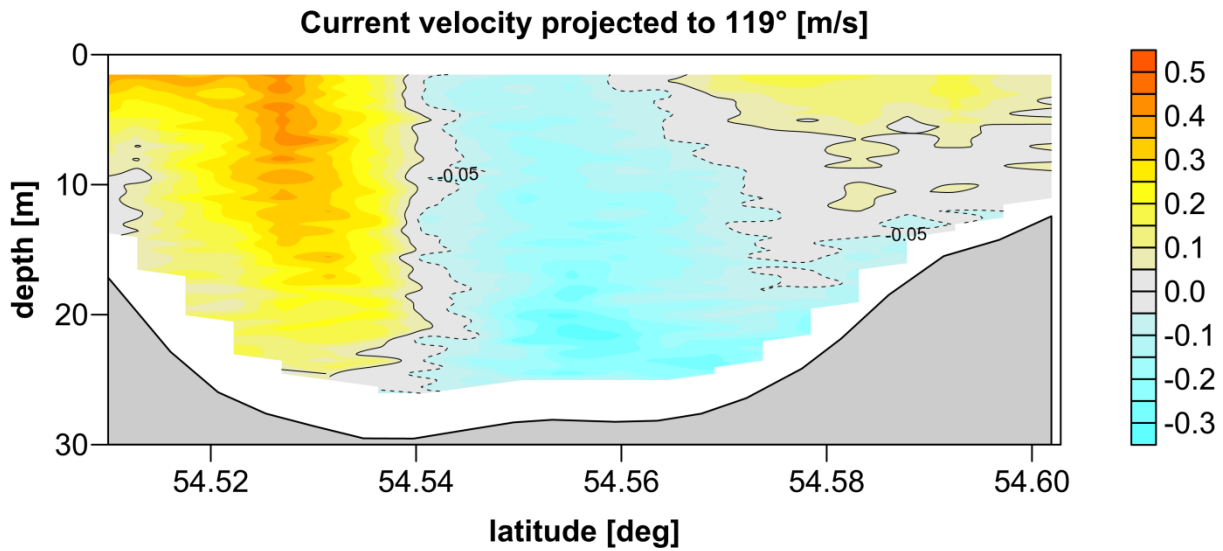


Fig. A.5.b Juni_2009_TADCP_05

17.06.2009 08:54 UTC - 17.06.2009 10:19 UTC.

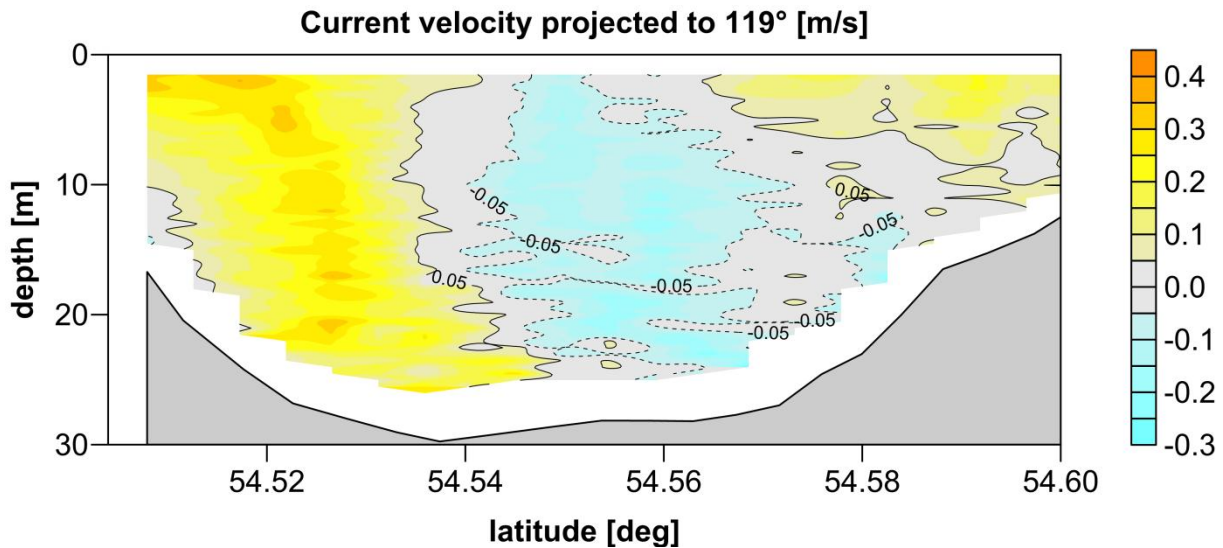




Fig. A.6.b Juni_2009_TADCP_06

17.06.2009 10:20 UTC - 17.06.2009 11:47 UTC.

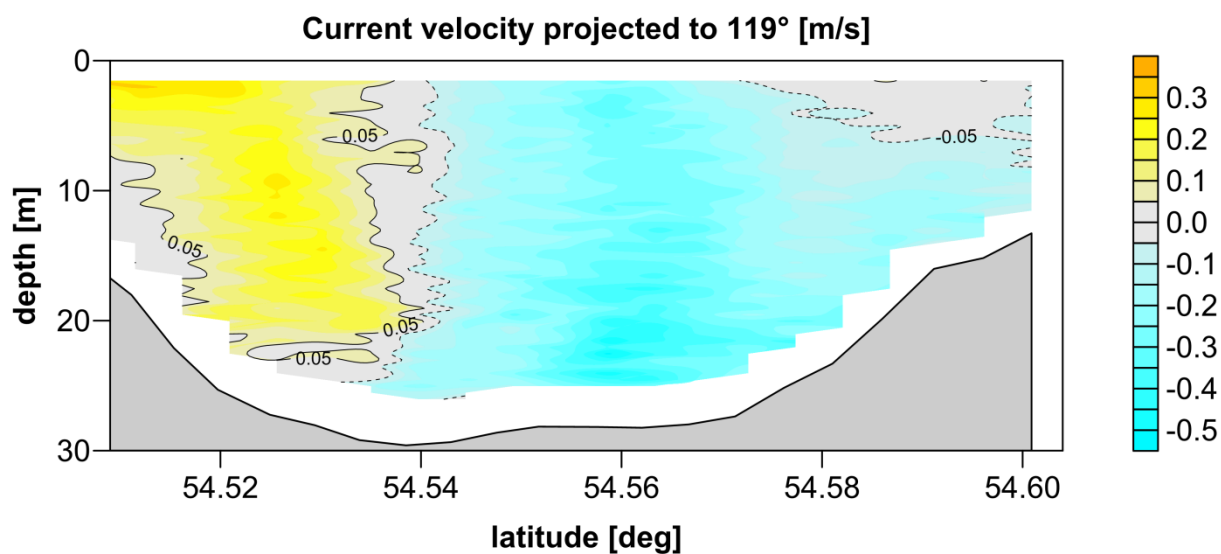


Fig. A.7.b Juni_2009_TADCP_07

17.06.2009 11:50 UTC - 17.06.2009 13:15 UTC.

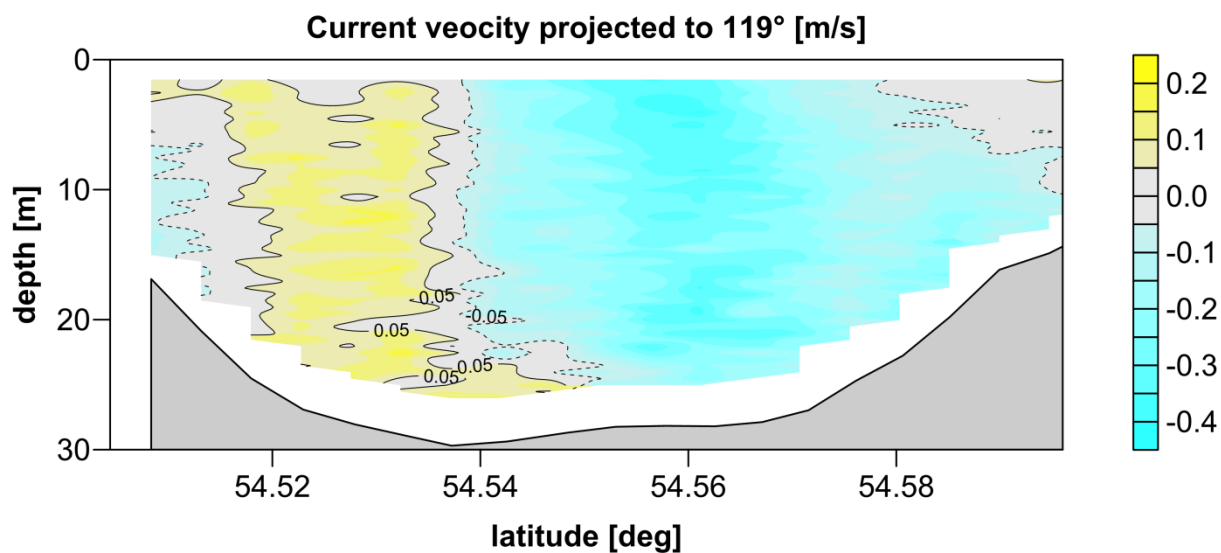


Fig. A.8.b Juni_2009_TADCP_08

17.06.2009 13:20 UTC - 17.06.2009 14:40 UTC.

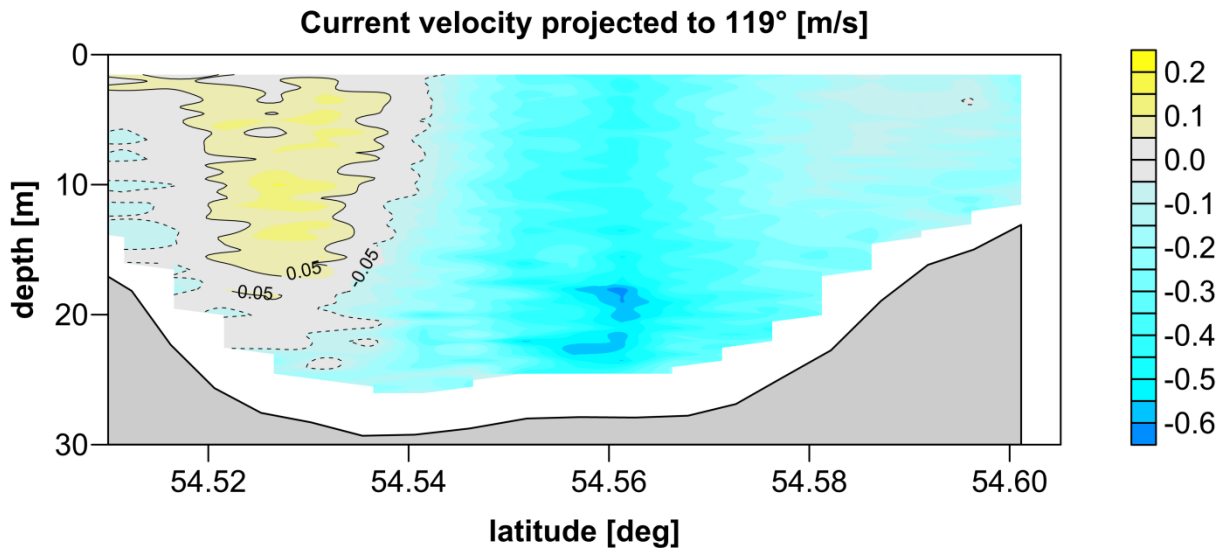


Fig. A.9.b Juni_2009_TADCP_09 17.06.2009 14:44 UTC - 17.06.2009 16:04 UTC.

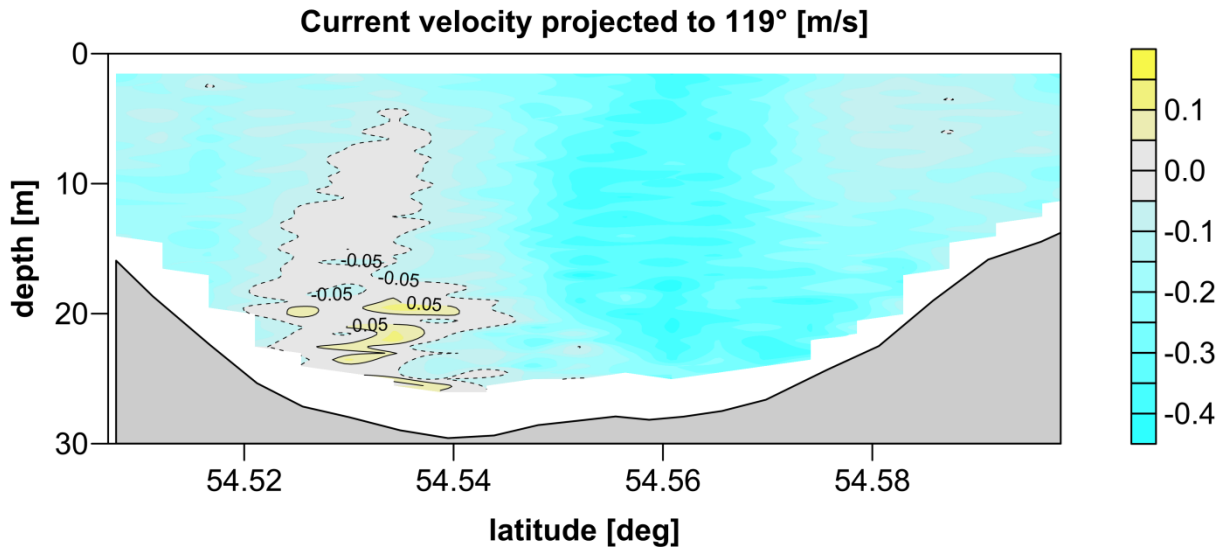


Fig. A.10.b Juni_2009_TADCP_10 17.06.2009 16:08 UTC - 17.06.2009 17:38 UTC.

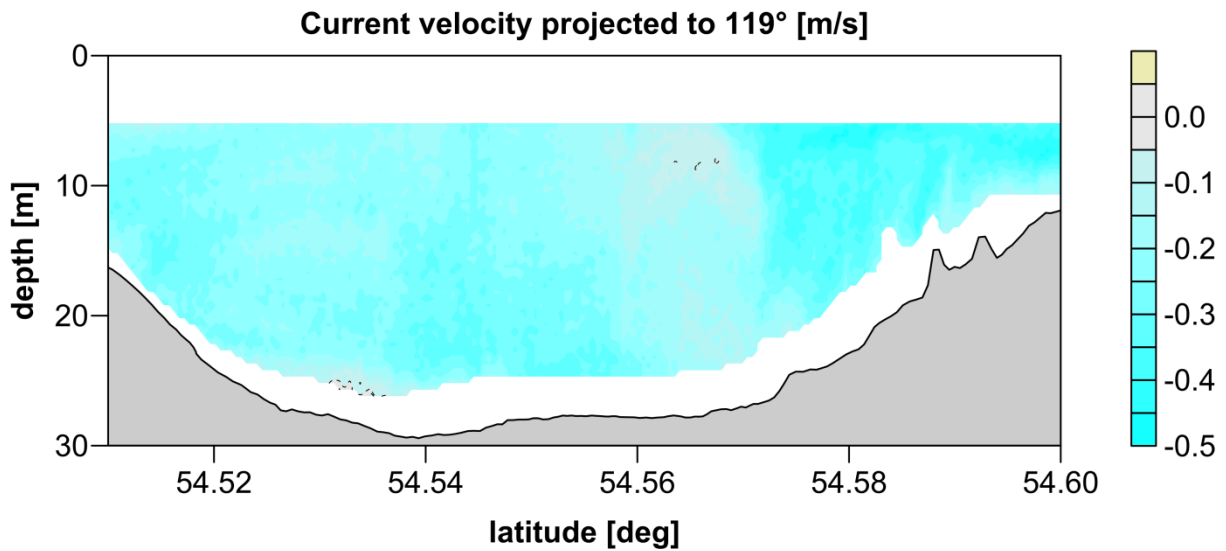


Fig. A.11 Juni_2009_ADCP_11 17.06.2009 19:01 UTC - 17.06.2009 22:16 UTC.

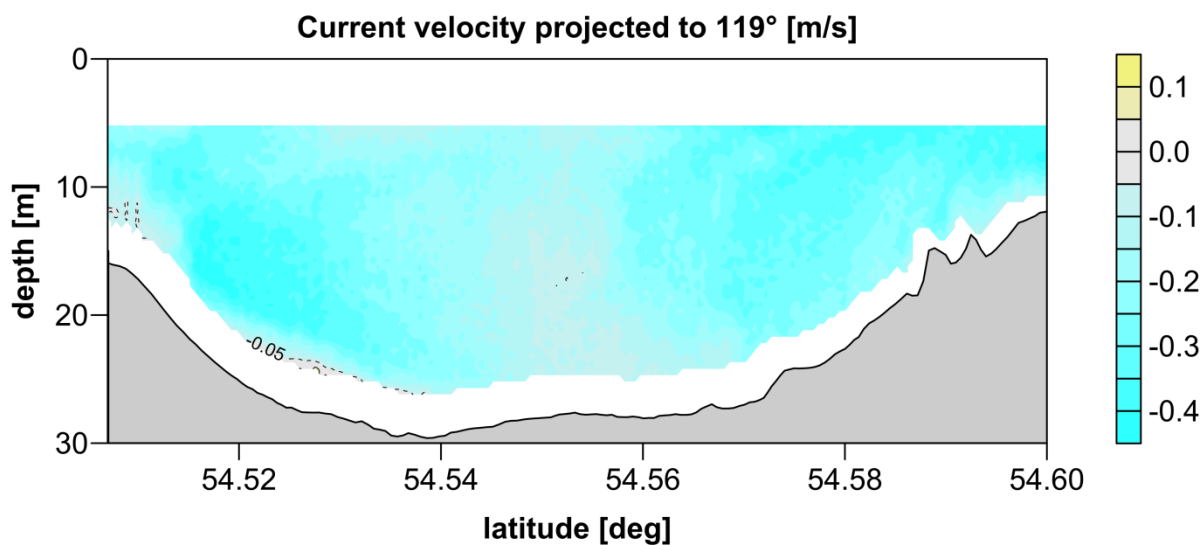


Fig. A.12 Juni_2009_ADCP_12 17.06.2009 23:17 UTC - 17.06.2009 01:24 UTC.

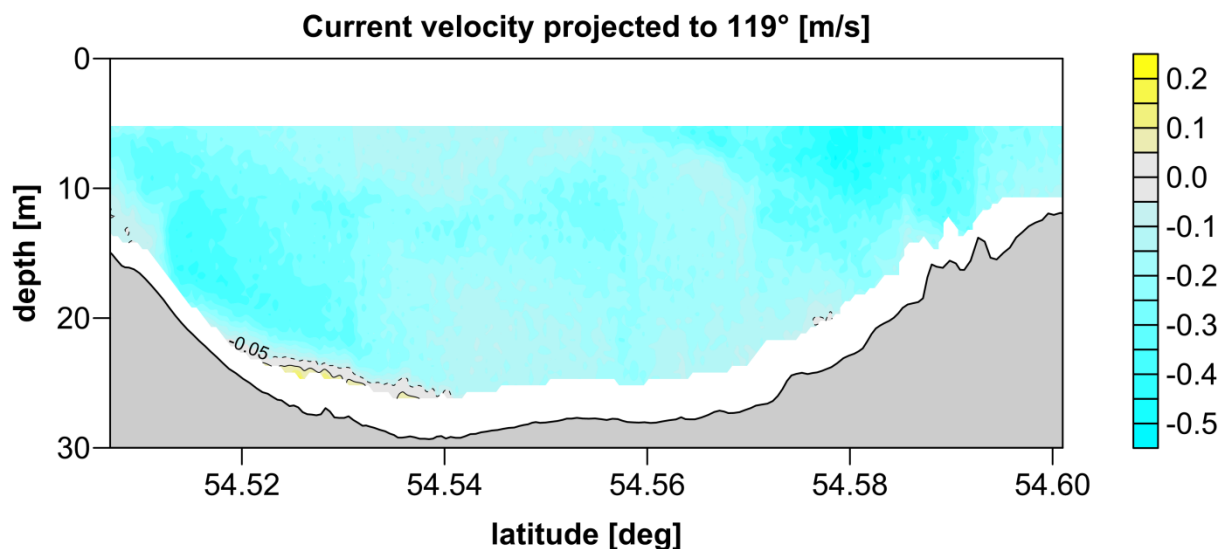


Fig. A.13 Juni_2009_ADCP_13 18.06.2009 01:30 UTC - 18.06.2009 04:49 UTC.

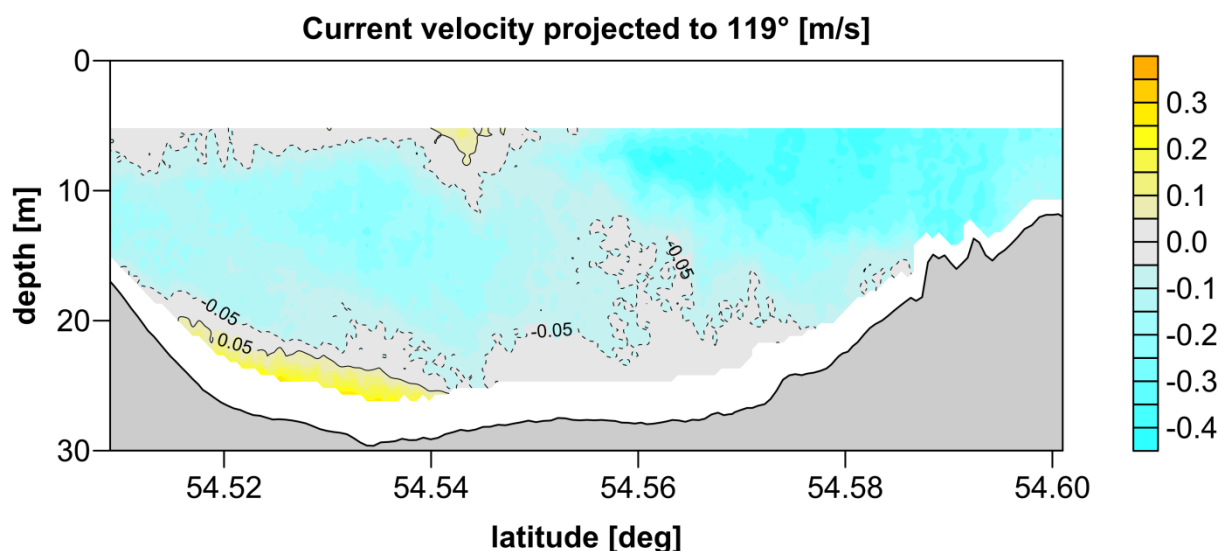


Fig. A.14 Juni_2009_ADCP_14 18.06.2009 04:50 UTC - 18.06.2009 07:25 UTC.

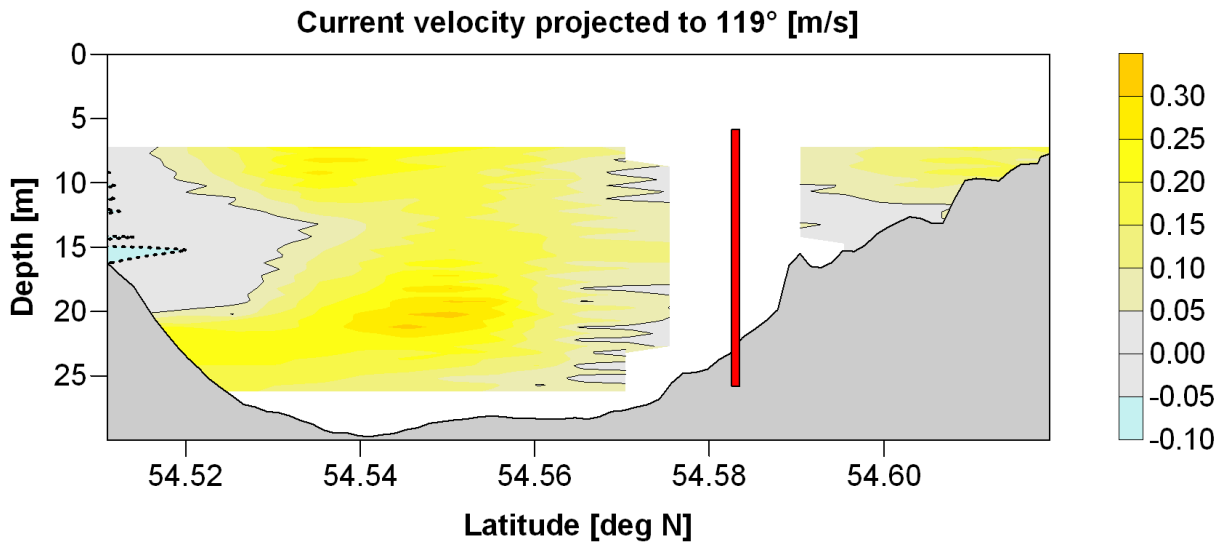
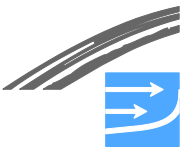


Fig. A.15 Juli-August_2009_1 25.07.2009 05:51 UTC - 25.07.2009 07:36 UTC.

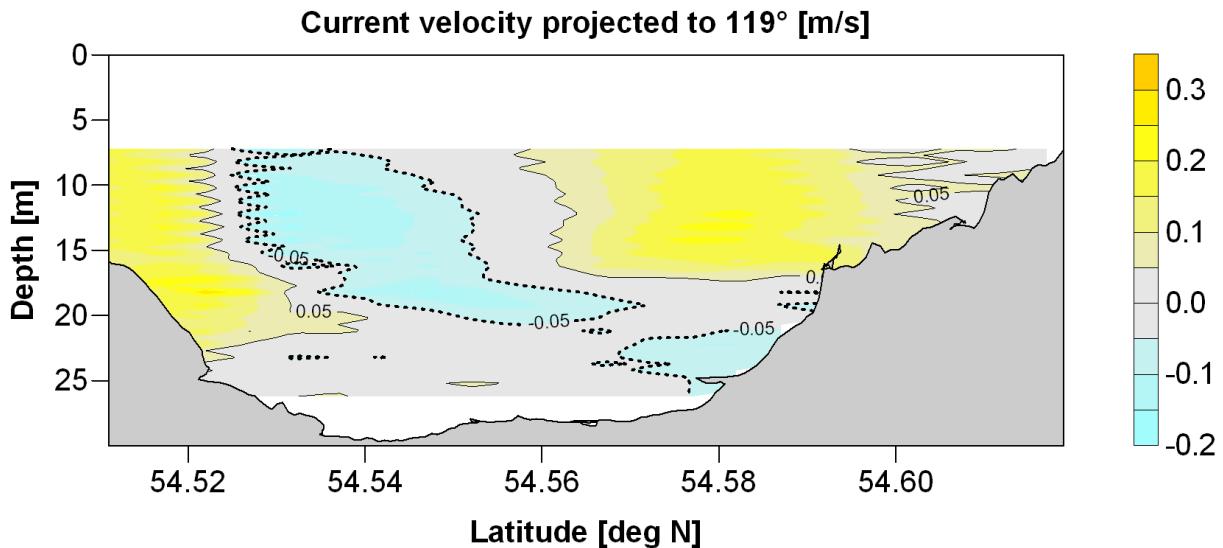


Fig. A.16 Juli-August_2009_2 28.07.2009 12:47 UTC - 28.07.2009 14:23 UTC.

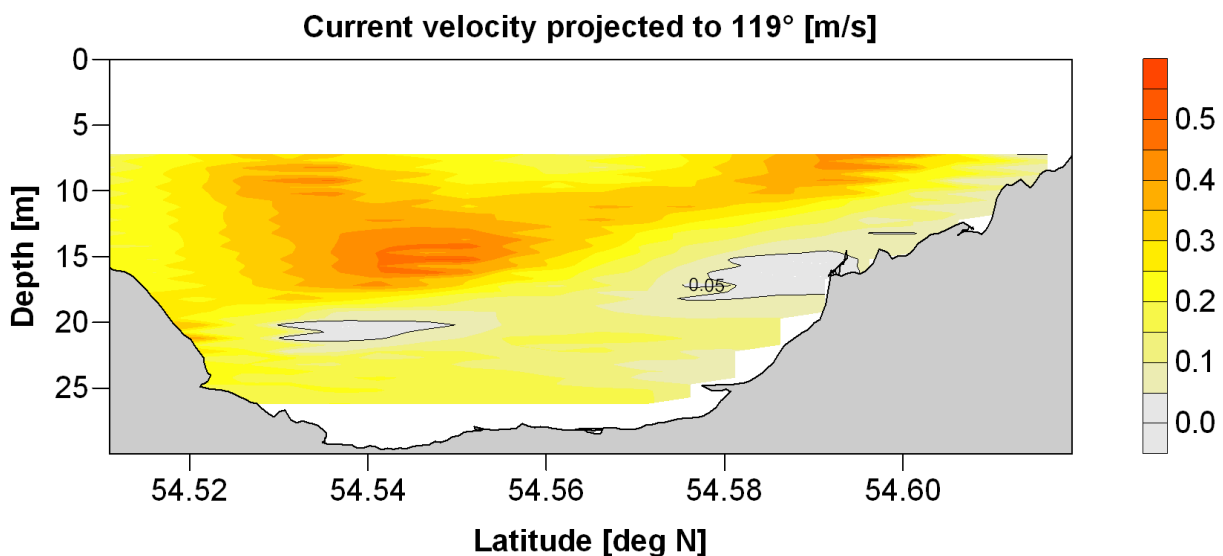


Fig. A.17 Juli-August_2009_3 01.08.2009 03:55 UTC - 01.08.2009 05:18 UTC.

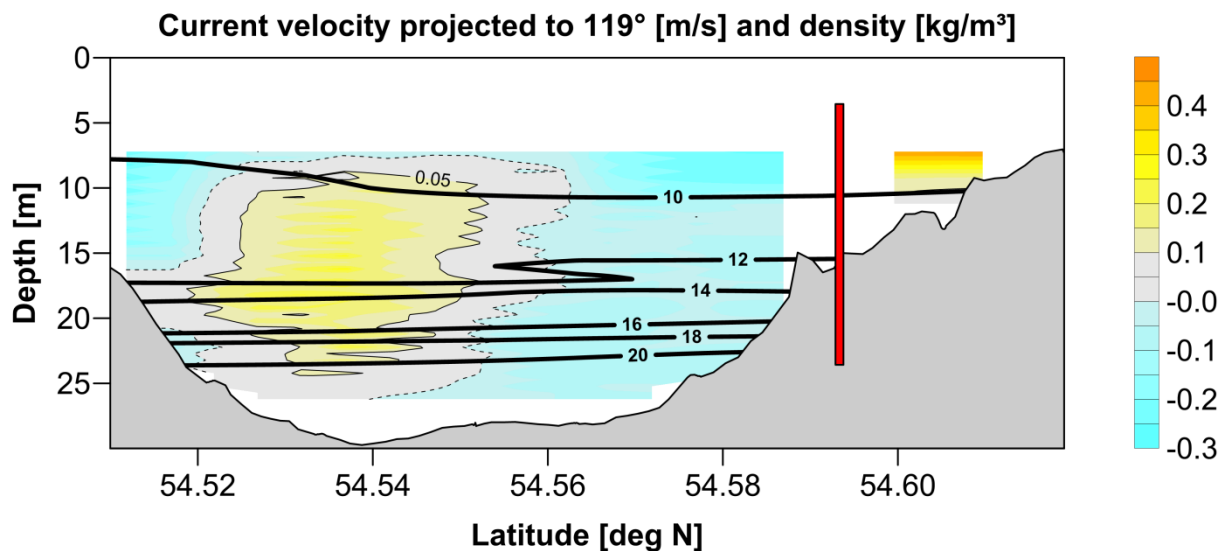


Fig. A.18 Juli-August_2009_4 01.08.2009 05:20 UTC - 01.08.2009 18:43 UTC.

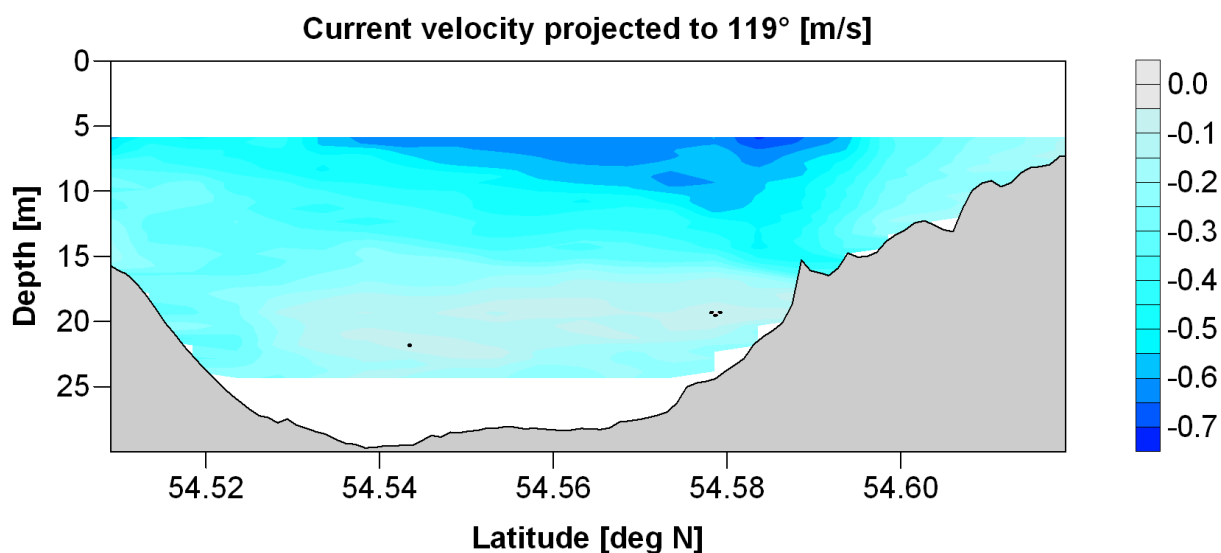


Fig. A.19 Aug-Sep_2009_1 24.08.2009 11:04 UTC - 24.08.2009 12:47 UTC.

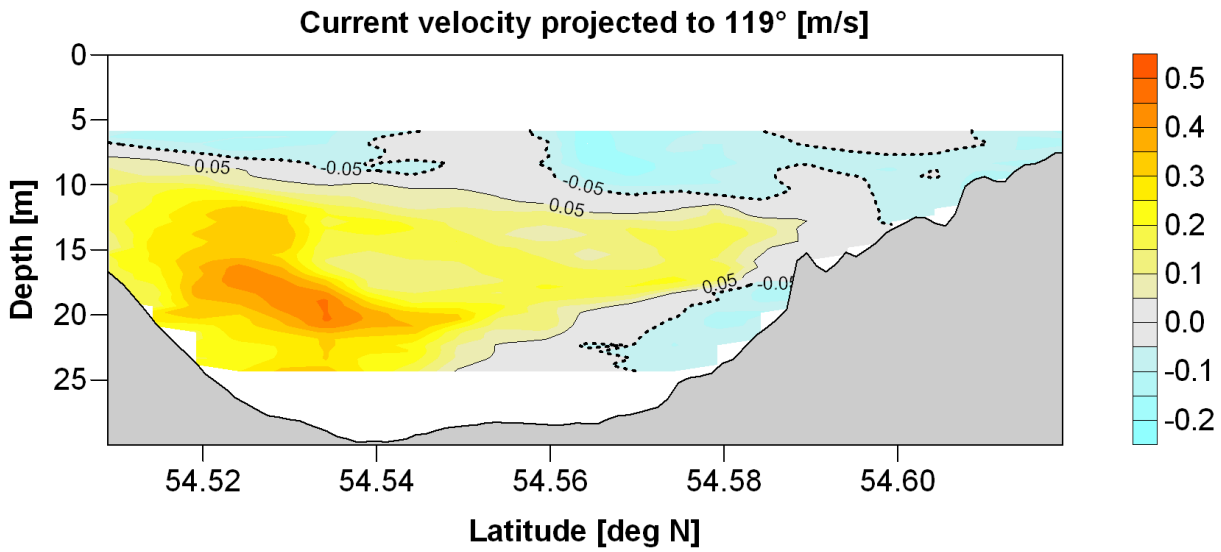


Fig. A.20 Aug-Sep_2009_2 27.08.2009 10:59 UTC - 27.08.2009 12:36 UTC.

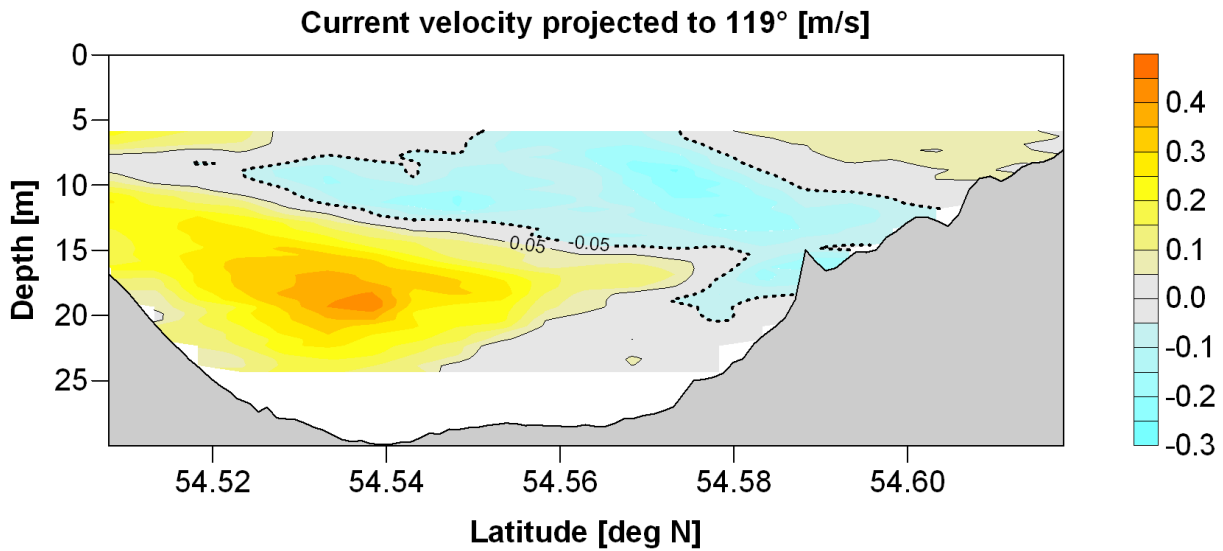


Fig. A.21 Aug-Sep_2009_3 28.08.2009 14:04 UTC - 28.08.2009 15:43 UTC.

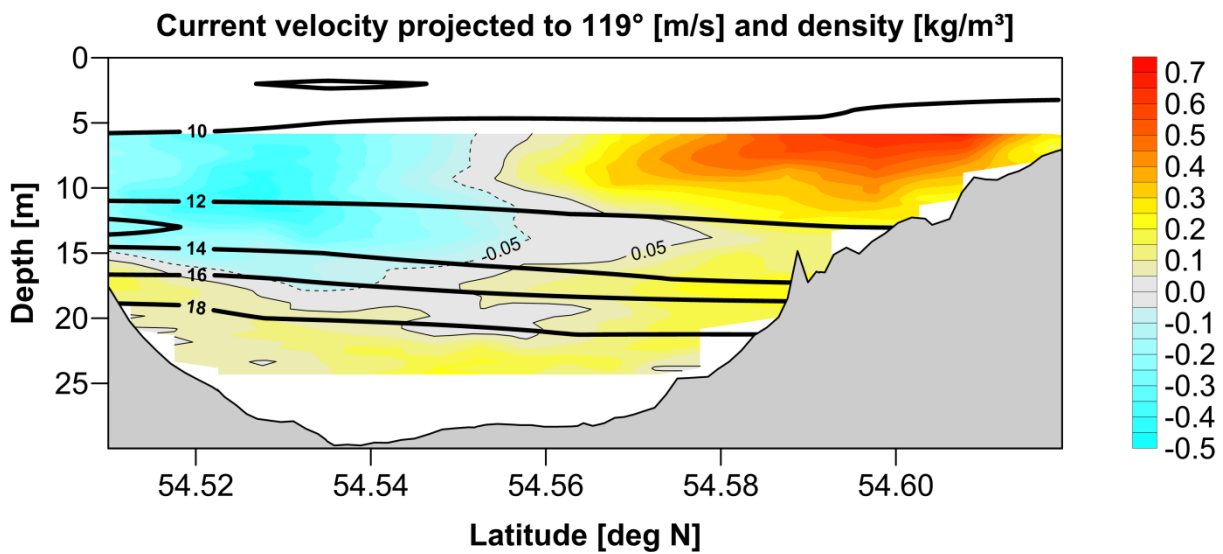


Fig. A.22 Aug-Sep_2009_4 31.08.2009 15:14 UTC - 31.08.2009 19:11 UTC.

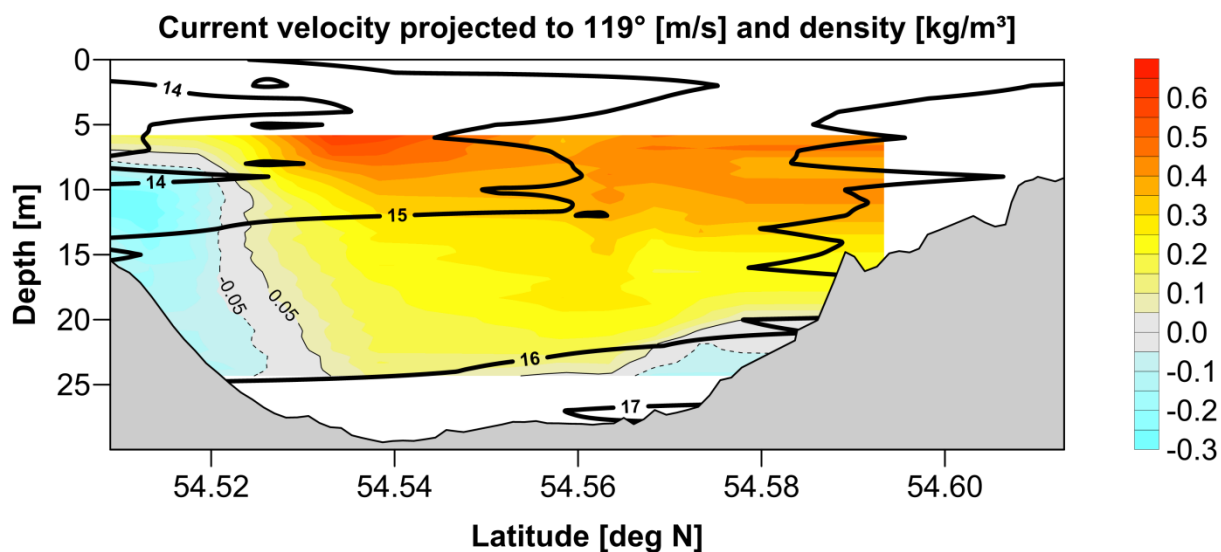


Fig. A.23 Sep-Oct_2009_1 28.09.2009 15:50 UTC - 28.09.2009 19:12 UTC.

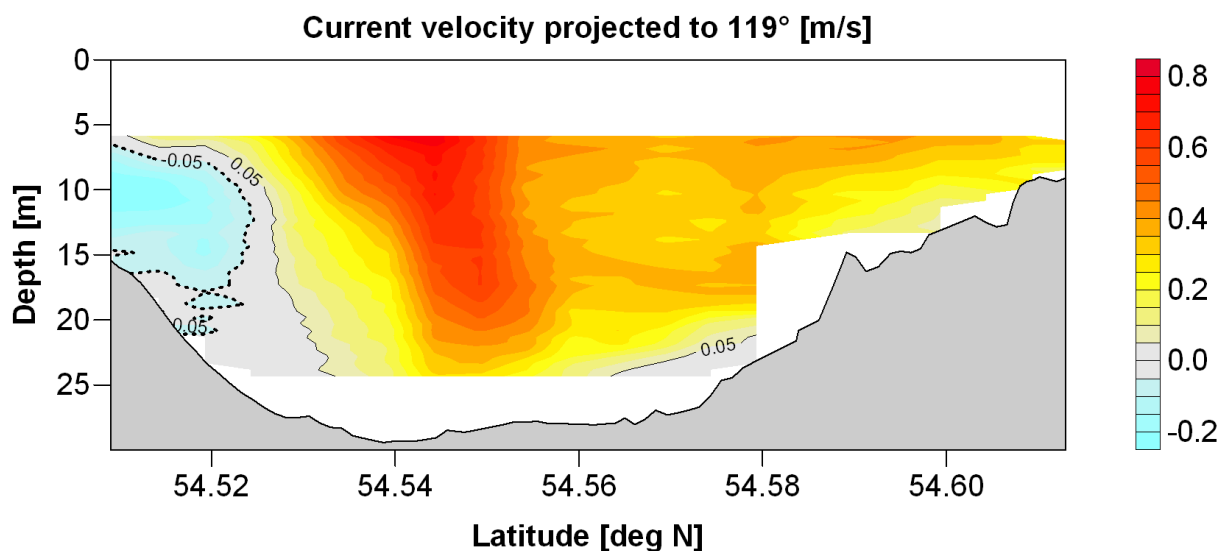


Fig. A.24 Sep-Oct_2009_2 28.09.2009 13:50 UTC - 28.09.2009 15:20 UTC.

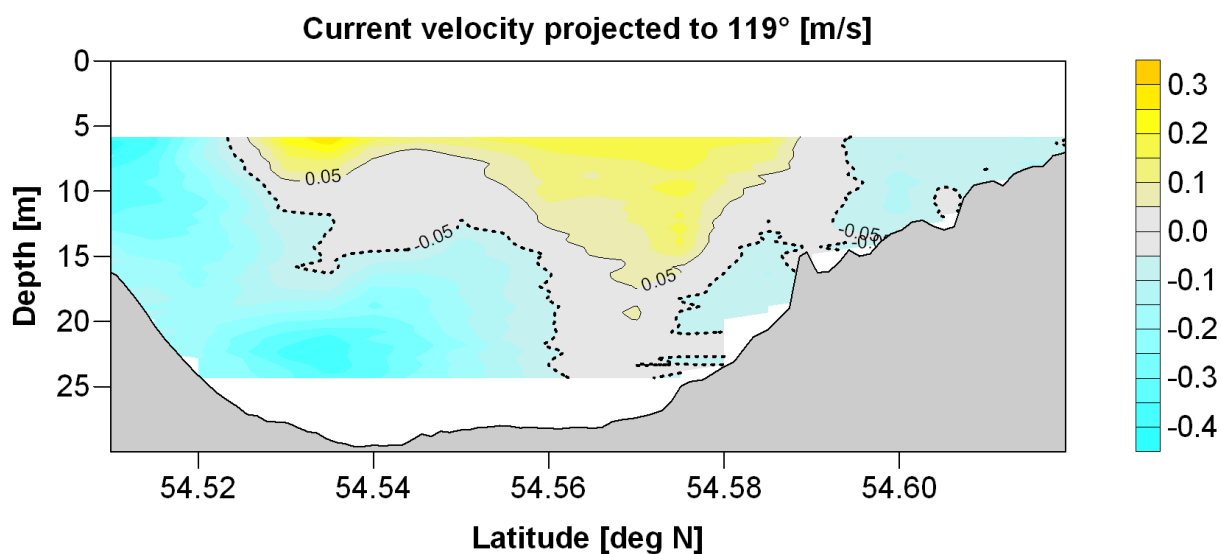


Fig. A.25 Sep-Oct_2009_3 30.09.2009 05:19 UTC - 30.09.2009 06:59 UTC.

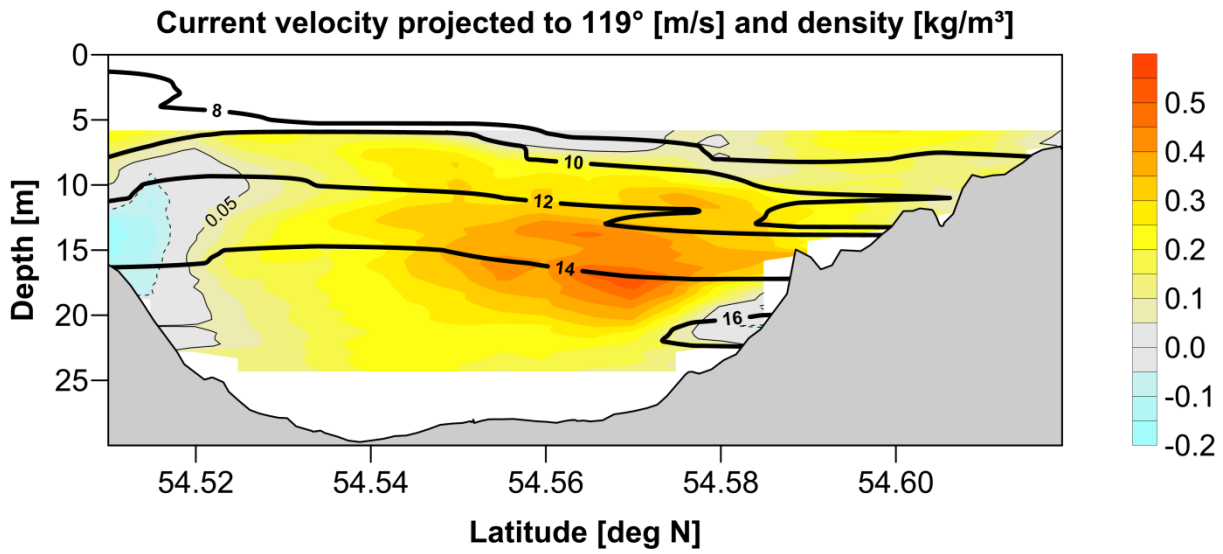


Fig. A.26 Oct-Nov_2009_1 27.10.2009 15:34 UTC - 27.10.2009 19:13 UTC.

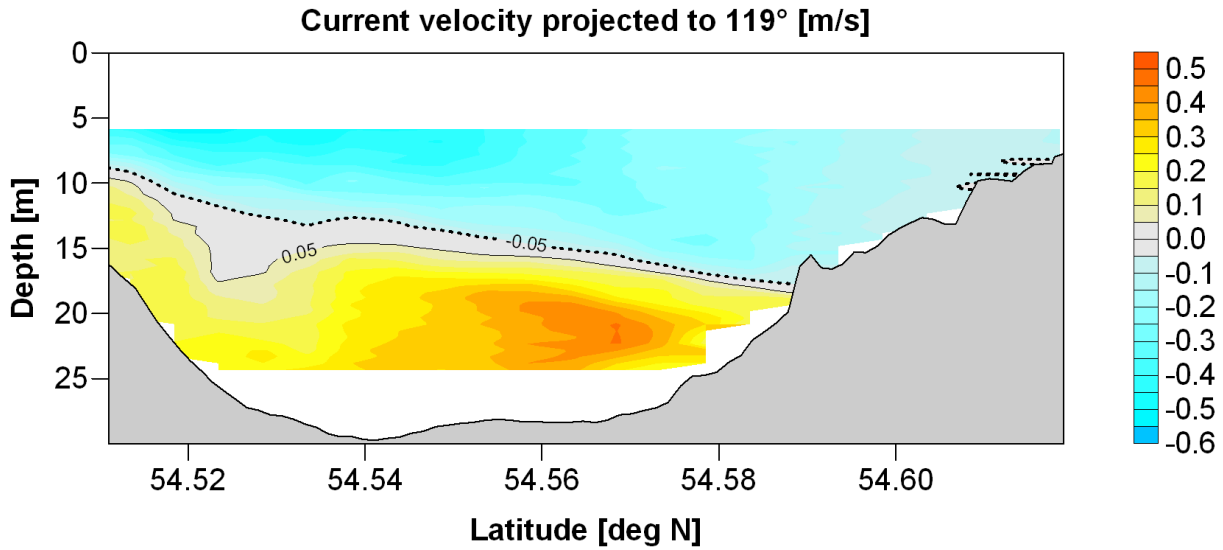


Fig. A.27 Oct-Nov_2009_2 30.10.2009 01:25 UTC - 30.10.2009 02:52 UTC.

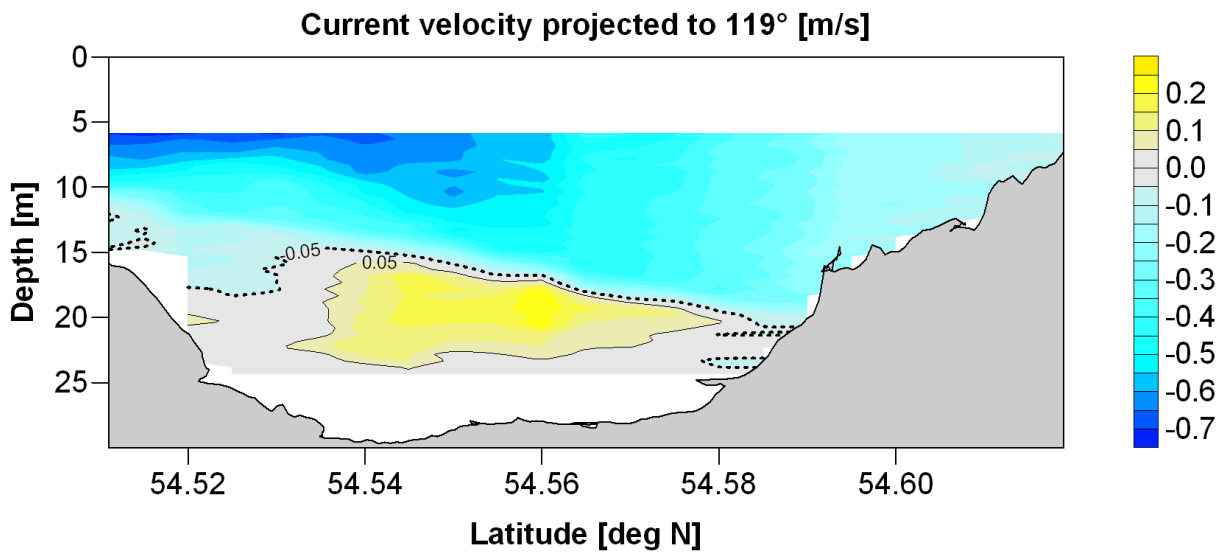


Fig. A.28 Oct-Nov_2009_3 01.11.2009 03:50 UTC - 01.11.2009 07:14 UTC.

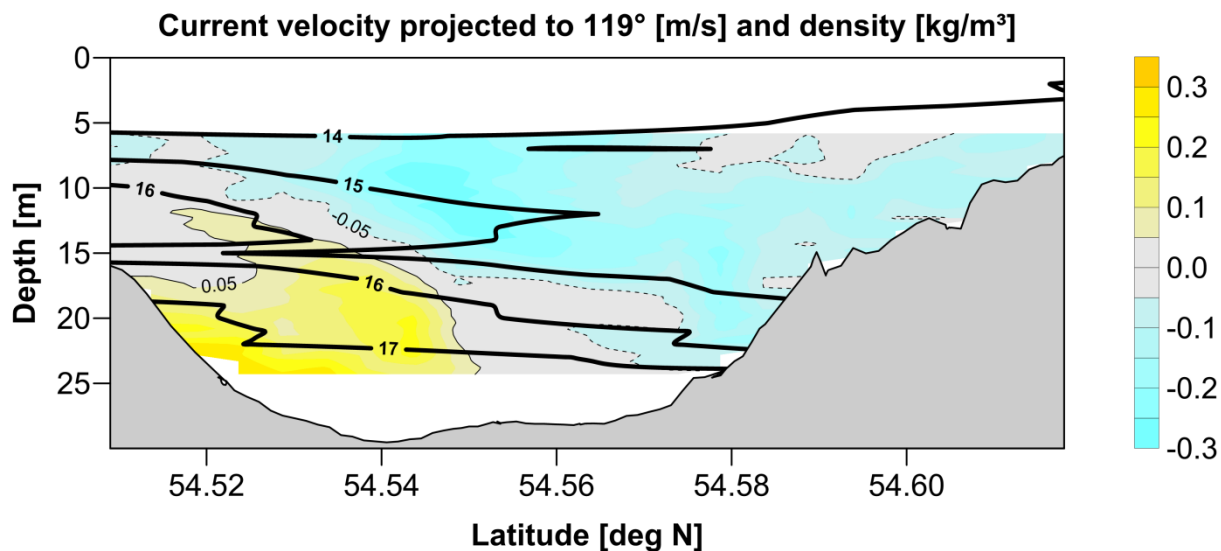


Fig. A.29 Nov-Dec_2009_1 30.11.2009 12:30 UTC - 30.11.2009 19:05 UTC.

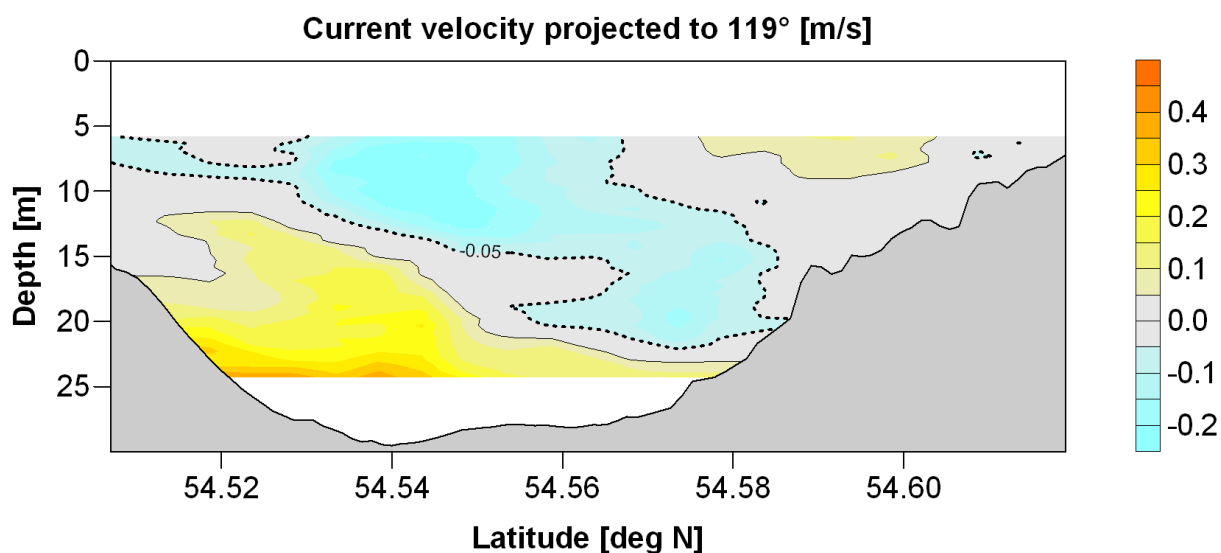


Fig. A.30 Nov-Dec_2009_2 30.11.2009 19:16 UTC - 30.11.2009 21:06 UTC.

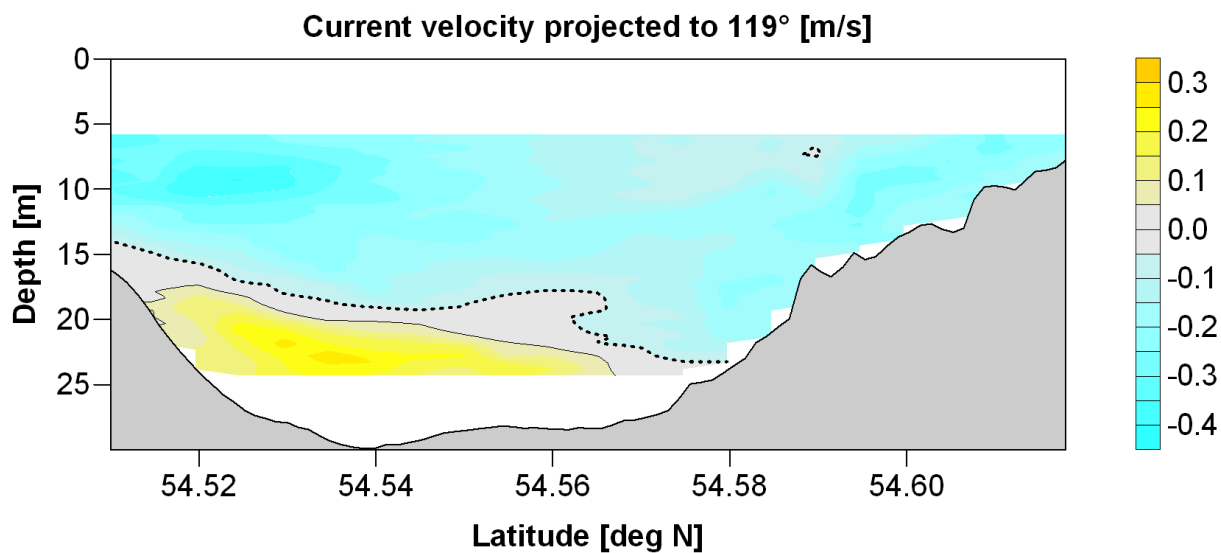




Fig. A.31 Nov-Dec_2009_3 02.12.2009 05:12 UTC - 02.12.2009 06:42 UTC.

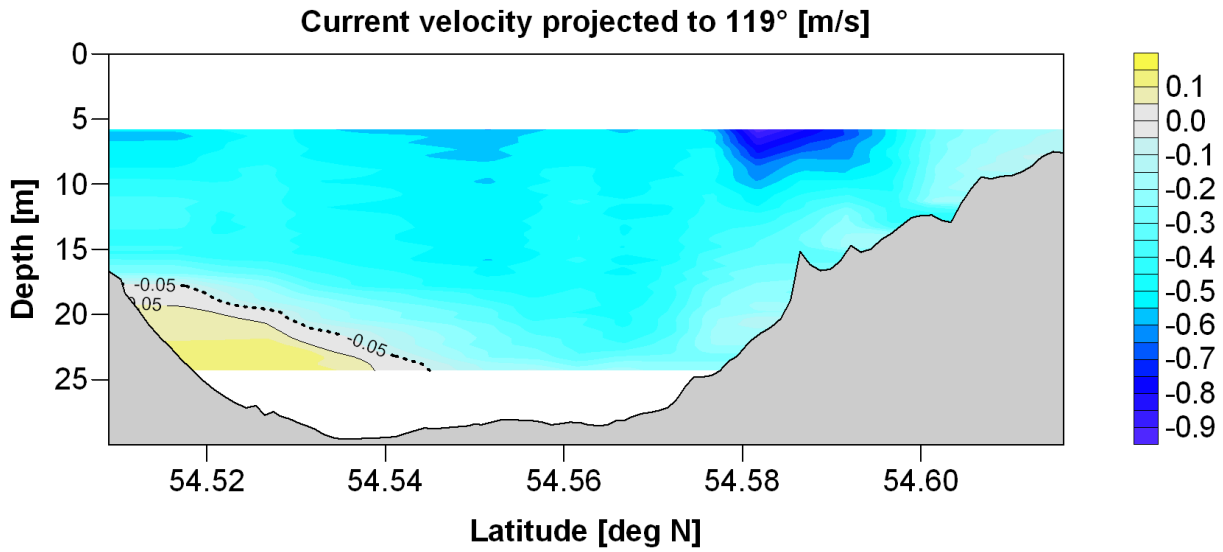


Fig. A.32 Nov-Dec_2009_4 05.12.2009 17:10 UTC - 05.12.2009 18:52 UTC.

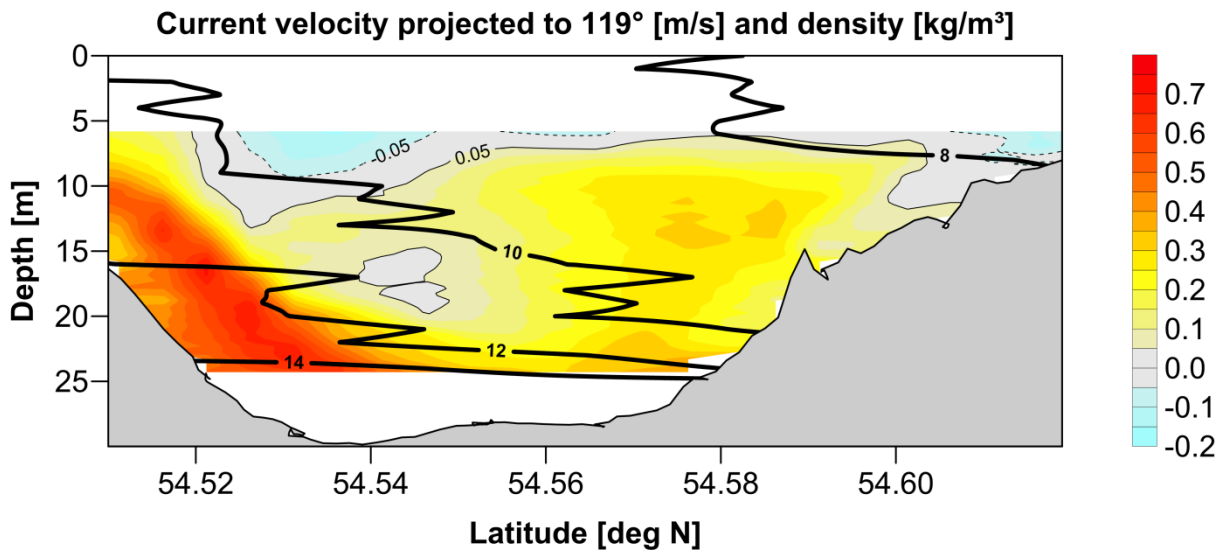


Fig. A.33 Januar_2010_1 11.01.2010 20:58 UTC - 12.01.2010 00:28 UTC.

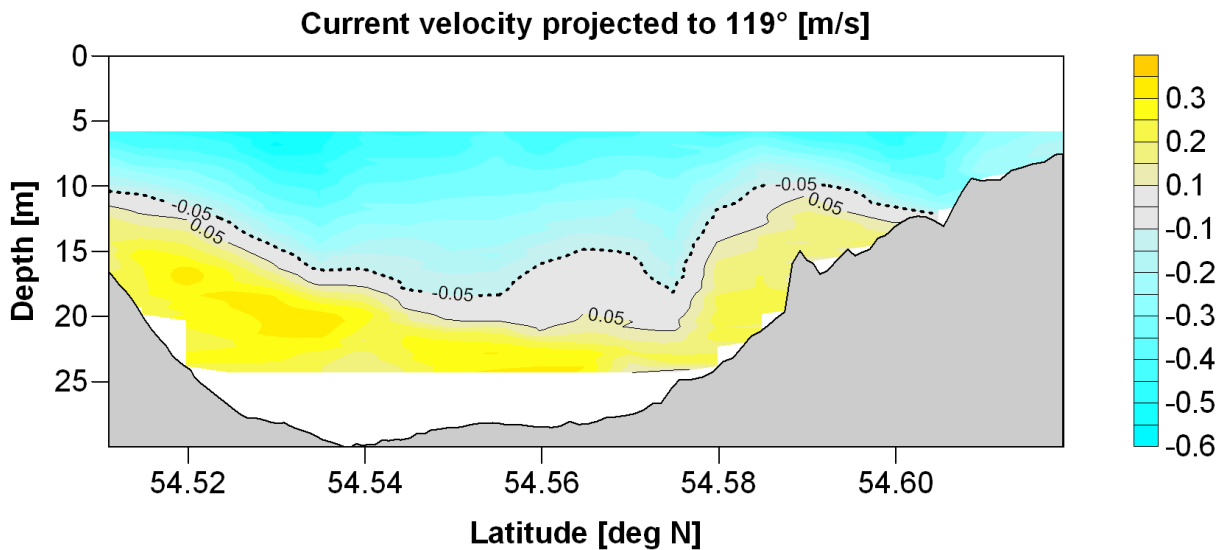




Fig. A.34 Januar_2010_2 13.01.2010 04:49 UTC - 13.01.2010 06:55 UTC.

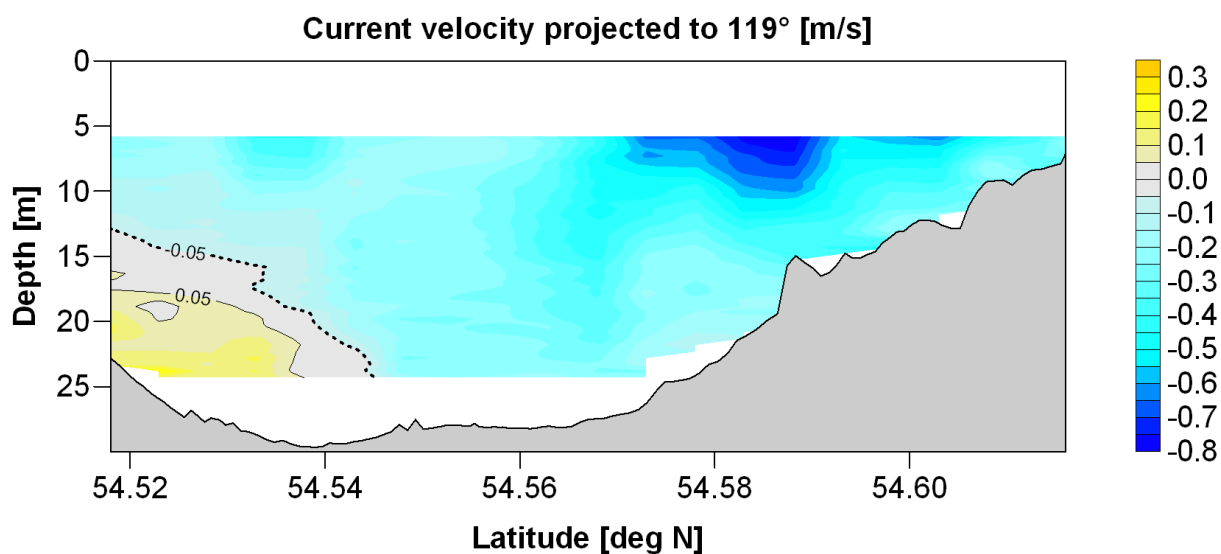


Fig. A.35 Januar_2010_3 16.01.2010 10:13 UTC - 16.01.2010 12:31 UTC.

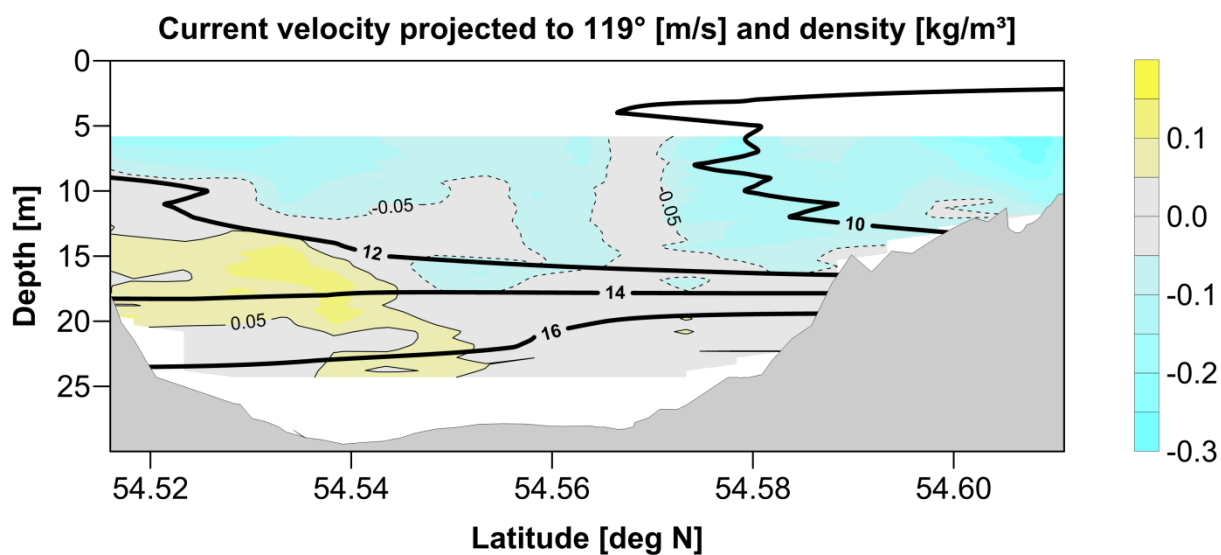


Fig. A.36 Februar_2010_1 16.02.2010 14:09 UTC - 16.02.2010 19:47 UTC.

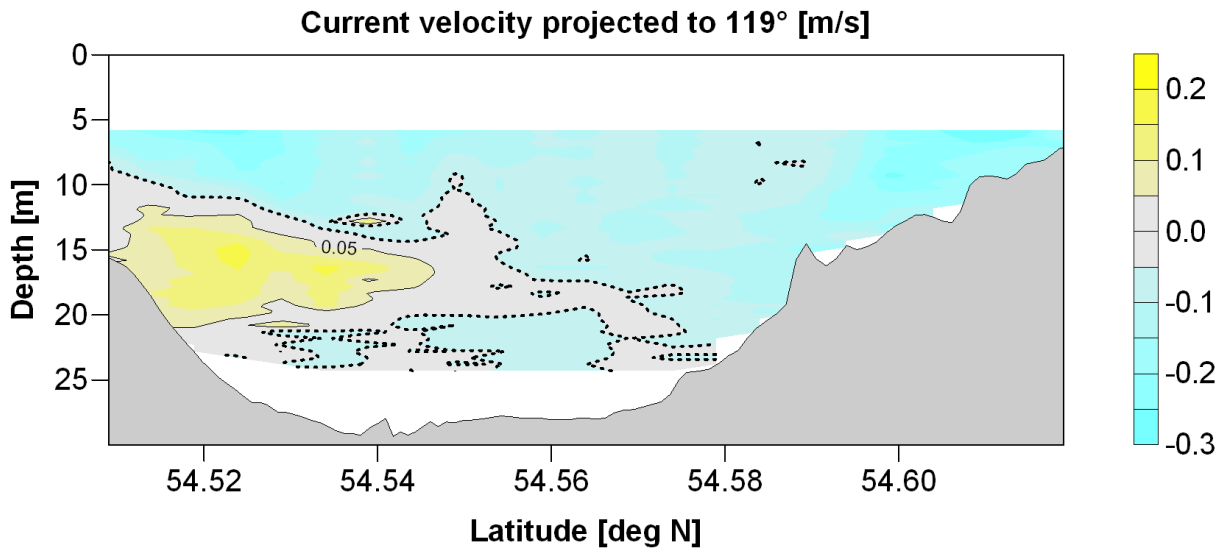
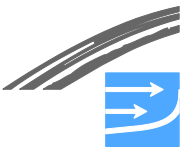


Fig. A.37 Februar_2010_2 16.02.2010 12:02 UTC - 16.02.2010 13:52 UTC.

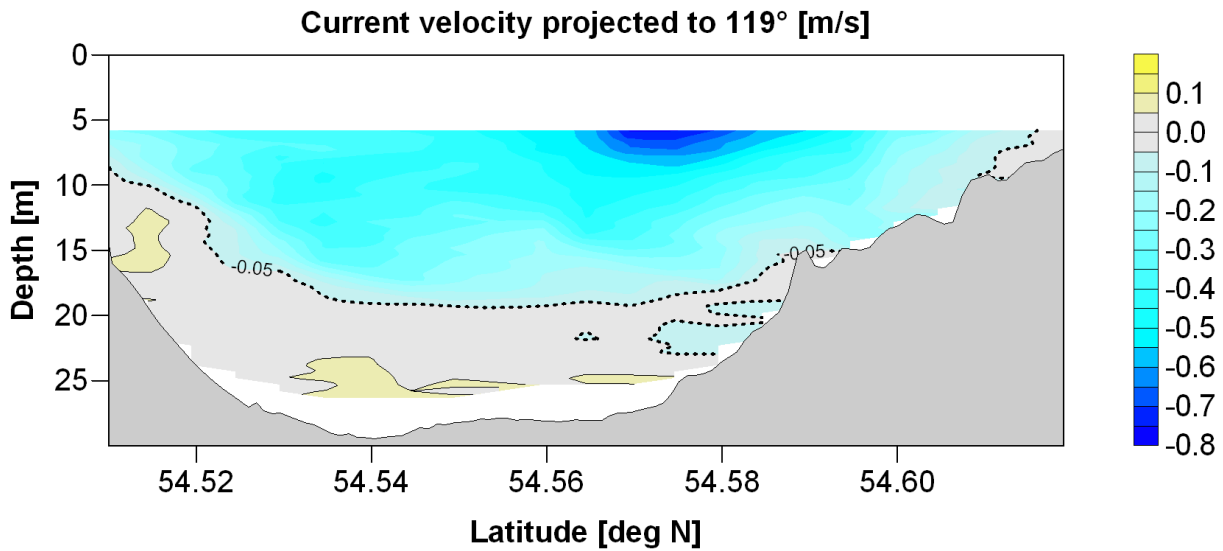


Fig. A.38 Februar_2010_3 18.02.2010 00:25 UTC - 18.02.2010 02:37 UTC.

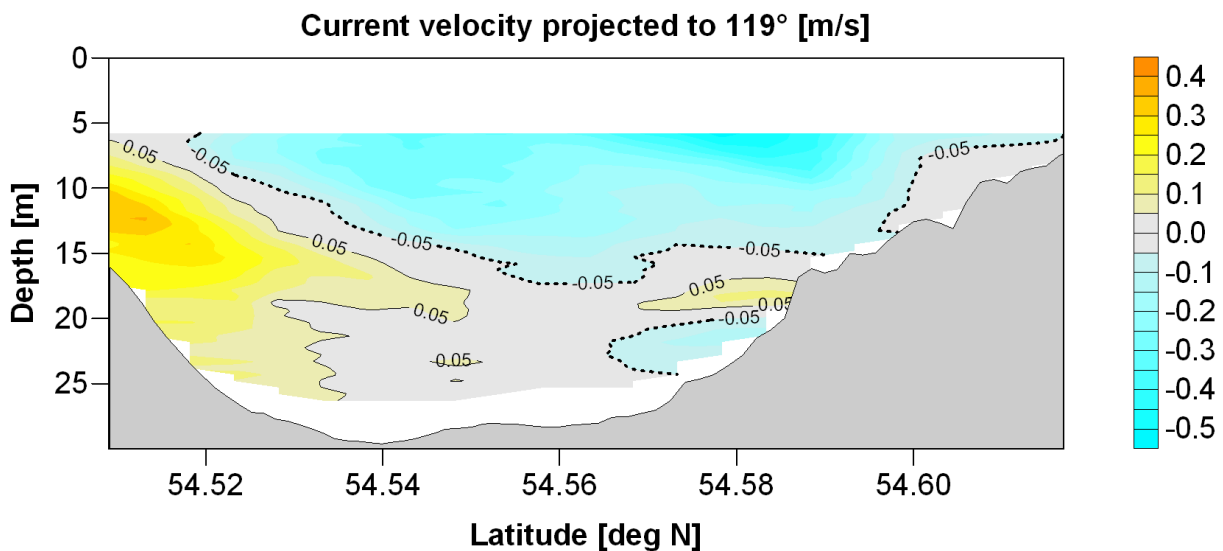
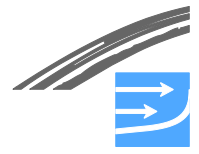


Fig. A.39 Februar_2010_4 19.02.2010 21:39 UTC - 19.02.2010 22:57 UTC.



A P P E N D I X B

Summary of wave model setup



Introduction and scope

This appendix summarizes the wave model setup and data applied in the Fehmarnbelt EIA. Waves in the project area of the Fehmarnbelt are governed primarily by the local wind conditions and the fetch limitations due to land such as Fehmarn to the South, Lolland to the North, Falster and Mecklenburg-Vorpommern to the E-SE and Langeland and Schleswig-Holstein to the West. However, occasionally waves from the Arkona Basin and Kieler Bay may contribute to the wave climate in the Fehmarnbelt. The wave conditions modelled for the present study consist of two parts:

1. Regional wave model covering the entire Baltic Sea
2. Local high resolution wave model covering the Fehmarnbelt area

The purpose of 1) is to supply boundary conditions for the local high resolution model, while the purpose of 2) is to provide detailed nearshore wave conditions as required for the morphological study.

Both wave models are run for the period 1989-01-01 to 2010-05-01 (21.3 years) resulting in a long-term detailed description of the wave conditions in and near the project area. The present appendix briefly describes the model setup, calibration and validation of the wave models and the overall results.

During the calibration and validation process it was found that the modelled wave directions showed a consistent pattern of deviations relative to measured values. The deviations seem to depend on the presence of land in the upwind direction. A similar pattern can be identified in the modelled wind data that are applied as forcing for the wave generation and wave growth in the wave models.

A summary of the deviations as well as a description of the adjustments to the modelled wave conditions are included in the baseline report (FEHY 2013d).

Wind and wave measurements

Wind measurements in the area of the Fehmarnbelt are adopted from the stations at Arkona, Darss Sill and Nysted and applied for comparisons with the modelled wind data. Wave measurements are acquired from the Arkona station and from the Fehmarnbelt main station ADCP's (MS01, MS02 and MS03) deployed by Femern A/S since March 2009. The main stations provide an overlap of up to about 1 year with the modelled wind data.

The locations of the wind and wave measurements are shown in Fig. B. 1. The period and frequency of available and valid data are given in Table B. 1 and Table B. 2 together with coordinates, height/depth and data provider. Due to the fairly large water depths in the Fehmarnbelt the main stations are not able to measure non-directional wave data (height and period) of waves shorter than 2.3 – 2.5s and directional wave data (peak and mean direction) of waves shorter than 3.5-4.2s.

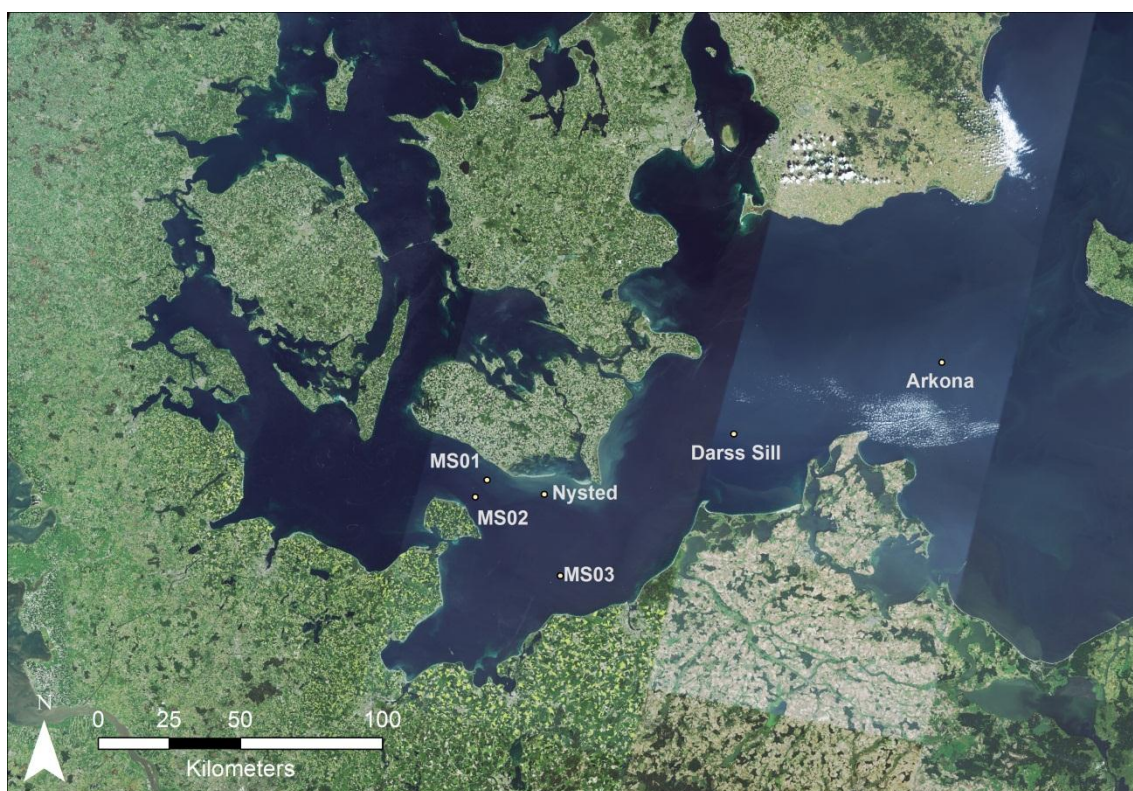


Fig. B. 1 Locations of wind and wave measurements

Table B. 1 Wind measurements

Station	Lon. °E	Lat. °N	Height m MSL	Period yyyy-mm-dd	Freq.	Device
Arkona	13.8667	54.8833	10	2003-09-29 – 2009-11-30	1h	Mast
Darss Sill	12.7000	54.7000	9.0	2003-04-11 – 2009-10-27	1h	Mast
Nysted	11.6627	54.5348	10/65 ¹	2004-06-07 – 2005-11-25	10min	Mast

¹ Wind speed was measured at 10 m and 65 m, while wind direction was measured at 65 m only.

Table B. 2 Wave measurements

Station	Lon. °E	Lat. °N	Depth m MSL	Period yyyy-mm-dd	Freq.	Device
Arkona	13.8667	54.8833	-46.0	2005-01-01 – 2005-12-31	1h	ADCP
MS01	11.3553	54.5859	-21.2	2009-03-07 – On-going	1h	ADCP ¹
MS02	11.2880	54.5340	-27.0	2009-03-30 – On-going	1h	ADCP ¹
MS03	11.7330	54.2750	-24.0	2009-03-29 – On-going	1h	ADCP ¹

¹ Bottom mounted.



Wave modelling tool

The wave conditions in this study are obtained by simulations of wave fields applying the numerical spectral wave (SW) model, MIKE 21 SW, developed by DHI. MIKE 21 SW is a third generation spectral wind-wave model. The model simulates the growth, decay and transformation of wind generated waves and swells in offshore and coastal areas. For further information regarding the MIKE 21 SW, see (DHI 2009a) and (DHI 2009b). For this study the simulations were executed in a UNIX environment with the developer version dated 2011-01-04 (including upgraded structure module).

Modelled wind data

Modelled wind data (fields of wind speed and wind direction varying in time and space) is required to force the wave models. In the Fehmarnbelt area the local wind forcing is the primary source of input for the wave models due to the fairly enclosed location well protected from (swell) waves from the large oceans. The accuracy of the local wind data is therefore of outmost importance. Wind data for this study is adopted from the latest WATCH simulation (EN5) provided by the Danish Meteorological Institute (DMI). This data set covers most of Europe with a geographical resolution of 0.11° and a temporal resolution of 1h during 1960 – 2010 (i.e. overlapping with the local wave measurements).

Modelled water level and currents

Water level and depth-averaged currents as input to the wave models are acquired from the established regional MIKE model (FEHY 2013e). This data set has a temporal resolution of 1h and covers the entire regional wave model area.

Regional wave model setup

The bathymetry for the regional wave model is compiled from the FEHY common local bathymetry and digital sea chart data provided by C-MAP Norway. The regional wave model domain entails the entire Baltic Sea from the Danish Straits and east- and north-eastward. The bathymetry and mesh in the south-western part of the Baltic Sea are shown in Fig. B. 2. The mesh has a characteristic element length in the range of 1,000–4,000 m in the Danish Straits and 4,000–7,000 m in the Arkona Basin.

The model boundaries in the Danish Straits are treated as closed, i.e. no incoming waves, since any wave energy entering from these locations is unlikely to affect the wave conditions in the project area significantly. The model is forced with the time and spatially varying winds, water levels and depth-averaged currents described above. The fully spectral, non-stationary formulation suitable for wave studies involving time-dependent wave events and rapidly varying wind conditions in space and time is applied and the model is calibrated with respect to bottom friction, wave breaking/dissipation etc. The settings for the regional wave model are summarised in Table B. 3.

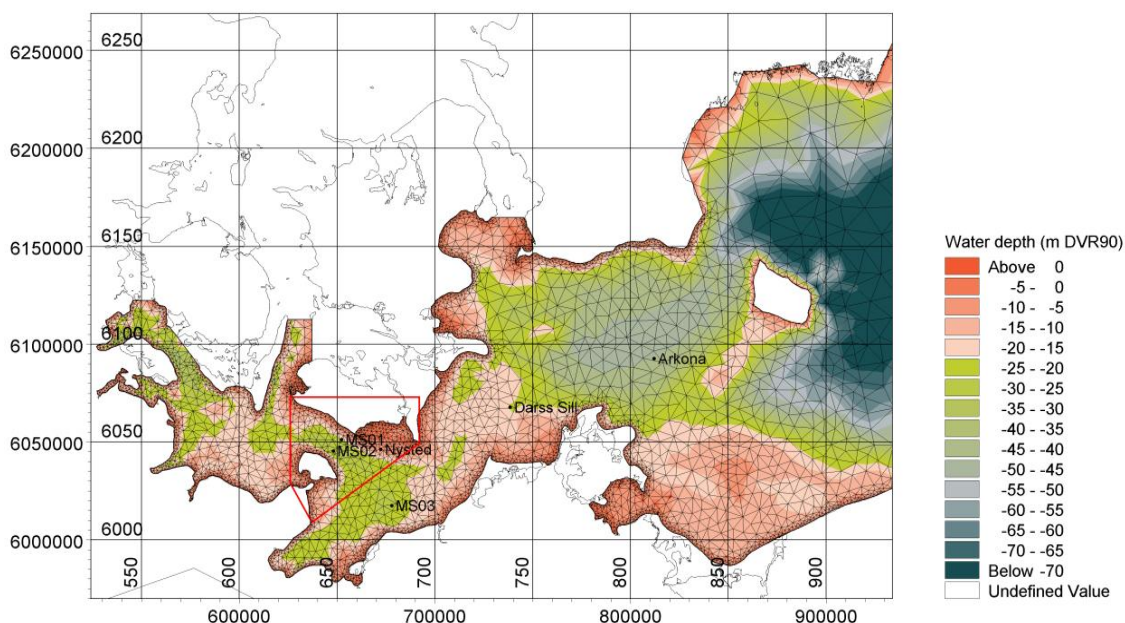


Fig. B. 2 Regional wave model bathymetry and mesh (south-western part). The red frame indicates the extent of the local wave model

Table B. 3 Summary of regional wave model settings

Setting	Value
Mesh resolution	1,000 – 4,000m (Danish Straits)
Simulation period	1989-01-01 – 2010-04-30
Basic equations	Fully spectral non-stationary ($\Delta t_{\max} = 300s$)
Discretisation	25 frequencies (1.5s - 12.5s), 32 directions
Water level	2D (temporally and spatially varying)
Current conditions	2D depth averaged (temporally and spatially varying)
Wind forcing	WATCH-EN5 (DMI), coupled, Charnock = 0.01
Boundary conditions	Closed
Wave breaking	Included, $\gamma=0.8$, $\alpha=1$
Bottom friction	Nikuradse, $k_N = 0.01m$
White capping	$C_{dis} = 6.0/4.6$, $\Delta_{dis} = 0.8$

Local Wave Model Setup

The bathymetry for the local wave model is compiled from a local bathymetry of 50x50 m. The mesh is highly refined in the link corridor and along the coastal areas adjacent to Rødby and Puttgarden harbours in order to properly resolve the bathymetrical features of importance for the nearshore wave transformation, se Fig. B. 3. The mesh size within the 7 m contour is less than 50 m in the vicinity of the harbours.

The model boundaries at the western and eastern side of the domain are forced by fully spectral line series saved from the regional wave model. The setup of the local wave model is identical to that of the regional model except that in order to apply the much higher spatial resolution within a reasonable computation time, the model is run with the quasi-stationary formulation of MIKE 21 SW. This method can be used for fetch limited conditions when individual wave events can be considered as



independent. A comparison between results from a model set up in non-stationary mode and the present model showed that the quasi-stationary formulation was capable of computing wave conditions with fully adequate accuracy even in events with rapidly time varying wind directions during a storm event.

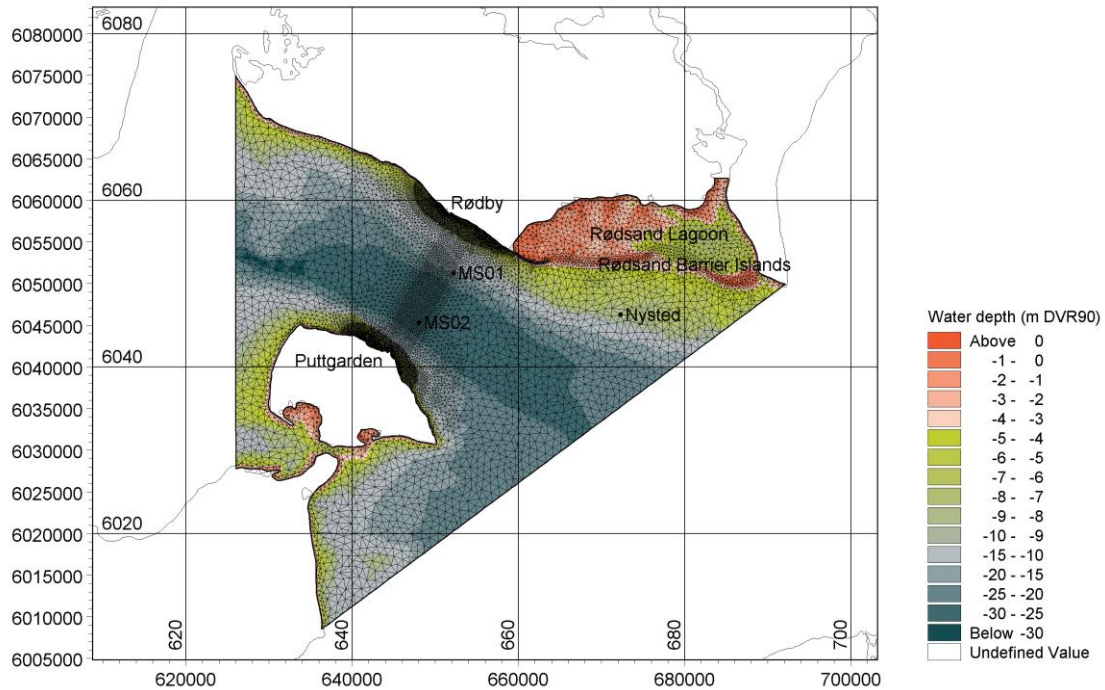


Fig. B. 3 Local baseline wave model bathymetry and mesh

Comparison of modelled and measured wind data

Wind roses at Nysted windfarm of the measured and modelled data are shown in Fig. B. 4. Both wind roses show predominant directions from south to west and some contribution from the eastern sector as well. The model data shows a slightly higher occurrence of wind from the SW sector than the measurements and a general tendency of clockwise rotated directions compared to the measurements.

It is noted that the measured wind data is representative of the exact location of the measurements, while the modelled data represents the average of a grid cell. The grid cell size of the WATCH-EN5 data is about 11 km at the Fehmarnbelt, which means that the model may not resolve very local conditions such as land-water boundaries in detail.

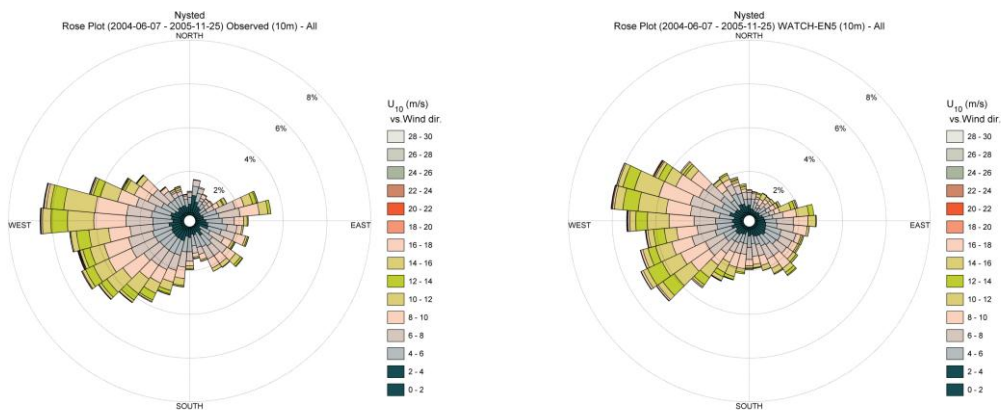




Fig. B. 4 Measured (left) and modelled (right) wind roses at Nysted

The yearly BIAS (mean difference) in wind speed (U_{10}) for measured wind speeds greater than 6 m/s is given in Table B. 4, showing that the medium to strong wind speeds are underestimated by 0.62 m/s at Arkona while slightly overestimated at Nysted windfarm by 0.23 m/s. At Darss Sill there is a distinct change from negative to positive BIAS between 2006- 2007. The sudden change in BIAS at Darss Sill may be explained by two jumps in the measured wind speeds just after 2007-09-06. Comparisons with other sources of modelled wind data show identical jumps indicating that the jumps originate from the measurements. It is thus not possible to assess the absolute BIAS at this station due to uncertainties in the measurements.

Table B. 4 Yearly BIAS in wind speed (modelled ÷ measured) for measured wind speeds greater than 6 m/s, N = number of valid measurements

U_{10} [m/s]	Arkona		Darss Sill ²		Nysted	
	Year	N	BIAS	N	BIAS	N
2003	1,600	-0.95	3,229	-0.39	-	-
2004	5,721	-0.54	5,740	-0.35	17,322	0.14
2005	5,804	-0.64	5,242	-0.33	25,862	0.29
2006	5,801	-0.76	5,315	-0.38	-	-
2007	5,518	-0.65	3,564	0.27	-	-
2008	5,645	-0.64	4,666	0.24	-	-
2009	5,068	-0.35	4,054	0.10	-	-
All years	35,153	-0.62	31,808	-0.14	43,184	0.23

² The BIAS changes significantly after 2007-09-06, due to two sudden jumps in the measurements.

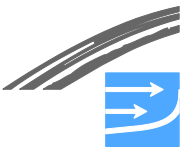
Similarly, the overall BIAS of wind direction varies significantly from year to year, see Table B. 5. It is assessed that the offset is related to the measured wind data but from the available data and information it is not possible to assess which level of offset is more correct and it may thus simply be concluded that the measurements show considerable uncertainties in the actual offset (mean wind direction).

Table B. 5 Yearly BIAS in wind direction (modelled ÷ measured) for measured wind speeds greater than 6 m/s, N = number of valid measurements

U_{dir} [deg]	Arkona ¹		Darss Sill ²		Nysted	
	Year	N	BIAS	N	BIAS	N
2003	1,600	9.74	3,229	-7.76	-	-
2004	5,721	8.54	5,740	-9.98	17,322	12.50
2005	5,804	9.95	5,242	-7.99	25,862	12.31
2006	5,801	6.69	5,315	9.45	-	-
2007	5,518	-3.47	3,564	13.73	-	-
2008	5,645	-5.65	4,666	15.41	-	-
2009	5,068	3.35	4,054	14.44	-	-
All years	35,153	3.61	31,808	3.31	43,184	12.38

¹ The offset changes significantly on: 2007-06-25, 2007-09-20, 2009-06-15, 2009-07-20.

² The offset changes significantly on: 2005-11-15.



It seems likely that the identified deviations have a correlation with the presence of upwind land. The effects of the upstream land in turning the wind directions may originate from the following:

- A relatively coarse spatial resolution in the wind model relative to the narrow straits and smaller land areas in the Fehmarnbelt region
- Uncertainty in the applied roughness parameter over land in the meteorological model
- Uncertainty in the prediction of static stability over land areas

The average deviation between modelled and measured wind directions at Nysted is +12.38 deg. for measured wind speeds greater than 6 m/s and is relatively constant during the observation period. One explanation for this could be an offset in the measured wind directions. In Fig. B. 5 the offset of 12.38 degrees is subtracted from the directional BIAS to illustrate the deviations in modelled wind directions in excess of the offset (overall BIAS). The "clockwise" and "anticlockwise" in the text added to the figure refer to this excess deviation. According to communication with Niels Woetmann Nielsen from DMI, a too high roughness over land (i.e. bullet 2 above) is a likely reason for the measured deviations in Fig. B. 5.

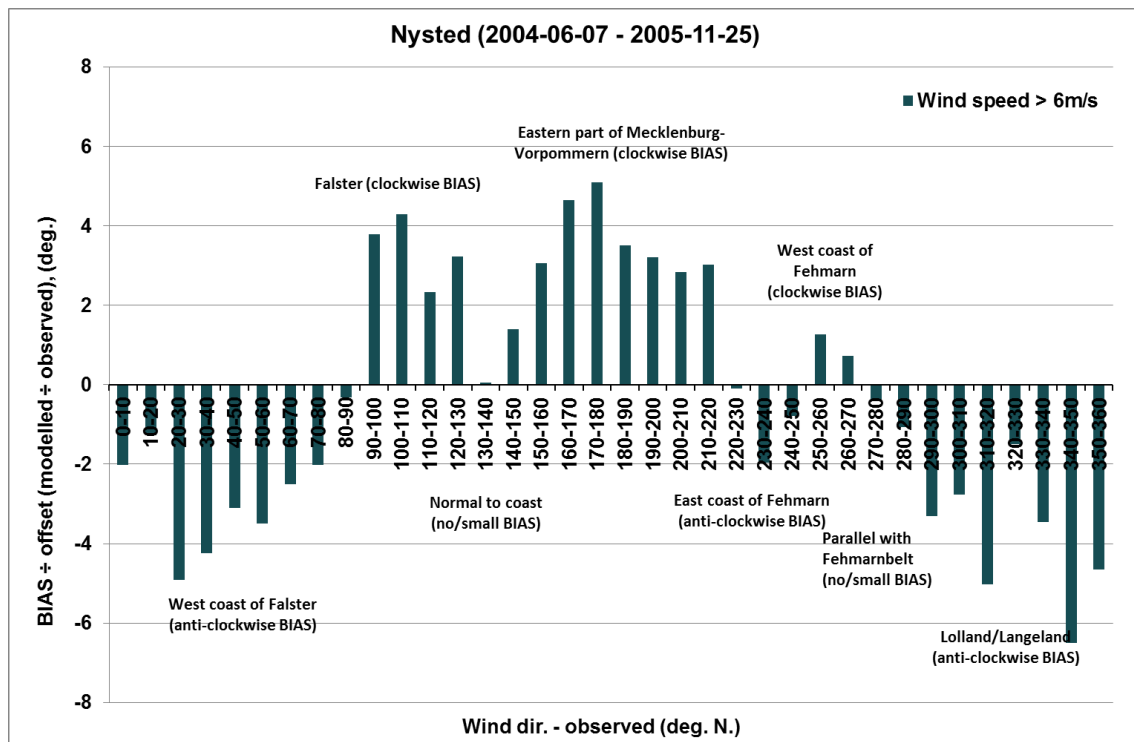


Fig. B. 5 BIAS ÷ offset (12.38 deg.) in wind direction (modelled ÷ measured), [deg.], at Nysted, measured wind speeds greater than 6 m/s. The locations on the diagram indicate the upwind land area

Comparison of modelled wave data

The local wave model is validated against measurements of significant wave heights (H_{m0}), mean wave periods (T_{01}) and mean wave directions (MWD) at the Fehmarnbelt Fixed Link main stations MS01 and MS02. The validations cover the entire period of overlapping data between measurements and models of approximately 1 year (March 2009 – April 2010).

Wave roses at MS01 ($H_{m0} > 0.6\text{m}$) and MS02 ($H_{m0} > 1.0\text{m}$) of the measured and modelled data are presented in Fig. B. 6 and Fig. B. 7. Both set of wave roses show dominating directions from WNW and SE, i.e. perpendicular to the Fehmarnbelt corridor and in the direction of the longest fetches for wave generation. The MWD at MS01 show a pattern of anti-clockwise rotated wave directions from the dominating directions of WNW and SE and clockwise rotated directions from the other remaining directions. A similar pattern was identified for the wind at Nysted. At MS02 the pattern is slightly different; however, this may not be entirely representative due to the limited number of data included.

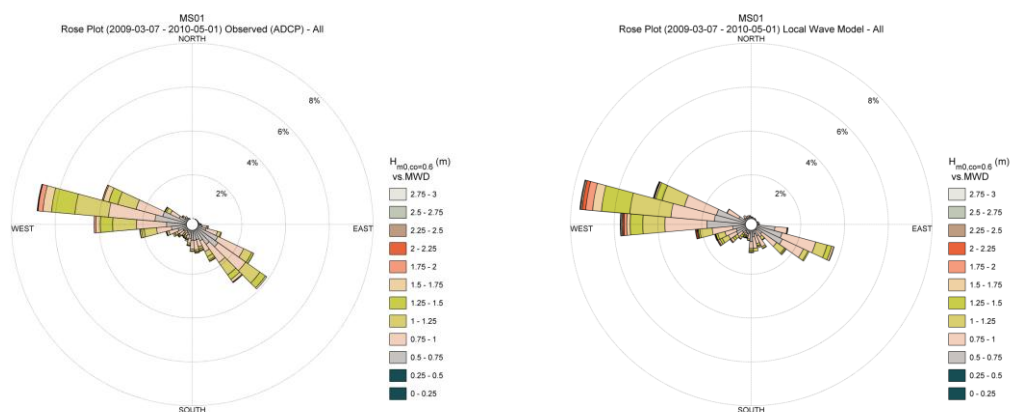


Fig. B. 6 Measured and modelled wave roses at MS01 for measured $H_{m0} > 0.6\text{ m}$

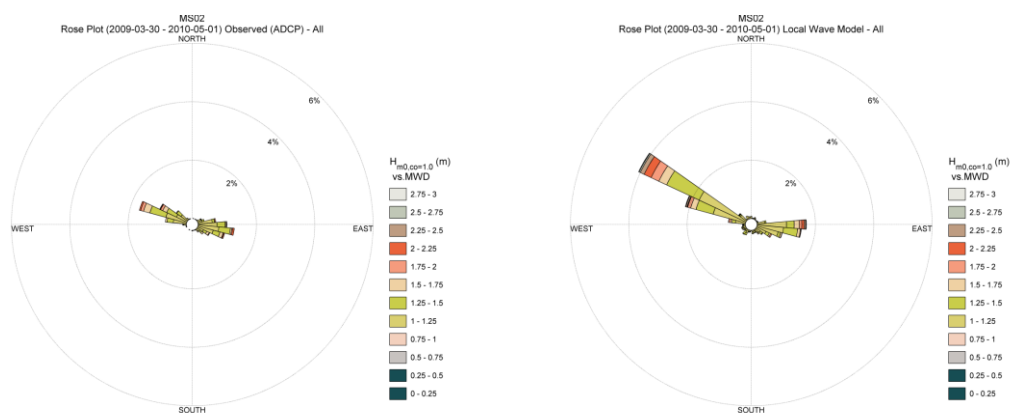


Fig. B. 7 Measured and modelled wave roses at MS02 for measured $H_{m0} > 1.0\text{ m}$

The average ratio between modelled and measured H_{m0} at MS01 ($H_{m0} > 0.6\text{m}$) and MS02 ($H_{m0} > 1.0\text{ m}$) for each directional bin of 10 deg. is shown in Fig. B. 8. Apparently there is some variation in the ratio for both stations. At MS01 the wave heights from the ESE and WNW directions are underestimated by up to about 10%, while waves from the SW sector are overestimated by up to 20% (waves from this sector are fairly infrequent though). At MS02 the wave heights from the E-SE sector are slightly underestimated by 5-10%, while the waves from the WNW sector are overestimated by 10-20% compared to the measurements.

In conclusion, the comparisons between modelled and measured wave conditions show some deviations between measured and modelled wave directions and heights. The magnitude of the deviations is found to vary with the directions from



which the waves approach the Fehmarnbelt area and seem to be related to the presence of 'upstream' land areas. The mean wave direction and significant heights applied for the morphological study have been adjusted for the nearshore wave conditions.

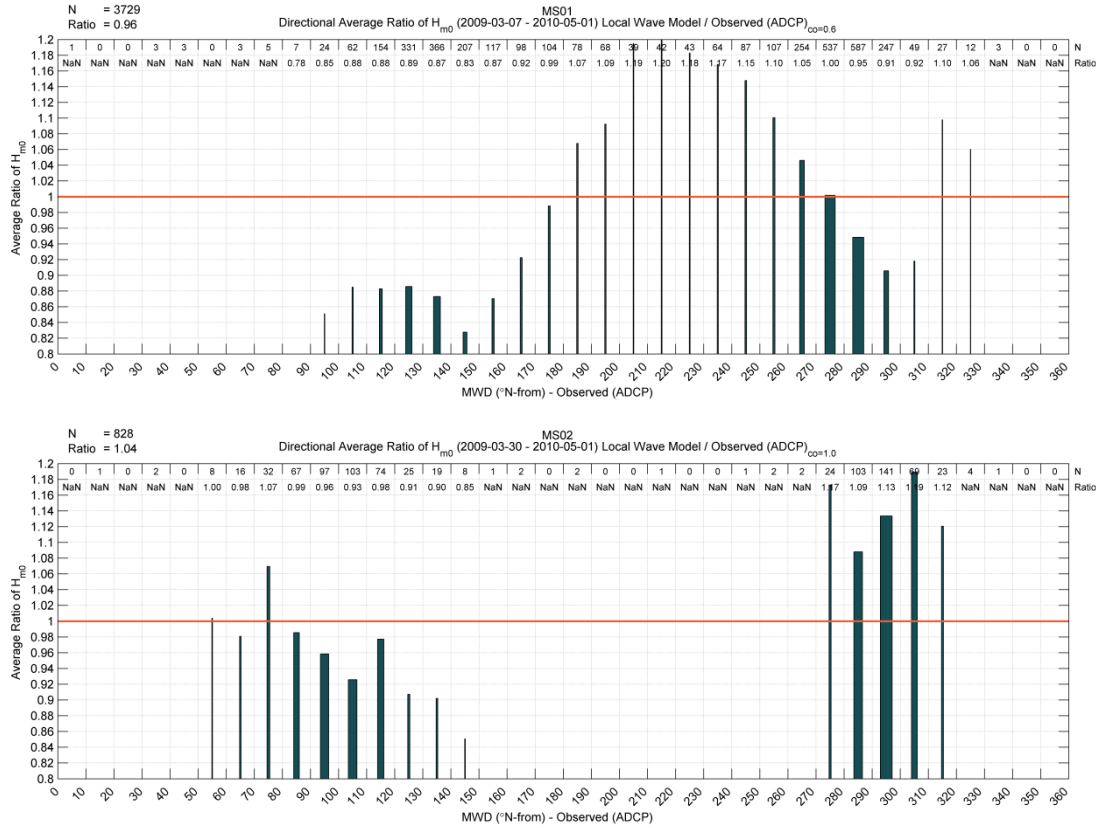


Fig. B. 8 Directional average ratio between modelled and measured wave height at MS01 (top, measured $H_{m0} > 0.6$ m) and MS02 (bottom, measured $H_{m0} > 1.0$ m).

Modelled wave conditions at MS01 and MS02

Wave data from the locations of MS01 and MS02 was extracted from the local baseline wave simulation as time series of 1-hourly values covering the period 1989-01-01 – 2010-05-01. The following conditions are based on the raw output from the wave model, i.e. without any corrections for the above identified deviations. Based on the time series the local wave conditions are illustrated in terms of:

- Wave roses (H_{m0} vs. MWD) see Fig. B. 9
- H_{m0} - U_{10} Scatter diagrams see Fig. B. 10
- H_{m0} - T_p Scatter diagrams see Fig. B. 11
- H_{m0} - T_{01} Scatter diagrams see Fig. B. 12

The wave conditions in the Fehmarnbelt are generally mild. The mean significant wave height during the simulation period is 0.66 m and 0.65 m at MS01 and MS02, respectively and the waves are short with most of the mean wave periods in the range of 1.5 s – 4.0 s and peak wave periods generally less than 6.5 s.



Due to the dominance of locally generated wind-waves in the Fehmarnbelt there is a strong correlation between wind speed and wave height and between wave period and wave height, cf. Fig. 6.10 - Fig. B. 12. The conditions are generally similar at MS01 and MS02 with respect to wave height and period.

The predominant wave direction of W-WNW at MS01 is more or less perpendicular to the link corridor, but a significant fraction of waves occurs also from the directions E-SE. The conditions at MS02 are very similar to those at MS01, except that the dominant directions are shifted to respectively WNW and E. Waves from N-NE are low in amplitude and occur rarely.

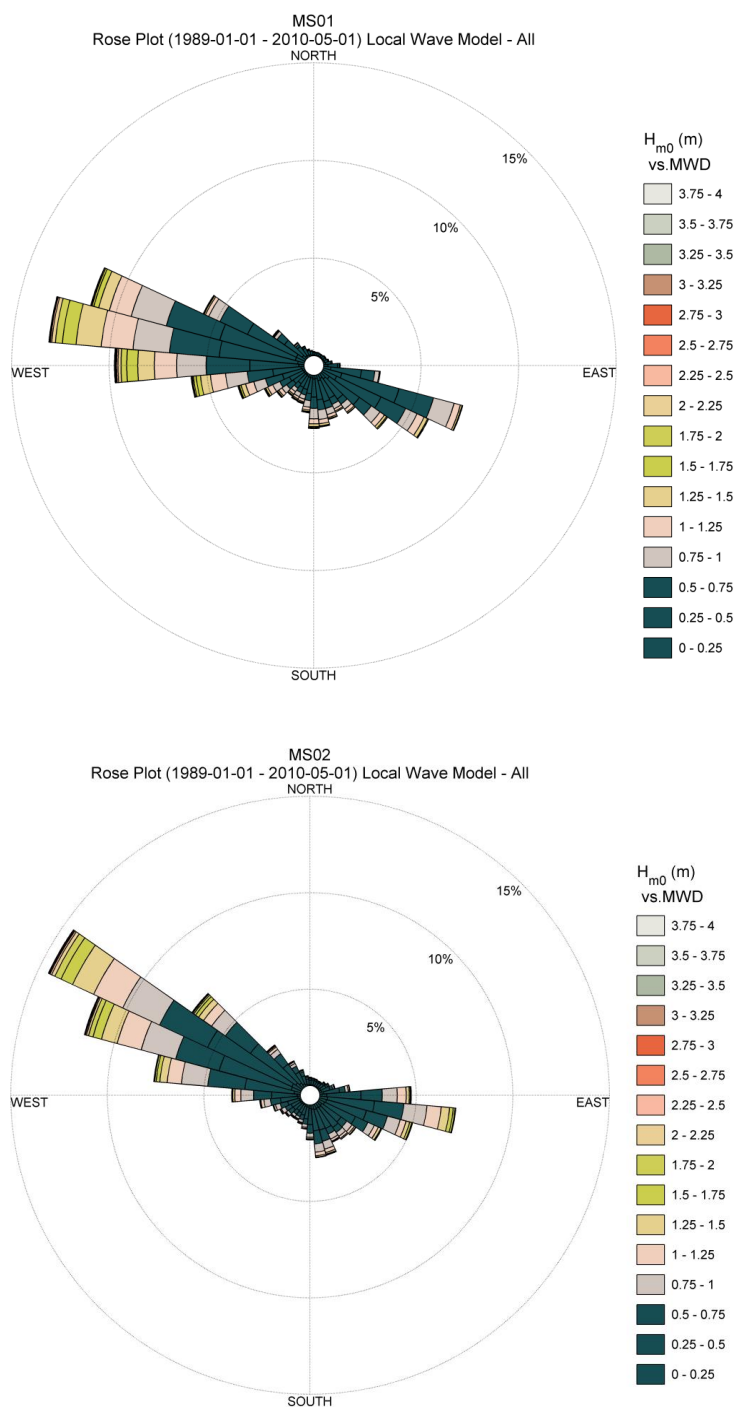


Fig. B. 9 Wave roses at MS01 (left) and MS02 (right)

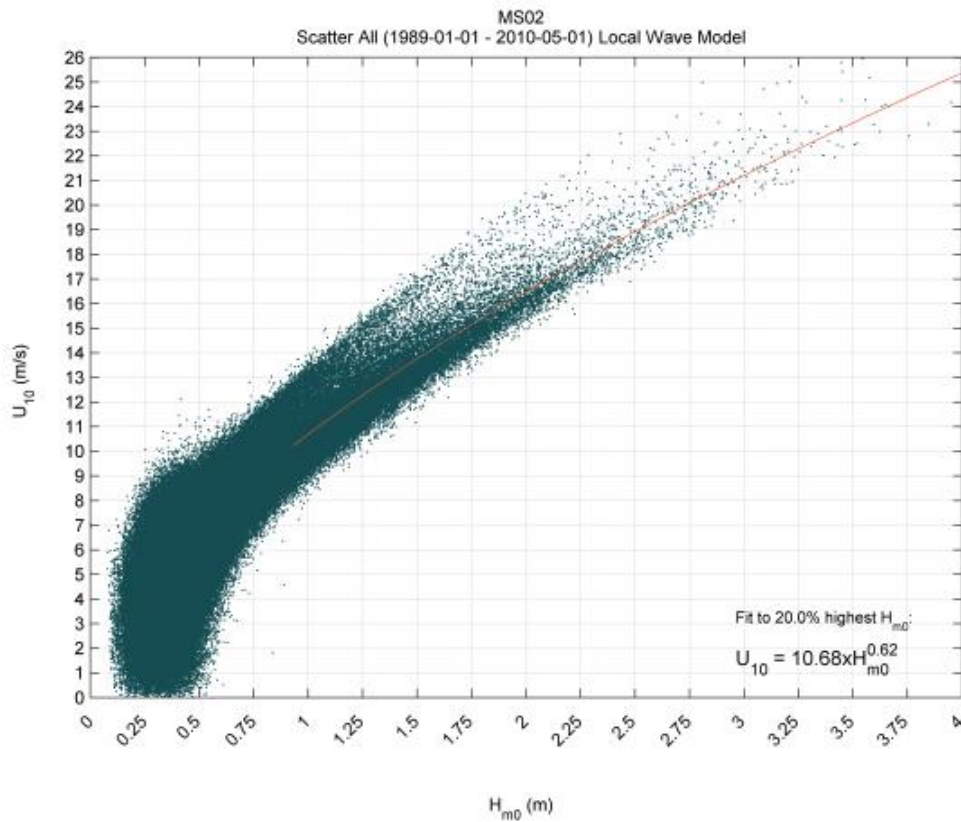
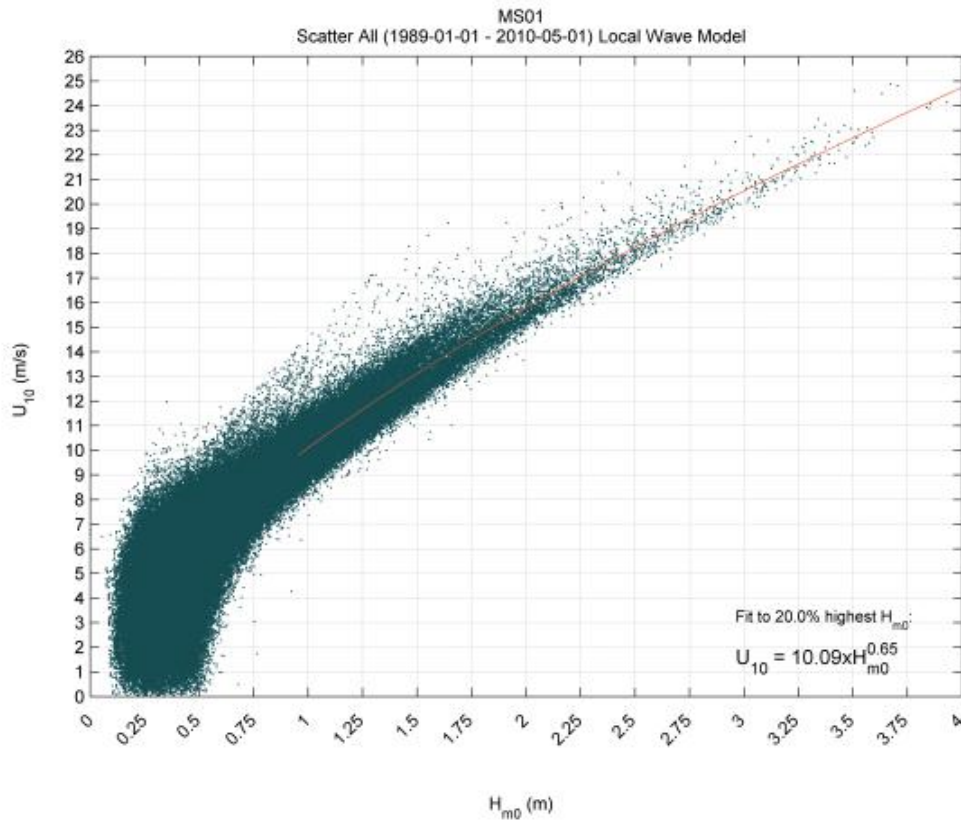


Fig. B. 10 H_{m0} vs. U_{10} scatter diagram at MS01 (left) and MS02 (right)

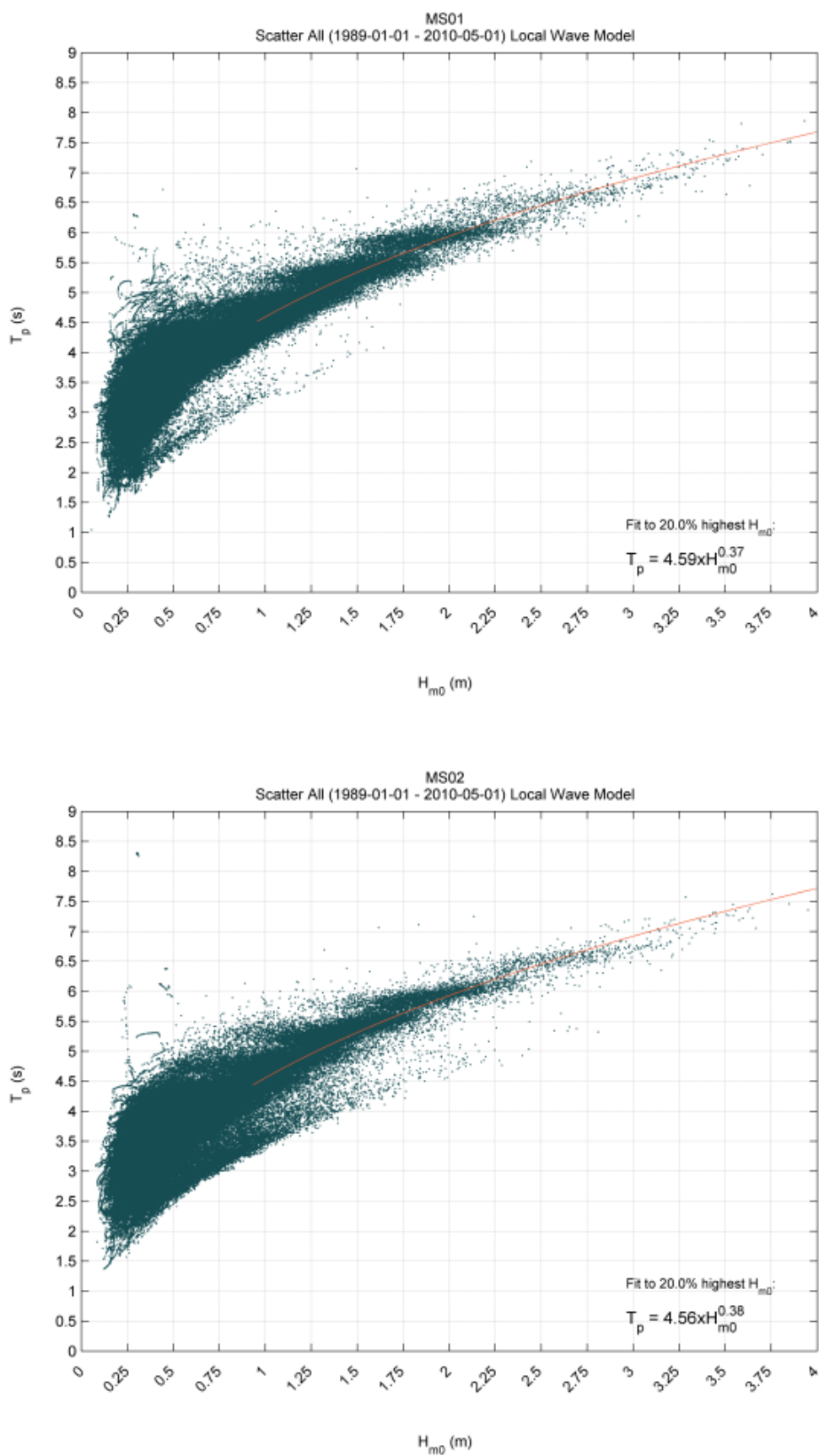


Fig. B. 11 H_{m0} vs. T_p scatter diagram at MS01 (left) and MS02 (right)

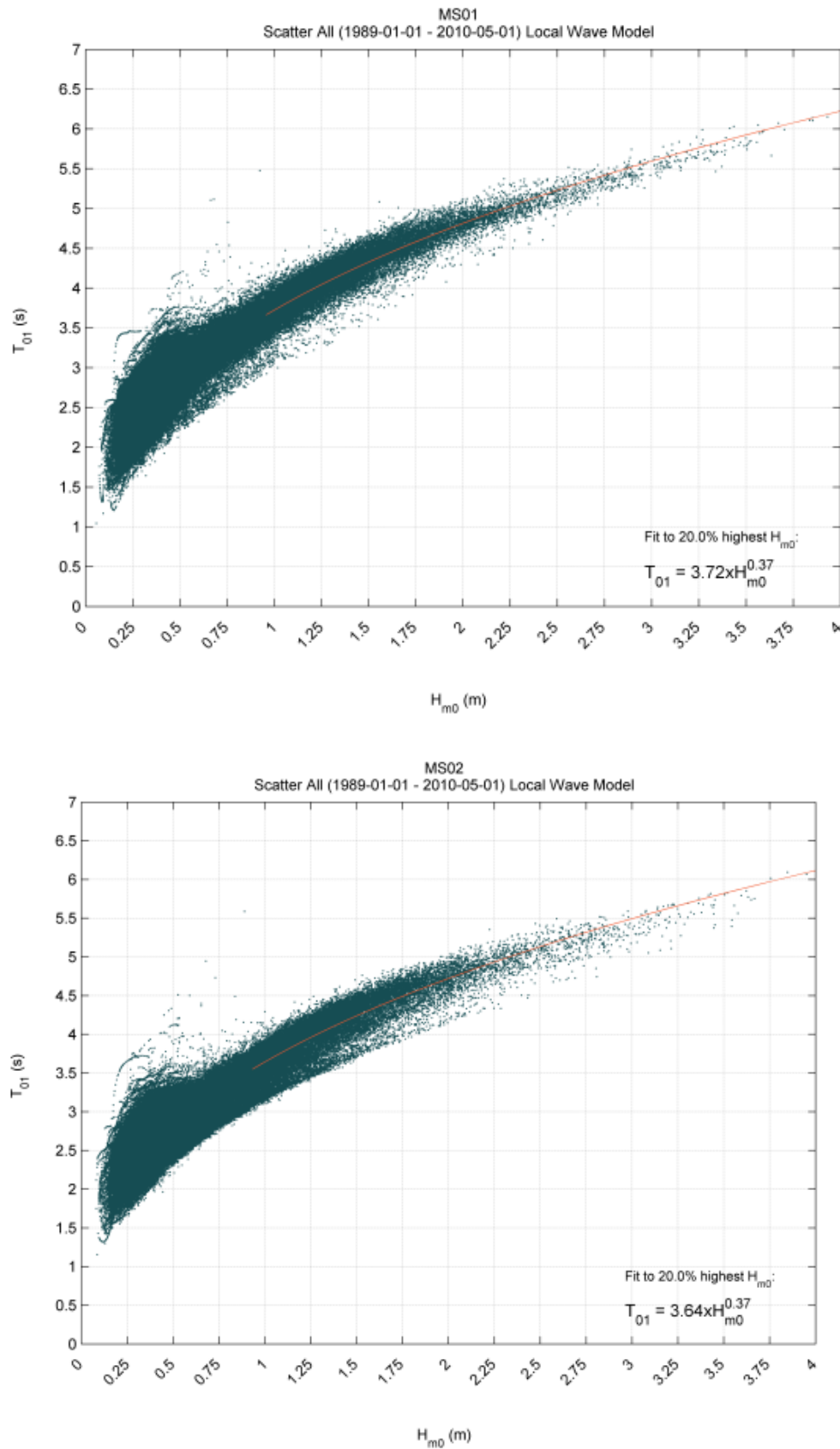
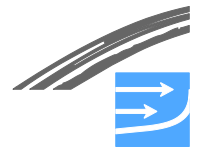


Fig. B. 12 H_{m0} vs. T_{01} scatter diagram at MS01 (left) and MS02 (right)



References

DHI (2009a): *MIKE 21 SW, Spectral Waves FM Module, User Guide.*

DHI (2009b): *MIKE 21, Spectral Wave Module, Scientific Documentation.*

FEHY (2013d): "Fehmarnbelt Fixed Link, Marine Soil - Baseline, Coastal Morphology along Fehmarn and Lolland, Report No. E1TR0056 Vol. III.

FEHY (2013e): Fehmarnbelt Fixed Link. Marine Water - Impact Assessment. Baltic Sea Hydrography, Water Quality and Plankton. Report No. E1TR0058 Volume I.